Boxplot: Electrical Conductivity @ 25°C

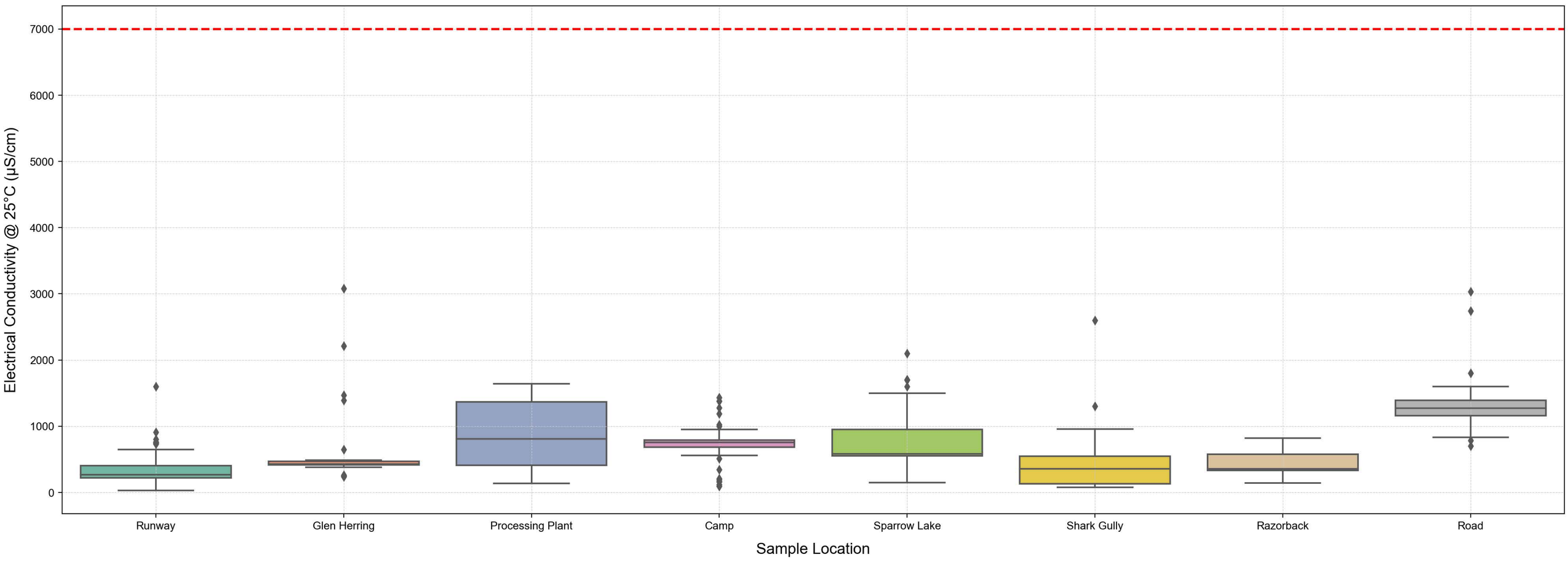

Boxplot: Ethylbenzene

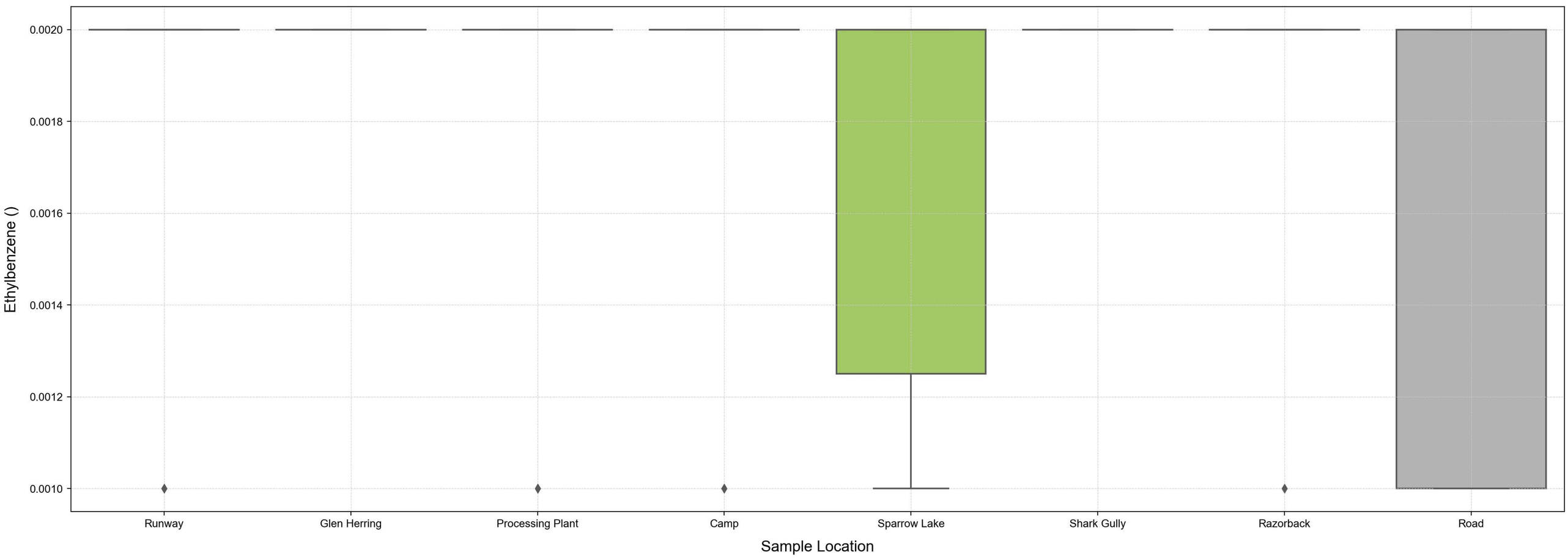

Boxplot: Field_EC

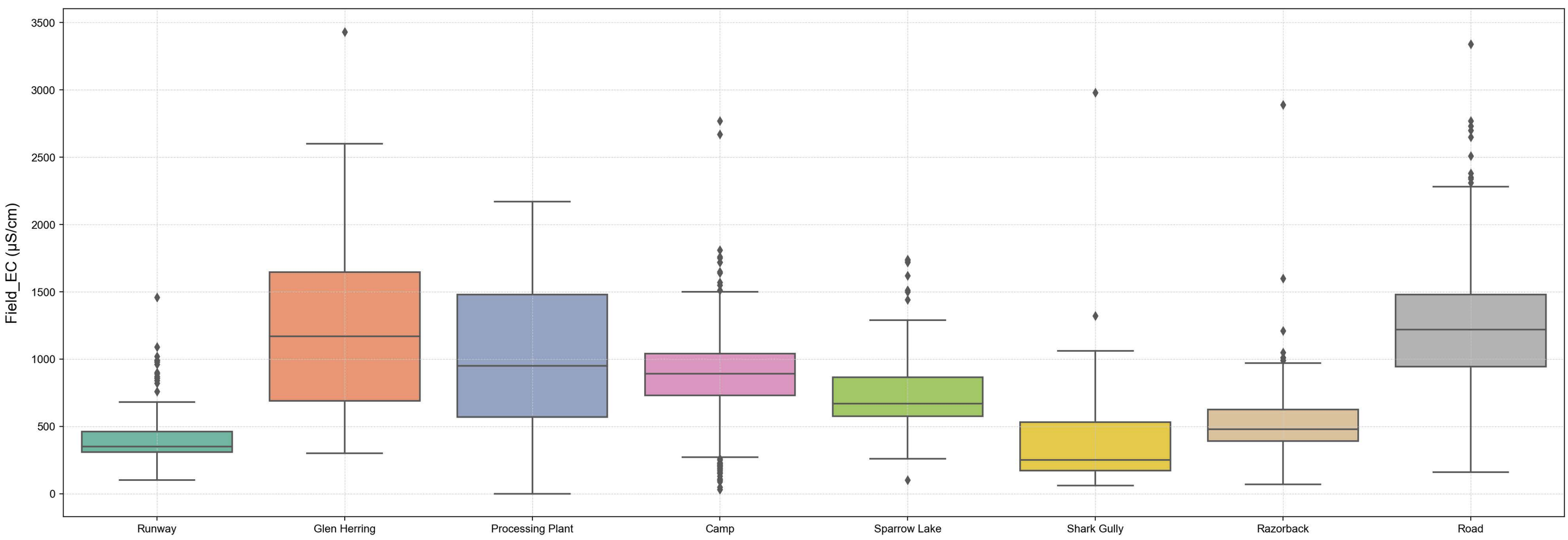

Boxplot: Field_pH

Boxplot: Fluoride

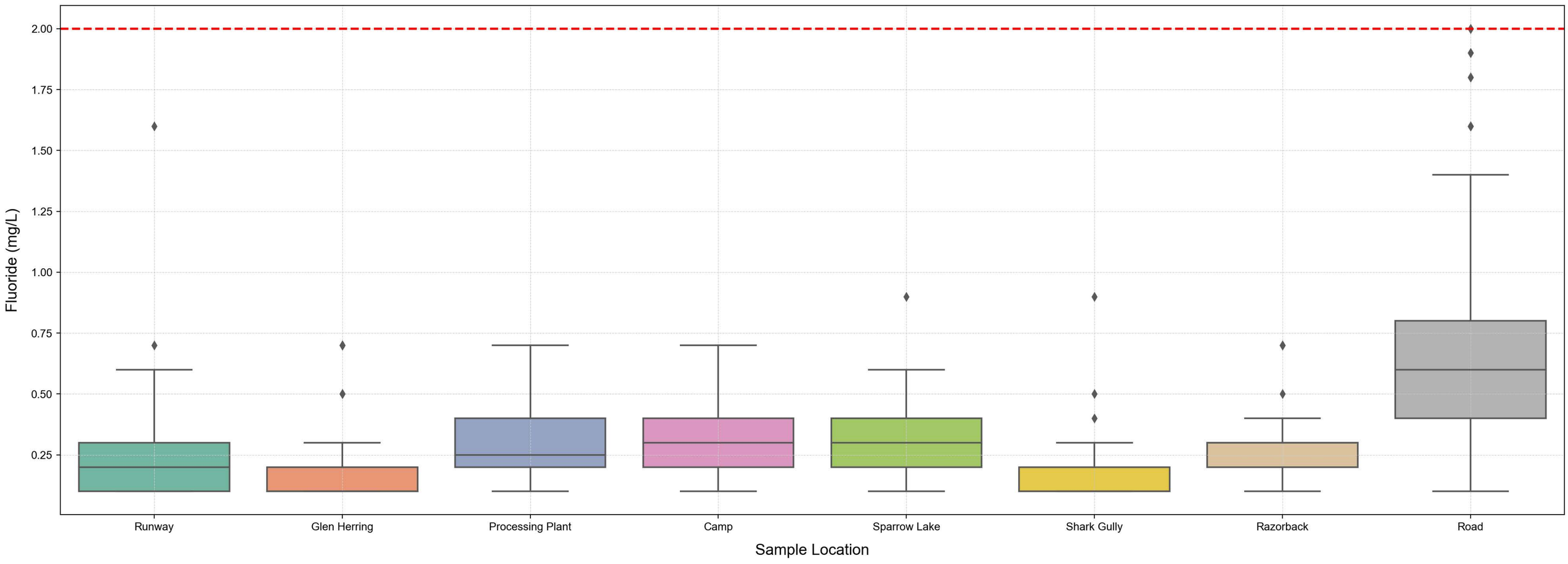

Boxplot: Hexavalent Chromium

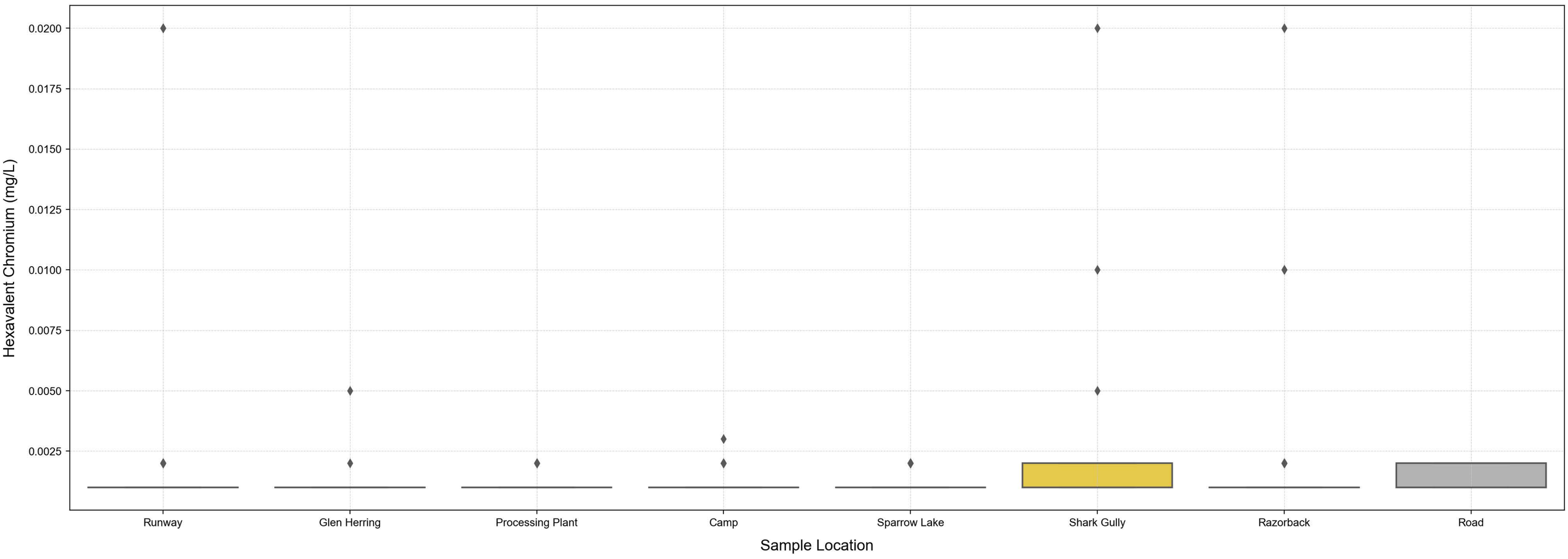

Boxplot: Hydroxide Alkalinity as CaCO3

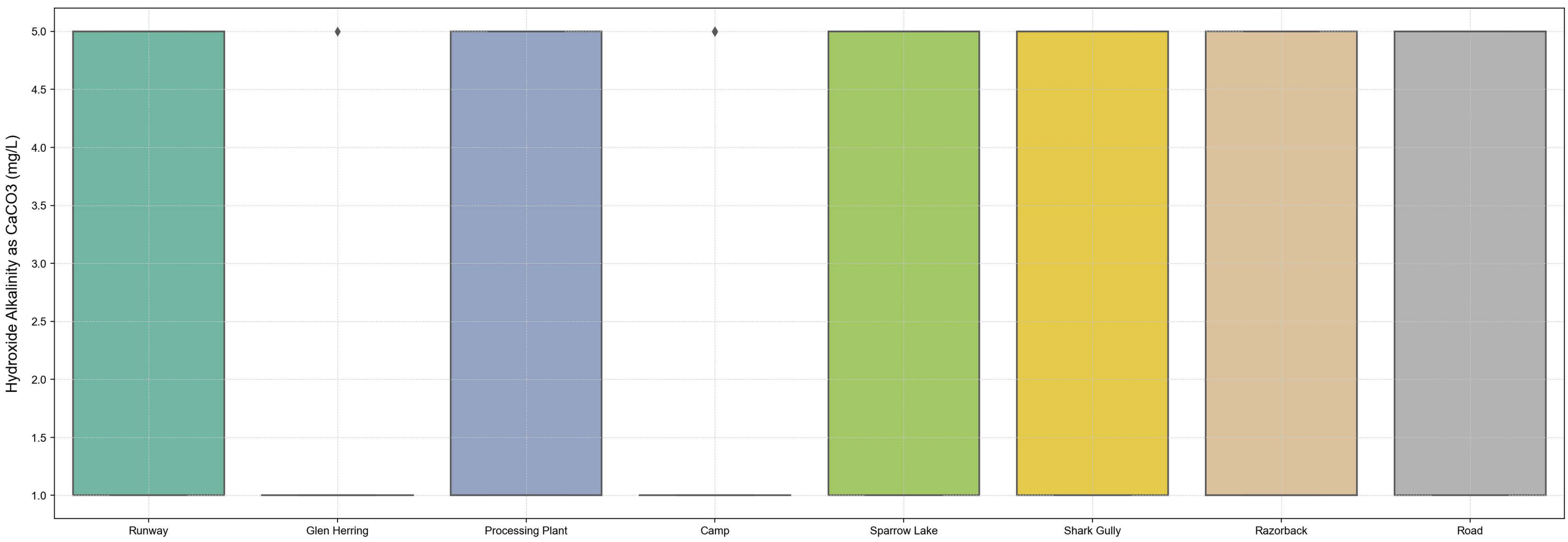

Boxplot: Ionic Balance

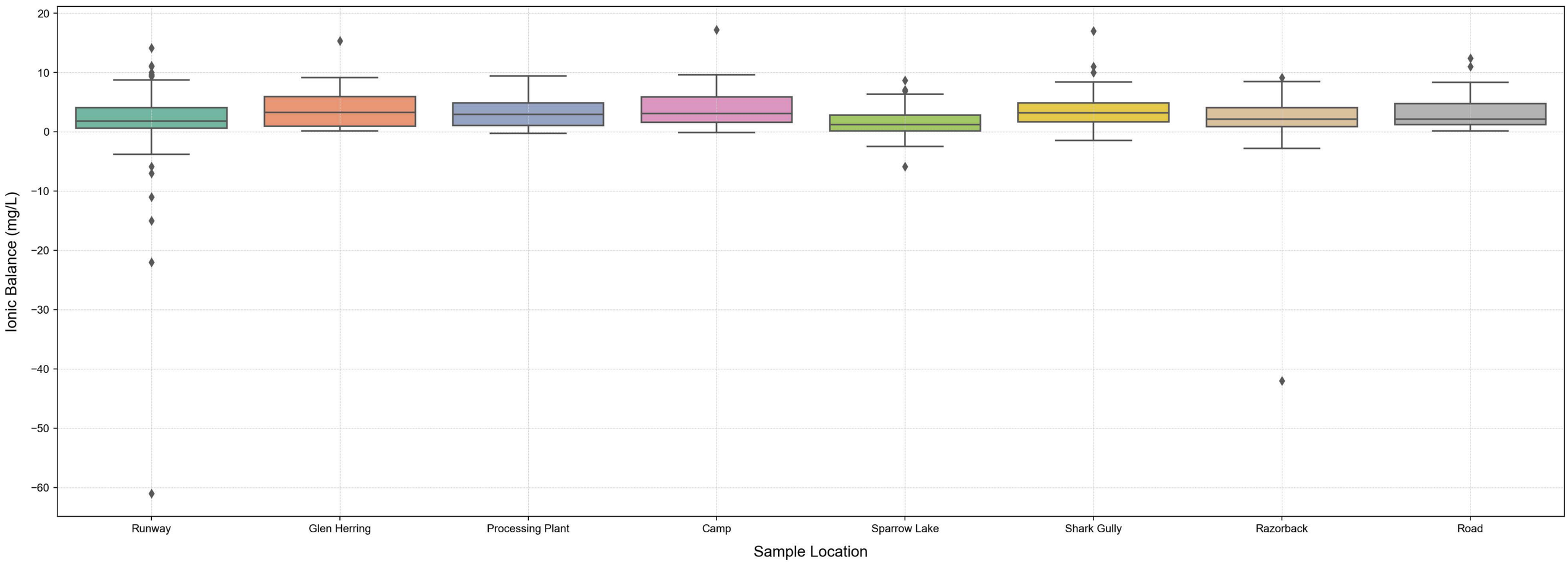

Boxplot: Iron

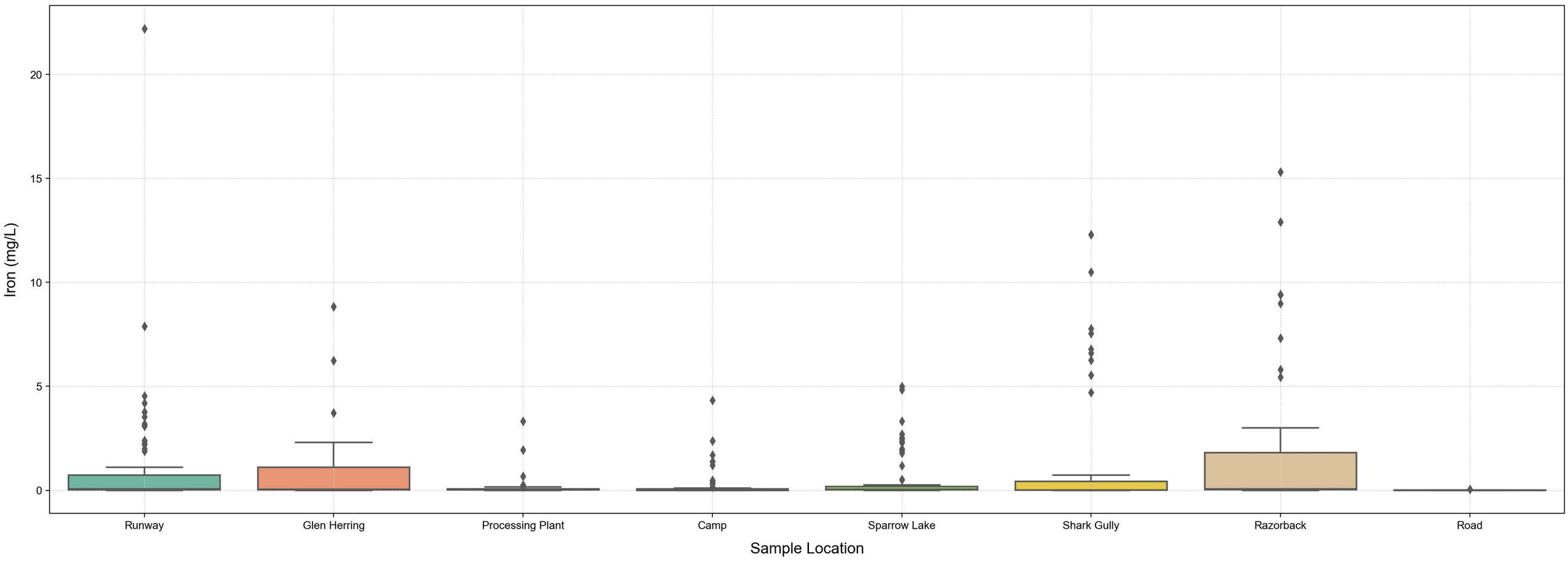

Boxplot: Lead

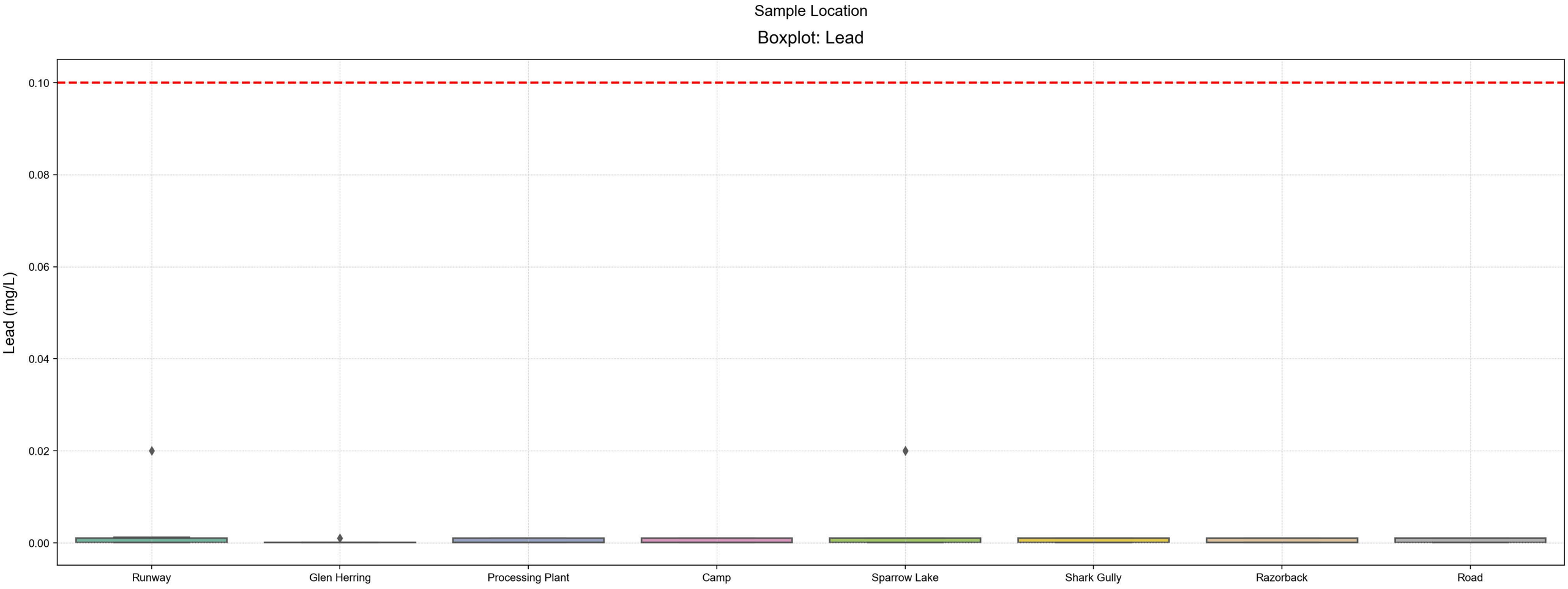

Boxplot: Magnesium

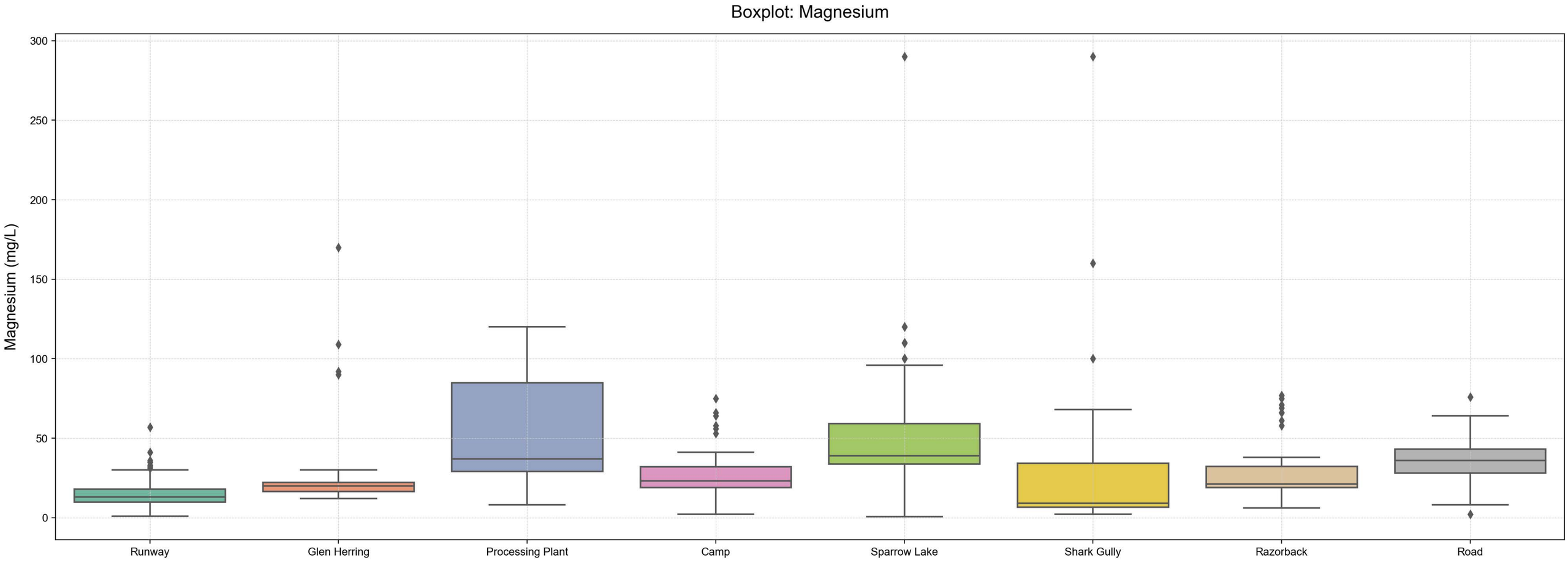

Boxplot: Manganese

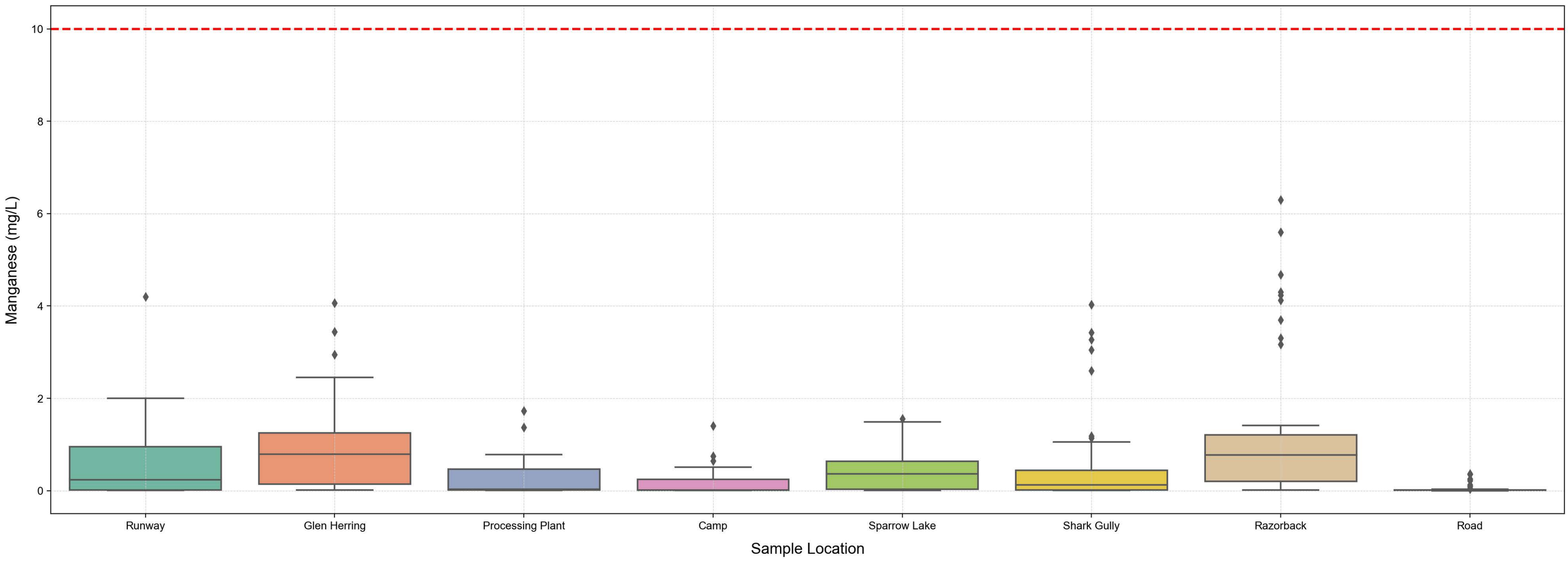

Boxplot: Mercury

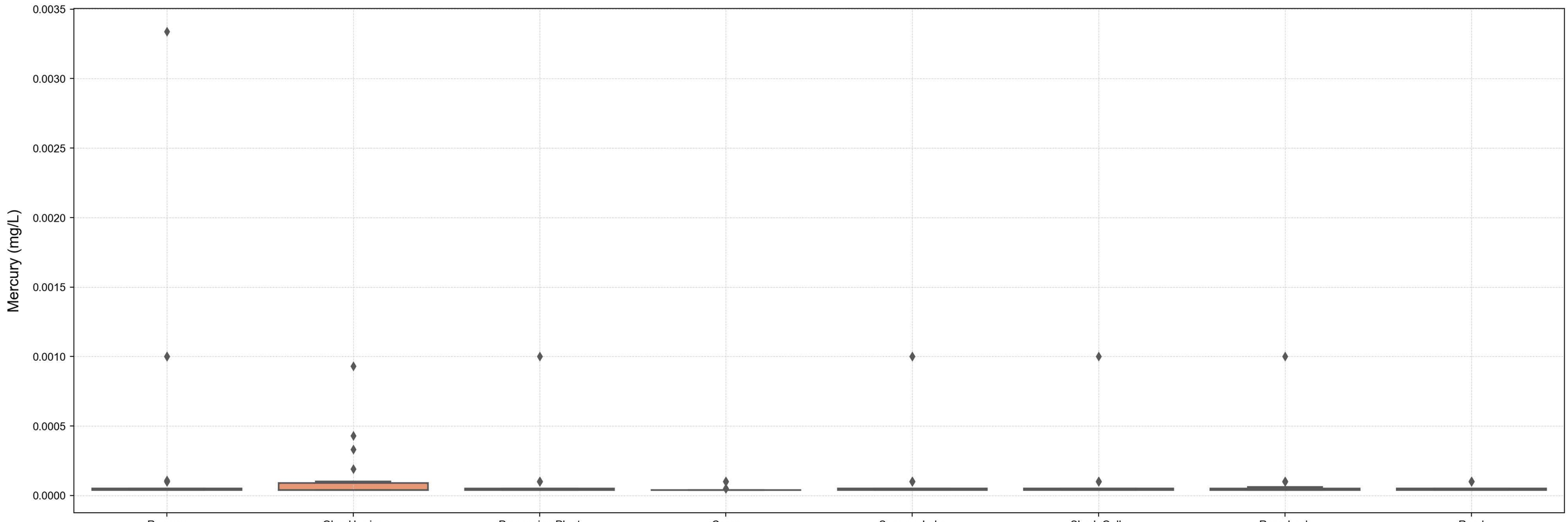

Boxplot: Molybdenum

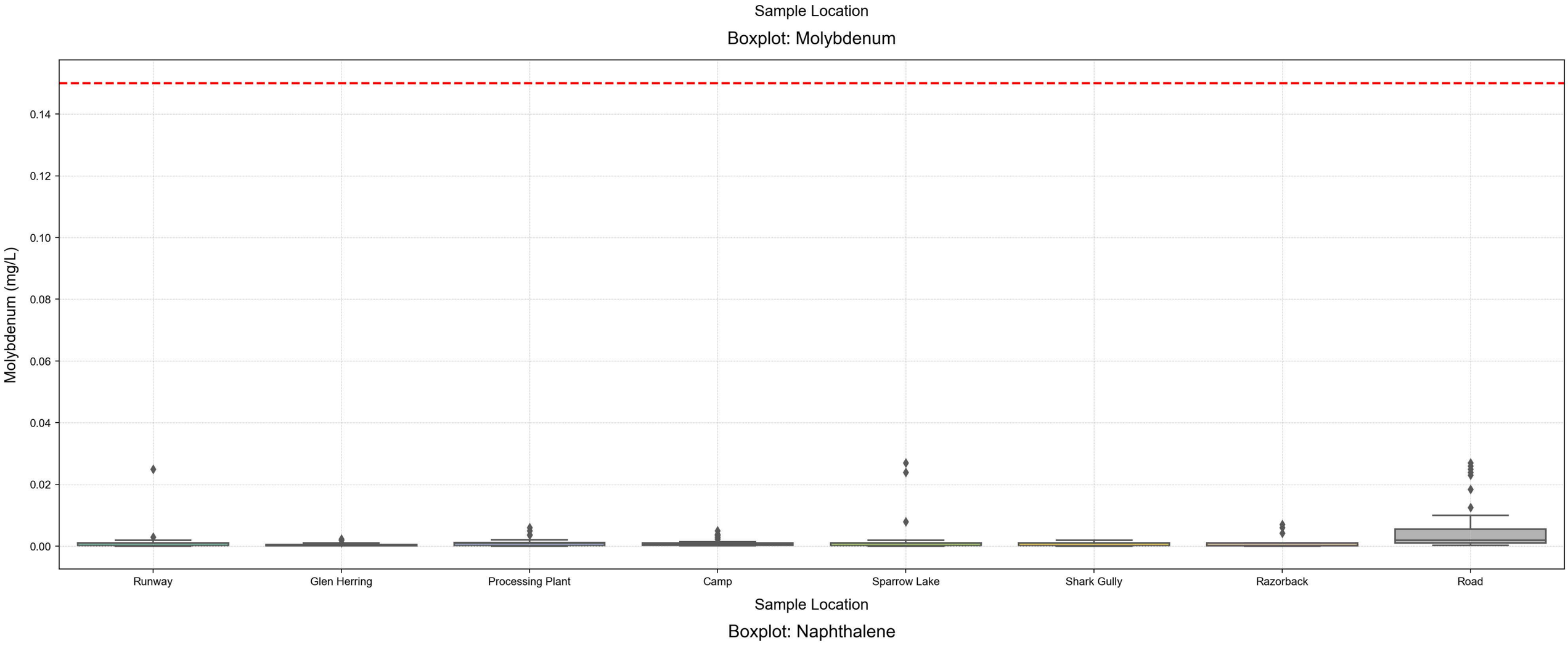

Boxplot: Naphthalene

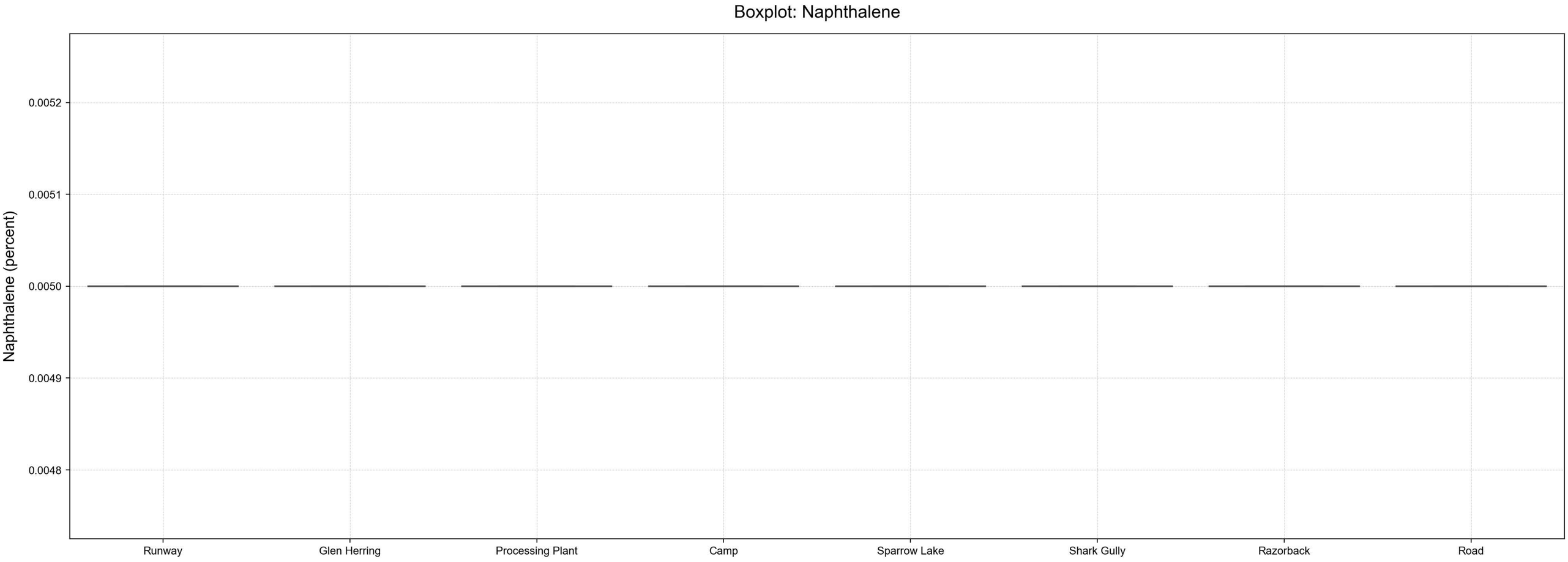

Boxplot: Nickel

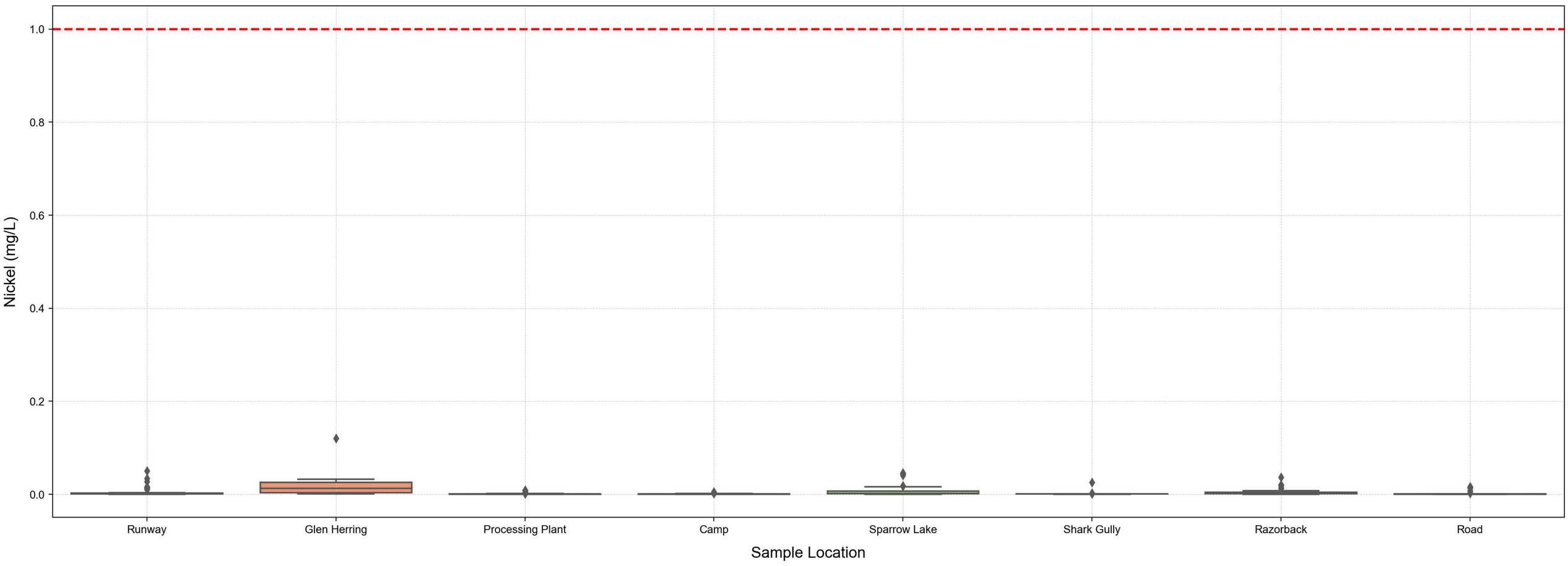

Boxplot: Nitrate as N

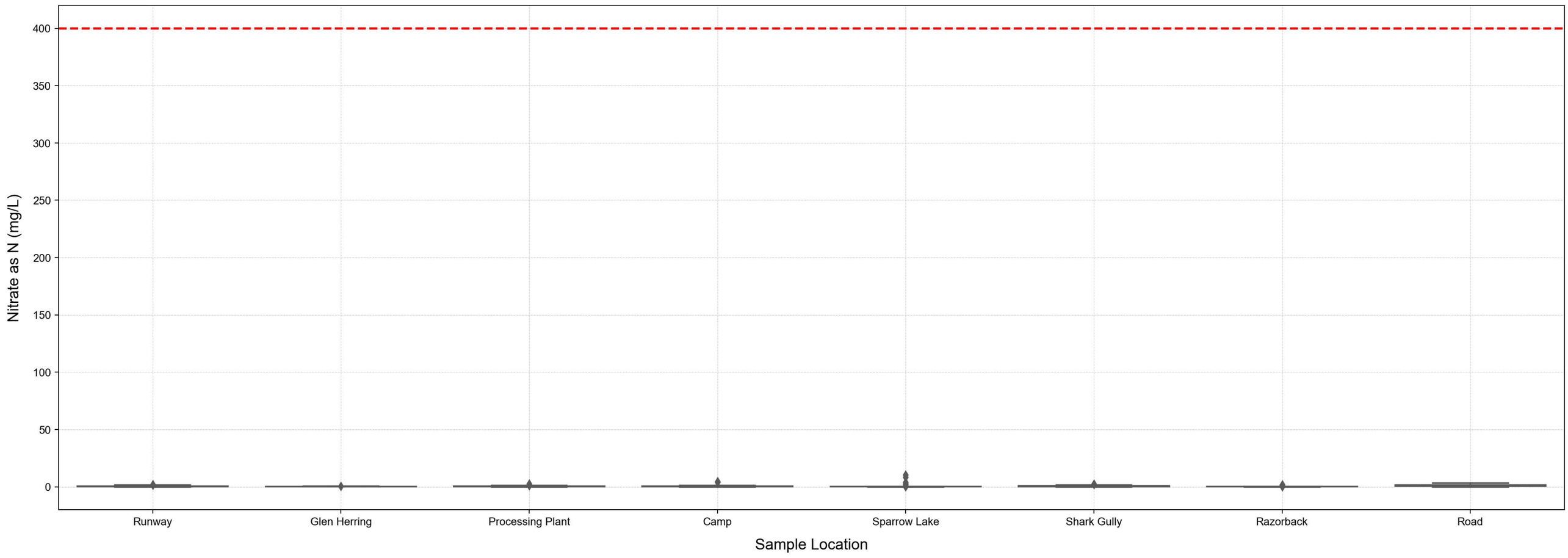

Boxplot: Nitrite + Nitrate as N

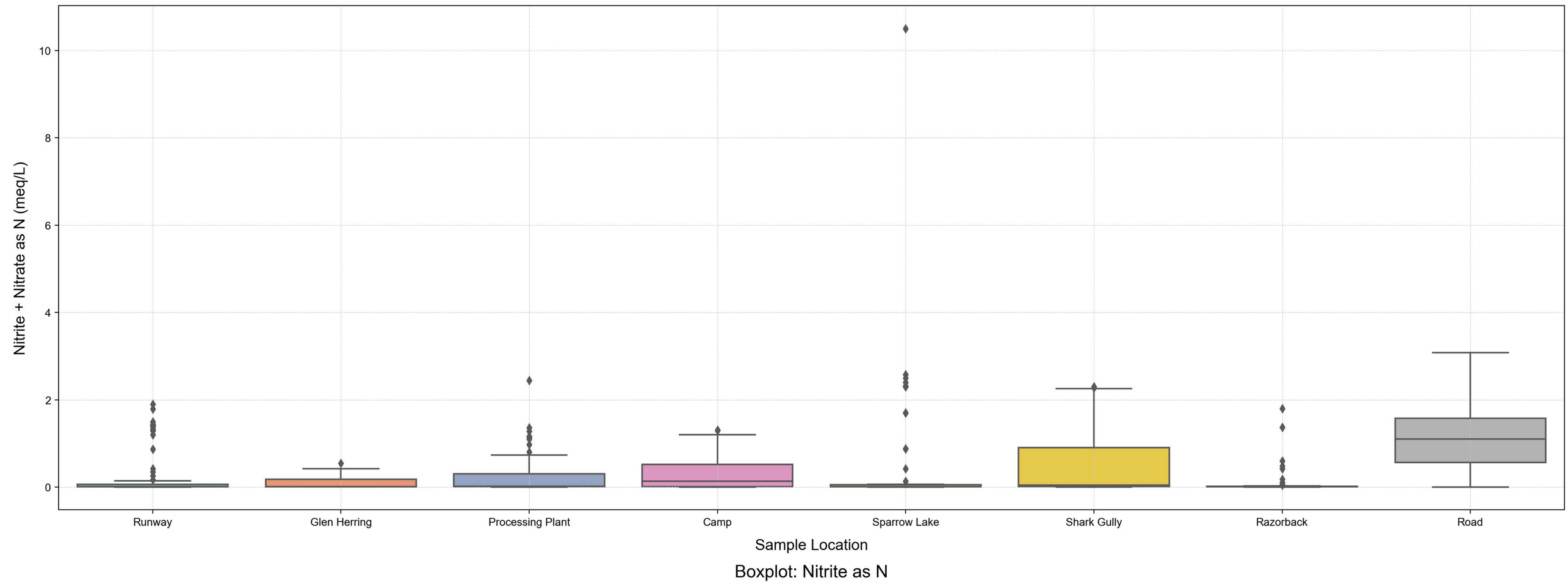

Boxplot: Nitrite as N

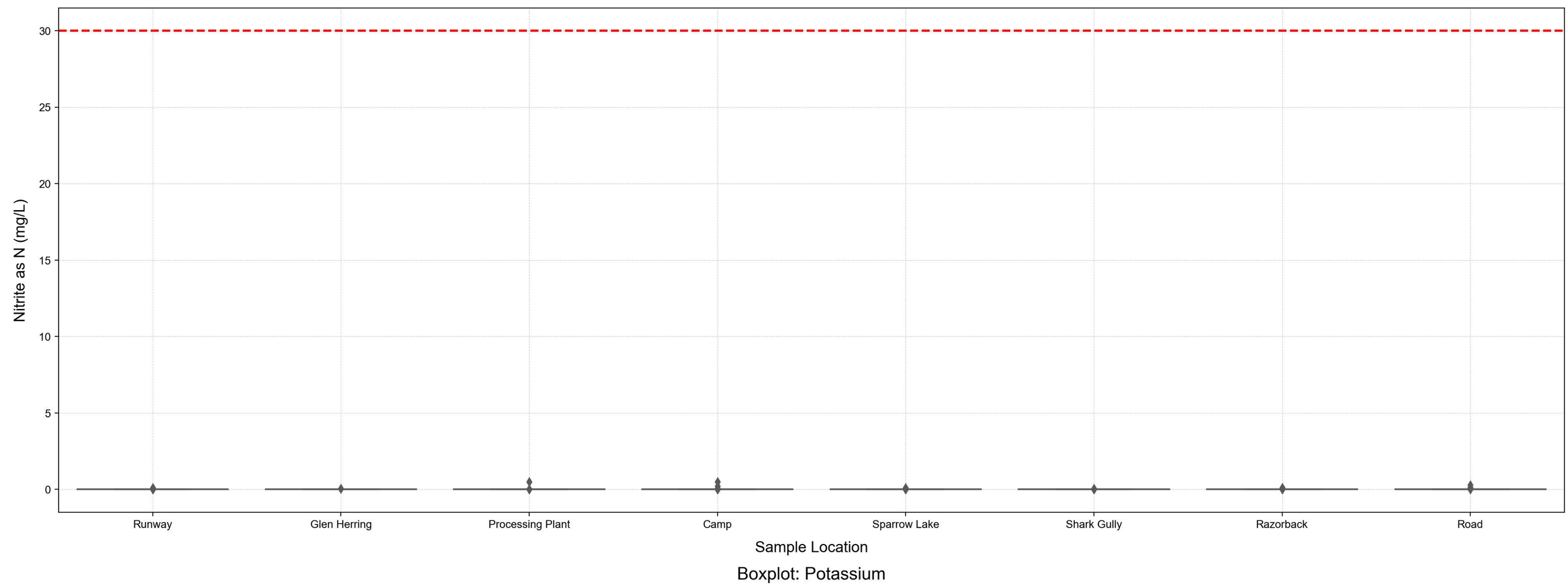

Boxplot: Potassium

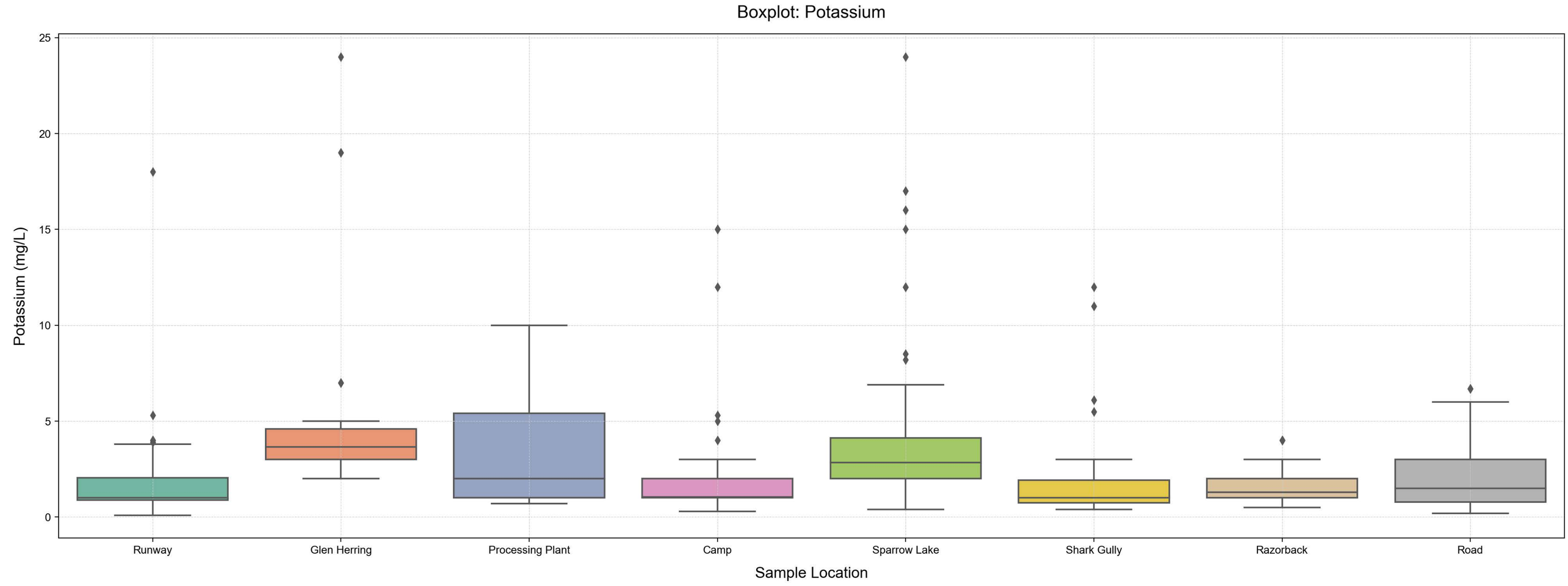

Boxplot: Selenium

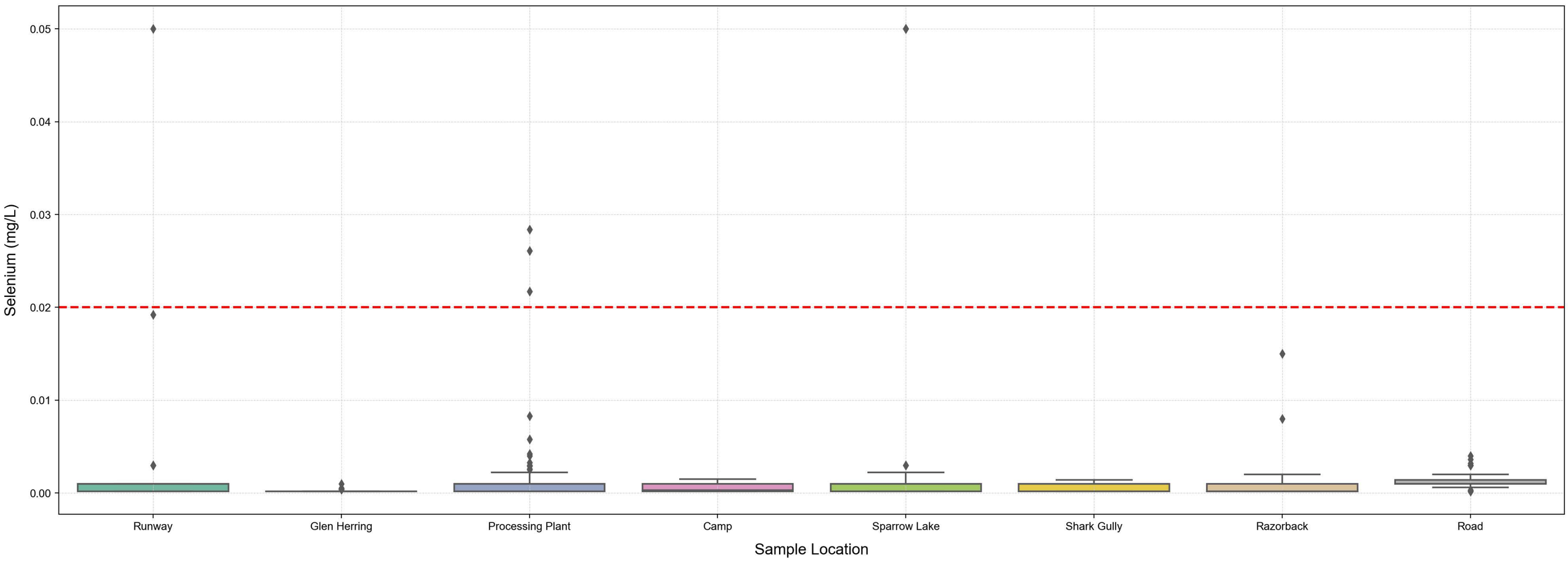

Boxplot: Silicon

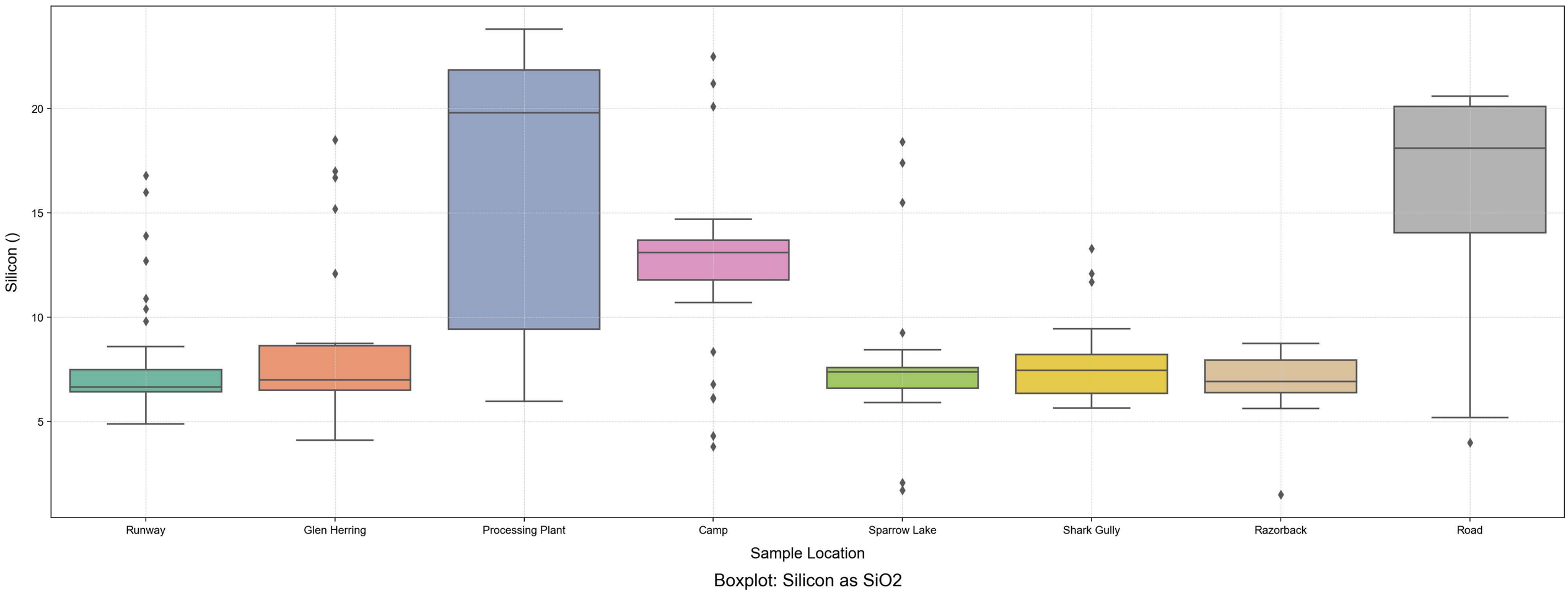

Boxplot: Silicon as SiO2

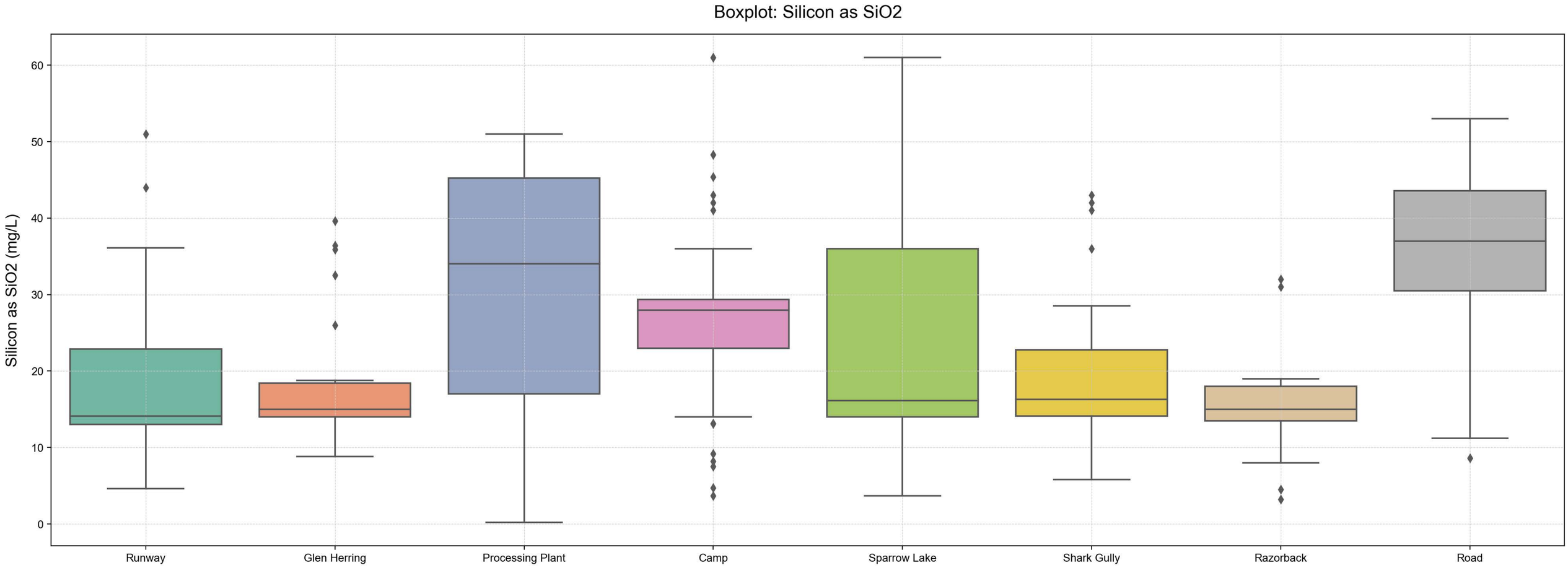

Boxplot: Silver

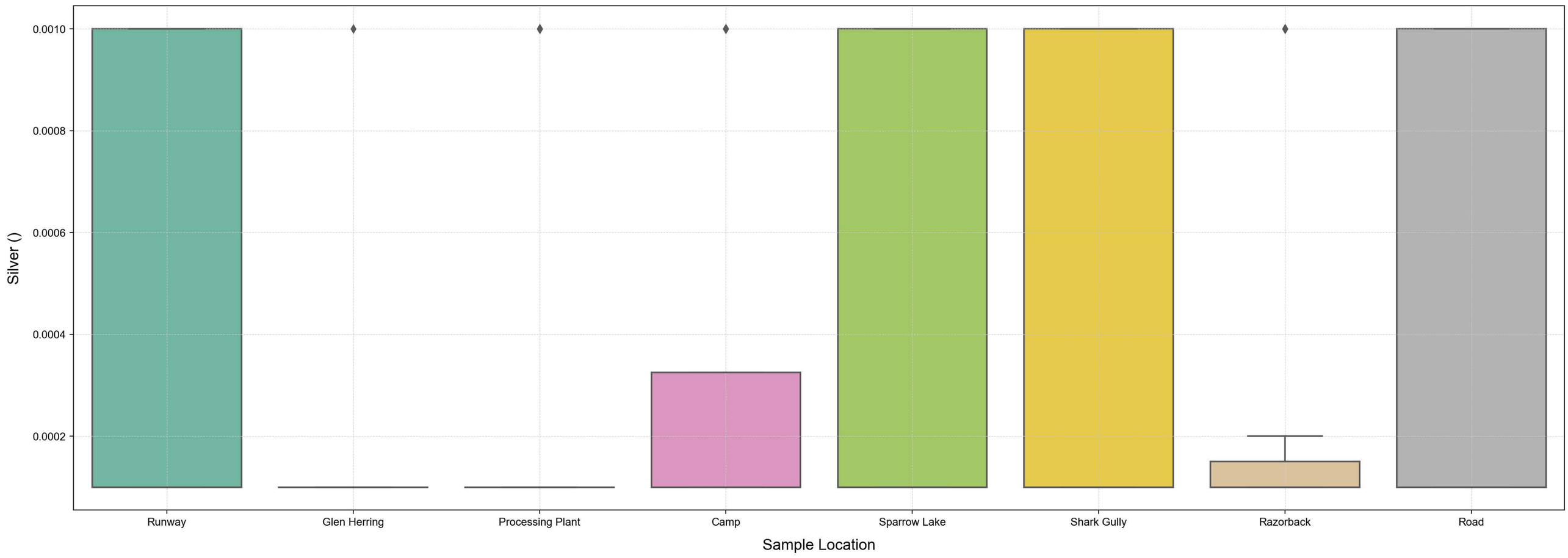

Boxplot: Sodium

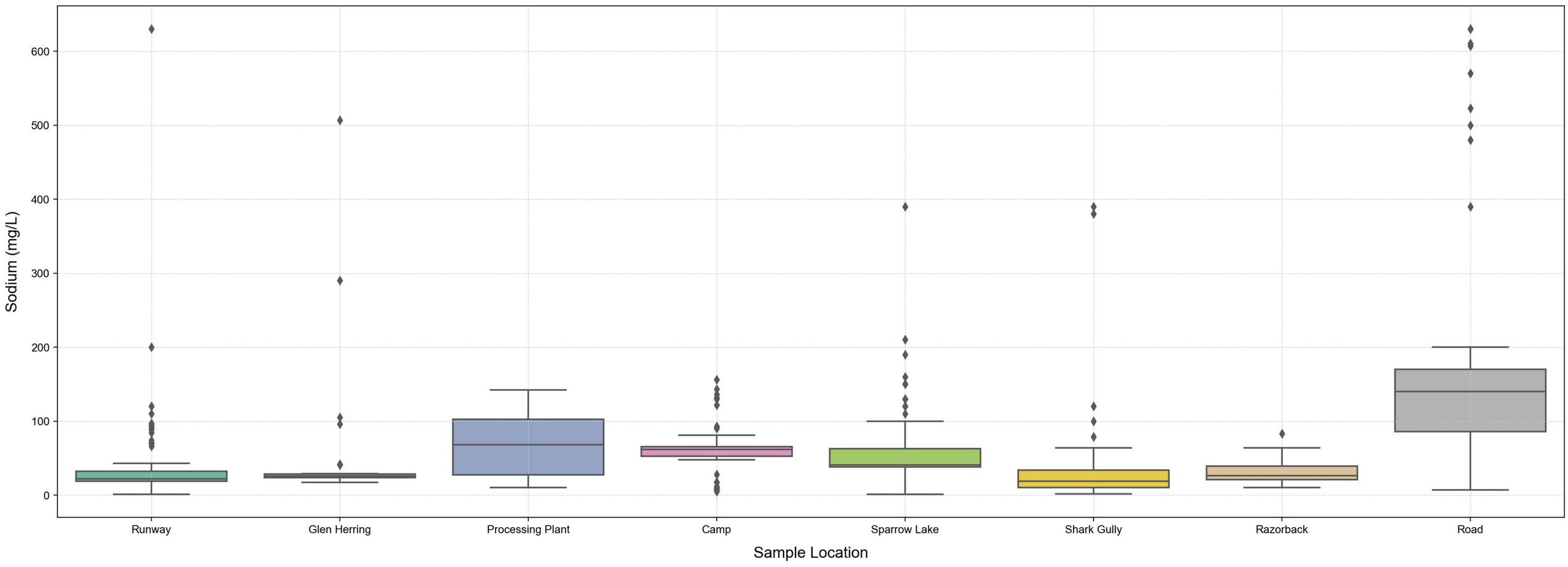

Boxplot: Strontium

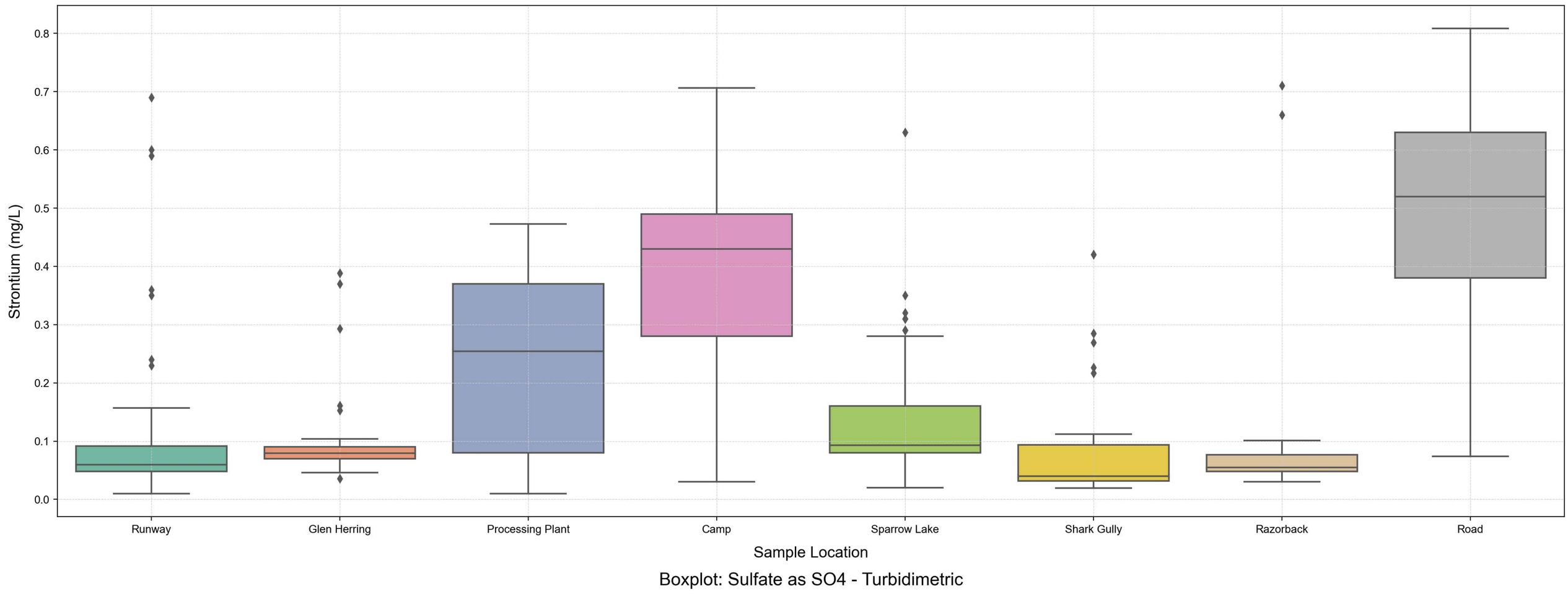

Boxplot: Sulfate as SO4 - Turbidimetric

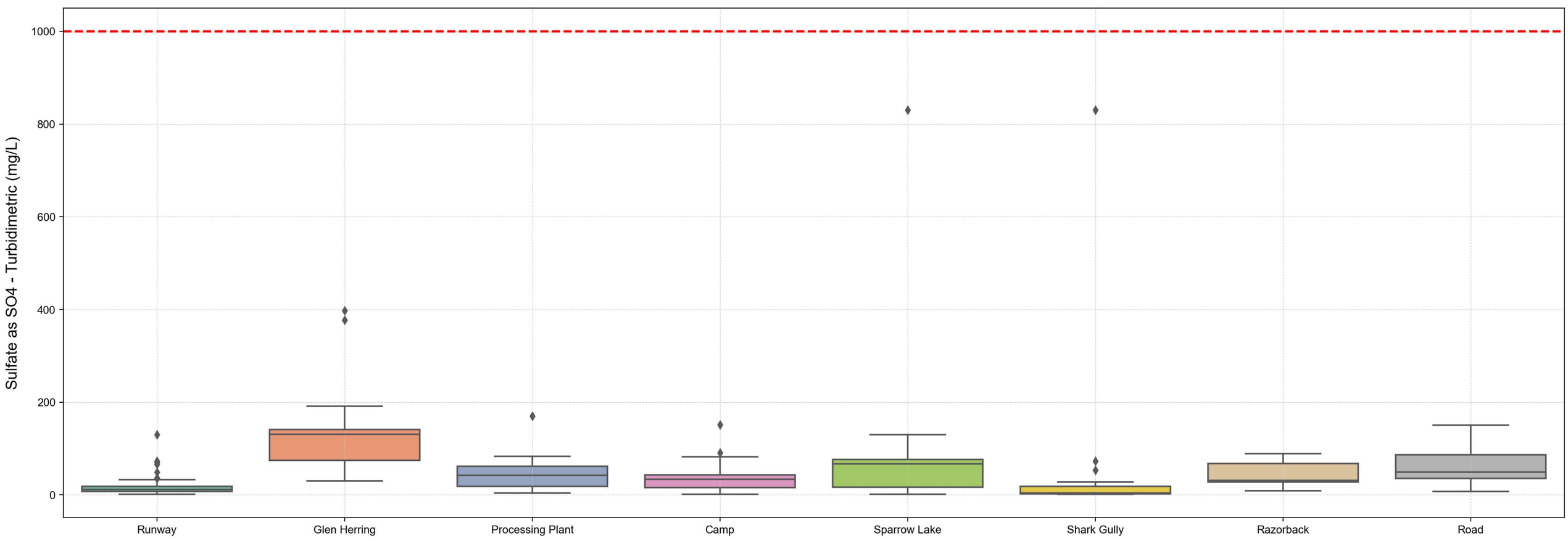

Boxplot: Sum of BTEX

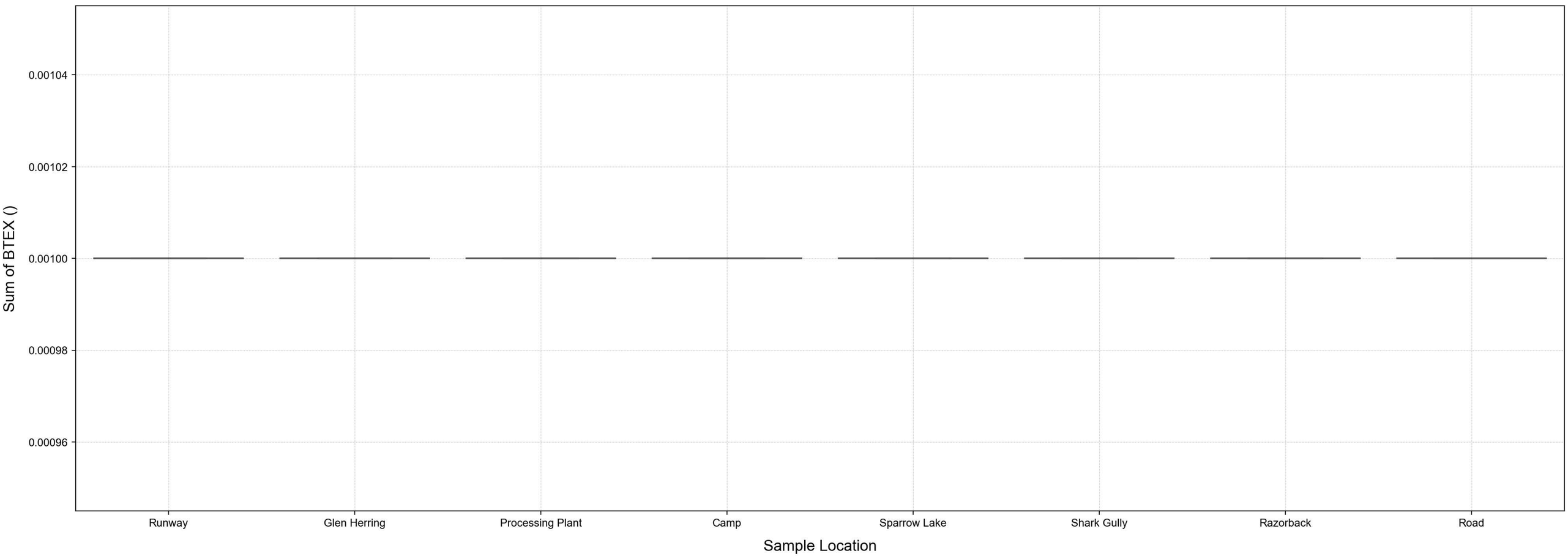

Boxplot: Suspended Solids (SS)

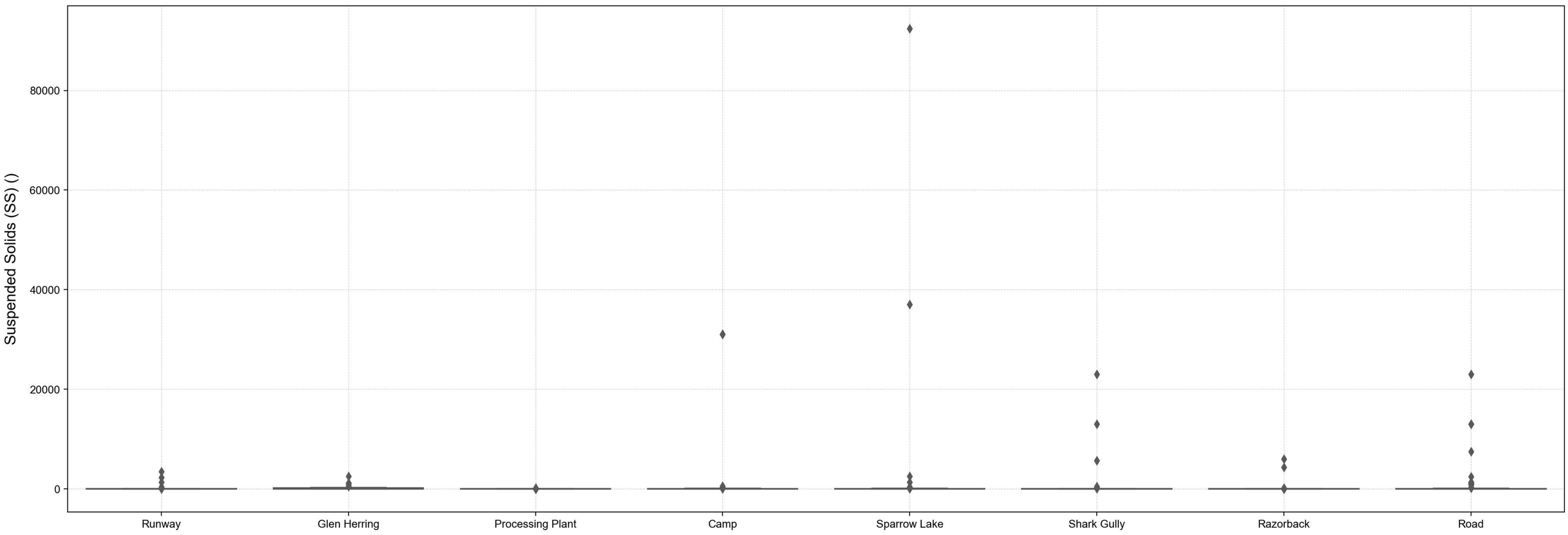

Boxplot: Tin

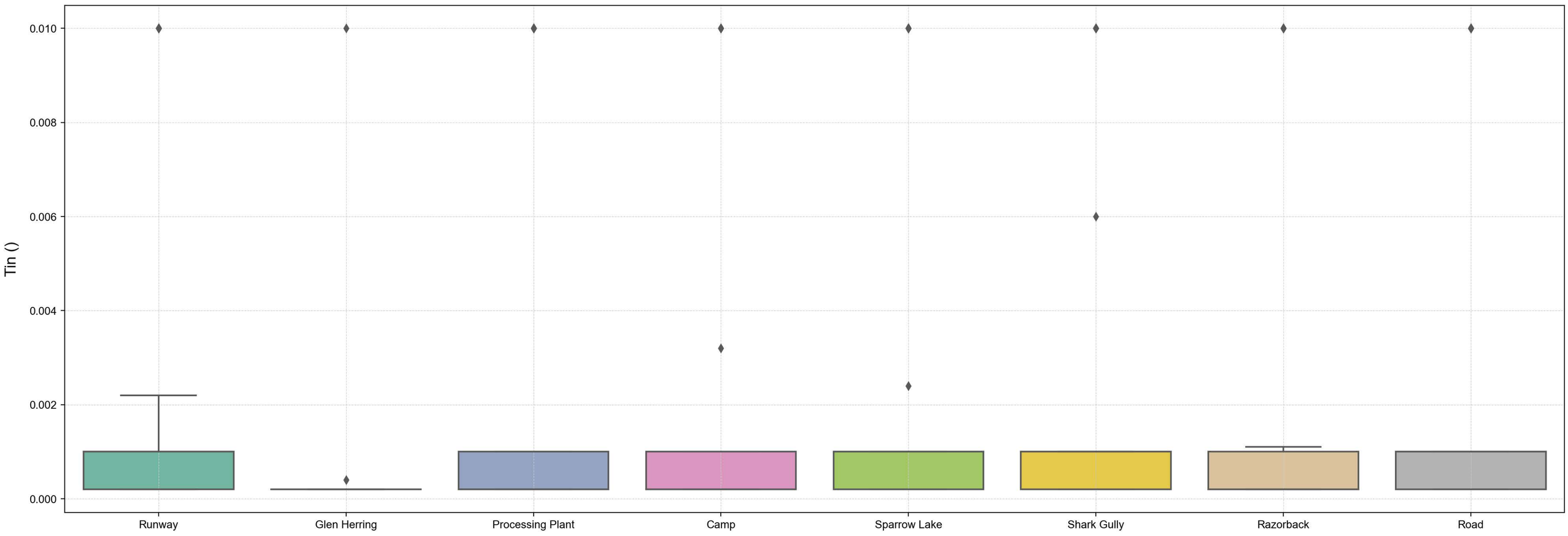

Boxplot: Toluene

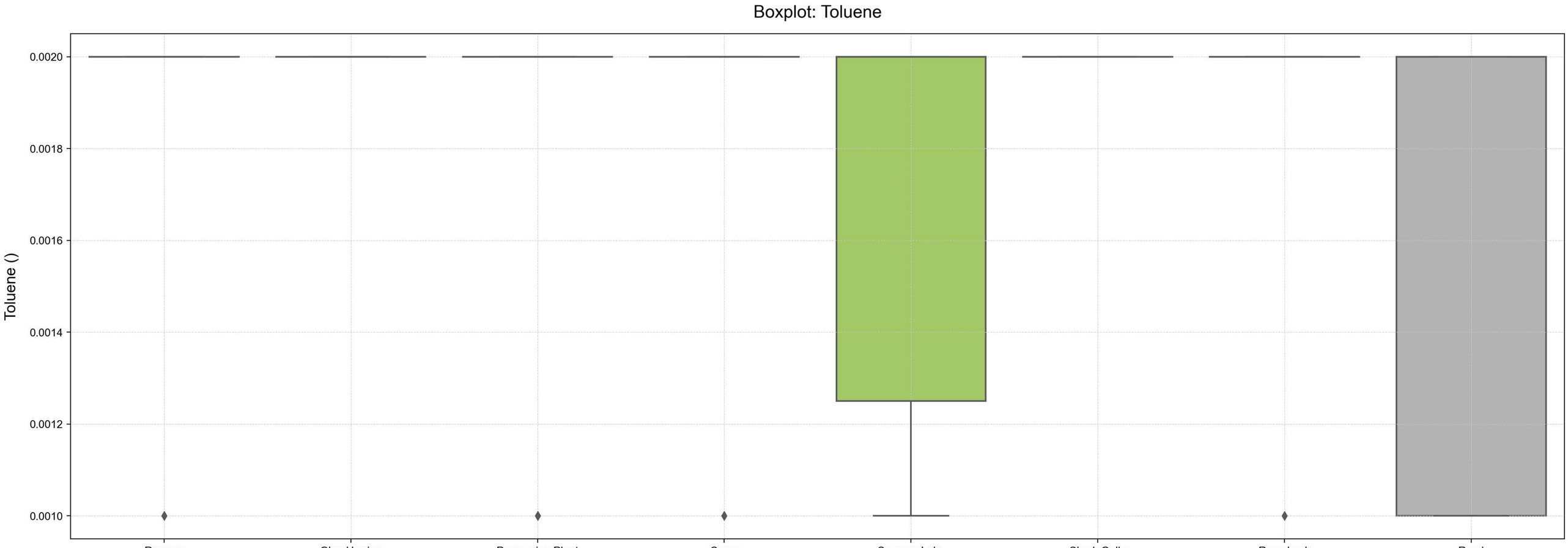

Boxplot: Toluene-D8

Boxplot: Total Alkalinity as CaCO3

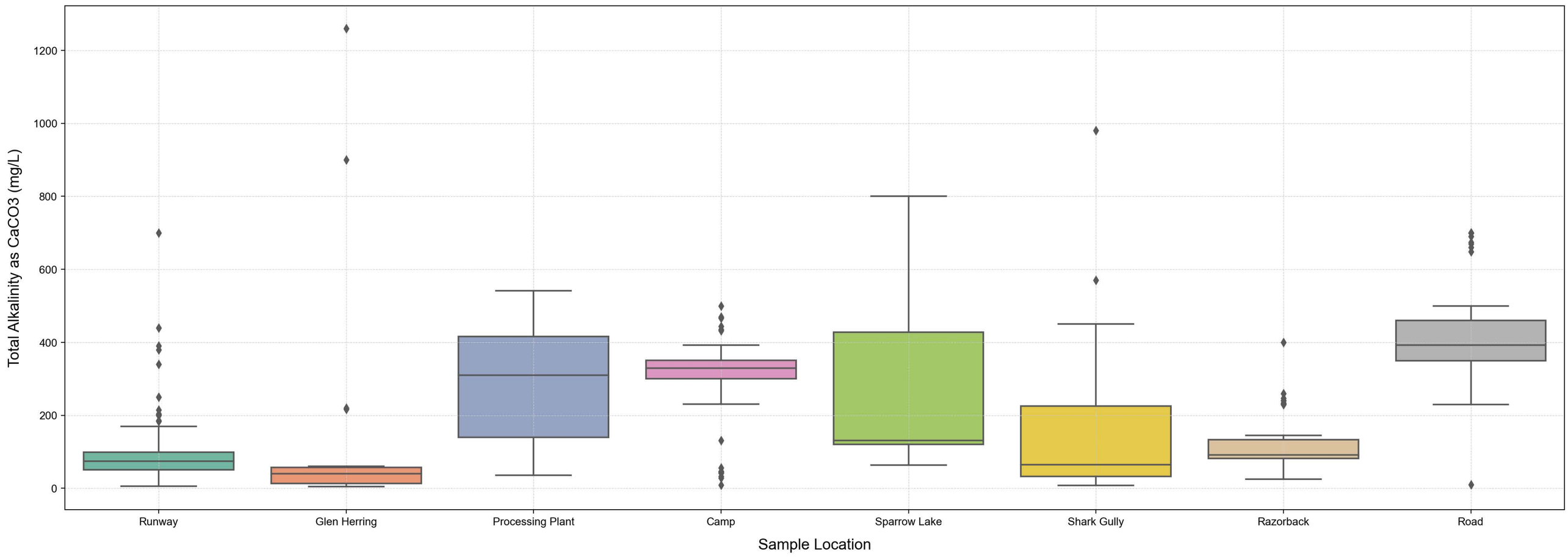

Boxplot: Total Anions

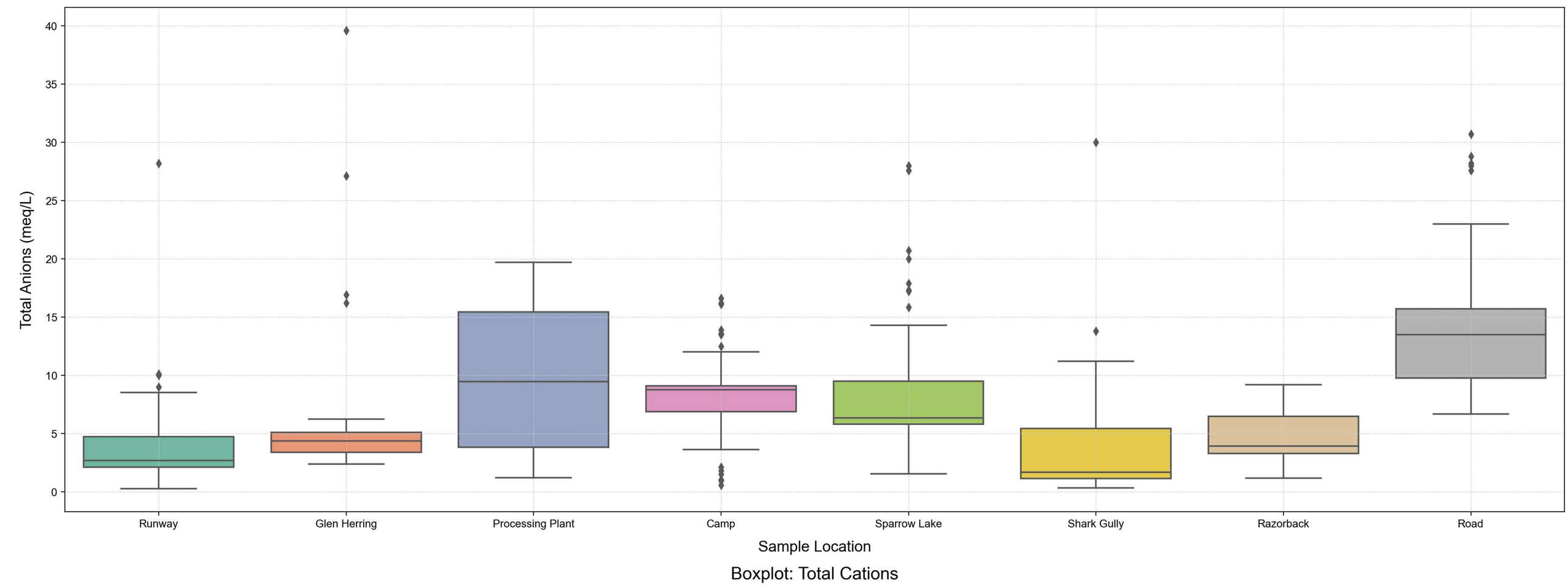

Boxplot: Total Cations

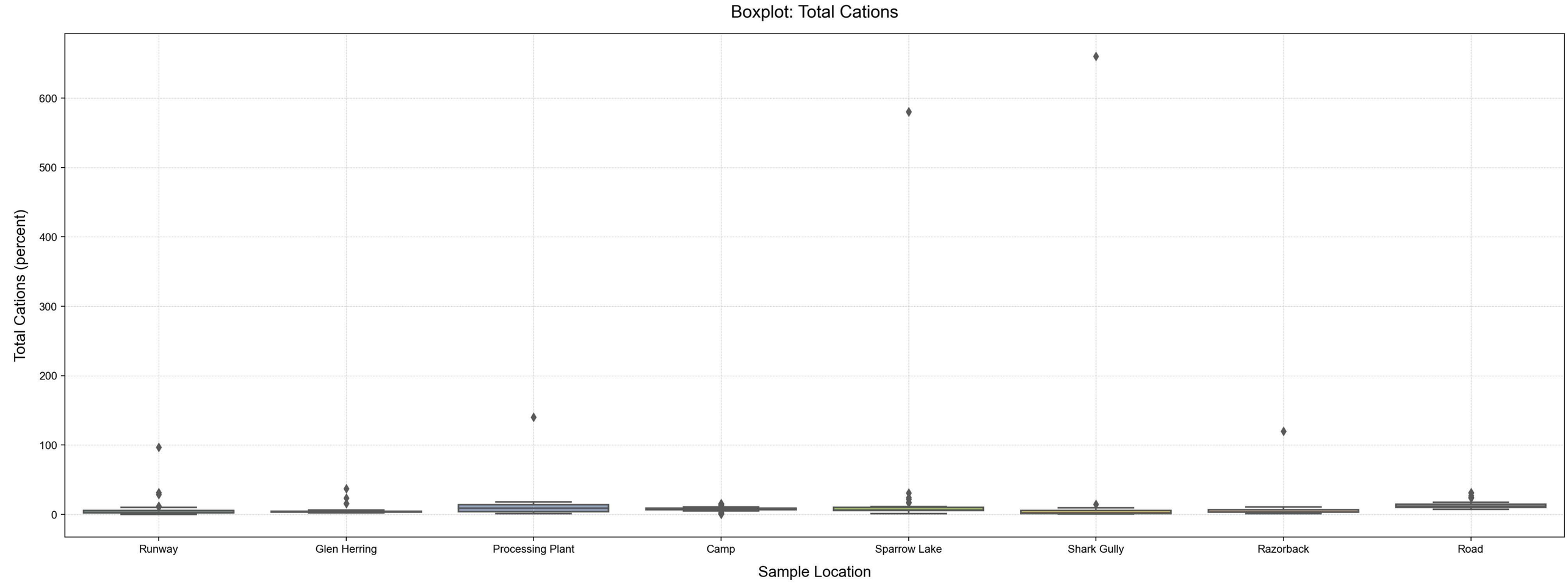

Boxplot: Total Dissolved Solids @180°C

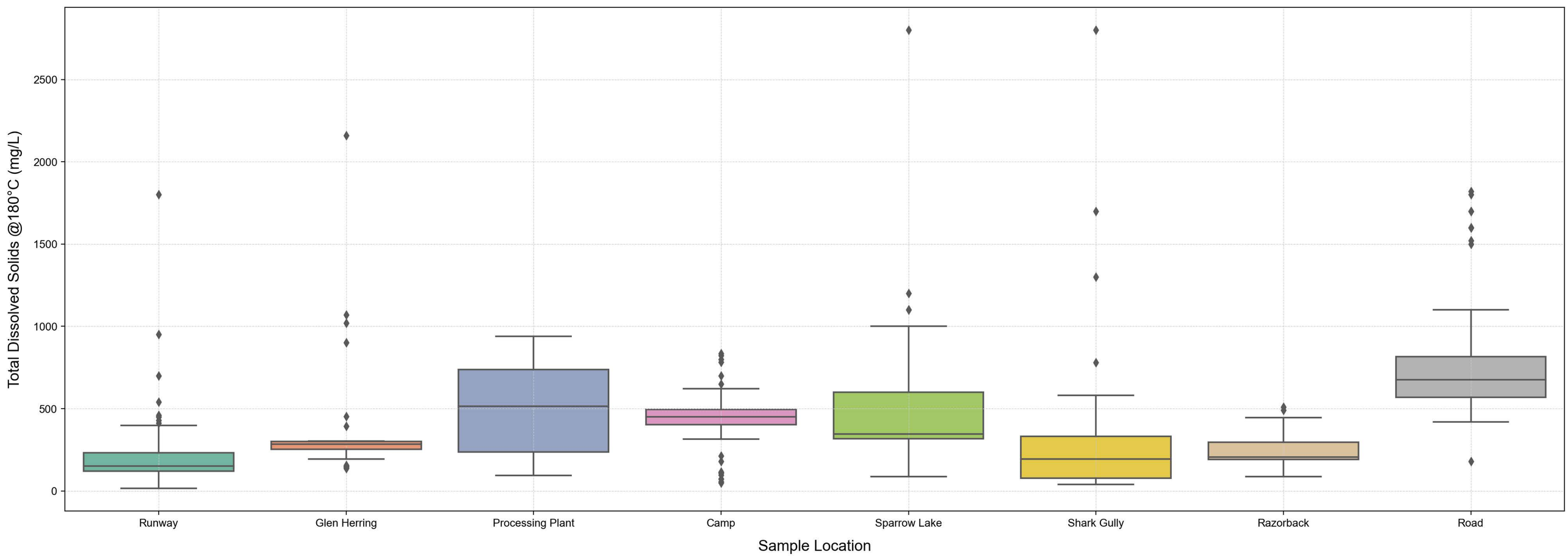

Boxplot: Total Hardness as CaCO3

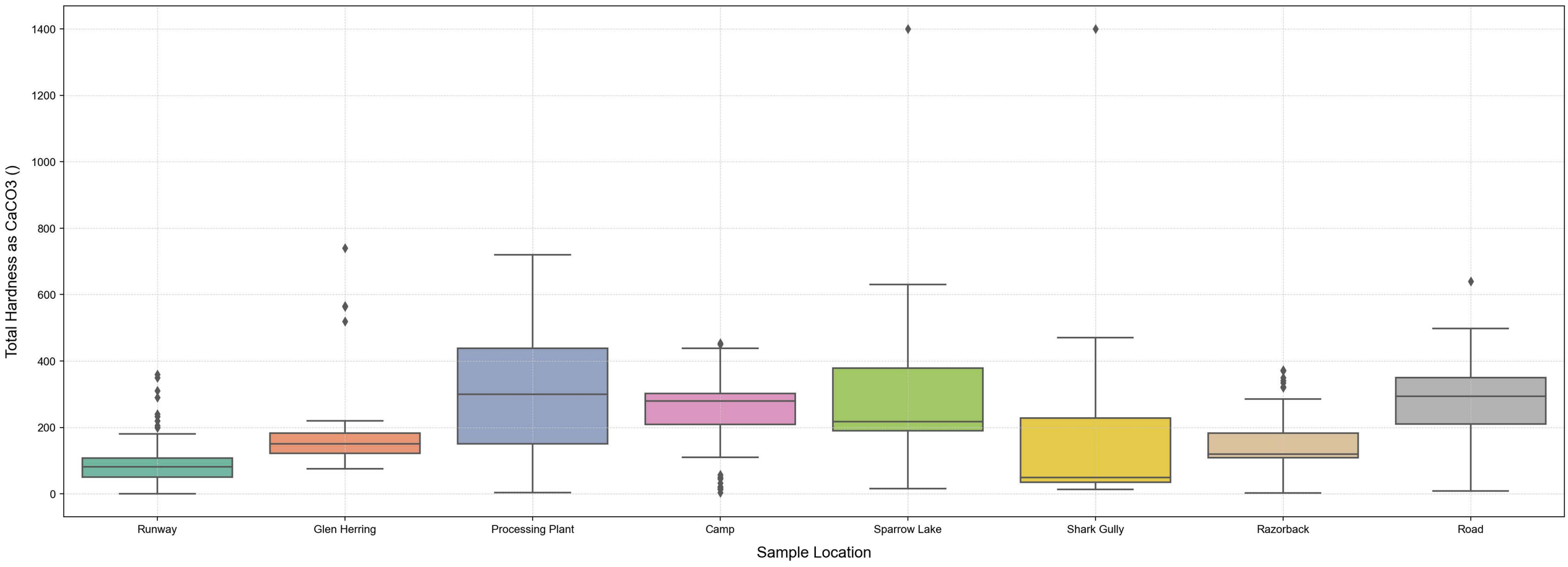

Boxplot: Total Xylenes

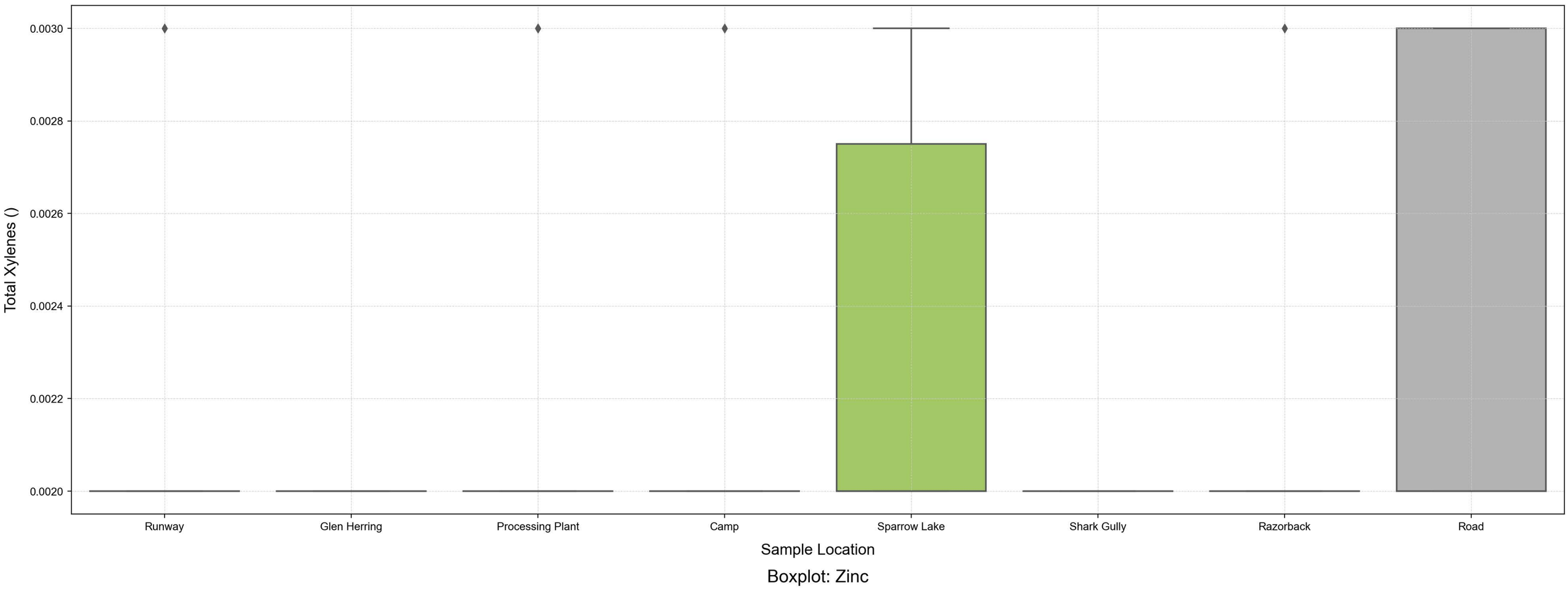

Boxplot: Zinc

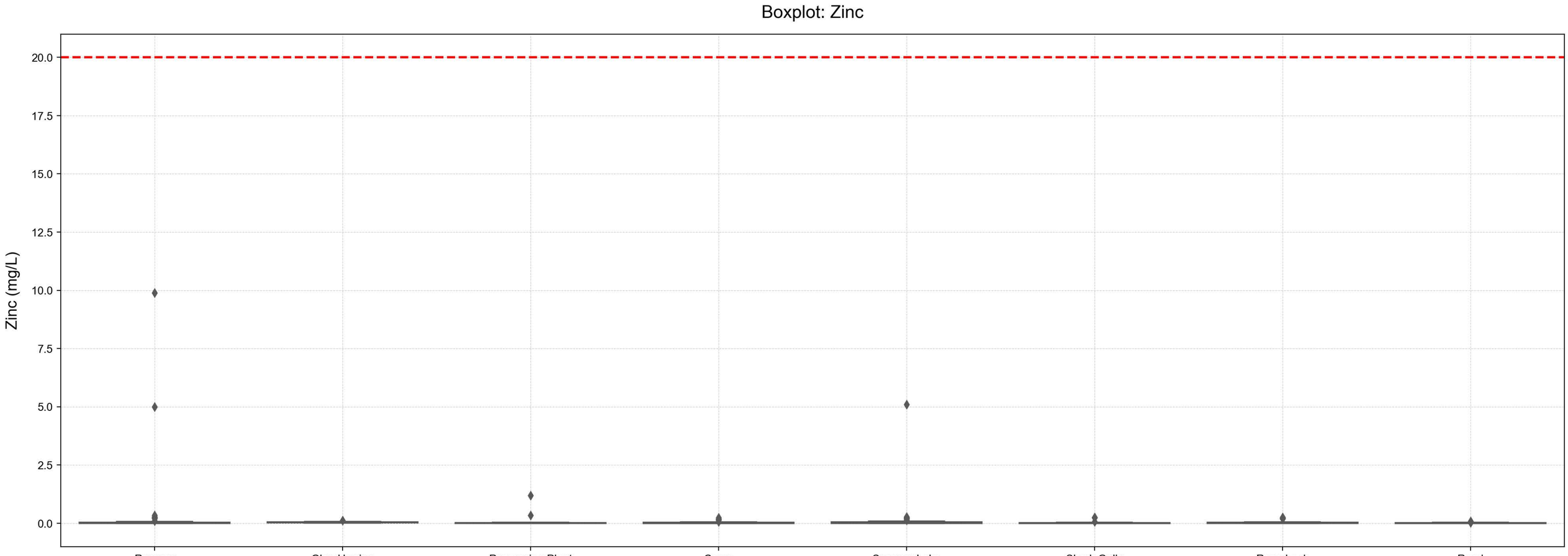

Boxplot: meta- & para-Xylene

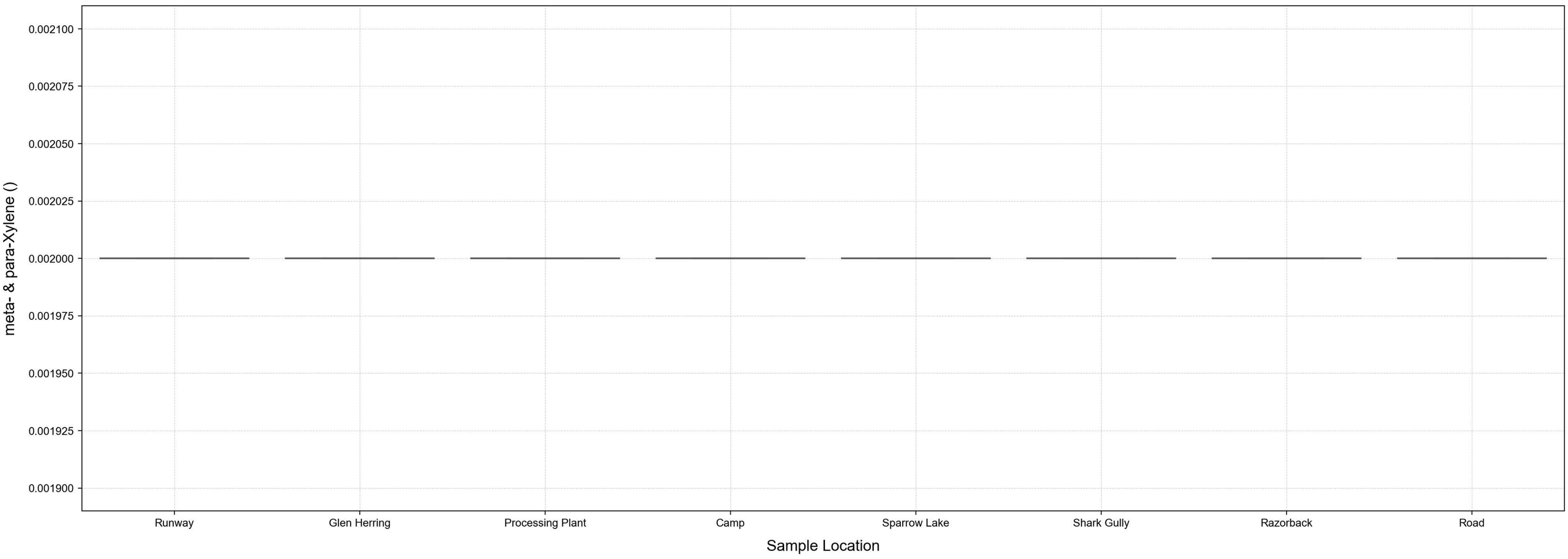

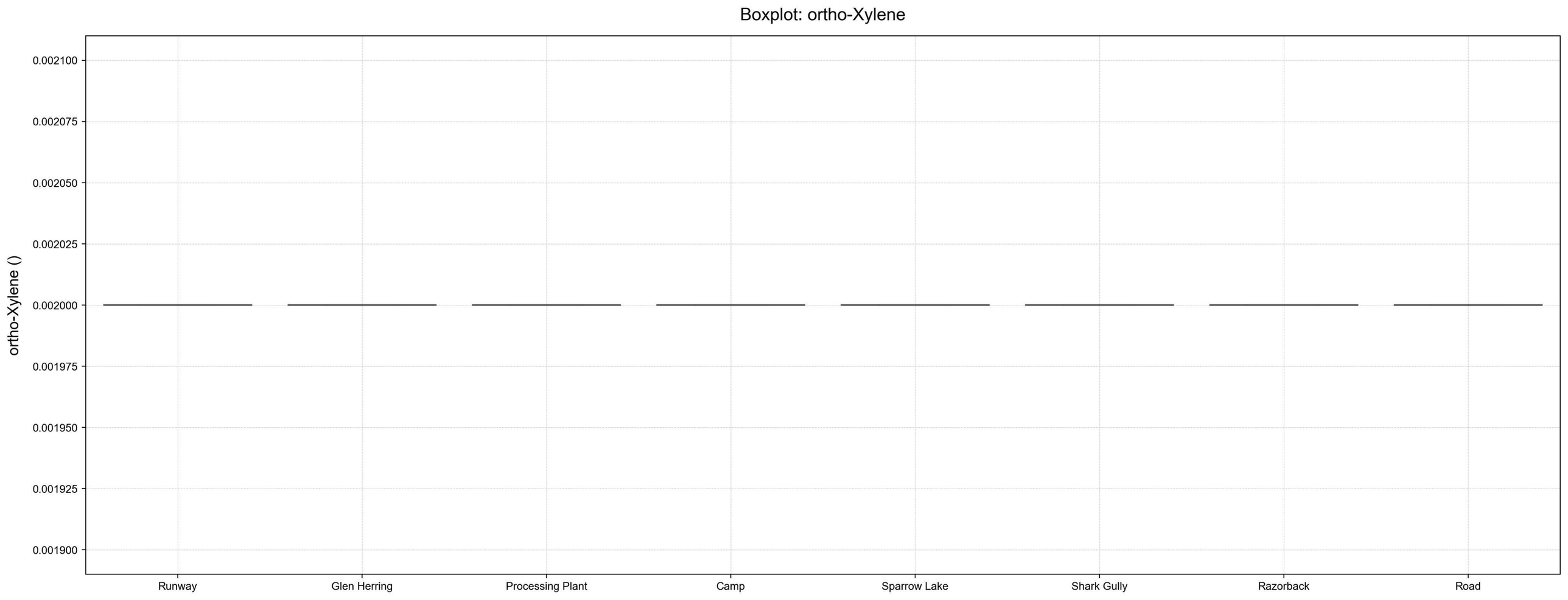
Boxplot: ortho-Xylene
ortho-Xylene ()
0.002100
0.002075
0.002050
0.002025
0.002000
0.001975
0.001950
0.001925
0.001900
Runway
Glen Herring
Processing Plant
Camp
Sparrow Lake
Shark Gully
Razorback
Road
Sample Location

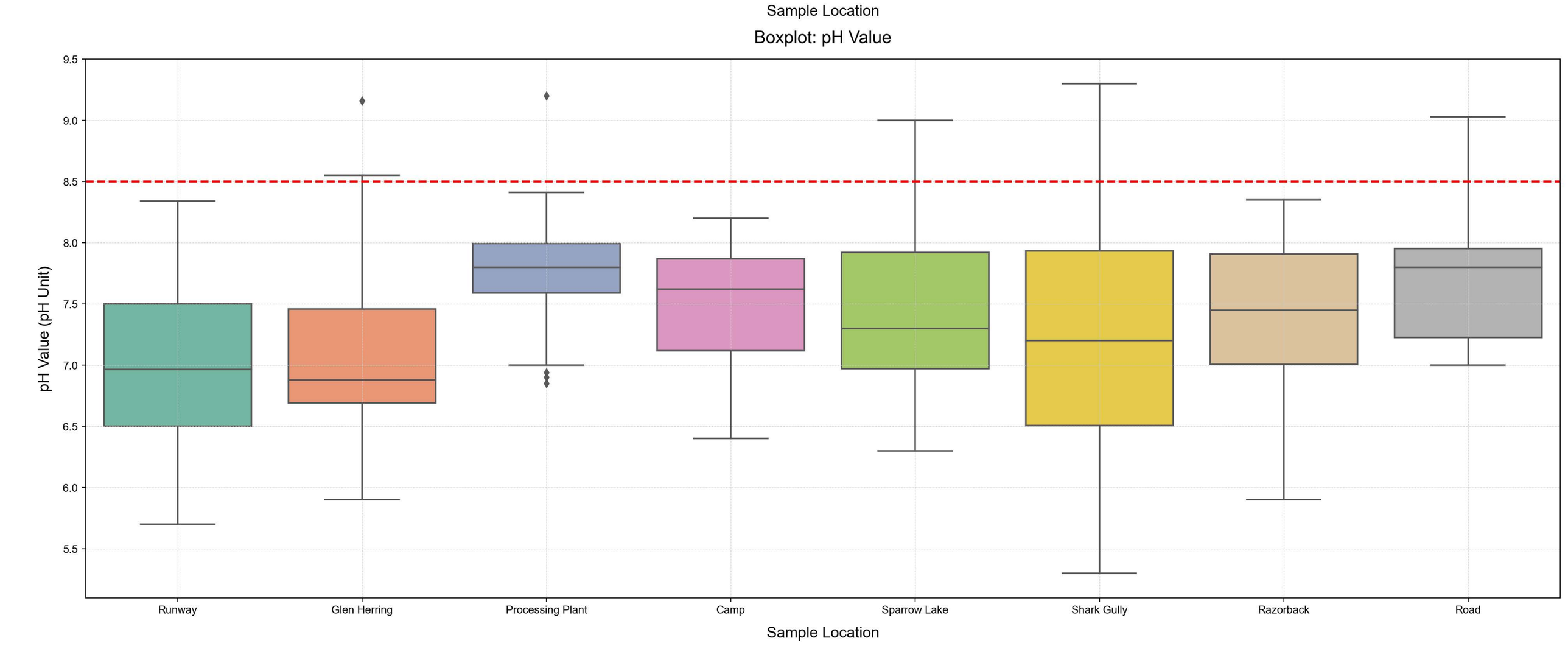
Boxplot: pH Value
pH Value (pH Unit)
9.5
9.0
8.5
8.0
7.5
7.0
6.5
6.0
5.5
Runway
Glen Herring
Processing Plant
Camp
Sparrow Lake
Shark Gully
Razorback
Road
Sample Location

ANZECC Limit

Appendix D Hydrographs

Area: Sparrow Lake

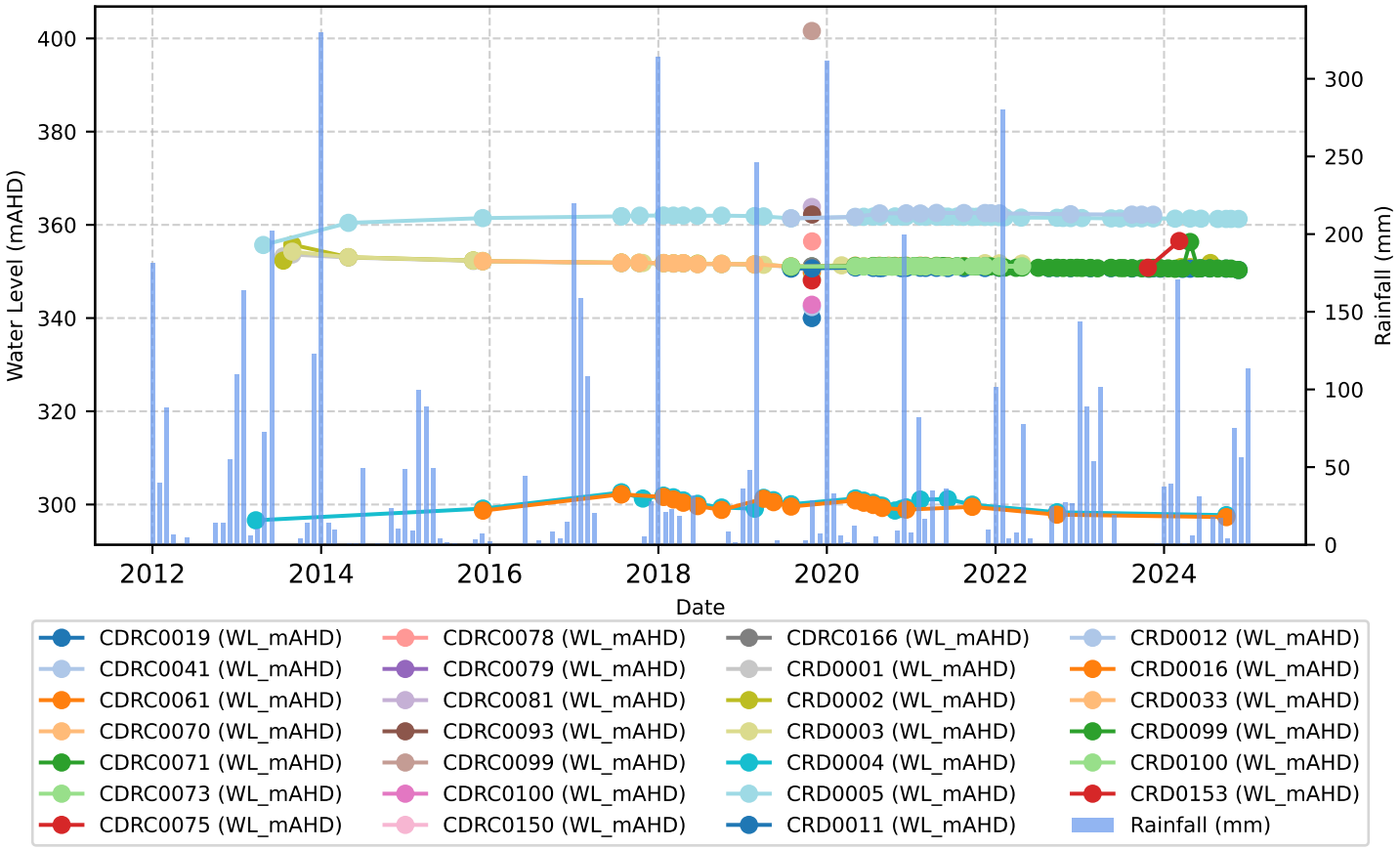

Area: Runway

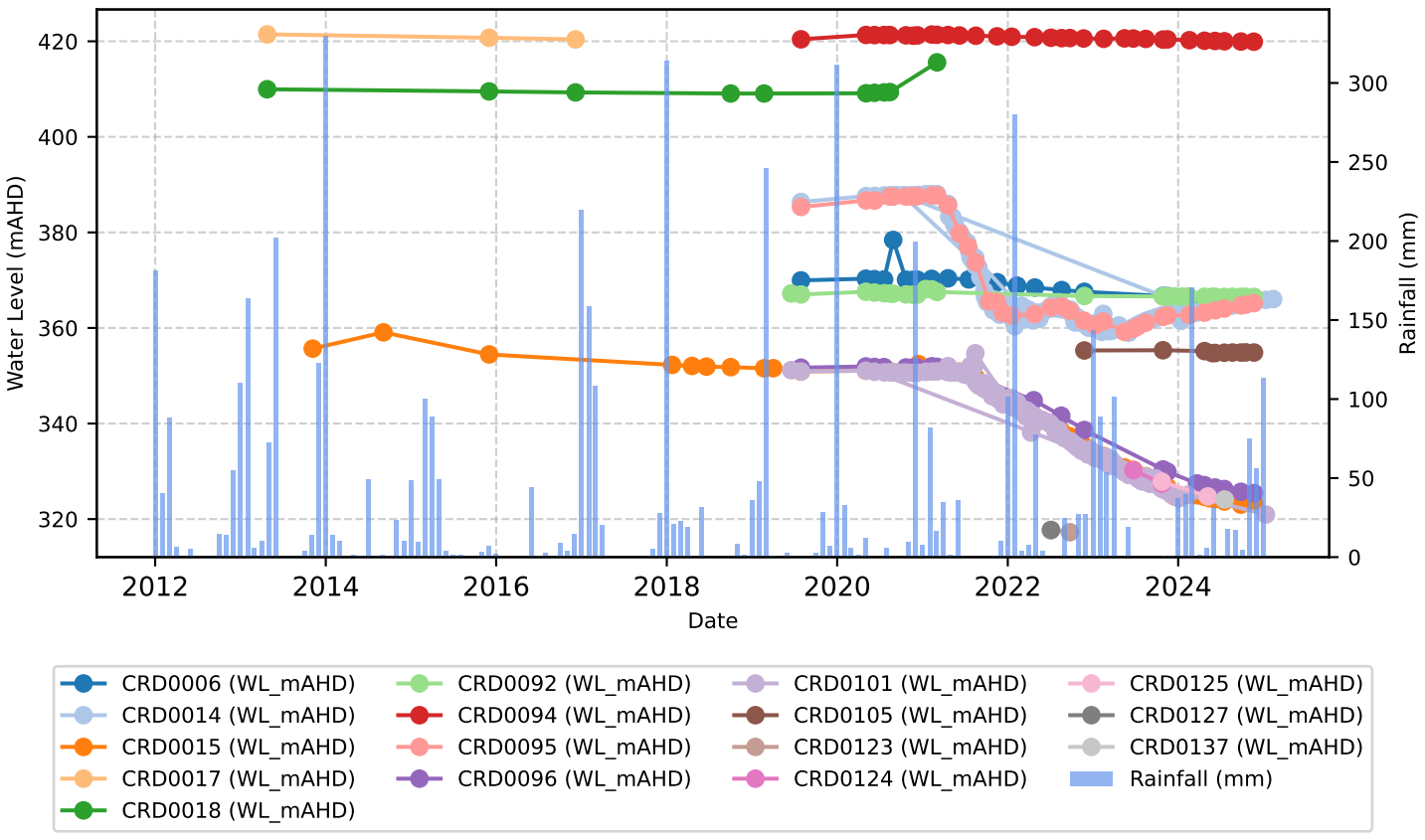

Area: Shark Gully

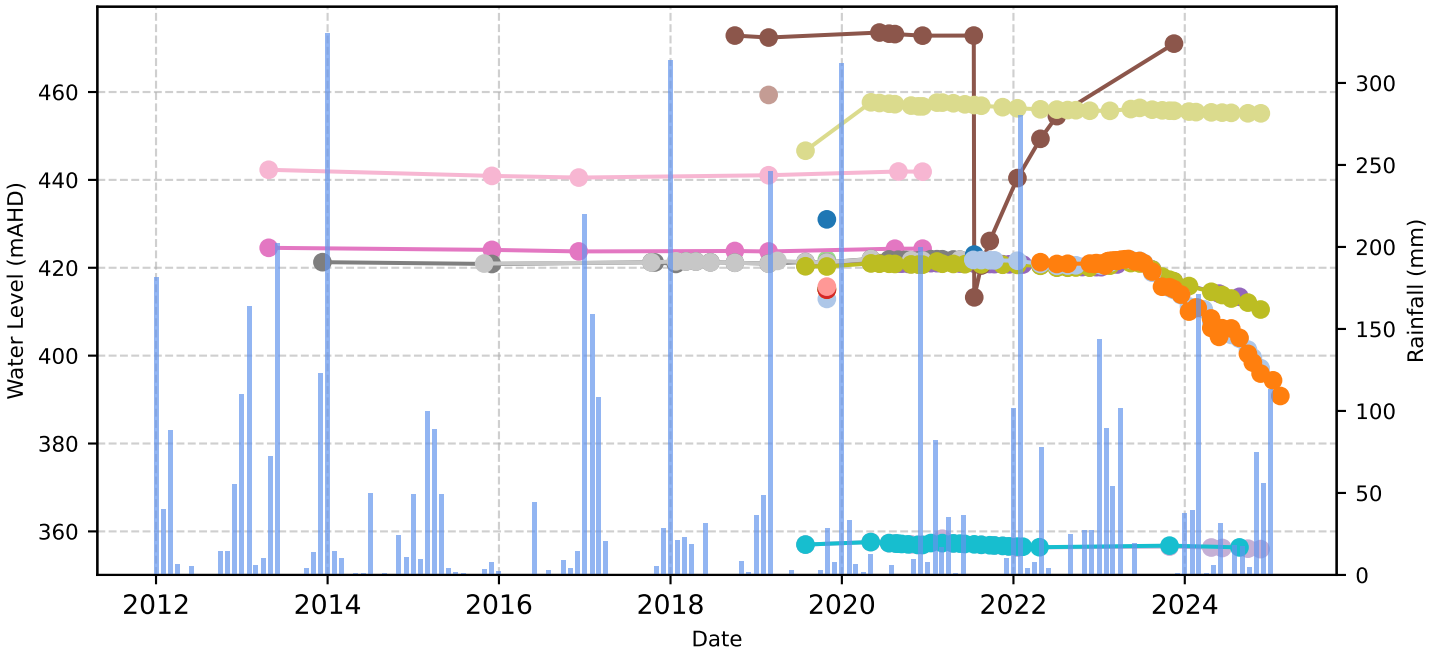

CDRC0204 (WL_mAHD)
CDRC0205 (WL_mAHD)
CDRC0207 (WL_mAHD)
CDRC0208 (WL_mAHD)
CDRC0209 (WL_mAHD)
CDRC0212 (WL_mAHD)
CDRC0213 (WL_mAHD)
CDRC0215 (WL_mAHD)
CRD0007 (WL_mAHD)
CRD0013 (WL_mAHD)
CRD0020 (WL_mAHD)
CRD0021 (WL_mAHD)
CRD0022 (WL_mAHD)
CRD0023 (WL_mAHD)
CRD0024 (WL_mAHD)
CRD0031 (WL_mAHD)
CRD0090 (WL_mAHD)
CRD0093 (WL_mAHD)
CRD0102 (WL_mAHD)
CRD0116 (WL_mAHD)
CRD0117 (WL_mAHD)
CRD0120 (WL_mAHD)
CRD0122 (WL_mAHD)
Rainfall (mm)

Area: Razorback

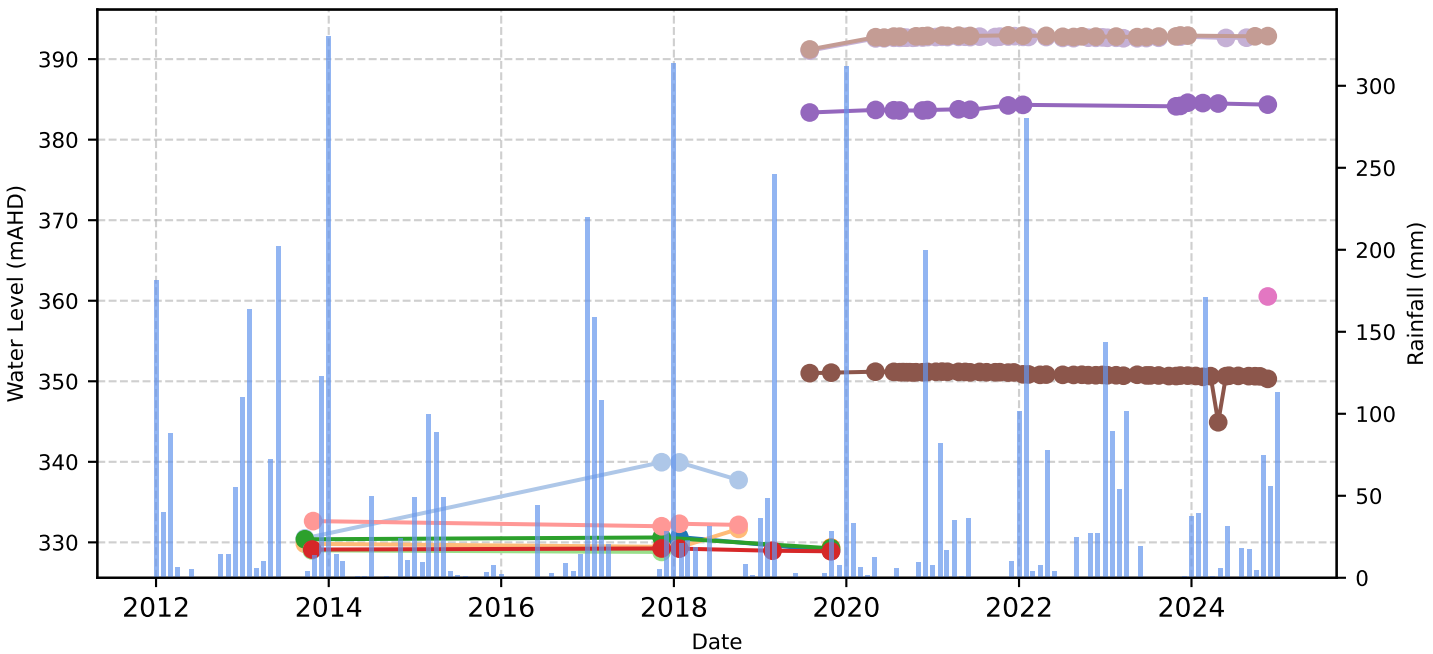

CDRC0122 (WL_mAHD)
CDRC0123 (WL_mAHD)
CDRC0124 (WL_mAHD)
CDRC0125 (WL_mAHD)
CDRC0127 (WL_mAHD)
CDRC0171 (WL_mAHD)
CDRC0173 (WL_mAHD)
CDRC0178 (WL_mAHD)
CRD0010 (WL_mAHD)
CRD0074 (WL_mAHD)
CRD0091 (WL_mAHD)
CRD0098 (WL_mAHD)
CRD0139 (WL_mAHD)
Rainfall (mm)

Area: Camp

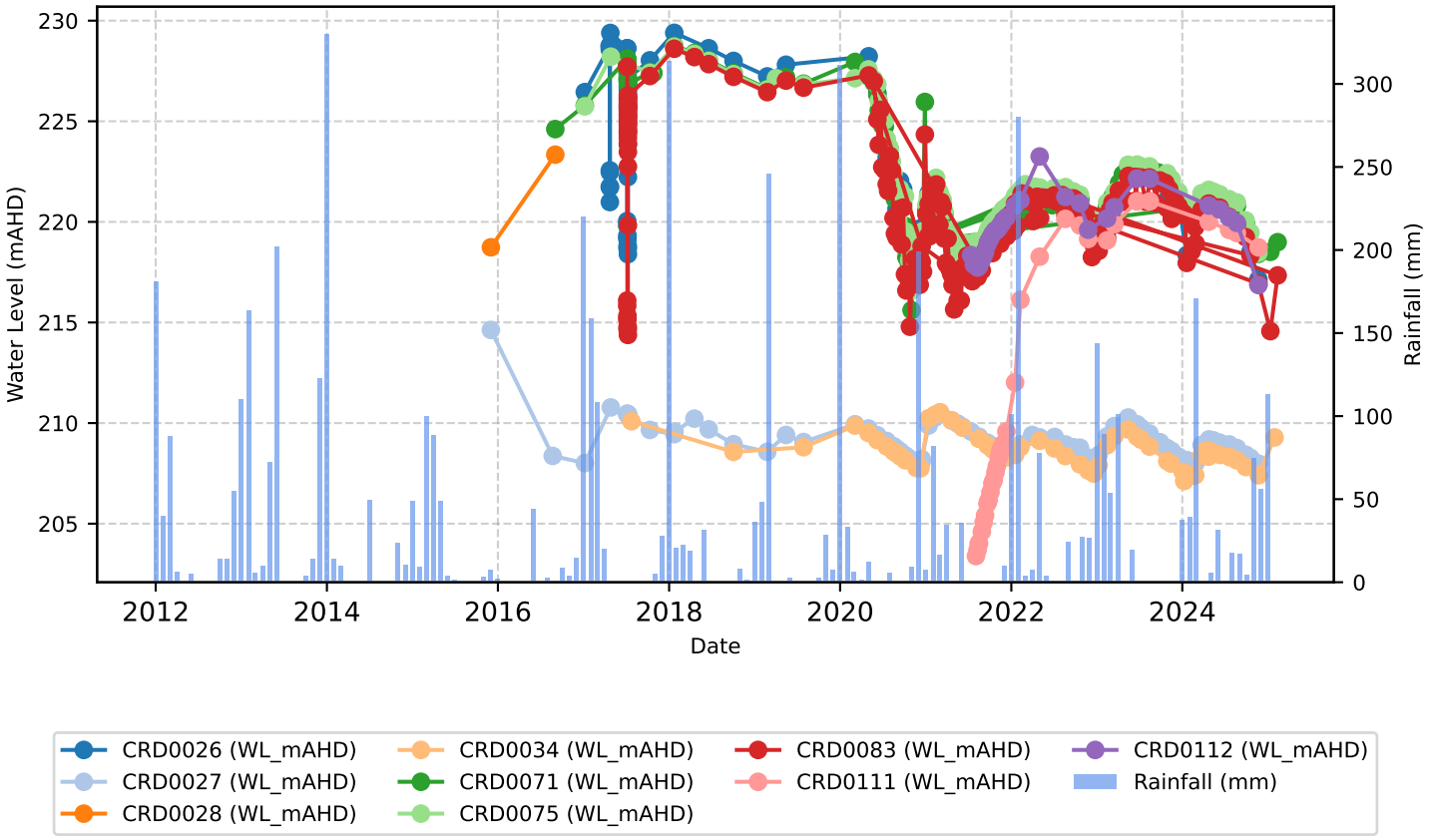

CRD0026 (WL_mAHD)
CRD0027 (WL_mAHD)
CRD0028 (WL_mAHD)
CRD0034 (WL_mAHD)
CRD0071 (WL_mAHD)
CRD0075 (WL_mAHD)
CRD0083 (WL_mAHD)
CRD0111 (WL_mAHD)
CRD0112 (WL_mAHD)
Rainfall (mm)

Area: Road

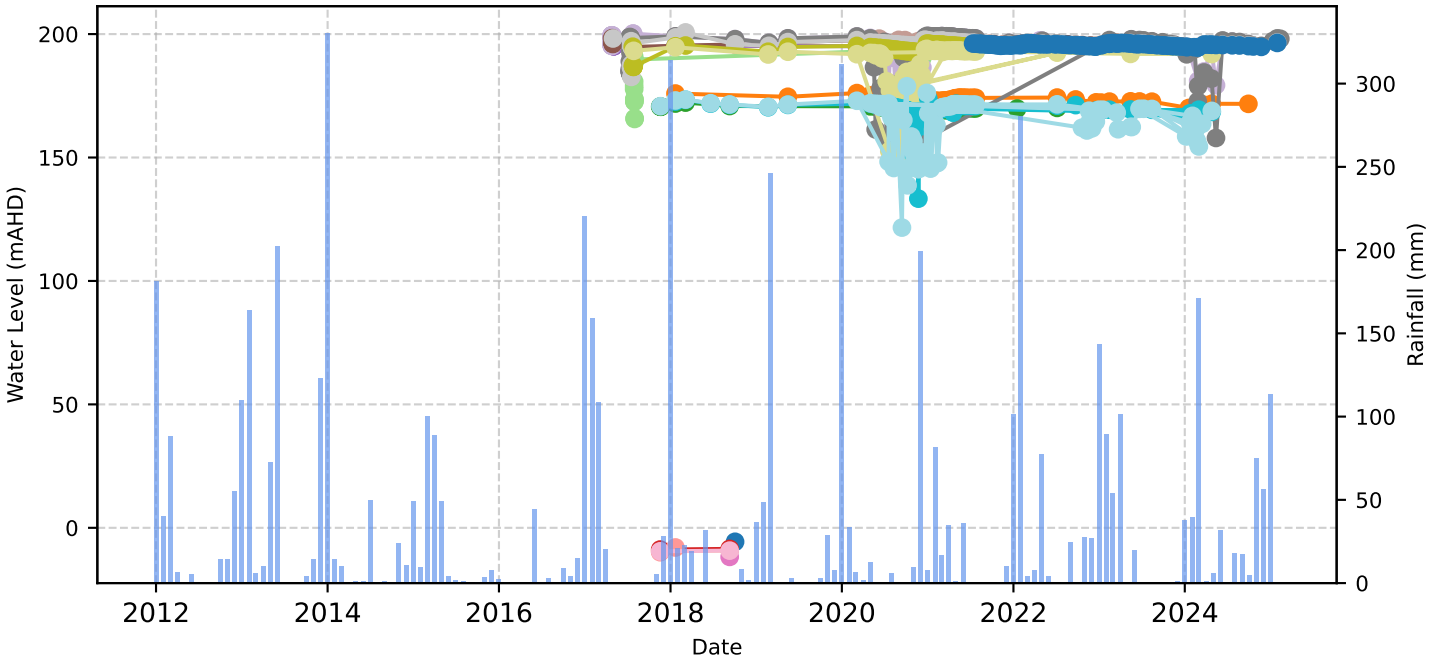

CRD0035 (WL_mAHD)
CRD0038 (WL_mAHD)
CRD0039 (WL_mAHD)
CRD0040 (WL_mAHD)
CRD0043 (WL_mAHD)
CRD0044 (WL_mAHD)
CRD0051 (WL_mAHD)
CRD0056 (WL_mAHD)
CRD0058 (WL_mAHD)
CRD0062 (WL_mAHD)
CRD0064 (WL_mAHD)
CRD0072 (WL_mAHD)
CRD0078 (WL_mAHD)
CRD0081 (WL_mAHD)
CRD0084 (WL_mAHD)
CRD0085 (WL_mAHD)
CRD0086 (WL_mAHD)
CRD0087 (WL_mAHD)
CRD0088 (WL_mAHD)
CRD0089 (WL_mAHD)
CRD0108 (WL_mAHD)
Rainfall (mm)

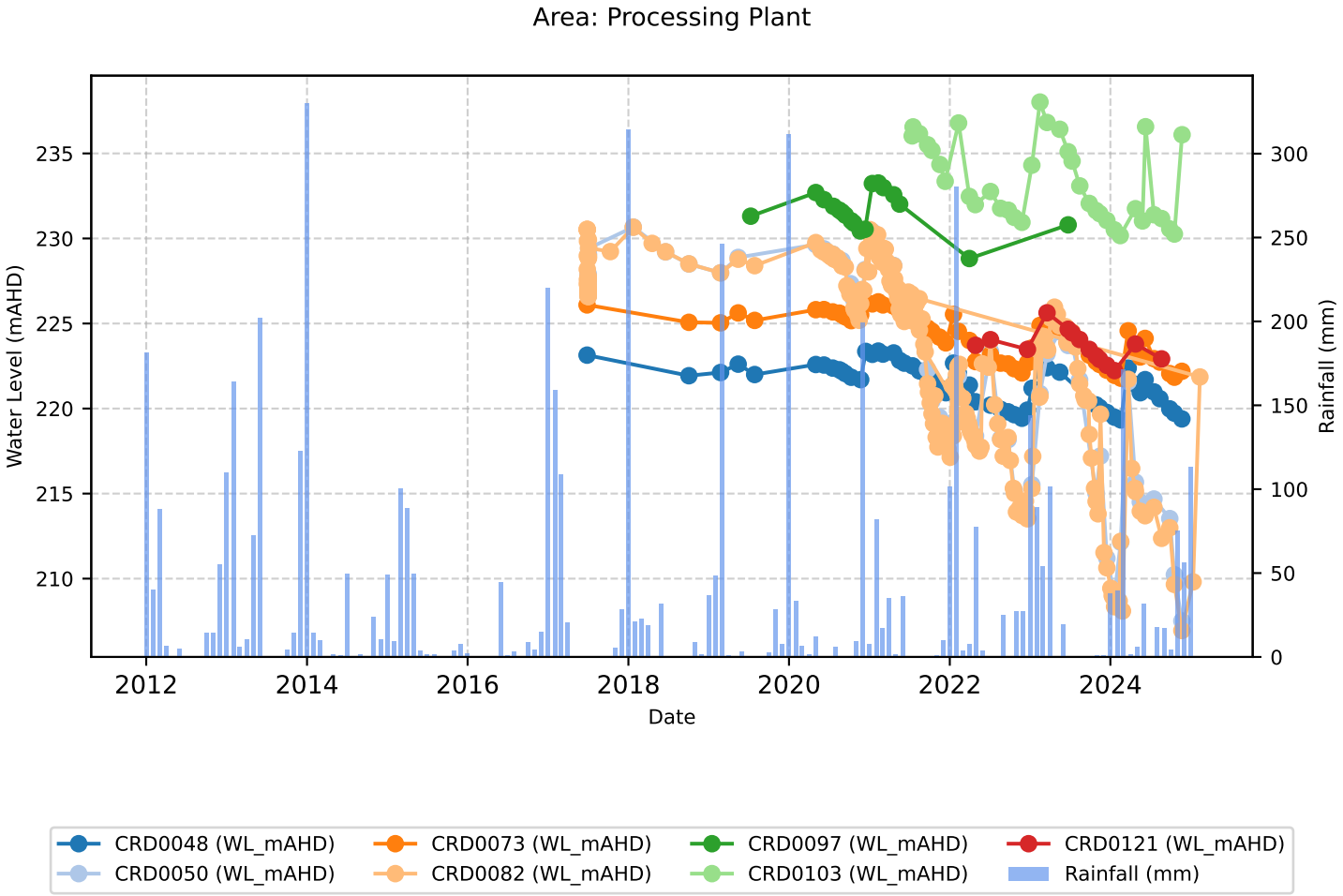
Area: Processing Plant
Water Level (mAHD)
Rainfall (mm)
Date
235
230
225
220
215
210
300
250
200
150
100
50
0
2012
2014
2016
2018
2020
2022
2024
CRD0048 (WL_mAHD)
CRD0050 (WL_mAHD)
CRD0073 (WL_mAHD)
CRD0082 (WL_mAHD)
CRD0097 (WL_mAHD)
CRD0103 (WL_mAHD)
CRD0121 (WL_mAHD)
Rainfall (mm)

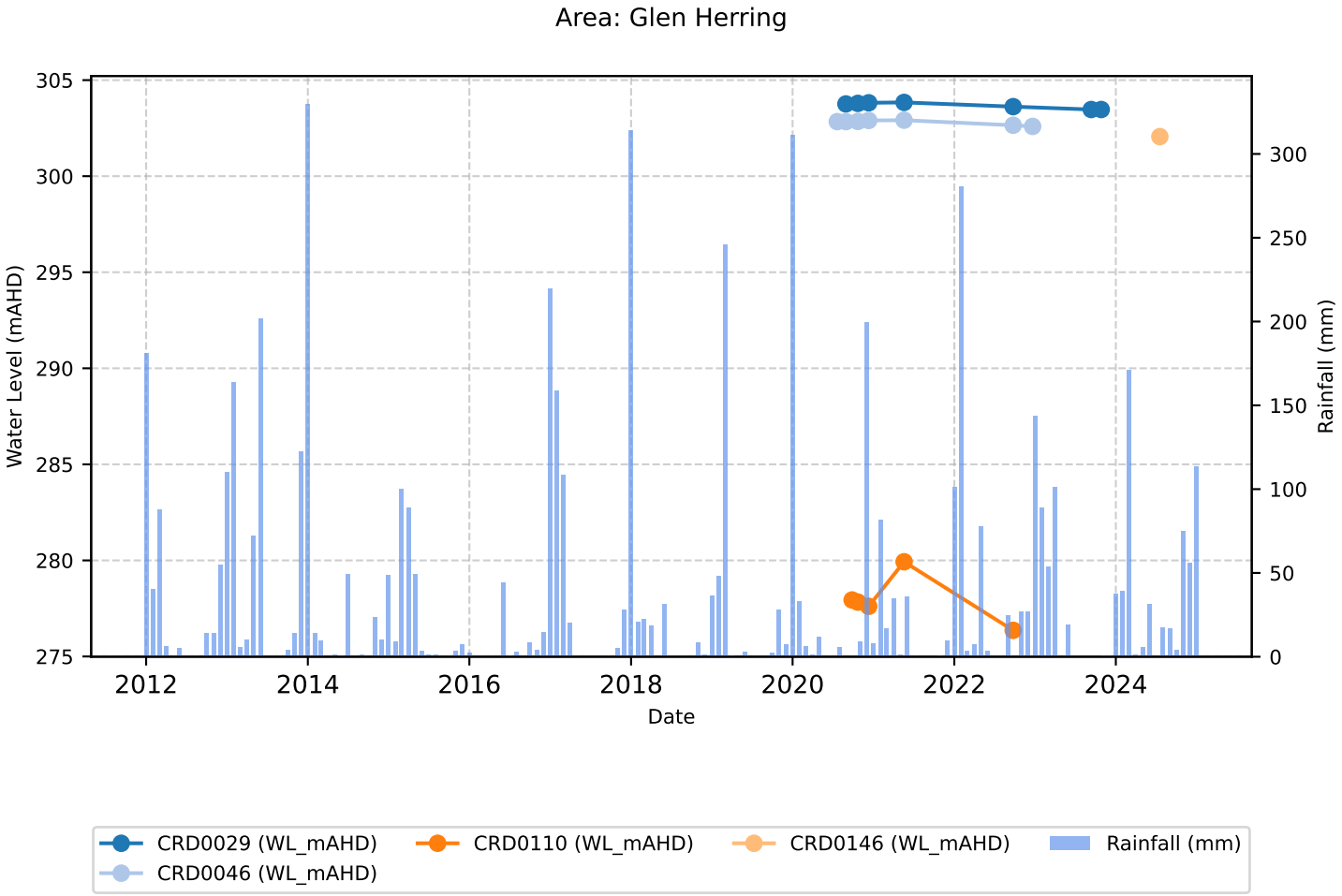
Area: Glen Herring
Water Level (mAHD)
Rainfall (mm)
Date
305
300
295
290
285
280
275
300
250
200
150
100
50
0
2012
2014
2016
2018
2020
2022
2024
CRD0029 (WL_mAHD)
CRD0046 (WL_mAHD)
CRD0110 (WL_mAHD)
CRD0146 (WL_mAHD)
Rainfall (mm)

Appendix E Surface Water Report

Sanjiv Ridge:

Hydrology Baseline and Impact Assessment 2025

Prepared For

Atlas Iron Pty Ltd

Report Prepared by

SMITH HYDRO

Smith Hydro Legal Entity:	Smith Hydro Limited
NZBN:	9429049427387
Smith Hydro Address:	41 Pandora Lane, Lincoln, Christchurch, 7672 New Zealand
Date:	16/05/2025
Project Number:	
Smith Hydro Project Director:	Francis Smith
Client Legal Entity:	Atlas Iron Pty Ltd
Client Address:	PO Box 7071, Cloisters Square WA 6850

Rev	Date	Issue	Author
1	16/05/2025	Atlas Iron via SRK Consulting (AU)	F. Smith
2	11/07/2025	Atlas Iron via SRK Consulting (AU)	F. Smith

Contents

1 EXECUTIVE SUMMARY

Atlas Iron Pty Ltd (Atlas) commissioned Smith Hydro (via SRK Consulting) to undertake a hydrological baseline study and surface water impact assessment for the Sanjiv Ridge Stage 5 Project.The Project area is located in the Pilbara region of Western Australia, approximately 33 km southwest of Marble Bar, and is situated on the escarpment encompassing the headwaters of regional catchments that contribute to the Coongan River and De Grey Rivers.

This hydrological baseline and impact assessment report assesses the impact of pit development as part of Stage 5 on the natural drainage network. This report provides a comprehensive baseline hydrological characterisation and impact assessment, incorporating both local site data and regional data analysis.

Topography

The Sanjiv Ridge mine site is situated within the middle reaches of the Coongan River catchment, which spans approximately 7000 km² in the Pilbara region of Western Australia. The region is characterised by rugged topography with steep gradients transitioning to flatter valley floors. The soils in the region are generally shallow, with a mix of rocky outcrops and sandy loams, which affect infiltration rates and runoff characteristics.

Climate

The climate of the Pilbara region can be classified as arid, with high temperatures and low, unpredictable rainfall, generally associated with tropical cyclones. The closest regional rainfall station is located at Marble Bar, which records an average annual rainfall of 390 mm. Rainfall is highly variable, with the highest amounts typically occurring in February and the lowest in September, with 80% of rainfall falling between December and March, often in short-duration, high intensity events resulting in significant ephemeral flood responses within the Project area. Temperature ranges are extreme, with average temperatures around 35°C in the summer months (December to February) and averaging around 20°C in the winter months (June to August). The region records high rates of evapotranspiration, averaging around 2500 mm annually. Climate change projections modelled using the Climate Futures Tool from the Bureau of Meteorology (BOM) indicate a significant future reduction in monthly rainfall and an increase in average monthly evapotranspiration, which could result in a 20-31% reduction in average peak flows and a total runoff volumetric reduction of between 26-28%. The frequency and intensity of large storm events however is projected to increase significantly, leading to a projected increase of up to 77% of the <1 hour design rainfall intensity, and 37% of the >24 hour intensity.

Hydrology

Streamflow monitoring was established by Atlas in 2024 at nine (9) locations within the project area, with long-term regional monitoring data of the Coongan River at Marble Bar also available. Rating curves have been defined using the conveyance estimation procedure based on topographic surveys of the channel and floodplains at each monitoring location. While the Coongan River itself is perennial, runoff within the Project area is driven by the steep gradients and shallow soils and is ephemeral in nature. High intensity rainfall events lead to rapid overland flow response, with only minor sustained flow within shallow alluvial deposits daylighting within depressions and small pools between rainfall events during the wet season. Pools play a crucial role in the region from both a cultural heritage perspective and an ecological standpoint, with several perennial pools identified within the Project area, as well as a number of ephemeral pools that are sustained through the wet season but dry out slowly throughout the dry season.

Hydrological Modelling

A physically based lumped hydrological model has been developed and calibrated to a limited number of recorded runoff events within the Project area. This model has utilised long-term Global Precipitation Measurement (GPM) rainfall records (Huffman et al, 2023) from 1998 to 2024 to generate a 26-year flow time series for the ephemeral stream network within the Project area. Baseline modelling indicates significant inter-annual variability, with notable sensitivity to dry and wet years, with limited runoff responses recorded during years of notable low rainfall (2016 and 2019). Average runoff coefficients are highly variable and subject to the intensity of rainfall events, with a range from 77% runoff in December 1999 which experienced several large, high-intensity rainfall events, to 10% in December 2000 which experienced lower-intensity and lower magnitude rainfall resulting in greater interception, infiltration and evapotranspiration losses.

Surface Water Impacts

An impact assessment model was built by modifying the calibrated baseline model to reflect the projected changes in catchment areas from the development of open pit areas, assessing the difference from a "natural pre-mine baseline" to the current state. This allows for a comparison of the impact from baseline through to the current state and how much more effect Stage 5 will have on surface runoff processes within the Project area, measured both against a pre-mine "baseline", and a current state (2025 operations) "baseline". Potential impacts arise mainly from catchment reduction due to open pit expansion and intercepted catchment areas. Detailed flood inundation mapping and runoff mapping will be completed as part of the wider water management scope of work.

Of all the surface water monitoring locations, SW009, SW007, and SW006 see the greatest change in catchment area due to pit expansion, ranging from a 19-67% reduction in catchment size relative to baseline conditions. Only four identified surface pools observe a reduction in catchment size, C0-WS-05, C0-WS-08, C0-WS-13 and C0-WS-14 ranging from 2-7%, with C0-WS-08experiencing the greatest reduction at 7%.

Impact modelling results suggest the greatest localised effect on streamflow occurs in the catchment with the greatest area reduction, SW009, with a 68% reduction in average peak runoff and a 75% reduction in runoff volume. This catchment hosts the largest pit in the Project (Sparrow Lake pit). SW009 is located downstream of Sparrow Lake pit; however, other monitoring locations highlight the decreasing effects with increasing distance downstream of the disturbance. SW001, for example, located downstream of SW002 and SW003, which observe up to a 14.4% reduction in peak runoff and 16% reduction in runoff volume, sees a reduced effect with increased non-disturbed catchment area contributing to runoff, with a 7.3% reduction in average peak runoff and 6% reduction in average volume.

Modelling impacts on the pools suggest a reduction in peak flow flushing between 2% and 7%, with a similar reduction in overall surface water volume recharge. It is not anticipated that this would have a significant effect on total storage due to the limited storage capacity of each pool versus the small reduction. The limiting factor remains the storage potential and evaporative losses during dry periods, rather than the overall total discharge volume and peak flow rates.

Climate Change

The combined impact of mining and climate change projections reveals that while mining operations have a localised effect on streamflow reduction, it is the climate change projections that present a far more significant impact to the hydrological flow regime of the area. Modelled projections for the Representative Concentration Pathway (RCP) 8.5 2090 baseline scenario (without mining operations) suggest an average decrease in average peak flow response of between 21-31%, with a 36-38% reduction of average annual runoff volume. Current state mining operations are likely to see this increase to between a 25-40% reduction in average peak flows, and between 37-47% reduction in average annual runoff volume. Stage 5 is likely to see this increase slightly more in affected catchments, with between a total of 25-77% decrease in average peak flow, and between 37-84% reduction in average annual runoff volume (noting SW009 is the most affected catchment). All percentage changes presented are relative to the baseline pre-mine scenario.

Conclusion

In conclusion, the impacts of Stage 5at Sanjiv Ridge are unlikely to have more than a minor effect on streamflow within the local area, with the exception of localised effects such as immediately downstream of locations such as SW009. The localised effects decrease rapidly with increasing distance from the mine, suggesting minimal long-term impact on the broader hydrological system, and no significant effects on identified Pools within the Project area.

Overall, the total catchment reduction due to Stage 5 represents less than 0.02% of the total Coongan River catchment, as measured from the Marble Bar gauge. This is a very small percentage of the regional catchment, suggesting that although alterations to the surface water flow regime may have a localised effect, small catchment reductions in streamflow response will be insignificant within the regional catchment, and dissipate rapidly with distance downstream from the mine as increasing areas of undisturbed catchment contribute to the stream flow response.

2 Introduction

Atlas Iron Pty Ltd (Atlas) propose to progress their Iron Ore Project at Sanjiv Ridge (the Project) in the Pilbara Region of Western Australia, to Stage 5, which will see pit development extend below the groundwater table and expansion of pit surface footprints in some areas. Sanjiv Ridge, herein referred to as the Project area, is approximately 33 km southwest of Marble Bar, and is situated within the middle reaches of the Coongan River catchment, on the escarpment encompassing the headwaters of regional catchments that contribute to the Coongan River and De Grey Rivers.

Smith Hydro Ltd (Smith Hydro) has been engaged by SRK Consulting (Australia) on behalf of Atlas to undertake a hydrological baseline study and hydrological impact assessment for Stage 5 of the Project.

This hydrological impact assessment report assesses the impact of pit development as part of Stage 5 on the natural surface drainage system. This report provides a comprehensive baseline hydrological characterisation and impact assessment, incorporating both local site data and regional data analysis.

This report presents a summary of the completed scope of works, and is structured as follows:

- Characterisation of the local topography and drainage system
- Characterisation of rainfall, using local and regional gauges in addition to satellite data to derive a suitable long-term rainfall time series for the Project area.
- Characterisation of temperature and evapotranspiration, using regional data to define a long-term dataset for the Project area
- Characterisation of potential climate change on rainfall and evapotranspiration in the Project area
- Long-term physically based hydrological model build and calibration using surface water monitoring data collected by Atlas within the Project area.
- Design rainfall/runoff modelling to determine Project area catchment response to extreme rainfall.
- Impact assessment: to determine the impact of Stage 5 on the surface water flow regime within the Project area, both compared to the current status quo, and a baseline (pre-mining operations) scenario. Impacts incorporating potential climate change are also included through to 2090.

3 Characterisation

3.1 Topography and Drainage

The terrain of the Project area is characterised by rugged topography featuring steep-sided, rocky ridges and hills. These landforms are predominantly composed of various hard rock outcrops such as greenstone, chert, sandstone, and dolomite. A significant geological characteristic of the area is the Banded Iron Formation (BIF). Well-developed drainage lines have deeply carved into the ridge areas, forming gorges and gullies made of ironstone and sandstone. Soils have been characterised previously (MWH, 2016a) as being generally shallow, classed as sandy loams prone to hard setting, and of moderately rapid drainage class with low water holding capacity.

The elevation within the Project area varies from around 460 meters above Australian Height Datum (mAHD) at the catchment divide close to the Sparrow Lake pit, to about 190 mAHD at the Marble Bar Flow Gauge location. The landscape transitions from the steep slopes associated with the ridges to more gentle and undulating slopes, valleys, and broad river floodplains at the base of these ridges.

The Project area is located in the mid-sections of the Coongan River catchment, which covers roughly 7,000 square kilometres, see Figure 1. This catchment is situated between the Chichester Ranges to the south and smaller ranges to the west and east. It includes numerous tributaries such as Budjen Creek, Triberlar Creek, Boobina Creek, Emu Creek, and Camel Creek. Additionally, the Coongan Catchment is part of the extensive De Grey River Basin, which spans an area of 57,000 square kilometres and encompasses major tributaries including the Strelley, Shaw, Coongan, Oakover, and Nullagine Rivers. The Coongan River joins the De Grey River at Mulyie Pool, about 41 km upstream of the confluence with the Shaw River, with a total combined catchment area of the De Grey River of approximately 56,890 km^2.

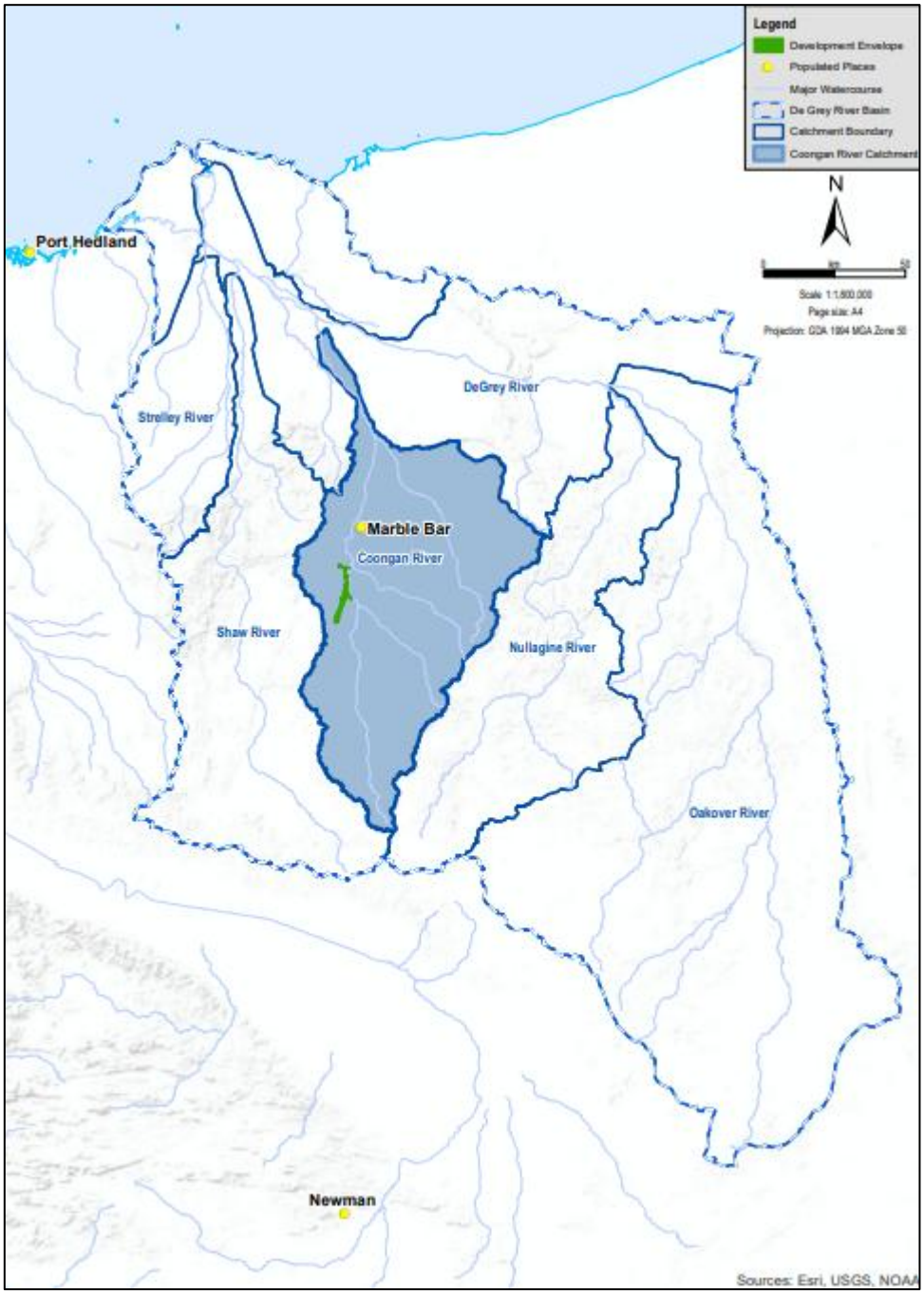

Figure 1 Regional Catchments (source: Atlas Iron Pty Ltd)

Runoff in the Project area sheds both sides of the north-south ridge line, ultimately towards the Coongan River. Steep gradients in the higher areas gradually flatten along the valley floors. The deeply incised drainage paths within the ridges and hill areas indicate high magnitude discharge in well-defined channels. Conversely, the flatter areas extending from the ridges show evidence of wide floodplains, suggesting out-of-bank flooding during high flow events.

The Coongan River is ephemeral, however is sustained by shallow groundwater baseflow contributions for periods following rainfall events. In contrast, the headwater catchments are ephemeral and respond directly to rainfall events only, due to the shallow, free-draining stony soils, steep catchments. While all rivers in the broader headwater region are ephemeral, surface water remains present year-round in pools along the main rivers and creeks, as well as within protected gullies and gorges. Major pools on the main branch of the Coongan River, such as the Nandingarra, Bookargemoona, and Doolena pools (Ruprecht & Ivanescu, 2000), are examples. These pools often reflect groundwater expressions within drainage alluvium or persist following surface runoff events for longer periods when shielded from direct sunlight and evaporative losses. A number of pools have been identified within the Project area; these are discussed in more detail within Section 4.1.2 24 of this report.

3.2 Rainfall

3.2.1 Available Data

Rainfall data for the Project area has been collected from several sources, providing valuable insights into the spatial and temporal variability of precipitation, as well as the overall magnitude. The sources include Mt Webber (MTW), Sanjiv Ridge Mine (SMR), McPhee Creek (MCP), Miralga (MIR), Marble Bar Combined, and satellite Global Precipitation Measurement (GPM) data. The distance between gauges in the region ranges from 23 to 60 km, as summarised in Figure 2 and Table 1.

Table 1. Rainfall Data Sources

Source	Location	Source
Mt Webber (MTW)	Approximately 53 km SW of Sanjiv Ridge	Atlas
Sanjiv Ridge Mine (SMR)	Located on Sanjiv Ridge, data prior to 21/03/2024 may not be reliable	Atlas
McPhee Creek (MCP)	Approximately 47km SEof Sanjiv Ridge	BOM
Miralga (MIR)	Approximately 63 km NW of Sanjiv Ridge	Atlas
Marble Bar (Combined)	Based on records from Marble Bar Comparison (Sta. No. 04020) and Marble Bar (Sta. No. 04106)	BOM
Satellite GPM Data	Provides rainfall estimation at a 3km resolution	NASA Global Precipitation Measurement Mission (Giovanni)

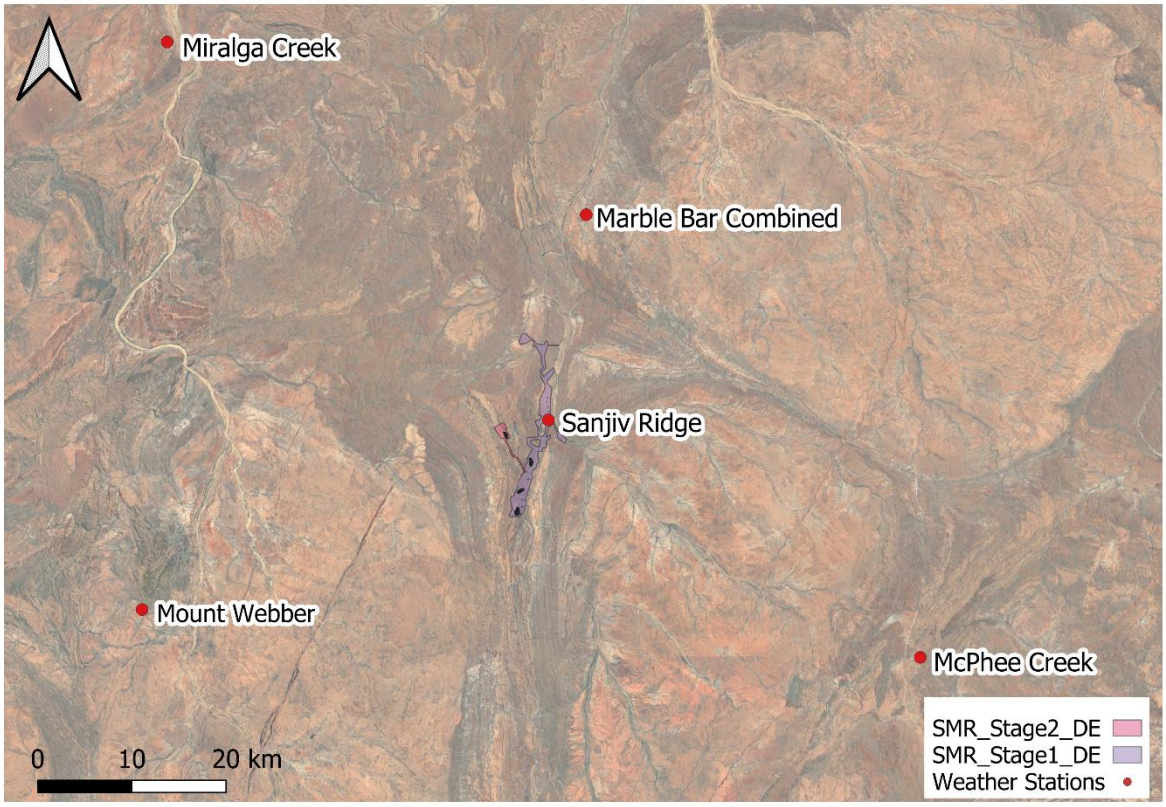

Figure 2. Rainfall Gauge Locations

3.2.2 Annual Rainfall

The Pilbara region's average annual rainfall, as measured by the Marble Bar gauge, is 380.8 mm. The minimum annual rainfall recorded at Marble Bar was 189 mm (2021), with a maximum annual rainfall recorded of 705.4 mm. This inter-annual variability is a notable characteristic of the rainfall patterns in the Pilbara region. The substantial differences in annual rainfall can be attributed to the frequency and intensity of cyclones. The Marble Bar gauge has recorded several significant storm events, where cyclones have significantly altered the annual rainfall. In March 2019 Cyclone Monica caused widespread rainfall with Marble Bar recording over 132 mm in a single day. In January 2020 Cyclone Blake resulted in over 200 mm of rain within a week. More recently Cyclone Zelia February 2025 recorded more than 200 mm across three days. Notable cyclonic events contribute to higher rainfall totals, while other years may see fewer cyclonic activities resulting in reduced annual rainfall.

On average, Marble Bar experiences about 24 days of rain annually. Of these, 23 days typically see rainfall exceeding 25 mm.

3.2.3 Seasonality

The Pilbara region experiences distinct seasonal rainfall patterns. The minimum, average and maximum monthly rainfall recorded at Marble Bar (Figure 3), clearly delineates the wet and dry seasons of the area as well as the significant inter-annual variability.

The wet season in the Pilbara typically spans from December to March. During these months, the region receives the majority of its annual rainfall, largely influenced by tropical cyclones and monsoonal rain. Cyclones bring intense

rainfall and can lead to significant flooding. Conversely, the dry season extends from April to November, characterised by minimal rainfall and arid conditions. During these months, the Pilbara region experiences long stretches of dry weather, with monthly rainfall often measuring less than 10 mm.

There are notable exceptions to these seasonal patterns. For instance, in June 2024, a 21 mm rainfall event was recorded at Sanjiv Ridge mine. Although this event was not associated with a cyclone, it was very intense and resulted in significant rainfall within a short period. Such events are often attributed to convective storms, which can develop rapidly and produce substantial rainfall despite not being part of the typical cyclonic or monsoonal activity.

Convective storms are localised weather systems that can generate intense rainfall over a short duration. These storms can occur due to various atmospheric conditions, including high temperatures and humidity levels, leading to rapid cloud formation and heavy, localised downpours. While cyclones remain a major contributor to rainfall in the region, these convective storms also play a significant role in the overall rainfall patterns, contributing to the observed bi-modal wet season that can occur.

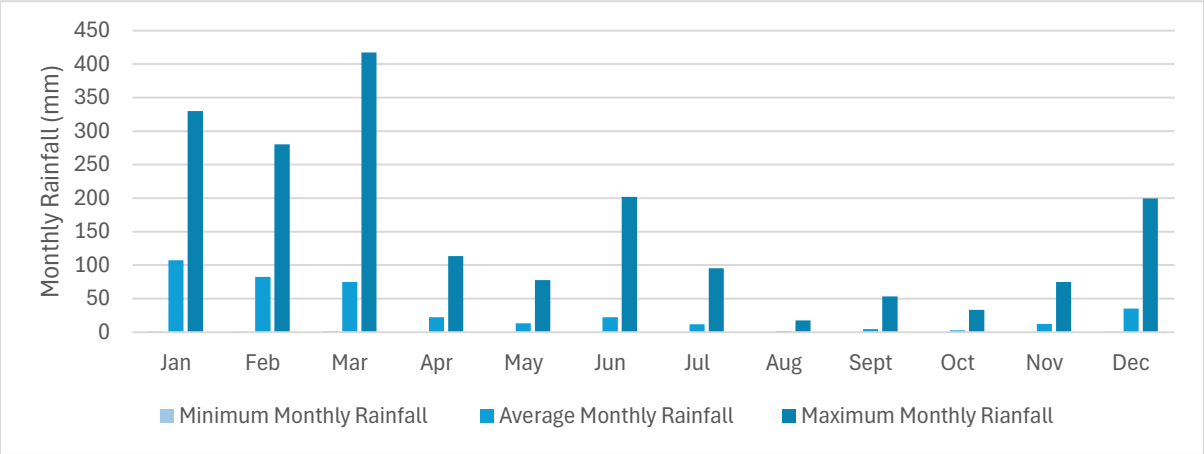

Figure 3. Marble Bar - Long-Term Rainfall

3.2.4 Spatial Variability

A monthly comparison of all overlapping data is presented in Figure 4, demonstrating strong agreement in seasonality between gauges, as expected, but notable differences in totals received per month across the area. For example, in March 2024, Miralga gauge recorded a total of 59.4mm compared to between 134-174mm recorded at the other gauges, suggesting significant spatial variability. This highlights the potential unsuitability of utilising rain gauges not located at Sanjiv Ridge to provide analogue infill data where data is unavailable at Sanjiv Ridge.

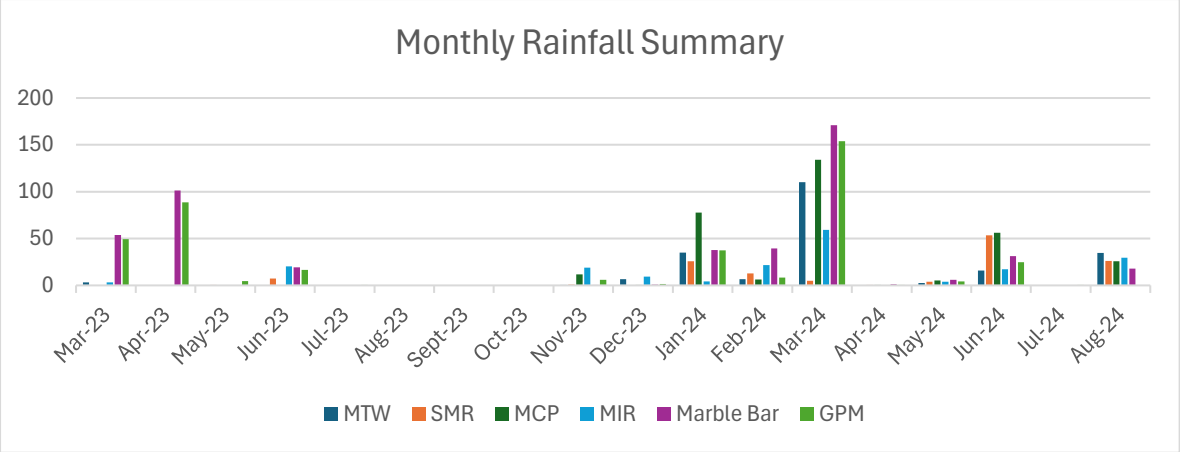

Figure 4. Monthly overlapping rainfall data.

The Sanjiv Ridge Mine (SMR) station, located on Sanjiv Ridge at the operation office location, has been operating since 2023, however an internal blockage in the rain gauge was discovered on 21 March 2024 and rainfall data prior to this may not be reliable. The blockage was subsequently cleared, and a number of rainfall events recorded in 2024. An isolated, high intensity storm event occurred on the 2 June 2024, with over 6mm of rain falling within a 15-minute period in the Project area, see Figure 5.

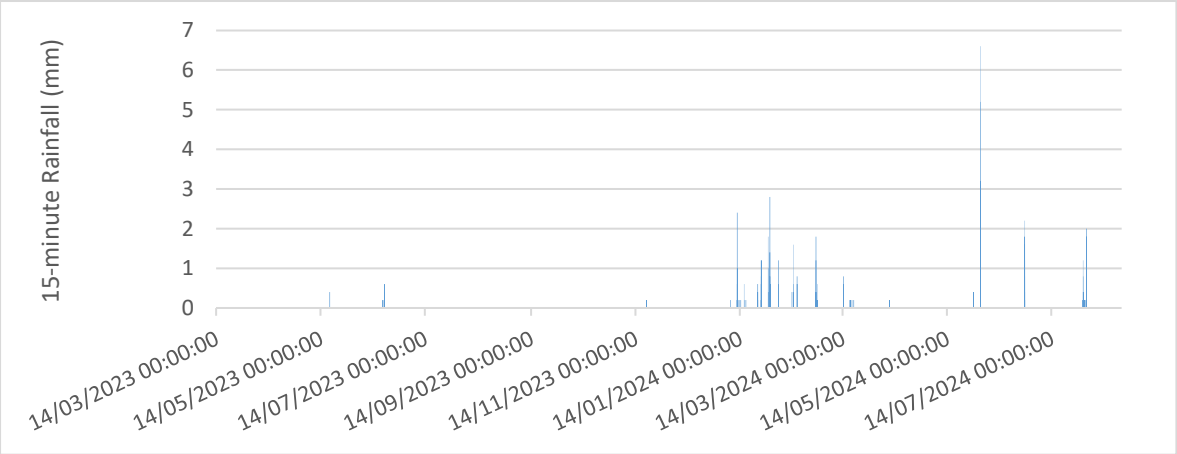

Figure 5. Sanjiv Ridge Rain Gauge - 15-minute record (SMR)

The intense storm event on the 2 June 2024 demonstrated considerable differences in rainfall intensity between gauges. As shown in Figure 6, Sanjiv Ridge experienced a more intense, middle-loaded event compared to other locations such as Mt Webber and Miralga, which recorded significantly lower intensities and overall magnitudes. McPhee Creek recorded lower intensities than Sanjiv Ridge but was closer in overall total rainfall due to an elongated rainfall period. Whilst not a high magnitude event, the intensity of such storms often result in significant surface runoff.

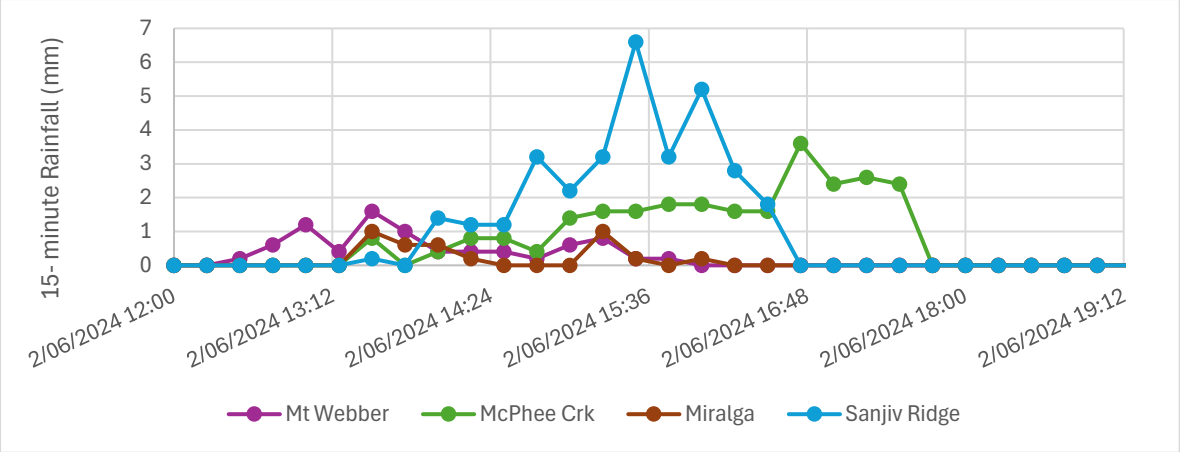

Figure 6. 2nd June Rainfall Event - 15 minute intensity

3.2.5 Long-Term Site Record

Typically, when only short-term data is available, a suitable analogue dataset is sought to provide a long-term perspective. Marble Bar (combined), due to its proximity, would usually be considered an appropriate surrogate. However, a poor correlation between daily rainfall data from Marble Bar and Sanjiv Ridge in 2024 exists, see Figure 7, indicating significant spatial variability even at this relatively short distance.

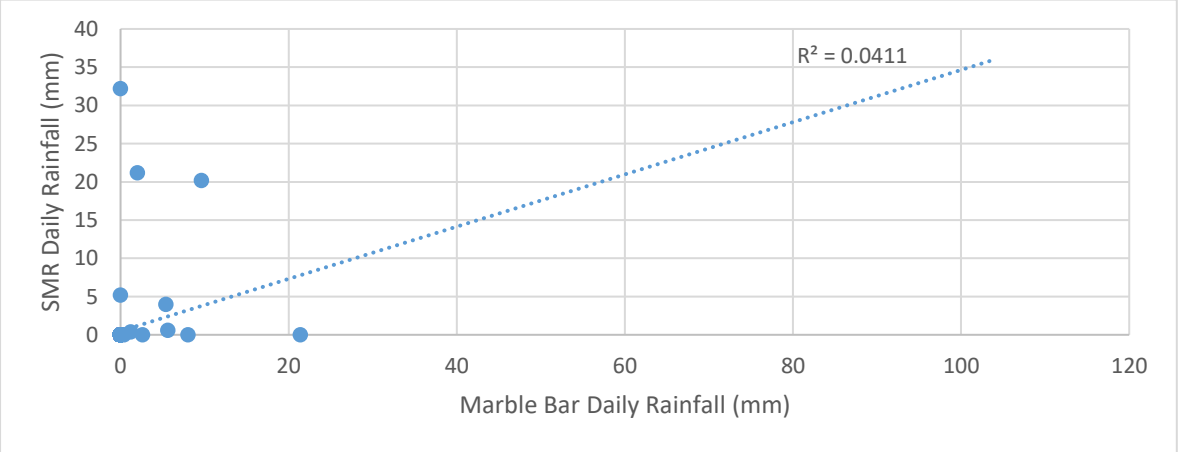

Figure 7. Marble Bar vs Sanjiv Ridge Gauge correlation

Consequently, satellite rainfall data from the GPM mission was evaluated as an alternative. The GPM mission, a joint initiative between NASA and the Japan Aerospace Exploration Agency (JAXA), provides high-resolution satellite data on precipitation. This data is collected using an advanced radar and microwave radiometer that can observe rainfall and snow worldwide, offering near real-time estimates of precipitation at a 3 km resolution. The GPM dataset, spanning from 1998 to the present, when validated against ground-sourced data, can provide a reliable long-term rainfall record.

The satellite GPM data demonstrated an acceptable correlation with both the short-term data recorded at Sanjiv Ridge (limited record) and the long-term data from Marble Bar (combined). Data from Marble Bar has gaps, including missing records for February 2011 and January to April 2016. After removing the gaps, a like-for-like correlation can be

performed to compare the days when rainfall has been recorded by Marble Bar versus GPM data, at a daily, monthly and annual timescale, see Figure 8, Figure 9 and Figure 10. Figure 11 and Figure 12 provides a long-term record comparison between GPM and Marble Bar gauge, demonstrating close agreement in seasonality and monthly rainfall, with some isolated exceptions.

These results indicate that GPM data, providing rainfall estimates at a 3 km^2 resolution, offers acceptable accuracy for representing local rainfall conditions to infill periods of time where the Sanjiv Ridge rainfall gauge has not recorded data. The GPM dataset spans from 1998 to the present, covering over 25 years, which is beneficial for long-term hydrological modelling and analysis.

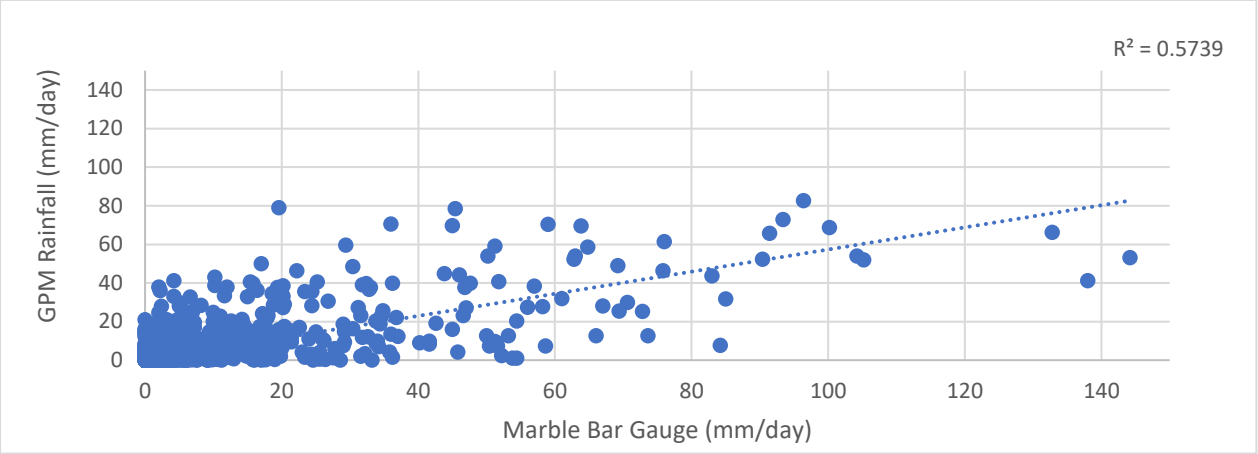

Figure 8. Daily rainfall Correlation (GPM vs Marble Bar (Combined))

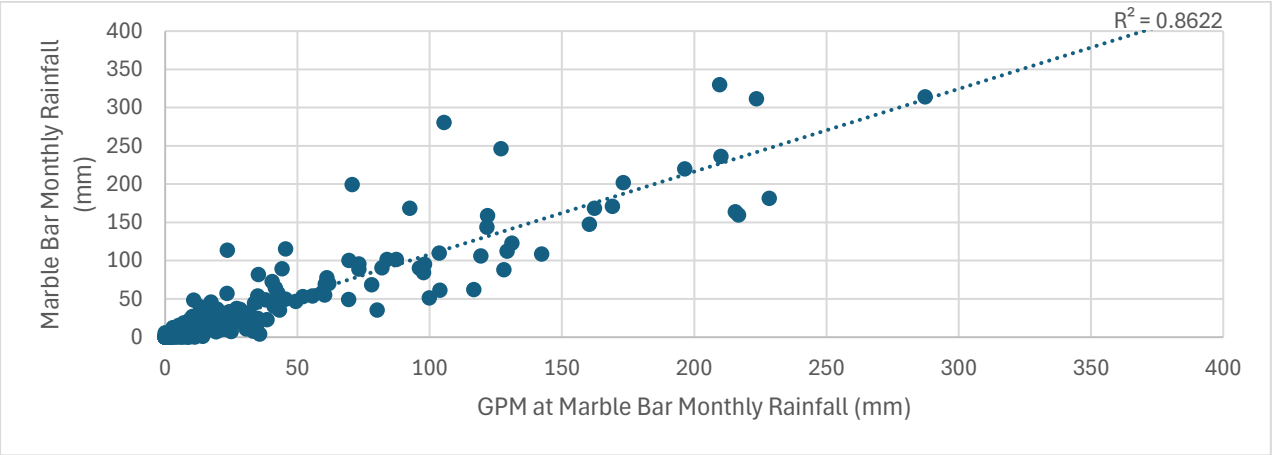

Figure 9. Monthly rainfall Correlation (GPM vs Marble Bar (Combined))

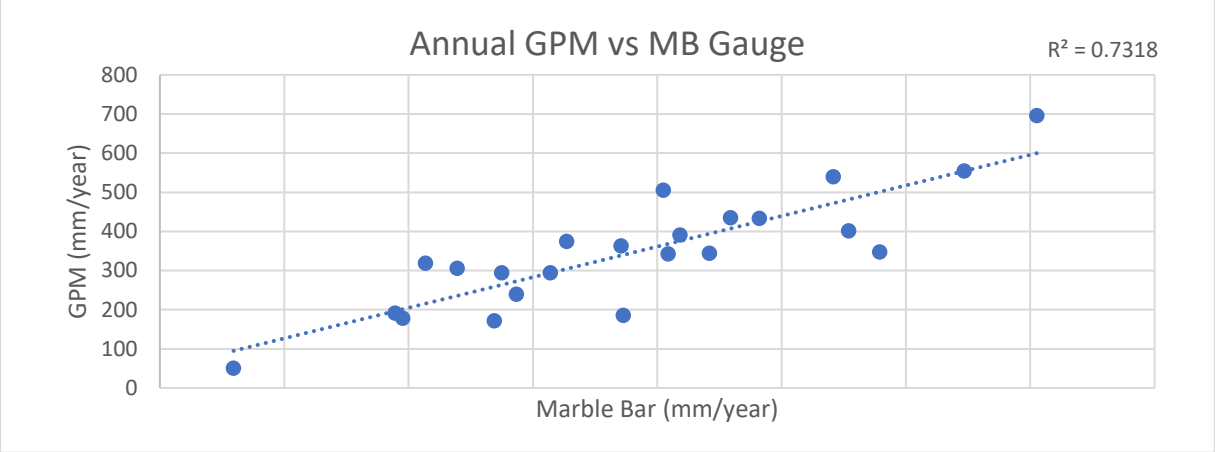

Figure 10. Annual rainfall correlation (GPM vs Marble Bar (Combined))

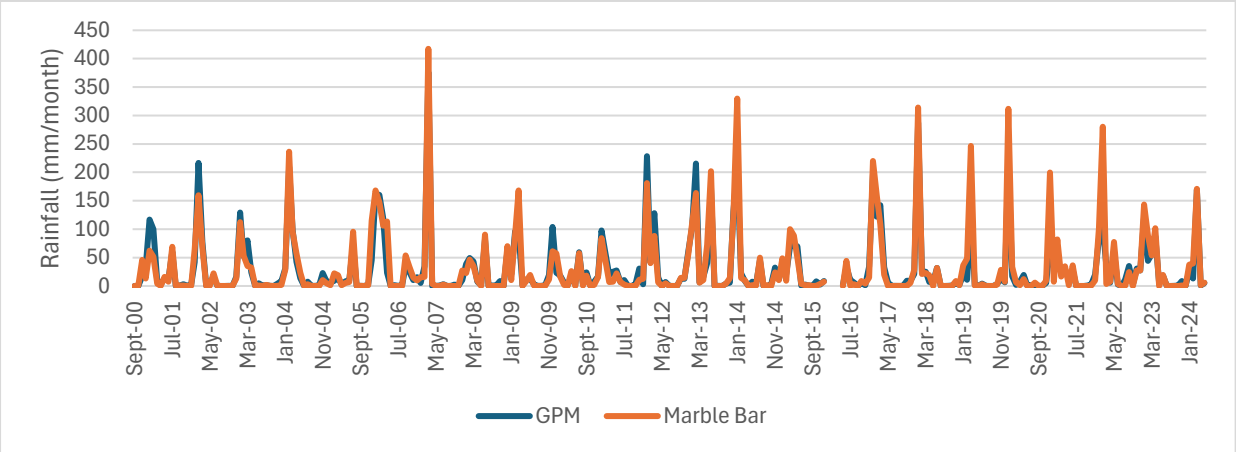

Figure 11. Seasonality - monthly rainfall 2000 - 2024 GPM vs Marble Bar

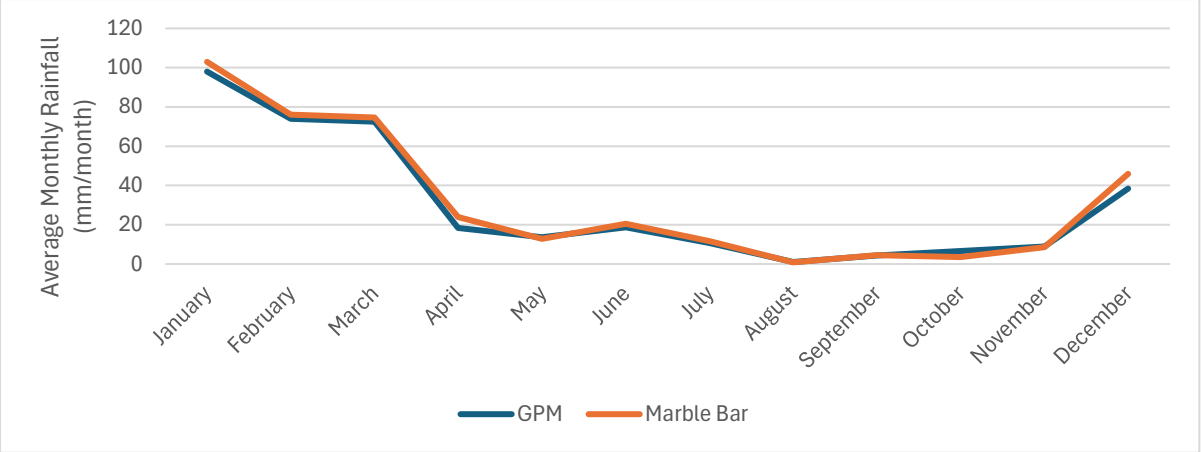

Figure 12. Average monthly rainfall GPM satellite vs Marble Bar gauge

3.2.6 Intensity Duration Frequency

The intensity duration frequency (IDF) data specific to the site has been obtained from the Bureau of Meteorology (BoM) Design Rainfall Data System (2016) (source: http://www.bom.gov.au/water/designRainfalls/revised-ifd/). This data is presented in Figure 13 and it provides valuable insights into the frequency and intensity of rainfall events over various durations across the Sanjiv Ridge Mine site for the purposes of flood modelling and stormwater management design.

IDF curves represent the relationship between rainfall intensity, duration, and frequency. The duration refers to the length of a rainfall event, while the frequency indicates how often a certain intensity of rainfall is likely to occur. Annual exceedance probability (AEP) is a key concept used in this analysis. It represents the probability of a specific rainfall intensity being equalled or exceeded in any given year. Understanding these parameters is crucial for simulating design runoff impact modelling, which has been completed as part of this study, and for informing future site-wide water management planning and design.

The BoM generates this information by analysing historical rainfall records and applying statistical techniques to determine the likelihood of different rainfall intensities occurring over specified time periods. This process involves the use of comprehensive climatic datasets and statistical techniques to produce more accurate and reliable IDF curves.

The BoM 2016 design rainfalls provided here are:

- Based on more than 30 years of additional rainfall data and data from extra rainfall stations than previous versions;
- More accurate estimates, combining contemporary statistical analysis and techniques with an expanded rainfall database;
- Better estimates of the 2% and 1% annual exceedance probability design rainfalls than the interim 2013 IFDs;
- Extended to include the subdaily rare design rainfalls.

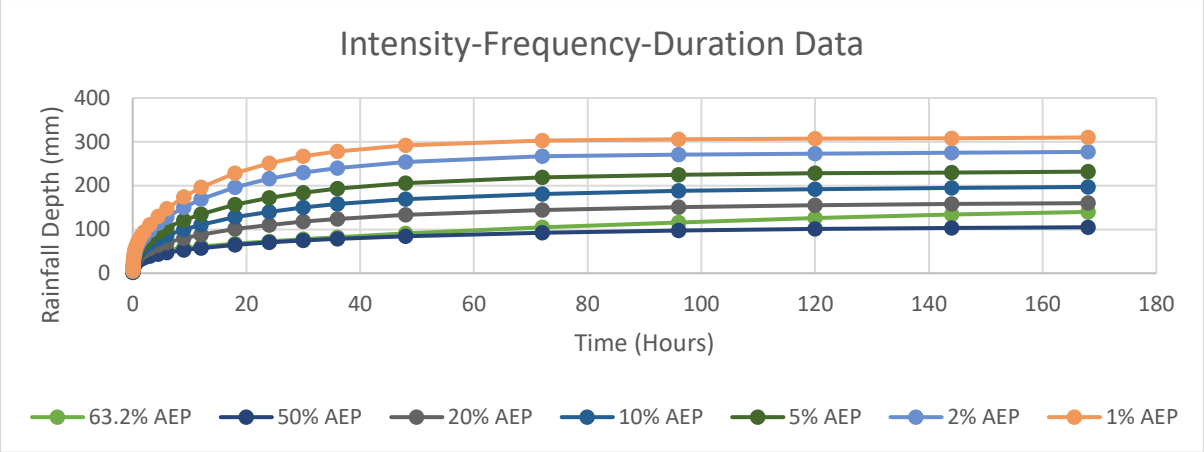

Figure 13. IDF data for Sanjiv Ridge (2025)

3.3 Temperature

The temperature regime in the area is important for understanding the climatic conditions affecting the Sanjiv Ridge Mine site. No long-term data is available for site, however Marble Bar is considered a suitable analogue for providing temperature data for the site due to its close proximity and the minimal variation in temperature over such short distances and at a similar general elevation (the Marble Bar gauge is located a few hundred metres lower than the main Sanjiv Ridge, at 182m).

Marble Bar is known for its significant temperature range. The recorded minimum temperature is 5 degrees Celsius, while the maximum temperature recorded was 49 degrees Celsius. The average daily temperature is relatively high, standing at 31 degrees Celsius. This wide range of temperatures is indicative of the extreme climatic conditions that can be experienced in the region. Figure 14 provides a summary of the monthly range of temperature statistics for the area.

Such high temperatures can lead to significant evaporative losses, thereby affecting the hydrological water balance of the region. Additionally, the prolonged dry periods and high temperatures increase the risk of soil hard panning of the soils, potentially resulting in rapid overland runoff during rainfall events.

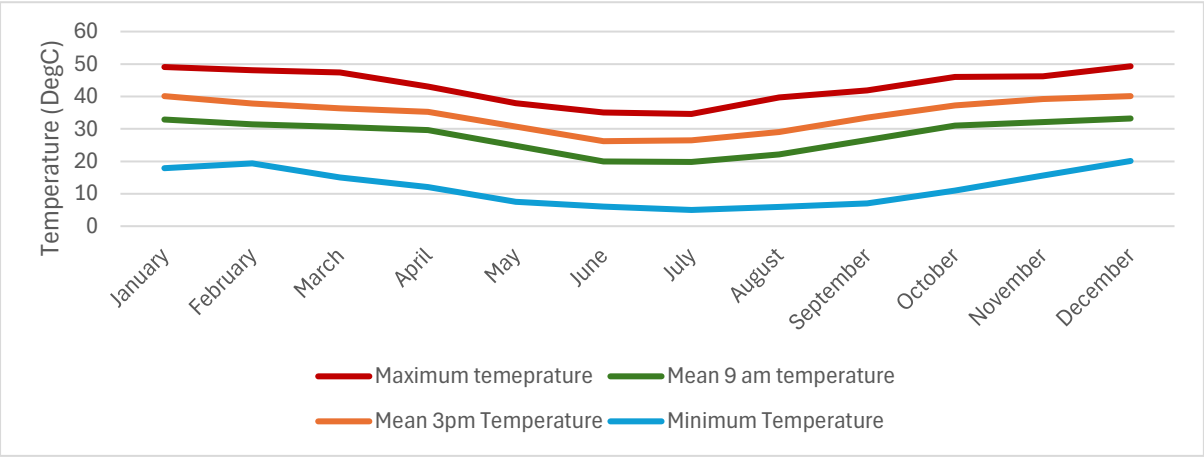

Figure 14. Monthly temperature ranges recorded at the Marble Bar weather station.

3.4 Evapotranspiration

Potential evapotranspiration is a critical factor in understanding the hydrological impacts of mining operations at Sanjiv Ridge. Long-term average potential evapotranspiration has been calculated using data from the Marble Bar weather station. This data reveals a clear seasonal pattern, with the highest potential evapotranspiration occurring during the wet season, linked to vegetative growth and the seasonal fluctuations in temperature.

During the months of June and July, when the minimum temperatures are recorded, we also observe the lowest levels of potential evapotranspiration. This correlation is crucial for hydrological modelling, as it provides insight into the seasonal water balance, with potential evapotranspiration representing a significant loss mechanism within the hydrological cycle of the area with an average annual potential evapotranspiration of 1635mm. High temperatures, as noted, lead to significant evaporative losses, with extended periods of dryness combined with high temperatures increase the risk of soil hard panning, which can result in rapid overland runoff during rainfall events.

Refer to Figure 15 for monthly average values of potential evapotranspiration.

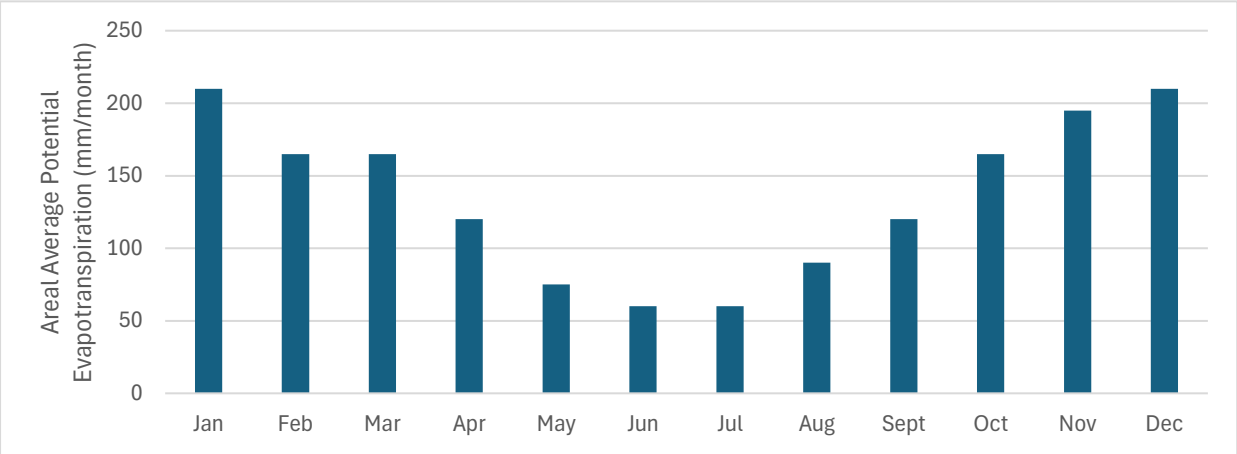

Figure 15. Monthly Average Potential Evapotranspiration (Marble Bar weather station)

3.5 Climate Change

Climate change analysis is important for understanding the potential future climate in the Sanjiv Ridge area. The future climate projections help in predicting changes in rainfall patterns, temperature, and evapotranspiration rates, all of which significantly influence the hydrological cycle and water balance in the region. This understanding is important for developing a hydrological model that includes a potential climate future, to determine potential effects of the mine combined with potential climate change effects.

In 2015, the Commonwealth Scientific and Industrial Research Organisation (CSIRO) and the BoM released the latest set of national climate projections for Australia. The research was funded by the Australian Government, CSIRO, and BoM. The CSIRO and BoM, Climate Change in Australia website makes all the results from this research available through a range of tools and downloadable reports. However, it is important to note that the climate projections provide general projections of the likelihood of certain climate futures only. They are based on scientific information, understanding, and quantitative modelling available at the time of their development.

Regional climate change projections are based on up to 40 Coupled Model Intercomparison Project Phase 5. (CMIP5) global climate model simulations driven by four emission scenarios. The ‘most likely’ case is the climate future represented by the greatest number of models. CSIRO defines the ‘most likely’ climate future as that which contains

more than one-third of the total number of models, where the number must be at least three times greater than the next most populous climate future. This criteria has been adopted for Sanjiv Ridge.

For the RCP 8.5 scenario in 2090, the projections present an average annual reduction in total rainfall received of -29.3%, see Table 2, with significant variation of effects throughout the year, with the greatest reduction projected for the dry season and lead up to the wet season.

Table 2. CSIRO/BOM Climate Change Projections, RCP8.5 scenario for 2090

	Projected Percentage Reduction in total rainfall (mm)
January	-22
February	-20.7
March	-30
April	-21.8
May	-35.4
June	-39.9
July	-39.9
August	-39.4
September	-47.2
October	-45.5
November	-30.9
December	-21
Annual	-29.3

Climate change projections for rainfall intensity, available from the BoM for the Sanjiv Ridge area, demonstrate that even though overall total rainfall is likely to reduce under RCP 8.5 2090, rainfall intensity is likely to increase, particularly for short-duration events. Whilst these increases should be considered generally as part of shorter term operational water management strategies, closure planning should take these potential large increases into account when designing closure water management solutions, particularly with regard to potentially increasing runoff and velocities as a result. The projections indicate an increase of up to 77% of the 1-hour intensity, with a projected 37% increase in the 24 hour intensity. These factors have been applied to the IDF data presented earlier in this section, to produce a projected IDF for the RCP 8.5 2090 climate scenario for Sanjiv Ridge (see Table 3. BOM Climate Change Factors for Sanjiv Ridge. and Figure 16).

Table 3. BOM Climate Change Factors for Sanjiv Ridge.

RCP-8.5										
Year	**<1 hour**	**1.5 Hours**	**2 Hours**	**3 Hours**	**4.5 Hours**	**6 Hours**	**9 Hours**	**12 Hours**	**18 Hours**	**>24 Hours**
2030	1.20	1.18	1.17	1.16	1.14	1.13	1.13	1.12	1.11	1.11
2040	1.26	1.24	1.22	1.20	1.18	1.17	1.16	1.15	1.14	1.14
2050	1.34	1.31	1.29	1.26	1.24	1.23	1.21	1.20	1.18	1.18
2060	1.42	1.38	1.35	1.32	1.29	1.28	1.26	1.24	1.22	1.21
2070	1.52	1.47	1.43	1.40	1.36	1.34	1.31	1.29	1.27	1.26

2080	1.63	1.57	1.52	1.48	1.43	1.40	1.37	1.35	1.33	1.31
2090	**1.77**	**1.69**	**1.64**	**1.58**	**1.52**	**1.49**	**1.45**	**1.42**	**1.39**	**1.37**
2100	1.86	1.77	1.71	1.64	1.58	1.54	1.50	1.47	1.43	1.41

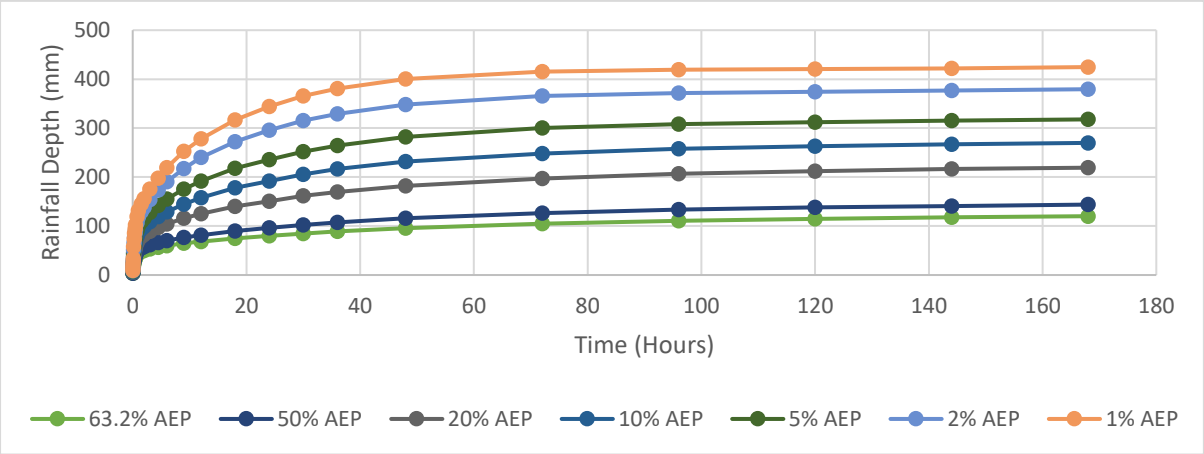

Figure 16. IDF data for Sanjiv Ridge - RCP 8.5 2090 climate change factors applied

For evapotranspiration, 97% of the 40 CMIP5 global climate model simulations suggest an average increase in evapotranspiration losses of 12%, linked to increased temperatures, by 2090 for RCP 8.5.

4 Surface Runoff

4.1 Monitoring Data

4.1.1 Stream Flow Monitoring

The closest long-term river gauge is located at the Coongan River at Marble Bar, with the record starting in December 1966, providing over 58 years of data, see Figure 19Figure 17. This provides a downstream monitoring location that includes the catchment areas of the Sanjiv Ridge mine, and demonstrates the significant inter-annual variability in runoff response, with key storm responses clearly evident within the record, such as the January 2nd Cyclone Blake response, which peaked within the Coongan at Marble Bar at over 1,150 m^3/s. Whilst typically ephemeral in nature, certain years (1999, 2000 for example) demonstrate a perennial response, likely as a result of sustained shallow groundwater discharge through the alluvial deposits within the floodplain and a higher than usual rainfall providing sufficient recharge for continued flows.

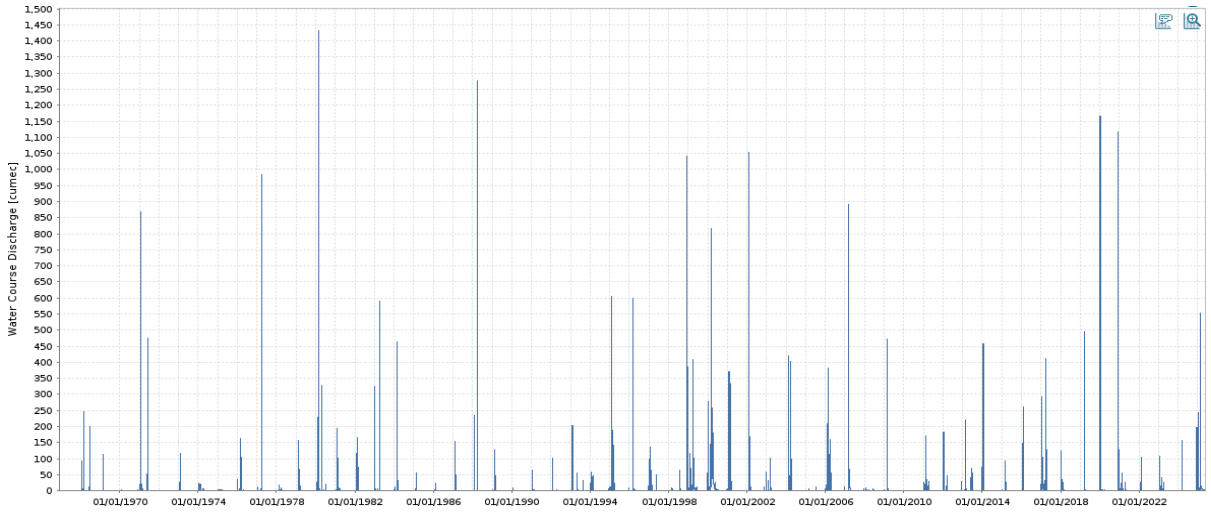

Figure 17. Coongan River Marble Bar Flow Record

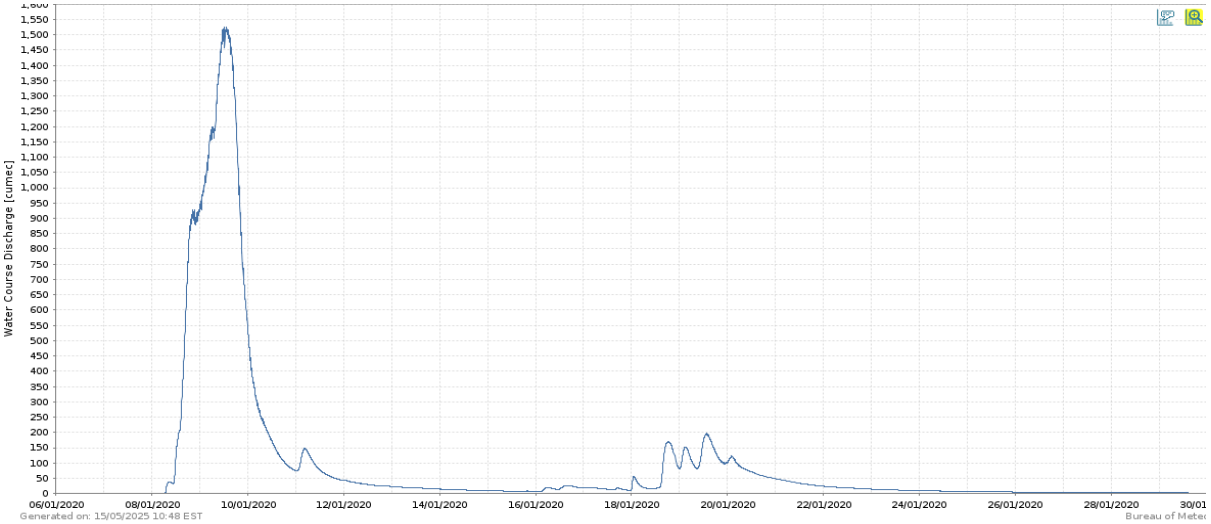

Figure 18. January 2nd 2020 - Cyclone Blake Flood Response

In late 2023, nine surface water monitoring sites were established during the dry season to monitor key catchments draining off the Sanjiv Ridge Mine, Refer to Figure 19 for a map of all monitoring locations.

These monitoring locations consist of:

- Seven sites monitoring eastward draining catchments that directly drain into the Coongan River.
- Two sites, SW007 and SW008, measuring runoff response in westward catchments that drain into a large ephemeral stream, which in turn drains into the Coongan River just northeast of the Glen Herring project area.

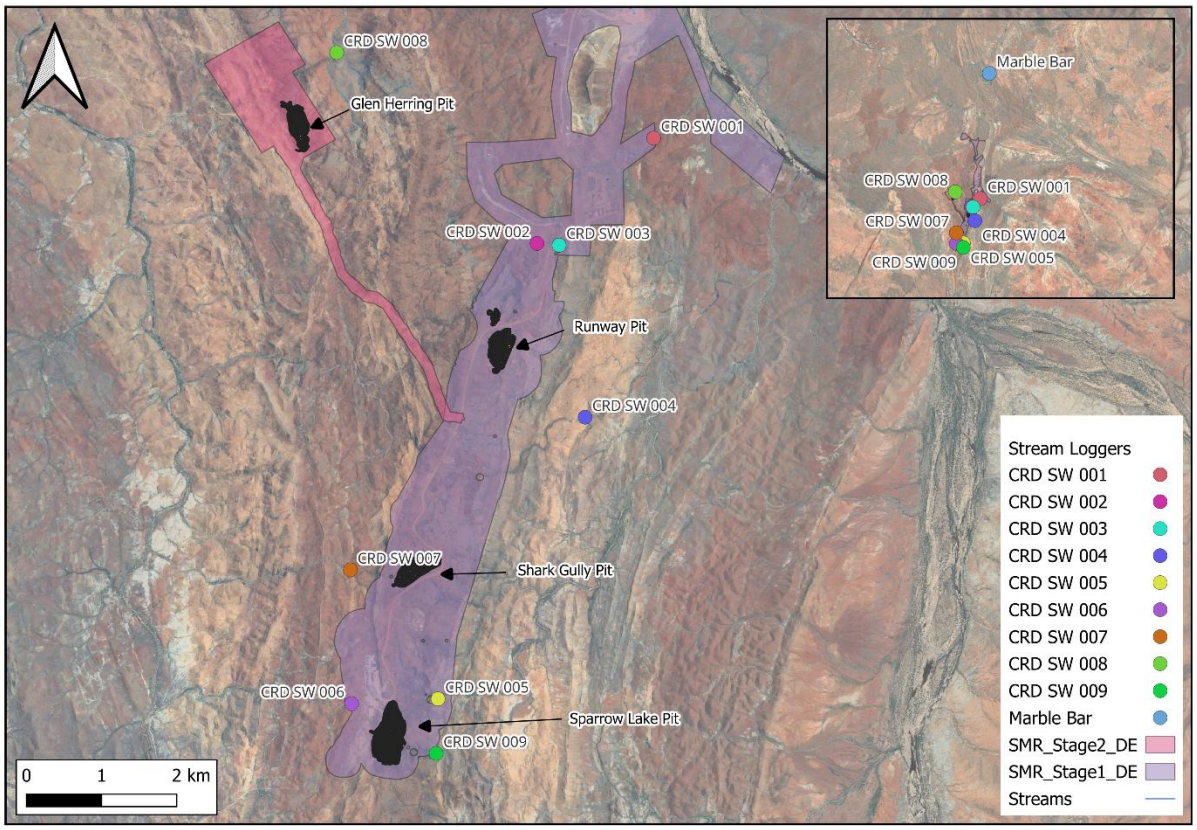

Figure 19. Surface Water monitoring locations

The monitoring sites use pressure transducers housed within slotted PVC pipes, which are securely fixed to the streambed. These devices record pressure readings that are manually downloaded by site staff. Pressure readings from the transducers are adjusted using a central barometric pressure logger located at CRD0096, a groundwater monitoring borehole. The barologger is installed at an elevation of 414.21 mAHD. For every one-meter rise in elevation, there is approximately a decrease of 0.012 kPa (0.12 cm). This pressure adjustment is essential to account for significant elevation differences between the surface water gauging sites and the baro position (for example, SW001 is installed at 221.87 mAHD).

The current record includes stream water level responses to rainfall events during the wet season of 2024. These water level readings require conversion to flow using rating curves. Rating curves have been created for each location where possible, providing a necessary calibration dataset for hydrological modelling. Further information is provided in Appendix A; however, Table 4 summarises the key information. Only SW001 and SW002 offer clear flow records suitable for hydrological modelling calibration, while SW003, SW007, and SW008 provide a limited dataset at the time of this reporting, useful for trend analysis but with uncertain accuracy. The remaining locations experienced technical issues, either related to barometric adjustment or potential damage, resulting in inconsistent data records. These locations have since been improved by site staff and will provide important ongoing monitoring data. SW001 and SW002 provide an ideal nested catchment monitoring dataset for modelling, with monitoring at different scales within the same overall catchment allowing for good characterisation of the catchment, which can be applied to other unmonitored areas that share similar characteristics.

Table 4. Stream monitoring location data summary

Site ID	Usable Stage Record?	Defined Rating Curve	Comment
SW001	Yes	Yes	Good data quality
SW002	Yes	Yes	Good data quality
SW003	Yes	Yes – but limited	Ok data quality except for logger displacement
SW004	No	No	No clear compensation
SW005	No	No	No clear compensation, drift apparent suggesting damaged sensor
SW006	No	No	No clear compensation, drift apparent suggesting damaged sensor
SW007	Yes	Yes – but limited	Compensation noise but usable as indicative response
SW008	Yes	Yes – but limited	Compensation noise but usable as indicative response
SW009	No	No	No clear compensation, drift apparent suggesting damaged sensor

A detailed breakdown for each location and rating curve derivation is provided in Appendix A.

Figure 20 and Figure 21 outline the runoff response to rainfall events in 2024, noting the known issue with the rainfall gauge prior to 21 March 2024 . Of note is the clearly ephemeral response at both, but prolonged recession of minor flows at SW001 through March and into April. This is not observed at SW002, which is located much higher up in the catchment and outlines the differences shallowing terrain and alluvial deposits within the channel make on shallow baseflow contributions. An out of season convective storm event occurred on the 2nd June 2024, observed at both gauges as a rapid, ephemeral flood response, with a 20-minute time to peak observed at SW001, see Figure 22. Interestingly, this event was not observed at the regional gauge on the Coongan River in Marble Bar, supporting the theory that these out of season events are localised convective storms, with runoff response infiltrating riverbed alluvial deposits with the shallowing terrain, prior to the Coongan River gauge at Marble Bar.

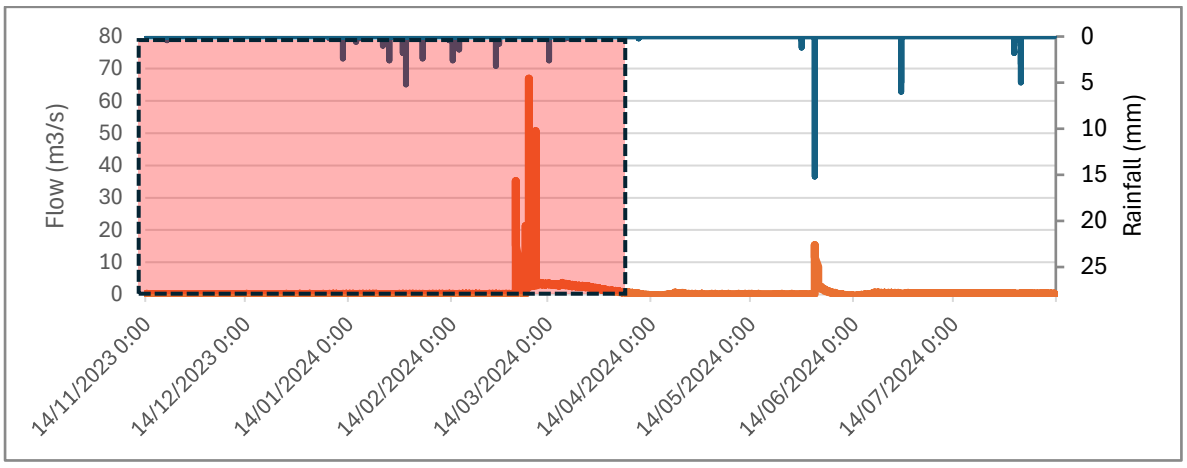

Figure 20. SW001 Flow Data

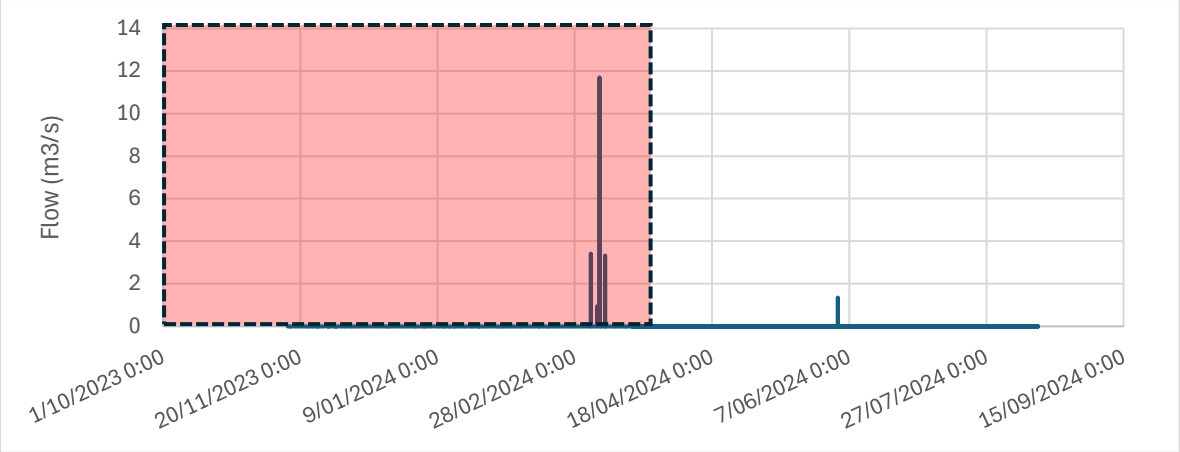

Figure 21. SW002 Flow Data

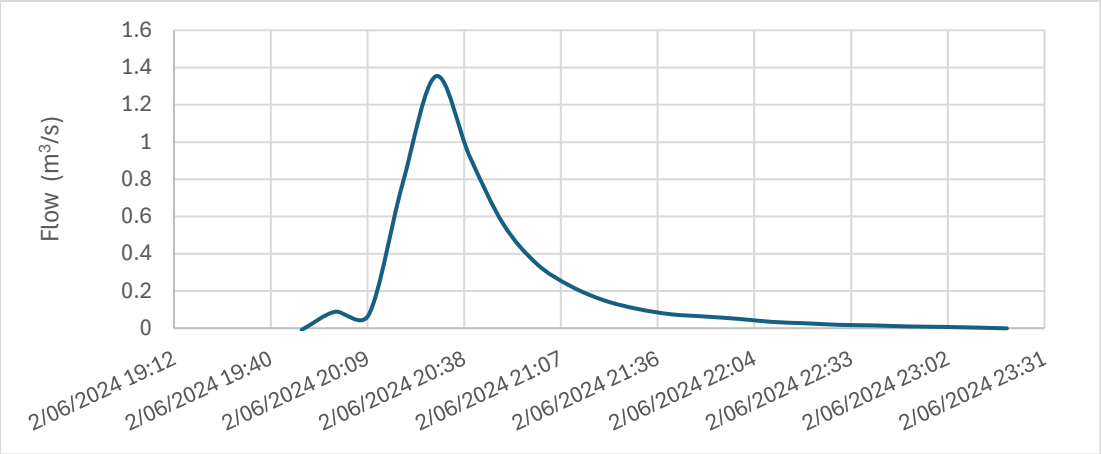

Figure 22. SW002 Isolated Storm Response

4.1.2 Pools

Eleven significant water sources were identified previously within the Project area (MWH, 2018a), see Figure 23. Pools were classified as ephemeral or perennial, with five of the eleven pools judged as perennial and four considered groundwater dependent (SRK, 2019), see Table 5. Pool CO-WS-14 is important as it supports the Pilbara Leaf-nosed Bat's breeding habitat linked to cave CO-CA-03 (MWH, 2018a), with water level monitoring suggesting whilst clear ephemeral storm runoff responses flushes through the pool in response to rainfall events, year round maintenance of water levels within the pool suggest a perennial recharge from groundwater, with CO-WS-12 demonstrating a similar trend with a gradual decline in water level consistent with evaporative losses and ongoing groundwater replenishment. Water level hydrographs from pools CO-WS-01, CO-WS-02, CO-WS-08, CO-WS-10, CO-WS-11 and CO-WS-13 suggest that whilst these pools may receive some minor contribution from groundwater, there is a steep antecedent trend indicative of a dominant evaporative influence following cessation of rainfall runoff response. All pools clearly show the influence of rainfall-runoff response forming a significant component of pool water recharge during the wet season. This has been analysed and reported on with similar conclusions in the past (MWH, 2018a, SRK, 2019)

Table 5. Pool Summary

Site ID	Permanency (SRK, 2019)
CO-WS-01	Perennial
CO-WS-02	Ephemeral
CO-WS-03	Ephemeral
CO-WS-05	Perennial
CO-WS-08	Ephemeral
CO-WS-09	Ephemeral
CO-WS-10	Perennial
CO-WS-11	Ephemeral
CO-WS-12	Perennial
CO-WS-13	Ephemeral
CO-WS-14	Perennial

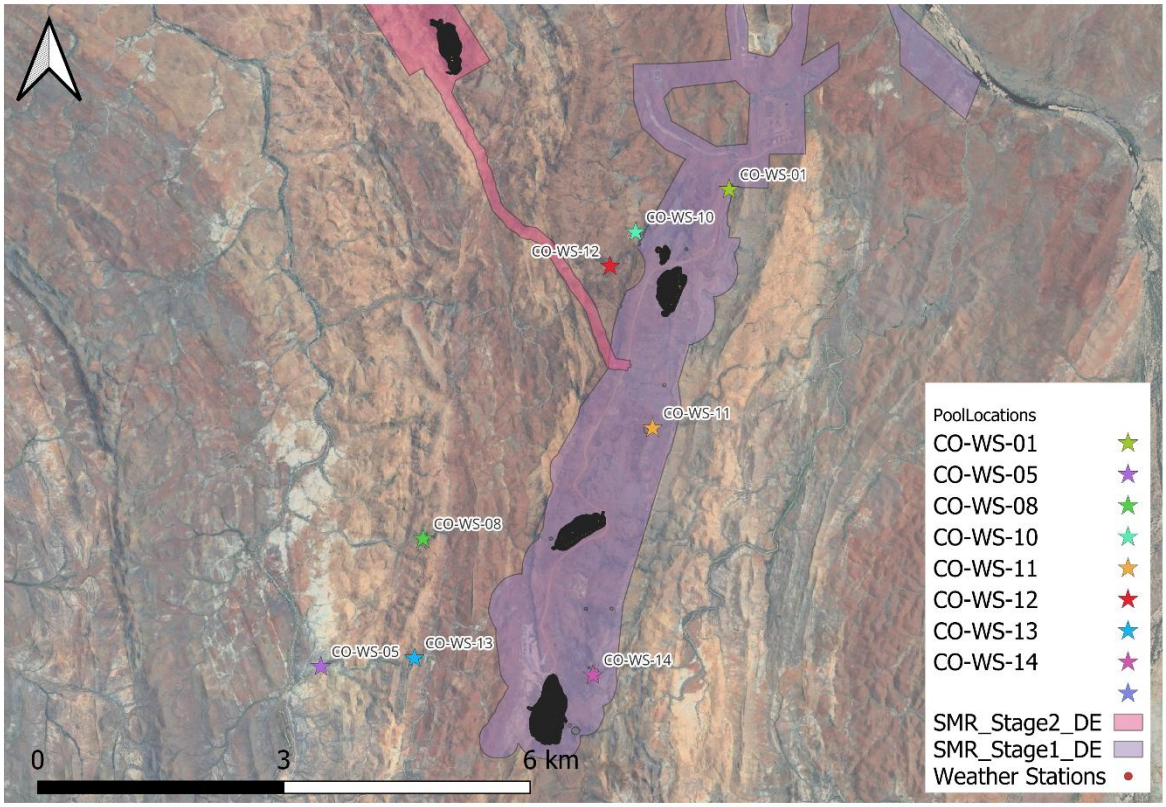

Figure 23. Pool Locations

5 Hydrological Modelling

5.1 Introduction

The hydrological model is essential for evaluating the long-term rainfall-runoff response within the Sanjiv Ridge drainage system. Current short-term monitoring of runoff response in the local catchments is insufficient for comprehensive assessments. By calibrating a hydrological model to this limited dataset and extending the model using long-term rainfall records, we can simulate the rainfall-runoff response over extended periods, providing data for use in assessing the Project impacts and in management and mitigation planning.. Additionally, the model will help determine the area's response to design runoff events for 1%, 2%, 20%, and 50% AEPs using 24-hour IFD data from BOM.

A Hydrologic Engineering Center – Hydrologic Modeling System (HEC-HMS) Linear Deficit and Constant model was used for this assessment, leveraging its capabilities for continuous simulation and design event modelling. HEC-HMS (Hydrologic Engineering Center's Hydrologic Modelling System) is a robust tool widely used for simulating precipitation-runoff processes. This approach employs physically based parameters, facilitating accurate simulation of loss and runoff mechanisms despite the limited calibration dataset. By calibrating infiltration and loss parameters, we extended the model's applicability well beyond the monitoring period, ensuring it can effectively represent hydrological responses during both wet and dry seasons.

The hydrological model was calibrated to represent the current 2025 catchments, incorporating modifications from pit areas, stockpiles, and haul roads that alter flow paths. Catchment removal through interception and storage, such as sediment ponds and pit inflows, were also considered. The following scenarios were then developed:

- Scenario 1: Baseline - a pre-mine natural catchment baseline.
- Scenario 2: Current (2025) - the calibrated model reflecting existing catchment modifications.
- Scenario 3: Stage 5 mining operations - modifications primarily limited to pit expansion areas and slight modifications to haul road and stockpile areas.
- Scenario 4: Baseline with climate change - the pre-mine natural catchment baseline with climate change effects for the RCP8.5 2090 scenario.
- Scenario 5: Current (2025) with climate change - the calibrated model reflecting existing catchment modifications, incorporating climate change effects for the RCP8.5 2090 scenario.
- Scenario 6: Stage 5 mining operations with climate change - modifications primarily limited to pit expansion areas and slight modifications to haul road and stockpile areas, including climate change effects for the RCP8.5 2090 scenario.

This comparative impact assessment quantified changes in runoff response between the current and baseline scenarios, future Stage 5 and baseline, and future Stage 5 and current scenarios, in addition to the effects of climate change on all of these scenarios. The potentially affected pools; C0-WS-05, C0-WS-08, C0-WS-13 and C0-WS-14 have been modelled separately to allow for a review of the potential impacts of Stage 5 on surface water flow regime through the pools, both for current climate and a future RCP 8.5 2090 scenario.

5.2 Methodology

A HEC-HMS Linear Deficit and Constant model was constructed for the hydrological assessment of the Sanjiv Ridge mine site. The model employed a simple canopy loss model and Snyder unit hydrograph transform method (Snyder, 1938). This approach follows industry best practise and is suitable for both continuous simulation of hydrological response and design event modelling in the small headwater catchments of Sanjiv Ridge.

The parameters described in Table 6 were established as initial parameter ranges prior to calibration following industry guideline values, reflecting the unique environmental conditions of the region and providing a starting point for further refinement. These initial values serve as starting points and will be refined through subsequent calibration based on site-specific data, as detailed in the following chapter.

Table 6. Initial model calibration parameter range

Parameter Type	Parameter	Value	Comments
Canopy Parameters	Initial Storage	0 -50%	Initial water stored in the canopy before any rainfall
Canopy Parameters	Crop Coefficient	0.3-0.5	Reflects the rate at which crops use water relative to a reference crop
Canopy Parameters	Maximum Storage	10 mm	Maximum amount of water that can be held in the canopy
Loss Parameters	Initial Deficit	10-20 mm	Initial soil water deficit before rainfall begins
Loss Parameters	Maximum Deficit	50-150 mm	Maximum soil water deficit capacity
Loss Parameters	Constant Rate	2 mm/hr	Rate at which water is lost due to processes like evaporation
Loss Parameters	Decay Factor	-4-0.8	Rate at which soil moisture deficit decays over time
Transform Parameters	Peaking Coefficient	0.6-0.9	Influence the hydrograph shape and time to peak/recession
Transform Parameters	Lag Time	Calculated based on catchment charateristics	Non-calibration parameter. Standard lag calculated using catchment characteristics via the Kirpich technique and represents the delay between peak rainfall and peak discharge in a river or stream.
Baseflow Parameters	No initial discharge	-	No initial water flow from groundwater
Baseflow Parameters	Recession Constant	0..5-0.9	Rate at which baseflow recedes after peak discharge
Baseflow Parameters	Threshold: Ratio to Peak	0.05-0.4	Threshold ratio used to adjust baseflow contribution

5.3 Model Calibration

The initial parameter values served as a starting point for the calibration process. These values were iteratively adjusted to enhance the model's accuracy in simulating the observed hydrograph characteristics. The primary focus was on achieving a good fit in terms of the hydrograph's response shape, which includes the time to peak, peak magnitude, total volumetric runoff yield, and recession shape, with a particular focus on the throughflow component from shallow sub-surface represented by the baseflow parameters, and the antecedent moisture conditions preceding rainfall events.

The two surface water locations used for model calibration/validation due to the availability of usable stage data and rating curves were:

SW001: Located in the lower catchment, this site provided clear runoff response data for periods of 2024 and was used for model calibration.

SW002: Positioned in the upper catchment, this site captured discharge data representative of headwater catchment response and served as the independent dataset for model validation.

The calibration process involved comparing the simulated hydrograph with the observed datasets from SW001. The goodness of fit was evaluated using several criteria, including the Nash-Sutcliffe Efficiency (NSE), the Root Mean Square Error (RMSE), and visual inspection of the hydrograph shapes. The model was then validated against the data from SW002.

5.4 Summary of Calibrated Parameters

Table 7 summarises the final calibrated parameters for the model.

Table 7. Summary of calibrated parameters

Parameter Type	**Parameter**	**Value**
Canopy Parameters	Initial Storage	0
Canopy Parameters	Crop Coefficient	0.3
Canopy Parameters	Maximum Storage	1 mm
Loss Parameters	Initial Deficit	10 mm
Loss Parameters	Maximum Deficit	50 mm
Loss Parameters	Constant Rate	2 mm/hr
Loss Parameters	Decay Factor	-3
Transform Parameters	Peaking Coefficient	0.43
Transform Parameters	Lag Time	Calculated in model
Baseflow Parameters	No initial discharge	-
Baseflow Parameters	Recession Constant	0.62
Baseflow Parameters	Threshold: Ratio to Peak	0.23

5.5 Goodness of Fit and Limitations

The calibrated model showed a satisfactory fit with the observed hydrographs, with high NSE values (>0.7) and low RMSE values (<0.3) indicating good model performance. Figure 24 and Figure 25 provide a zoomed in comparison between the final calibrated simulated flow and cumulative volume for the 2nd June 2024 runoff event as an example, compared to that observed (measured) at SW001.

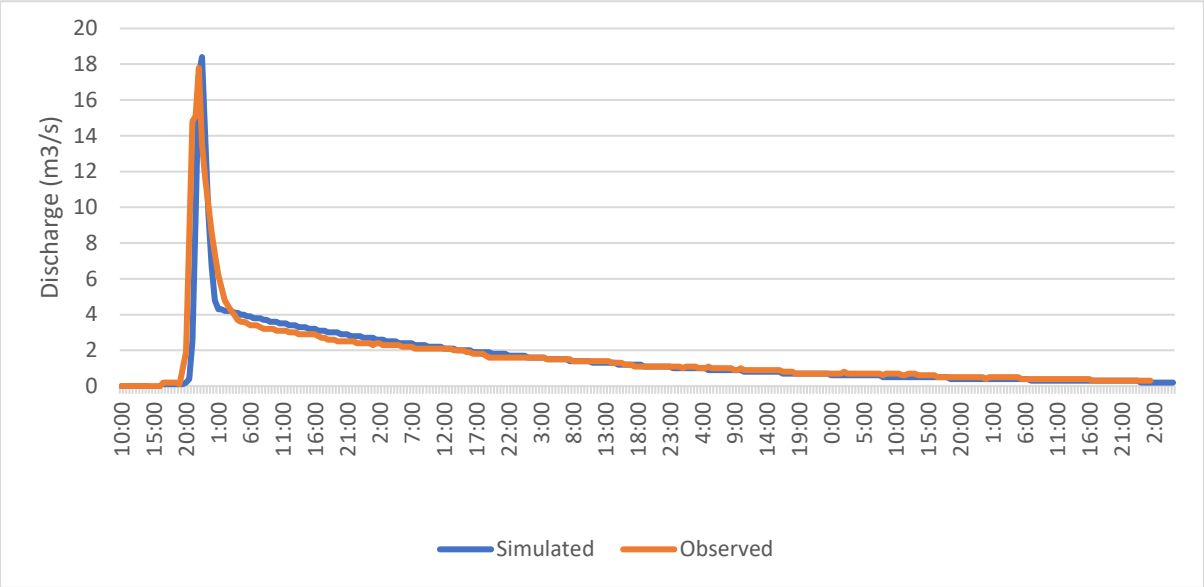

Figure 24. Fit to 2nd June 2024 runoff event

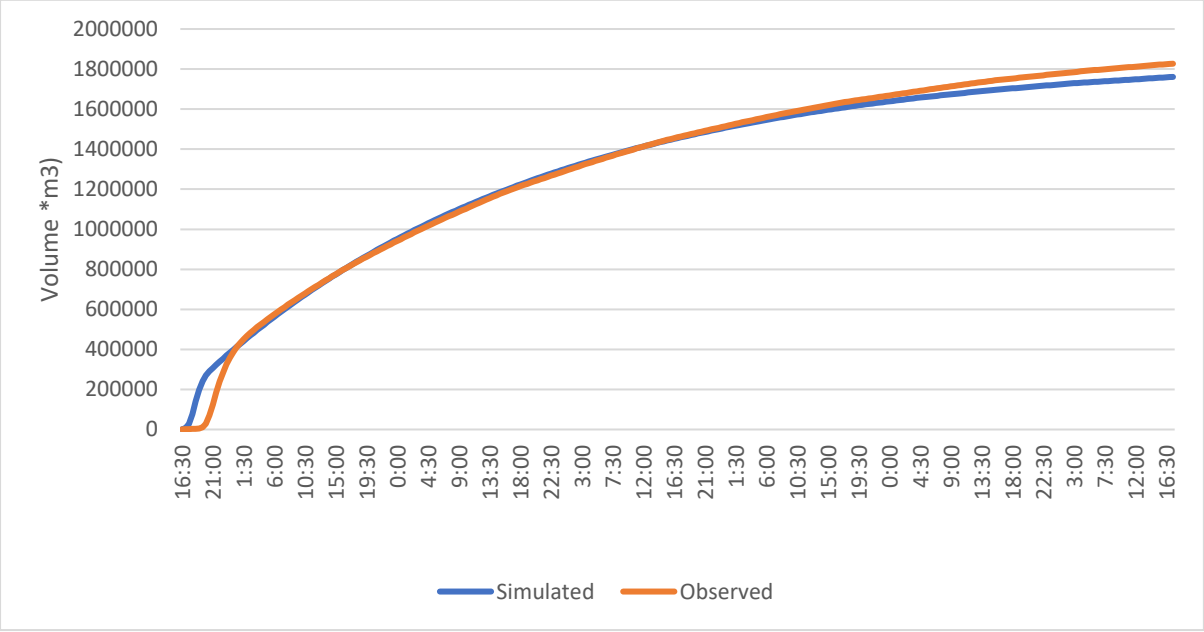

Figure 25. Cumulative volume comparison between final calibrated model and observed dataset for 2nd June 2024 event

It is necessary to consider the limitations of the short record length. Typically, a multi-year dataset would be utilised for long-term simulation calibration to capture the wetting and drying patterns within the catchment

comprehensively. However, due to the extreme ephemeral response associated with sporadic and intense rainfall and limited soil water storage post-rainfall, the short calibration record is not deemed a critical flaw in the model. The 2024 dataset includes a full range of events with extended dry periods, which allows the physical parameters of the catchment to be accurately represented in the model. This provides assurance that the model can be extended to simulate periods outside the calibration using site-specific rainfall data to effectively simulate the runoff response shape, time to peak, peak magnitude, total volumetric runoff yield, and recession shape. It is not uncommon for impact assessments to be based upon uncalibrated models, however this introduces significant uncertainty. The modelling completed in this assessment provides a significant improvement and provides greater certainty around the range of potential effects, particularly across different scenarios, including the potential effects of climate change.

6 Impact Assessment

6.1 Long-Term Simulation

6.1.1 Modelled Scenarios

The calibrated hydrological model followed industry best practise methodology and utilised long-term GPM rainfall data and evapotranspiration values, (a detailed background to these datasets is provided in 3.2 of this report), to produce a long-term record of stream flow response across the Sanjiv Ridge drainage network.

This section details the modelling results for all of the following scenarios

- Scenario 1: Baseline - a pre-mine natural catchment baseline.
- Scenario 2: Current (2025) - the calibrated model reflecting existing catchment modifications.
- Scenario 3: Stage 5 mining operations - modifications primarily limited to pit expansion areas and slight modifications to haul road and stockpile areas.
- Scenario 4: Baseline with climate change - the pre-mine natural catchment baseline with climate change effects for the RCP8.5 2090 scenario.
- Scenario 5: Current (2025) with climate change - the calibrated model reflecting existing catchment modifications, incorporating climate change effects for the RCP8.5 2090 scenario.
- Scenario 6: Stage 5 mining operations with climate change - modifications primarily limited to pit expansion areas and slight modifications to haul road and stockpile areas, including climate change effects for the RCP8.5 2090 scenario.

The following catchment reductions characterised key changes between scenarios, with the current “2025” scenario demonstrating notable catchment reductions in certain areas with no change moving forward to Stage 5, and other catchments experiencing more significant changes at Stage 5, notably SW009, see Table 8. Of the 11 identified pools in the Project area, only C0-WS-01, C0-WS-05, C0-WS-08, C0-WS-13 and C0-WS-14 lie within catchments potentially affected by changes to surface water runoff response through Stage 5.

Surface water intercepted by pits and stormwater management sediment ponds will ultimately be discharged back to the watercourse after the event via pumps and pipe infrastructure (in accordance with licence conditions and/or industry guidelines (such as the Water Quality Protection Guidelines for Mining and Mineral Processing Guidelines (Water and Rivers Commission, 1999)). However, although it is likely that most of the intercepted surface water will be discharged to watercourses, these typically fall under constant rate discharges of significantly lower magnitude than the natural rainfall-runoff response. It is unlikely that much of the discharge will remain at surface beyond the immediate headwater reaches, (which are predominantly rocky outcrops/shallow soils), but instead percolate through the shallow alluvial deposits within the stream. This impact assessment considers a worst-case scenario, where these returned discharges are no longer considered as contributing to the overland volumetric yield of surface water within the local drainage network.

Scenario 4 serves as a valuable baseline for understanding the potential isolated impact of climate change on the natural catchment, devoid of any mining activities. This allows for a clear separation of climate change response from mining activity effects. In contrast, scenarios 5 and 6 facilitate a review of the combined effects of climate change and mining operation. It is important to highlight that the continuation of mining activities through to 2090 is not anticipated; thus, these scenarios are purely hypothetical, assuming that the current or Stage 5 impacts persist without considering future closure plans that could potentially mitigate some of these effects.

Table 8. Percentage reduction in catchment area. Blank denotes no change.

Site ID	Current	Stage 5
SW001	5.83%	
SW002	6.80%	7.17%
SW003	12.62%	
SW004	0.46%	
SW005		2.44%
SW006		36.73%
SW007		19.34%
SW008		3.62%
SW009	4.44%	66.76%
C0-WS-01	12.72%	
C0-WS-05		2.10%
C0-WS-08		7.05%
C0-WS-13		2.77%
C0-WS-14		2.40%

6.1.2 Results

Scenario 1: Baseline

The simulation results for the baseline scenario indicate significant inter-annual variability, see SW001 example in Figure 26, reflecting the model's sensitivity to both dry and wet years. During low rainfall years such as 2016 and 2019, the modelled runoff response was limited. On the other hand, substantial runoff was simulated during wet years, demonstrating the model's ability to handle varying climatic conditions.

The average peak flow (the average monthly maximum flow) and runoff coefficients were highly variable, closely linked to rainfall intensity, see Figure 26 and Figure 27. The average peak flow is a useful metric in an ephemeral system as it allows the evaluation of peak flow trend changes, not just isolated events. For example, December 1999 had a runoff coefficient of 77% due to several high-intensity events, whereas December 2000 had a coefficient of just 10% due to lower-intensity rainfall, resulting in higher interception, infiltration, and evapotranspiration losses.

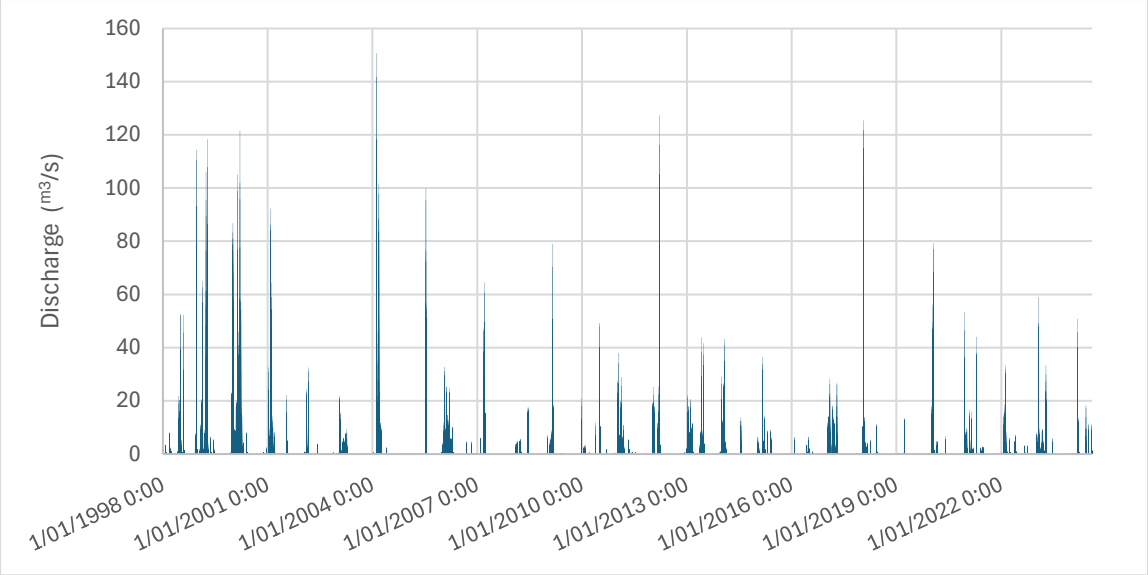

Figure 26. Modelled SW001 Baseline Flow Record

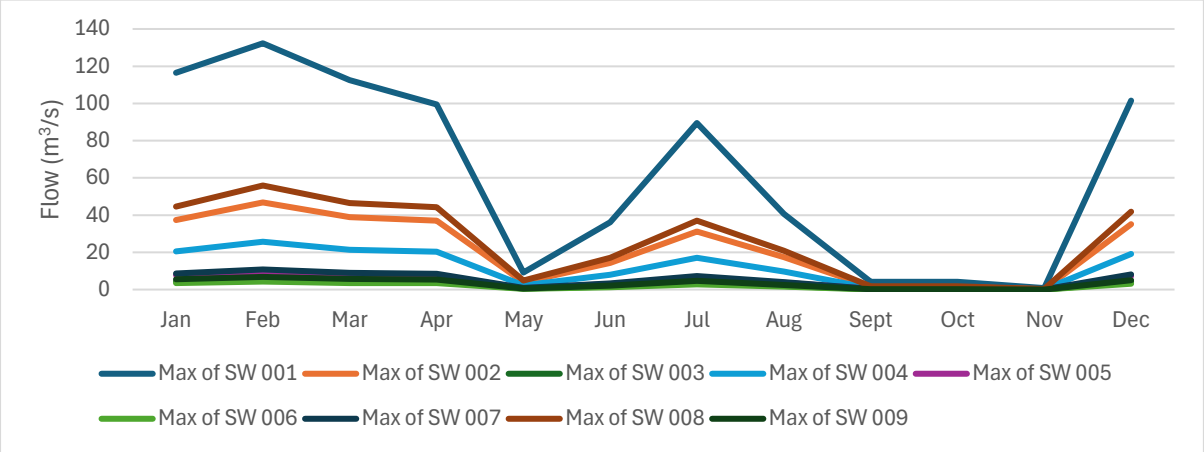

Figure 27. Modelled Average Maximum Flows

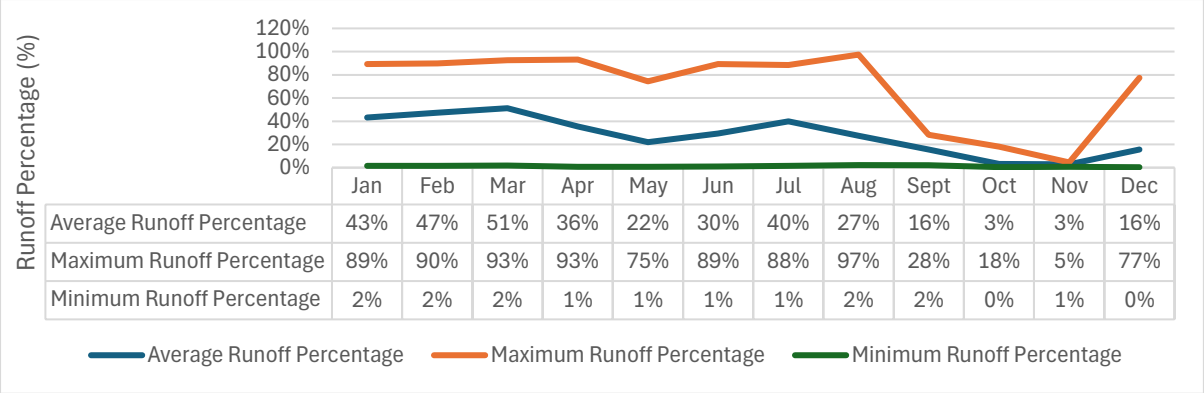

	Jan	Feb	Mar	Apr	May	Jun	Jul	Aug	Sept	Oct	Nov	Dec
Average Runoff Percentage	43%	47%	51%	36%	22%	30%	40%	27%	16%	3%	3%	16%
Maximum Runoff Percentage	89%	90%	93%	93%	75%	89%	88%	97%	28%	18%	5%	77%
Minimum Runoff Percentage	2%	2%	2%	1%	1%	1%	1%	2%	2%	0%	1%	0%

Figure 28. Modelled Runoff Percentages

Scenarios 2 and 3

Scenarios 2 and 3: Modelling Results

The modelling results for scenarios 2 and 3 highlight reductions in average peak flow and annual volume across various locations. Figure 29 demonstrates that Scenario 2 ("2025") shows an average peak flow reduction of up to 13%, with SW003 experiencing the greatest reduction due to catchment loss. Interestingly, SW001, located downstream of SW003, exhibits a 7.21% catchment loss, illustrating the diminished effect downstream due to inflows from unaffected areas. Scenario 3: Stage 5 results reveal several locations remaining unchanged from Scenario 1. However, catchments such as SW009, SW006, and SW007 observe notable peak flow reductions of between 13% and 67%.

Figure 30 demonstrates that for Scenario 2, locations SW001 through SW003 experience the greatest reductions in average annual volume, up to 16%. Scenario 3 shows a decrease in peak runoff of up to 75% at SW009. This reduction is significantly less at other sites. The SW009 monitoring site, located near the proposed Sparrow Lake pit expansion area, highlights immediate effects compared to other locations where contributing areas unaffected by the scenarios influence the flow response.

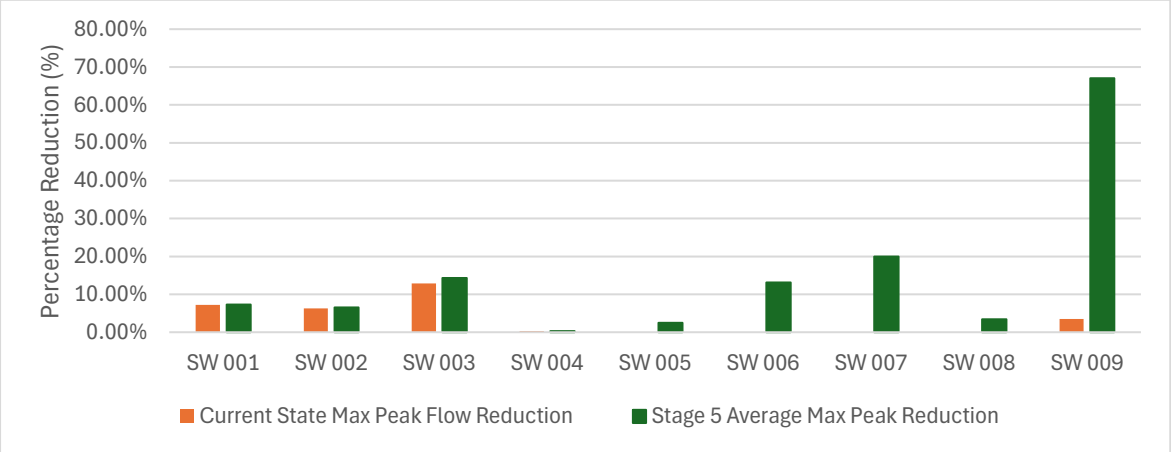

Figure 29. Scenarios 2 and 3: Average peak flow reduction (%)

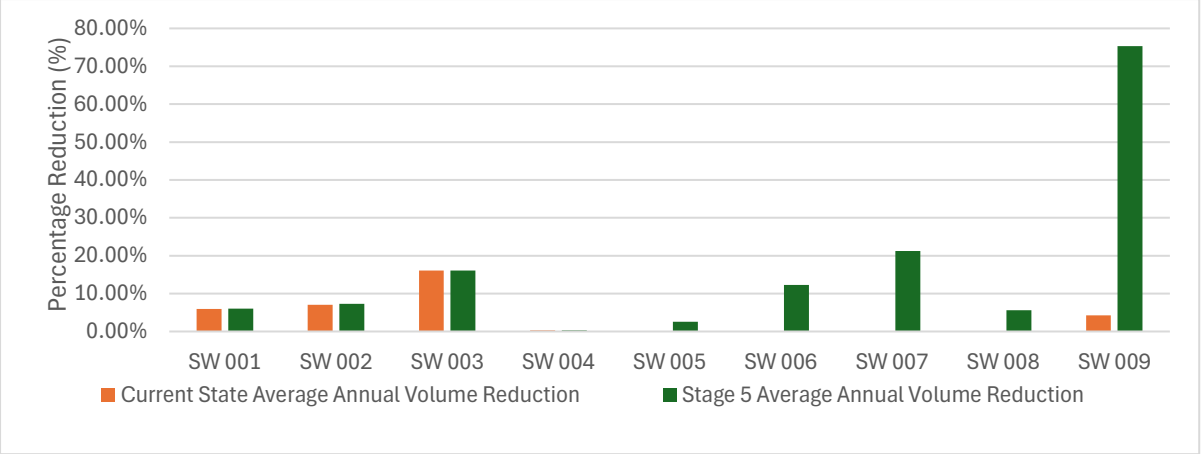

Figure 30. Scenarios 2 and 3: Average annual volume reduction (%)

The results of scenarios 4 through 6 incorporate the climate change RCP8.5 2090 scenario, simulating a long-term record for the year 2090. This modelling aims to understand the impacts of projected climate conditions on average peak flow and annual volume runoff within the catchment areas.

Figure 31 presents the average peak flow reduction, which clearly shows a significant reduction in average peak flow for all scenarios in response to the climate change RCP 8.5 scenario for the year 2090. In Scenario 4: Baseline with climate change, a 23% and 33% reduction in peak flow was observed. This demonstrates the substantial impact that the changing climate could have on hydrological response, even under baseline conditions.

Scenario 5 builds on the baseline by incorporating current conditions alongside the climate change projections. Locations such as SW001 through SW003 and SW004 observed an additional 1% to 9% reduction in peak flow compared to Scenario 4. This indicates that the current mining effects on surface water, when combined with climate change effects, could further reduce peak flow response in certain affected catchments at a local level.

Scenario 6 simulates Stage 5under the climate change projections. While some locations remained unchanged from Scenario 5, reductions were noted in areas such as SW006, SW007, and SW009. These locations saw an increased reduction in average peak flow ranging from 38% to 57%. This scenario highlights areas that may be particularly vulnerable to climate change impacts and Stage 5 operations, however the modelling also highlights the decreasing effect with distance travelled downstream of mining operations and stormwater management.

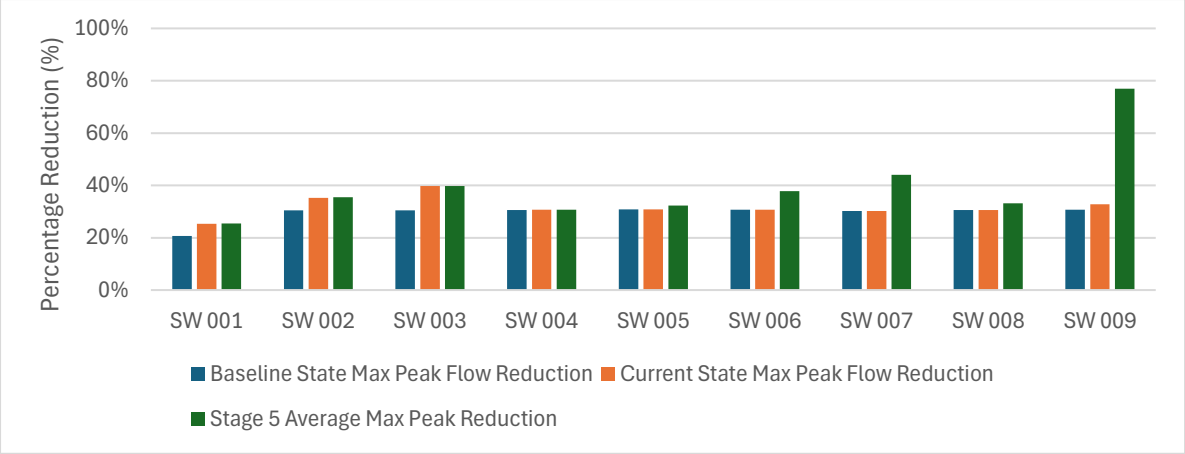

Figure 31. Scenarios 4, 5 and 6: Average peak flow reduction (%)

Volume reduction follows a similar general trend to peak flow reductions, as can be seen in Figure 32. Scenario 4, the baseline with climate change, demonstrated between a 36% and 38% reduction in average annual volume runoff. This reduction increased by an additional 3% to 10% for certain catchments such as SW003 under Scenario 5. For Scenario 6, key catchments like SW006, SW007, and SW009 experienced further reductions ranging from 7% to 44%.

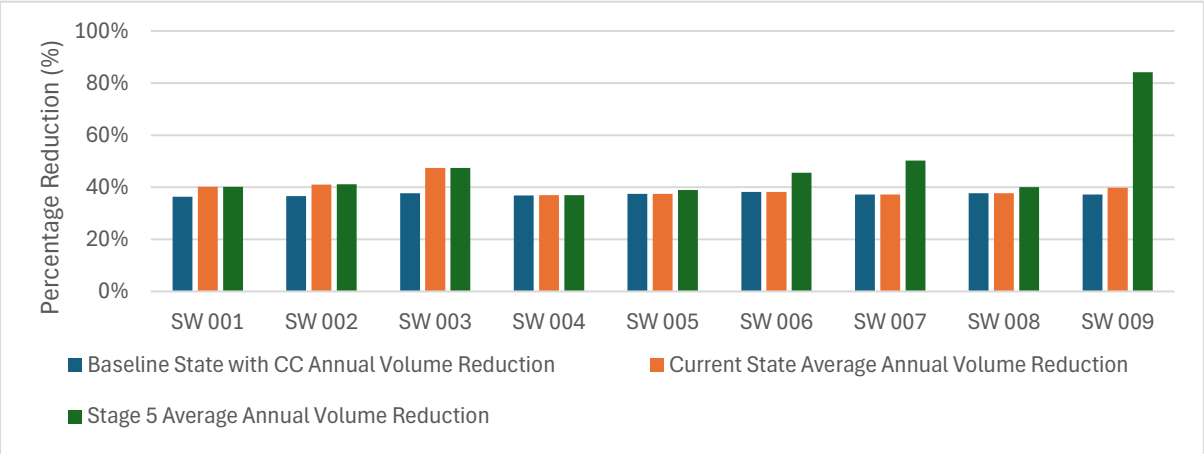

Figure 32. Scenarios 4, 5 and 6: Average annual volume reduction (%)

The progression through to Stage 5 of operations has been modelled to understand its potential impact on hydrological responses within the identified at risk pools. The simulations indicate an average reduction in peak flows of between 2-7%, as illustrated in Figure 33. Similarly, annual volume reductions show a decrease of between 2-7.2%. Among the pools, CS-WS-08 experiences the greatest potential impact. However, this impact still represents less than a 10% reduction in the surface water volumetric yield flowing through CO-WS-08.

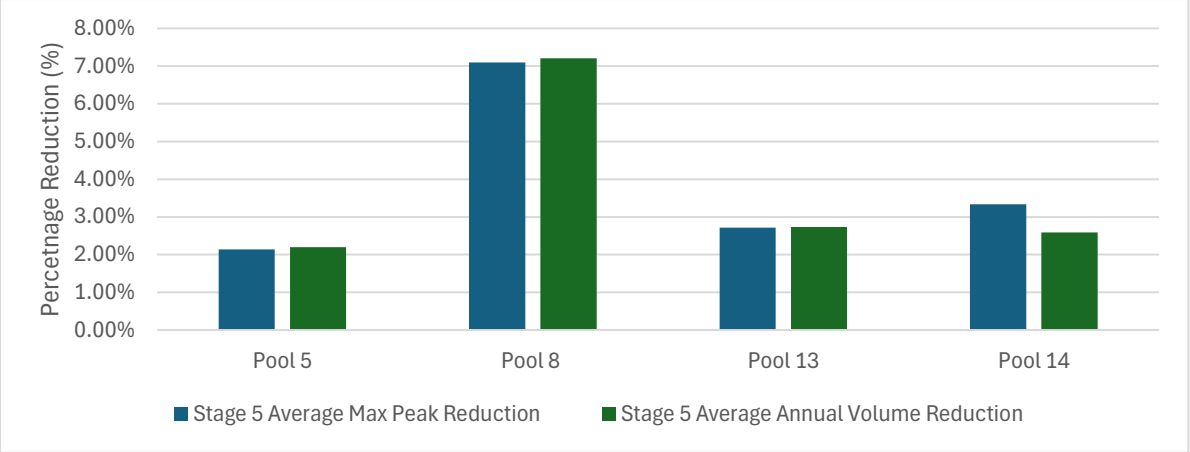

Figure 33. Stage 5 Pool Impacts: Average peak flow and volume reduction

When considering the climate change RCP8.5 scenario for the year 2090, the potential impacts become significantly more pronounced, as summarised in Figure 34. The modelling suggests a much greater reduction in average peak flow response, ranging between 32-35%, and a reduction in annual volume of between 38-41%. These projected changes underscore the influence that climate change could have on the local pool flow regime, surpassing the impacts observed from Stage 5alone.

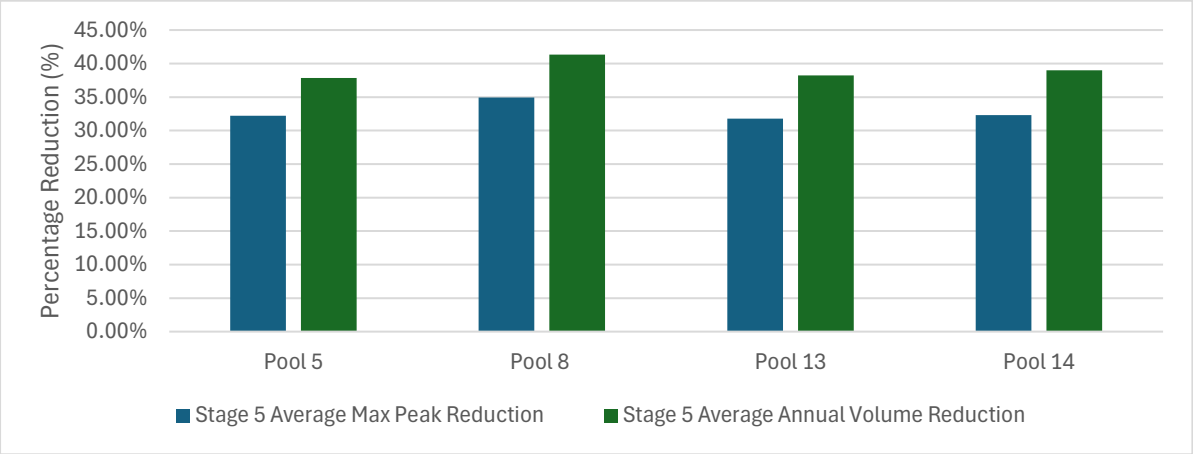

Figure 34. Stage 5 Pool Impacts with Climate Change: Average peak flow and volume reduction

Overall, climate change may have a significant effect on catchment runoff, both in terms of average peak flow and total volumetric yield. It is important to note that these results reflect average peak and volumetric responses and do not account for extreme events, which climate change projections predict to increase in intensity. These extreme events have been modelled separately in the following section as individual design events.

6.2 Design Runoff

6.2.1 Introduction

The previous chapters have detailed the methodology, simulation results, and analysis of a calibrated hydrological model validated against datasets from sites SW001 and SW002. This chapter presents the application of the same calibrated model to simulate design runoff events in line with industry best practise methodology. These simulations are important in understanding the hydrological response under extreme conditions, specifically for the 1%, 2%, 20%, and 50% Annual Exceedance Probability (AEP) events using 24-hour Intensity-Frequency-Duration (IFD) data derived from the Bureau of Meteorology (BOM) in Australia. It also allows for incorporation of predicted climate change affects, which as summarised earlier, is projected to increase the intensity of extreme rainfall events by as much as 77%.

Six scenarios have been modelled, following the same procedure as for the long-term simulation modelling, described as follows:

- Scenario 1: Baseline - a pre-mine natural catchment baseline.
- Scenario 2: Current (2025) - the calibrated model reflecting existing catchment modifications.
- Scenario 3: Stage 5- modifications primarily limited to pit expansion areas and slight modifications to haul road and stockpile areas.
- Scenario 4: Baseline with Climate Change - the pre-mine natural catchment baseline with climate change effects for the RCP8.5 2090 scenario.
- Scenario 5: Current (2025) with Climate Change - the calibrated model reflecting existing catchment modifications, incorporating climate change effects for the RCP8.5 2090 scenario.
- Scenario 6: Stage 5with Climate Change - modifications primarily limited to pit expansion areas and slight modifications to haul road and stockpile areas, including climate change effects for the RCP8.5 2090 scenario.

6.2.2 Intensity-Frequency-Duration Data

The design runoff events were simulated using 24-hour IFD data provided by the BOM. This data is used for estimating the rainfall intensities for specified AEPs, which represent the probability of a particular rainfall event occurring in any given year. The AEPs considered in this study include:

- 1% AEP – representing a 100-year average recurrence interval
- 2% AEP – representing a 50-year average recurrence interval
- 20% AEP – representing a 5-year average recurrence interval
- 50% AEP – representing a 2-year average recurrence interval

Climate change adjustment factors for RCP 8.5 2090, as described in 3.5, have been used to scale the IDF data for Sanjiv Ridge.

6.2.3 Results

The design runoff modelling results, presented in Table 9, illustrate the differences in peak flow responses at various locations, from Scenario 1: Baseline conditions through to Scenario 6: Stage 5with climate change. For the baseline scenario, which simulates a pre-mine drainage system, climate change projections under RCP8.5 2090 see a significant increase from 102.2 m^3/s for the 1% AEP event at SW001 to 193 m^3/s. As presented in Table 11, this represents an 89% increase in peak flow response.

For Stage 2: Current scenario, there is a reduction in extreme runoff peak flow for the current climate scenario of between 3-13%. Notably, SW003 experienced the most significant proportion of catchment changes. In Stage 5, the

reduction in peak flow increased at several locations, with SW007 and SW009 experiencing between 19-67% reduction in the 1% AEP peak flow.

The reductions observed are significantly offset under the RCP 8.5 2090 climate change scenarios modelled in Scenarios 4 through 6. There is an increase in baseline 1% AEP peak flows of between 89-91% across all modelled catchments due to the projected climate change impacts, see Table 10. However, mining effects see this increase slightly reduced. In Scenario 5: Current including climate change, the increase observed is between 64-89%. Scenario 6: Stage 5 including climate change sees further reductions at key locations such as SW007, with a 52% increase. The exception is SW009, which experienced a 38% reduction in the 1% AEP peak flow response.

Table 9. Design Event Modelling Results (m3/s).

Baseline	**1% AEP**	**1% AEP wCC**	**2% AEP**	**2% AEP wCC**	**20% AEP**	**20% AEP wCC**	**50% AEP**	**50% AEP wCC**
SW001	102.2	193	90.0	171.1	49.2	99	30.2	65.8
SW002	44.4	84.2	39.1	74.8	21.3	43.3	12.9	28.5
SW003	8.3	15.7	7.3	14	4	8	2.4	5.3
SW004	23.5	44.6	20.7	39.6	11.3	22.9	6.9	15.1
SW005	14.2	26.9	12.5	23.9	6.8	13.8	4.1	9.1
SW006	6.5	12.4	5.8	11	3.1	6.3	1.9	4.2
SW007	21.8	41.1	19.2	36.6	10.4	20.9	6.4	13.9
SW008	38.6	73.1	34.0	64.9	18.6	37.5	11.4	24.9
SW009	9.5	18.1	8.4	16.1	4.6	9.3	2.8	6.1
Current State	**1% AEP**	**1% AEP wCC**	**2% AEP**	**2% AEP wCC**	**20% AEP**	**20% AEP wCC**	**50% AEP**	**50% AEP wCC**
SW001	96	181.3	84.5	160.7	46.2	92.9	28.3	61.8
SW002	41.3	78.4	36.4	69.7	19.8	40.3	12.1	26.5
SW003	7.2	13.6	6.3	12.1	3.4	6.9	2.1	4.6
SW004	23.4	44.4	20.6	39.5	11.2	22.8	6.8	15.1
SW005	14.2	26.9	12.5	23.9	6.8	13.8	4.1	9.1
SW006	6.5	12.4	5.8	11	3.1	6.3	1.9	4.2
SW007	21.8	41.1	19.2	36.6	10.4	20.9	6.4	13.9
SW008	38.6	73.1	34	64.9	18.6	37.5	11.4	24.9
SW009	9.2	17.4	8.1	15.5	4.4	8.9	2.7	5.9
Stage 5	**1% AEP**	**1% AEP wCC**	**2% AEP**	**2% AEP wCC**	**20% AEP**	**20% AEP wCC**	**50% AEP**	**50% AEP wCC**
SW001	95.8	181	84.4	160.5	46.1	92.8	28.3	61.8
SW002	41.2	78.1	36.3	69.5	19.8	40.2	12	26.5
SW003	7.2	13.6	6.3	12.1	3.4	6.9	2.1	4.6
SW004	23.4	44.4	20.6	39.5	11.2	22.8	6.8	15.1
SW005	13.9	26.2	12.2	23.4	6.6	13.4	4	8.9
SW006	5.9	11.1	5.2	9.9	2.8	5.7	1.7	3.8
SW007	17.6	33.2	15.5	29.6	8.4	16.9	5.1	11.2
SW008	37.2	70.4	32.7	62.4	17.9	36.1	10.9	24
SW009	3.1	5.9	2.8	5.3	1.5	3	0.9	2

Note: wCC denotes scenarios modelled with climate change effects

Table 10. Percentage change in design runoff

	Scenario 2:Current State			
Site ID	**1% AEP**	**2% AEP**	**20% AEP**	**50% AEP**
SW001	-6%	-6%	-6%	-6%
SW002	-7%	-7%	-7%	-6%
SW003	-13%	-14%	-15%	-13%
SW004	0%	0%	-1%	-1%
SW005	0%	0%	0%	0%
SW006	0%	0%	0%	0%
SW007	0%	0%	0%	0%
SW008	0%	0%	0%	0%
SW009	-3%	-4%	-4%	-4%
	Scenario 3: Stage 5			
Site ID	**1% AEP**	**2% AEP**	**20% AEP**	**50% AEP**
SW001	-6%	-6%	-6%	-6%
SW002	-7%	-7%	-7%	-7%
SW003	-13%	-14%	-15%	-13%
SW004	0%	0%	-1%	-1%
SW005	-2%	-2%	-3%	-2%
SW006	-9%	-10%	-10%	-11%
SW007	-19%	-19%	-19%	-20%
SW008	-4%	-4%	-4%	-4%
SW009	-67%	-67%	-67%	-68%

Table 11. Percentage change in design runoff including climate change

	Scenario 4:Baseline			
Site ID	**1% AEP wCC**	**2% AEP wCC**	**20% AEP wCC**	**50% AEP wCC**
SW001	89%	90%	101%	118%
SW002	90%	91%	103%	121%
SW003	89%	92%	100%	121%
SW004	90%	91%	103%	119%
SW005	89%	91%	103%	122%
SW006	91%	90%	103%	121%
SW007	89%	91%	101%	117%
SW008	89%	91%	102%	118%
SW009	91%	92%	102%	118%
	Scenario 5:Current State			
Site ID	**1% AEP wCC**	**2% AEP wCC**	**20% AEP wCC**	**50% AEP wCC**
SW001	77%	79%	89%	105%
SW002	77%	78%	89%	105%
SW003	64%	66%	73%	92%

SW004	89%	91%	102%	119%
SW005	89%	91%	103%	122%
SW006	91%	90%	103%	121%
SW007	89%	91%	101%	117%
SW008	89%	91%	102%	118%
SW009	83%	85%	93%	111%
	Scenario 6:Stage 5			
Site ID	**1% AEP wCC**	**2% AEP wCC**	**20% AEP wCC**	**50% AEP wCC**
SW001	77%	78%	89%	105%
SW002	76%	78%	89%	105%
SW003	64%	66%	73%	92%
SW004	89%	91%	102%	119%
SW005	85%	87%	97%	117%
SW006	71%	71%	84%	100%
SW007	52%	54%	63%	75%
SW008	82%	84%	94%	111%
SW009	-38%	-37%	-35%	-29%

7 Summary

Of all the surface water monitoring locations, SW009, SW007, and SW006 see the greatest change in catchment area due to pit expansion, ranging from a 19-67% reduction in catchment size relative to baseline conditions. Only four identified surface pools observe a reduction in catchment size, C0-WS-05, C0-WS-08, C0-WS-13 and C0-WS-14 ranging from 2-7%, with CO-WS-08 experiencing the greatest reduction at 7%.

Impact modelling results suggest the greatest localised effect on streamflow occurs in the catchment with the greatest area reduction, SW009, with a 68% reduction in average peak runoff and a 75% reduction in runoff volume. The SW009 monitoring location is located closely downstream of the proposed Sparrow Lake pit; however, other monitoring locations highlight the decreasing effects with increasing distance downstream of the disturbance. SW001, for example, located downstream of SW002 and SW003, observes up to a 40% reduction in peak runoff and 16% reduction in runoff volume under the current operation compared to baseline, with a reduced effect with increased non-disturbed catchment area contributing to runoff, with a 12.5% reduction in average peak runoff and 6% reduction in average volume. Only a 0.14% decrease in peak flow is projected at SW002 under Stage 5 operations, which translates to 0% change at SW001 due to additional undisturbed inflows. Overall, although some locations such as SW009 indicate significant reductions in both peak flow and volume, these are localised effects, and these effects are shown to diminish exponentially with distance downstream.

Modelling impacts on the pools suggest a reduction in peak flow flushing between 2% and 7%, with a similar reduction in overall volume. It is not anticipated that this would have a significant effect on total storage due to the limited storage capacity of each pool versus the small reduction, with seasonal throughflow likely to persist. The limiting factor remains the storage potential and evaporative losses during dry periods, rather than the overall total discharge volume and peak flow rates.

The combined impact of mining and climate change projections reveals that while mining operations have a localised effect on streamflow reduction, it is the climate change projections that potentially present a far more significant impact to the hydrological flow regime in the Project area. Modelled projections for the RCP 8.5 2090 baseline scenario

(without mining operations) suggest an average decrease in average peak flow response of between 21-31%, with a 36-38% reduction of average annual runoff volume. Current state (2025) mining operations are likely to see this increase to between a 25-40% reduction in average peak flows, and between 37-47% reduction in average annual runoff volume. Stage 5 is likely to see this increase slightly more in affected catchments, with between a 25-77% decrease in average peak flow, and between 37-84% reduction in average annual runoff volume (noting SW009 is the most affected catchment, by a significant margin).

In conclusion, the impacts of Stage 5 at Sanjiv Ridge are unlikely to have more than a minor effect on streamflow within the local area, except for localised effects such as immediately downstream of locations such as SW009. The localised effects decrease rapidly with increasing distance from the mine, suggesting minimal long-term impact on the broader hydrological system, and no significant effects on identified pools within the Project area.

Overall, the total catchment reduction due to Stage 5represents less than 0.016% of the total Coongan catchment, as measured from the Marble Bar gauge. This is a very small percentage of the regional catchment, suggesting that although alterations to the surface water flow regime may have a localised effect, small catchment reductions in streamflow response will be insignificant within the regional catchment, and dissipate rapidly with distance downstream from the mine.

7.1 Limitations and Future Work

While the current modelling provides valuable insights as to the potential impact of both mining operations and climate change on the local and regional flow regime, there are limitations that could be addressed in future work. The calibration of the hydrological model has been based on a relatively short-term record of surface water discharge, however provides significantly lower uncertainty compared to the use of an uncalibrated model. Incorporating more years of monitoring data would potentially enhance the accuracy of the model in the future, allowing for calibration across both wet and dry years which would help capture the variability in hydrological responses and improve the robustness of the predictions.

8 REFERENCES

Ball, J et al., 2016, Australian Rainfall and Runoff: A Guide to Flood Estimation, Commonwealth of Australia, Available from: http://arr.ga.gov.au/arr-guideline

Bureau of Meteorology (BOM), 2016a. Climate Data Online [online]. Available at: http://www.bom.gov.au/climate/data/. Accessed November 2025.

Bureau of Meteorology (BOM) 2016b. Intensity Frequency Duration (IFD) data http://www.bom.gov.au/water/designRainfalls/ifd/. Accessed November 2025.

Clarke JM, Whetton PH, Hennessy KJ (2011) 'Providing Application-specific Climate Projections Datasets: CSIRO's Climate Futures Framework.' Peer-reviewed conference paper. In F Chan, D Marinova and RS Anderssen (eds.) MODSIM2011, 19th International Congress on Modelling and Simulation. Perth, Western Australia. December 2011 pp. 2683-2690. ISBN: 2978-2680-9872143-9872141-9872147. (Modelling and Simulation Society of Australia and New Zealand). http://www.mssanz.org.au/modsim2011/F5/clarke.pdf.

Corunna Downs Project: Soil Resource Assessment And Waste Characterisation, MWH, December 2016

Department of Water (DOW), 2016. Water Information Reporting (WIR) [online]. Available at: http://wir.water.wa.gov.au/Pages/Water-Information-Reporting.aspx, accessed November 2025.

Department of Mines and Petroleum (DMP), 2006, Guidelines for Mining Proposals in Western Australia. [online]. Available at: http://dmp.wa.gov.au/

Kokic P, Breckling J, Lübke O (2002) 'A new definition of multivariate M-quantiles.' in Statistical Data Analysis Based on the L1-Norm and Related Methods. (Y Dodge ed.) pp. 15-24. (Birkhäuser Verlag: Basel).

Huffman, G.J., D.T. Bolvin, E.J. Nelkin, and NASA/GSFC/GMAO (2023), *IMERG Final Precipitation L3 Half Hourly 0.1° x 0.1° V06*, Greenbelt, Maryland, USA, Goddard Earth Sciences Data and Information Services Center (GES DISC), Accessed: November, 2024, https://giovanni.gsfc.nasa.gov/giovanni/Ruprecht et al, 2000. Surface Hydrology of the Pilbara Region, Summary Report. Water and Rivers Commission, Surface Water Hydrology Report Series, Report No SWH 32

Snyder, F. F. (1938). Synthetic Unit-Graphs. Transactions, American Geophysical Union, 19, 447–45

Water and Rivers Commission. (1999). *Water Quality Protection Guidelines (Nos. 1–11), Mining and Mineral Processing*. Water and Rivers Commission, Government of Western Australia. ISSN 1329-0746. Retrieved from Water Quality Management in Mining and Mineral Processing – WA Government

Whetton P, Hennessy K, Clarke J, McInnes K, Kent D (2012) 'Use of Representative Climate Futures in impact and adaptation assessment.' Climatic Change 115, 433-442. 10.1007/s10584-012-0471-z.

Appendix F Water Balance Report

SRK Consulting (Australasia) Pty Ltd
Level 3, 18–32 Parliament Place
West Perth WA 6005
Australia

ABN: 56 074 271 720

+61 8 9288 2000

info@srk.com.au
www.srk.com

Final – Rev2

Technical Memorandum

To	David Nyquest	**Client**	Atlas Iron Pty Ltd
From	Lachlan Gibbins	**Project**	ATL009
Cc	Richard Cheal	**Date**	27 May 2025

Subject Pit Void Water Balance Modelling: Sanjiv Ridge Stage 5 Below Water Table Mining Hydrogeology Study, WA, Australia

1 Introduction

Atlas Iron Pty Ltd (Atlas) is currently developing the Sanjiv Ridge (formerly Corunna Downs) project (the Project) from Phase 4 (above the water table) to Stage 5 (below the water table). The Project is located in the Pilbara region of Western Australia and involves the mining of iron ore from five open pits using conventional drill and blast methods (Figure 1.1). Atlas engaged SRK Consulting (Australasia) Pty Ltd (SRK) to complete hydrogeological drilling, testing and modelling during the Phase 4 mining studies that were completed in 2019. Atlas further engaged with SRK during 2023 and 2024 on the following Phase 5 studies:

- hydrogeological drilling and testing
- surface water catchment characterisation and flood modelling
- groundwater numerical modelling
- pit void water balance modelling.

Post closure, following cessation of dewatering, it is anticipated that permanent pit lakes will form within the pit voids mined below the water table (Runway, Shark Gully and Sparrow Lake [formerly Split Rock] pits) and that the pit lake elevations will be below the local groundwater table. It is anticipated that the lakes will act as permanent groundwater sinks (based on pit lake water balances generated for supplied pit shell designs).

Post-closure water balances were developed for the pit lakes that are anticipated to form within the pit voids present at the end of life of mine. These voids comprise Glen Herring South, Runway South, Shark Gully and Sparrow Lake (formerly Split Rock).

Figure 1.1: Atlas Project approximate layout

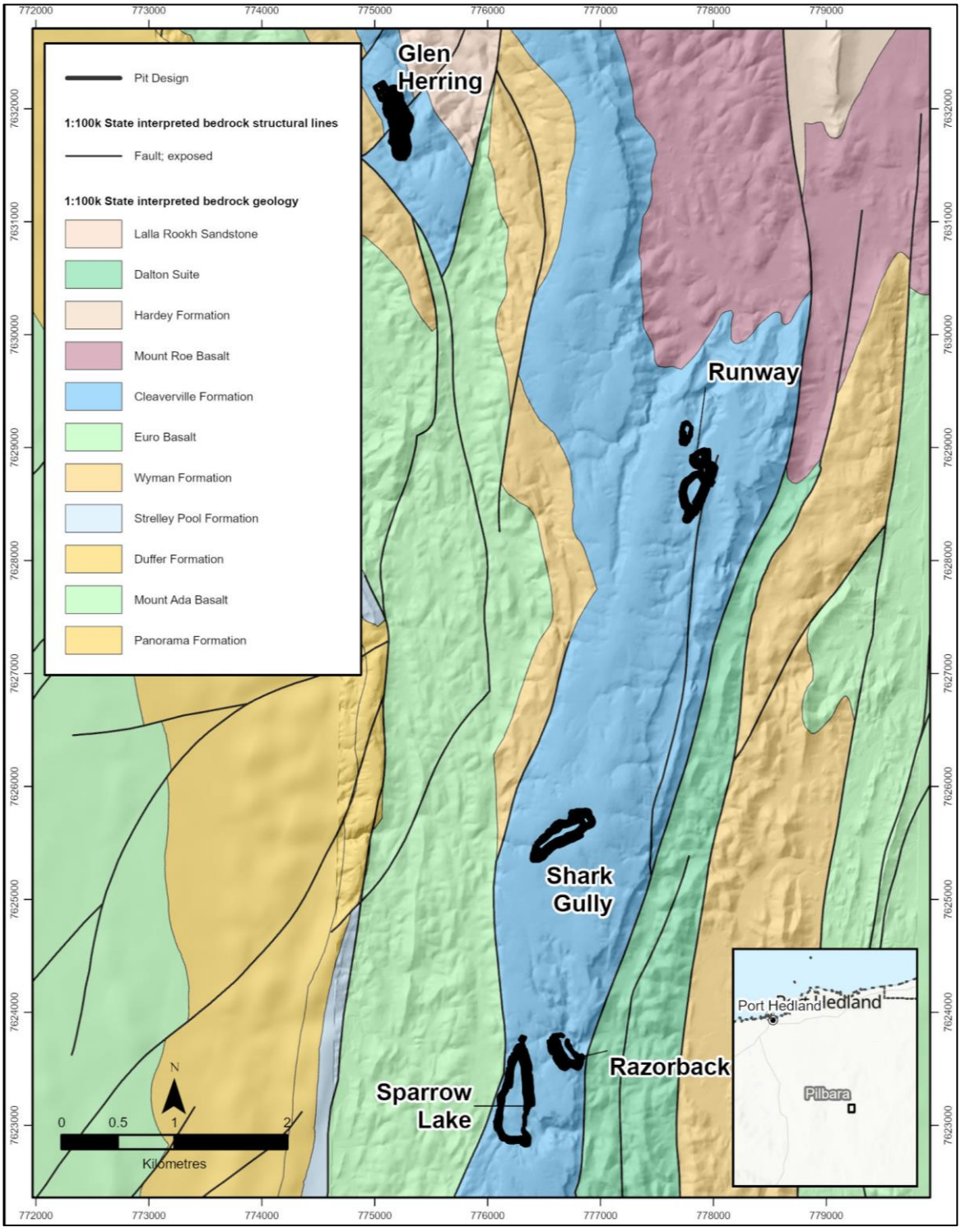

Source: SRK

A conceptual post-closure water balance for the pit void is as follows:

$$\textit{Change in pit lake water volume over time} = \sum \textit{inflows} - \sum \textit{outflows}$$

which can be expressed as:

$$\Delta \textit{ pit lake water volume} = P_{precip} + R_{runoff} + GW_{inflow} - E_{pit}$$

where:

- P_{precip} is the inflow from direct precipitation falling on the surface of the pit lake (m^3/time step)
- R_{runoff} is the inflow from pit wall runoff (the fraction of precipitation falling on the pit walls that ultimately reports to the pit lake)
- GW_{inflow} is the groundwater inflow to the pit lake (m^3/time step) and is positive when the water level of the lake is below the local water table, zero when it is at the same elevation, and becomes negative (i.e. outflow) if the level rises above the local water table
- E_{pit} is the open water evaporation from the pit lake surface based on a modified pan evaporation rate applied to the pit lake surface area (m^3/time step).

2 Modelling objectives

The model was developed as a tool to evaluate the final water level after closure for Sanjiv Ridge pits with the specific objective to:

- assess the range of pit lake water elevations for the post-closure period, including estimating the minimum water levels and potential for spillage to surface water outside of the pit.

3 Model construction

To meet the model objective a preliminary predictive pit lake water balance has been developed, using a dynamic system model in the GoldSim (v. 15) software platform. The GoldSim platform can be used for probabilistic simulation (Monte Carlo) to evaluate the potential uncertainty and variability in model input parameters related to groundwater and surface water.

The model runs on a daily time step and reports on a monthly time step basis, consistent with the level of data available. The pit water balance contemplates closure conditions (400 years). Note that an arbitrary start date of 1 January 2026 is adopted for the simulations.

3.1 Climate

3.1.1 Rainfall

The WGEN weather simulator uses monthly and annual statistics to generate daily time series of precipitation, minimum temperature, maximum temperature and solar radiation (Figure 3.1). The occurrence of rain on a given day has a major influence on temperature and solar radiation for the day. The approach that is used is to generate precipitation for a given day independently of the other variables. Maximum temperature, minimum temperature and solar radiation are then generated according to whether a wet day or dry day was previously generated. The model is designed to preserve the dependence in time, the correlation between variables, and the seasonal

characteristics in actual weather data for the location. Data used to inform the WGEN model come from the Marble Bar weather station (station number 4106) (SILO, 2024) for the period from 1 January 1956 to 14 April 2025.

Figure 3.1: WGEN simulated precipitation for modelled period

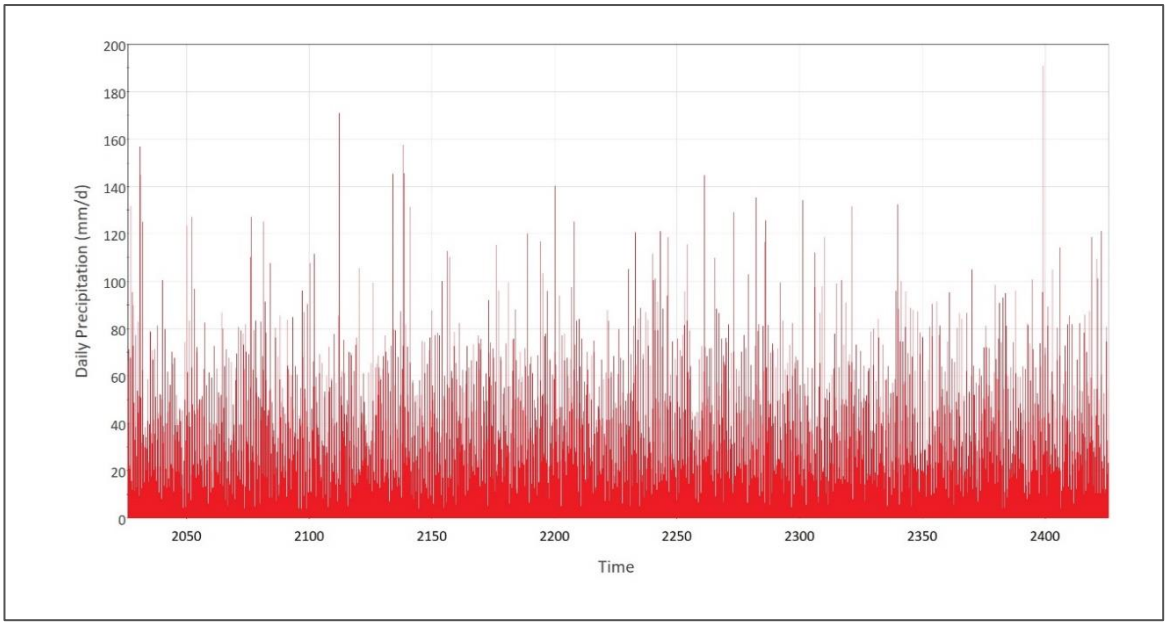

3.1.2 Evaporation

This model uses two methods to estimate evaporation:

1. The Hargreaves-Samani equation to estimate evaporation on exposed pit walls. The model is run on a 1-day time step and estimates evapotranspiration (ET0) using only minimum and maximum daily temperature time series and latitude inputs (Figure 3.2). This model is a model considered suitable for sites that lack measured radiation data. As ET0 is a reference evapotranspiration, a suitable conversion factor is applied to estimate actual evaporation from pit walls and open ground.
2. Hamon Lake Evaporation method to estimate daily evaporation from the pit lake surface. The Hamon method is a widely used approach for calculating evaporation based on climate drivers such as air temperature, solar declination and maximum daylight hours.

Figure 3.2: Simulated evaporation for modelled period

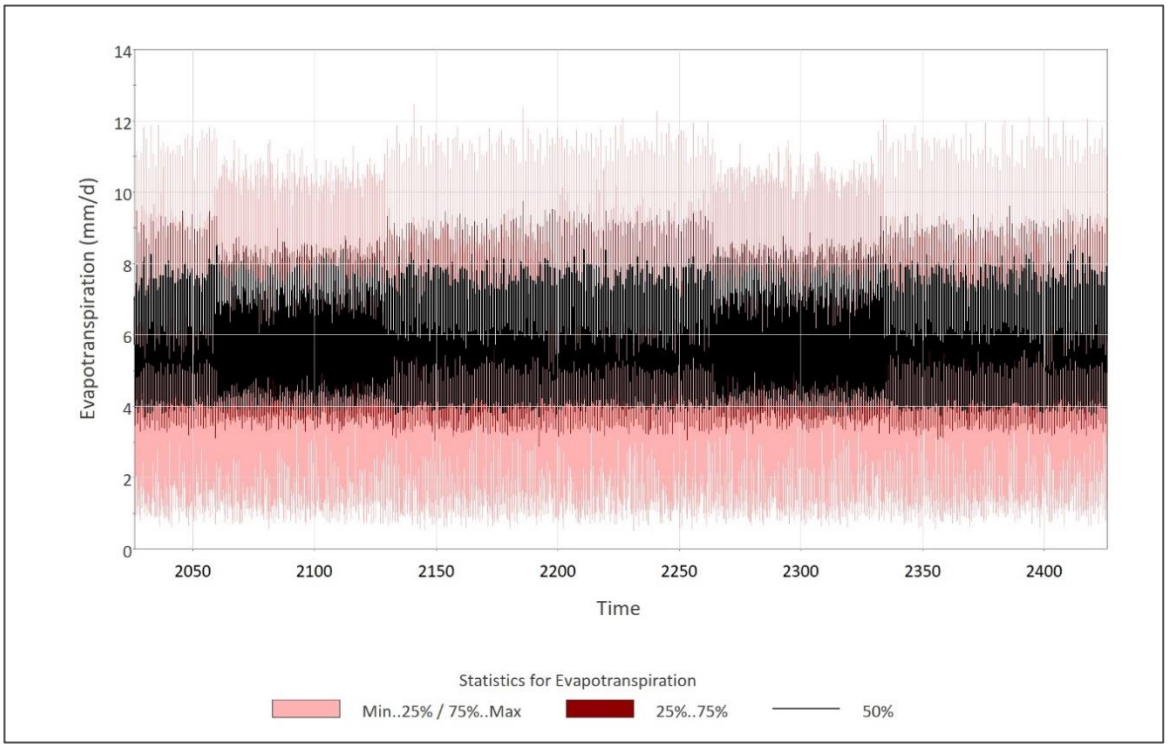

3.2 Pit water balance inflows

3.2.1 Pit wall runoff

The methodology for determining runoff estimates from the pit wall was developed using the Australian water balance model (AWBM). The AWBM is a lumped, daily rainfall-runoff model developed for the estimation of flows in ungauged catchments (see Boughton, 2003). The model applies daily rainfall and estimated evaporation data to derive daily runoff based on a set of model parameters. Surface runoff volumes are calculated daily and vary relative to time between rainfall events proportional to water volumes in near surface storage (infiltration). Total runoff volume is produced by the model by summing surface runoff and seepage from near surface storage.

3.2.2 Direct precipitation

Direct precipitation to the pit floor (or pit lake during closure) is calculated for each time step by multiplying the stochastic precipitation data by the surface area of the pit lake when formed.

3.2.3 Upgradient catchment runoff

It is assumed that the pit is bunded, i.e. upgradient catchment runoff is diverted and is not factored into the water balance.

3.2.4 Groundwater Inflow

Groundwater inflow values were taken from the modelled groundwater inflow values produced by SRK (2025) (Figure 3.3). The water level around the pits is known to be variable due to structurally controlled lithological compartmentalisation.

For the purposes of the water balance, water levels for Shark Gully, in late 2024, range between 400 and 410 mADH (30–40 m below current pit base). Water levels for Runway at the same time, range between 320 and 370 mADH (5–55 m below current pit depth), and water levels for Sparrow Lake range between 350 and 360 mADH (40–50 m below current pit base)

Figure 3.3: Groundwater inflow relative to pit lake elevation

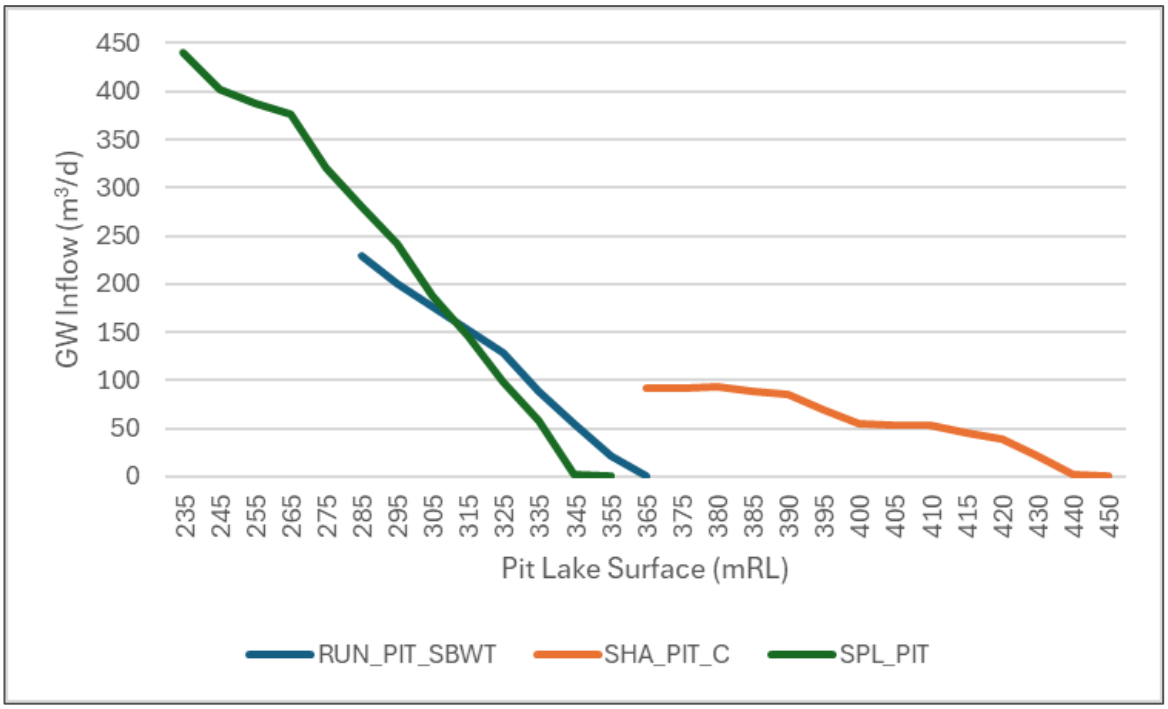

Source: SRK

3.3 Pit water balance outflows

3.3.1 Evaporation

Evaporation in the model is applied separately to the pit lake and the exposed pit walls, where the area of exposed pit wall is proportionally reduced by the area covered by water.

When calculating runoff from the pit wall, the AWBM method accounts for evaporation from the soil by multiplying the catchment area by the daily calculated evaporation factor. In this model, the ET0 value has a factor of 1.3 applied to represent evaporation from open ground.

Loss of water by evaporation from the pit lake surface is calculated for each time step by multiplying the stochastic evaporation data from the Hamon Lake Evaporation model by the surface area of the pit lake. The quantity of water lost to the atmosphere via evaporation is proportional to the area of the pit lake and varies with time.

3.3.2 Seepage to groundwater

It is assumed that while the pit lake is below the water table the lake will be in balance and there will be no losses to the groundwater table.

3.4 Pit geometry

The pit geometry is input using look-up tables for the pit elevation versus surface area (2D) and pit elevation versus volume correlations based on the final pit geometries (Table 3.1). The relationships used in the model between elevation and area, and elevation and volume, are shown for each pit in Figure 3.4 and Table 3.2.

Table 3.1: Data sources for Sanjiv Ridge geometries

Pit name	Source	Comments
RUN_PIT_SBWT	RUN_PIT_C_SBWT2_V1.dxf	Below water table pit
SHA_PIT_C	SHA_PIT_C_BWT_V2.dxf	Below water table pit
SPL_PIT	SPL_PIT_C_BWT2_V3.dxf	Below water table pit

Source: Atlas Mining

3.5 Basis of design

Table 3.2: Model input parameters

Parameter	Proposed value	Comment
Site	Sanjiv Ridge Mine, Western Australia	Client
Coordinate zone	GDA94/MGA zone 50	Client
Pit areas (km^2)	RUN_PIT_SBWT 161.2 SHA_PIT_C 158.7 SPL_PIT 286.5	Client data
AWBM parameters	A1 0.134 A2 0.433 A3 0.433 C1 5 C2 20 C3 40 C_Avg 27 BFI 0 Kb 0.95 Ks 0.35	SRK assumption
Climate inputs	Marble Bar weather station (station number 4106) Period 01/01/1956 to 14/04/2025 ■ Temperature ■ Solar radiation ■ Rainfall	Silo, 2024

Figure 3.4: Stage elevation and stage area curves for Project pits

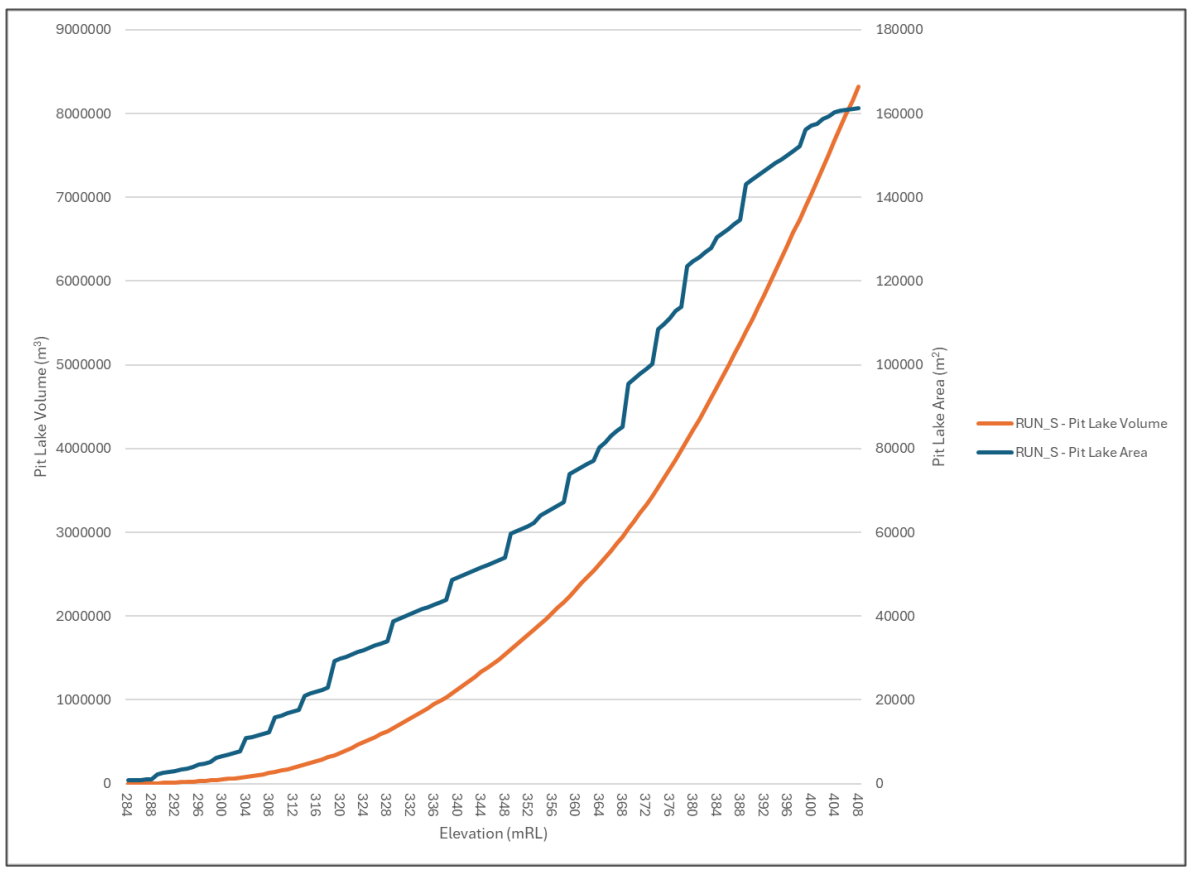

Runway South

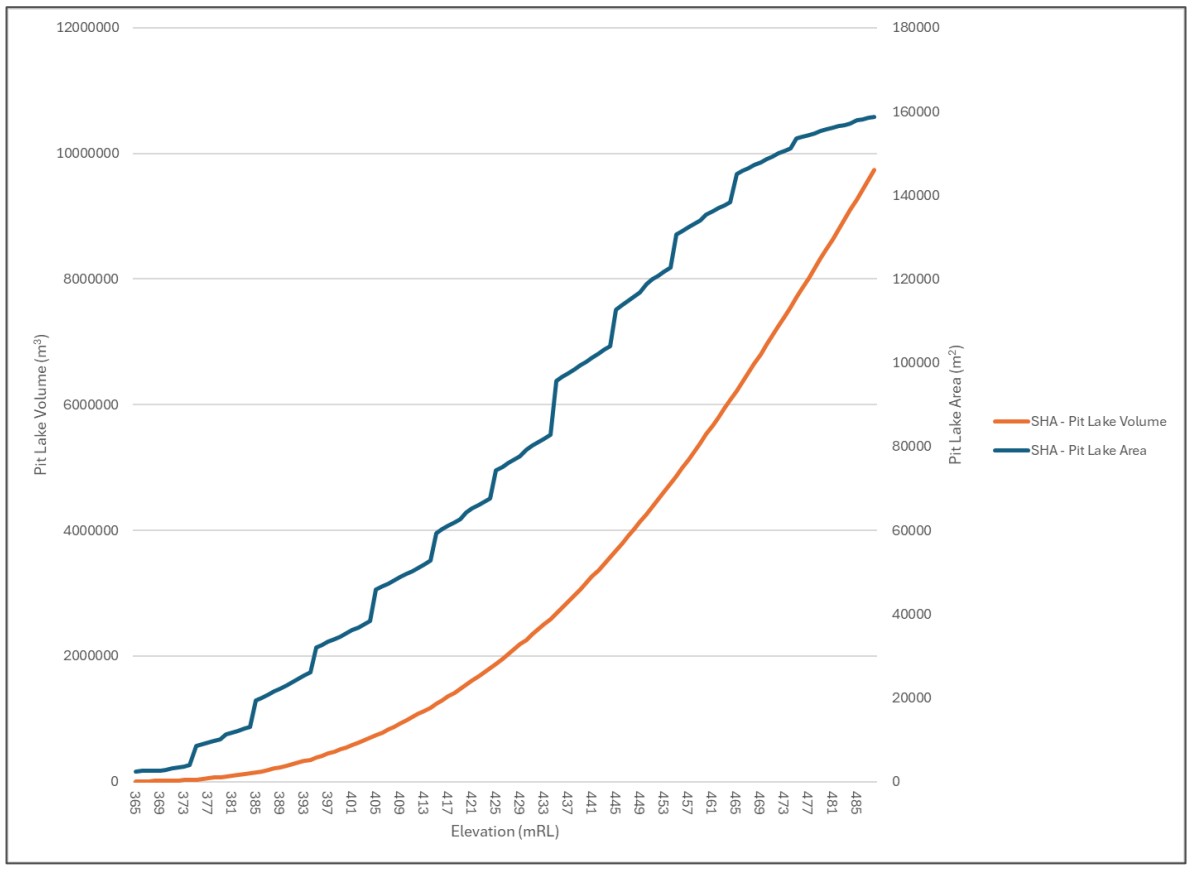

Shark Gully

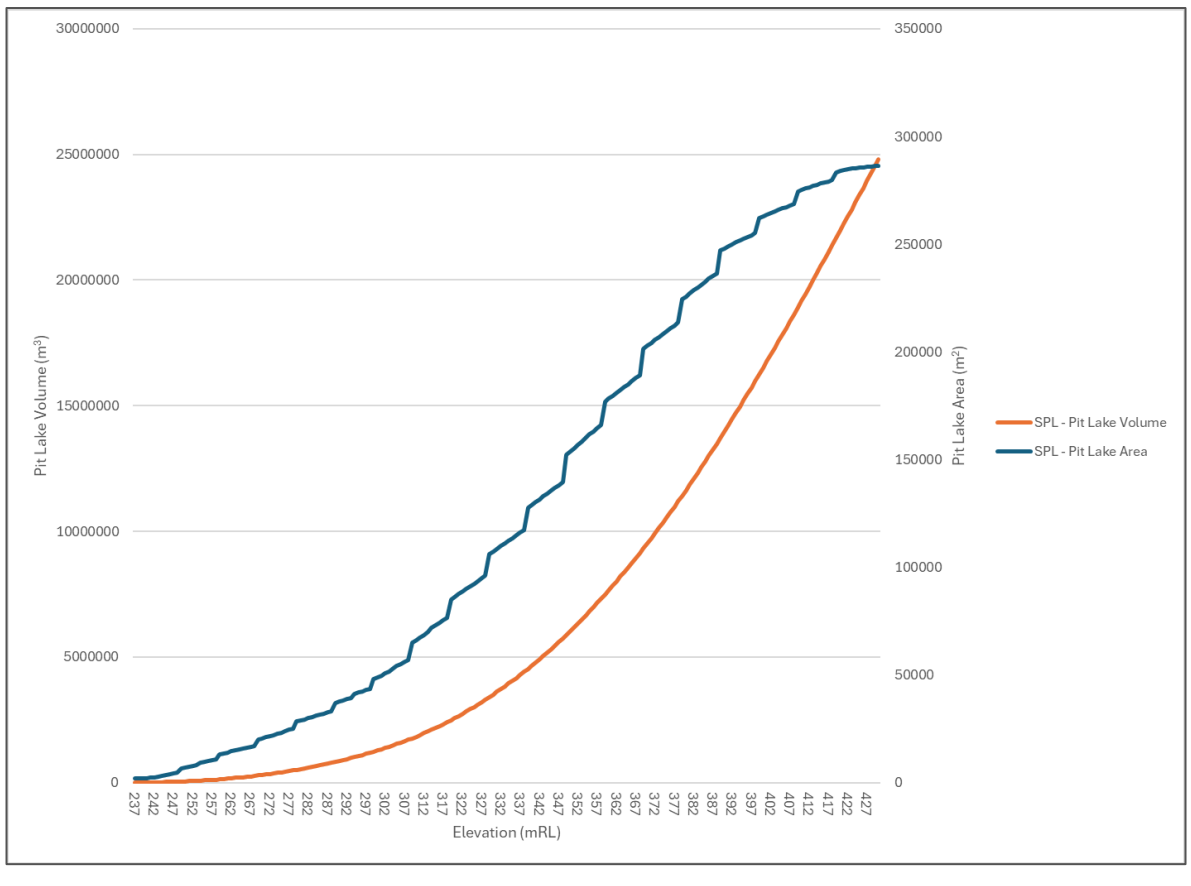

Sparrow Lake

4 Results

The model was constructed to simulate the system on daily time steps from a nominal start date of 1 January 2026 for a 400-year period post closure. The results are presented as statistical probabilities based on the results of 100 realisations of a Monte Carlo analysis. Probabilistic Monte Carlo statistical results are presented to allow assessment of uncertainty in model results to climatic (precipitation and evaporation) inputs.

4.1 Runway South

The post-closure predicted pit lake fluxes for the Runway South pit are presented in Figure 4.1 and predicted pit lake rebound is presented in Figure 4.2. Results for the pit lake rebound include the minimum, maximum, median, 5th percentile and 95th percentile Monte Carlo statistical results and are summarised in Table 4.1.

Table 4.1: Summary of Runway South steady state conditions

Parameter	Units	Minimum	5th percentile	Average	Median	95th percentile	Maximum
Runway South water levels	mRL	389.9	391.9	393.3	393.4	394.6	396.6

The median result shows that the steady state water level in the Runway South pit occurs at 393 mRL after around 31 years post closure and with a maximum variation of around 4 m, indicating that the pit will remain a groundwater sink over the long term under the modelled conditions.

The long-term average of post-closure pit water level is expected to remain below the regional groundwater level, and therefore it is not expected to spill to the surface or contribute water to local aquifers.

Figure 4.1: Runway South post-closure pit flux

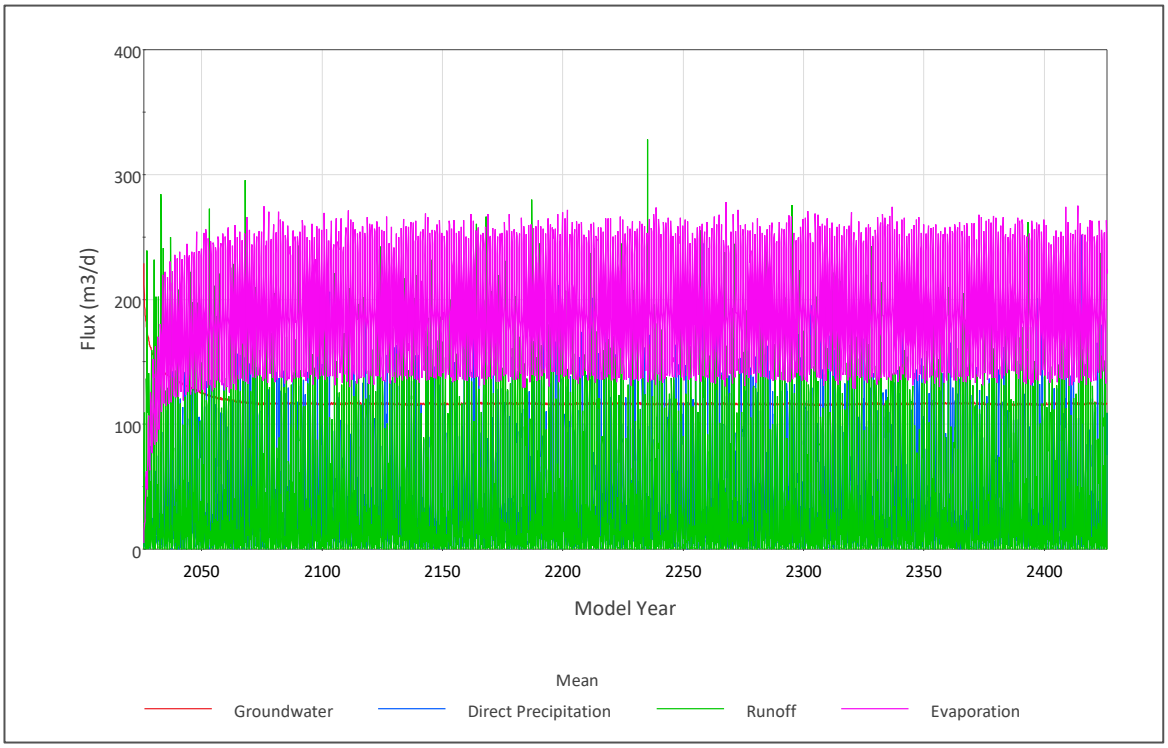

Figure 4.2: Runway South pit lake rebound

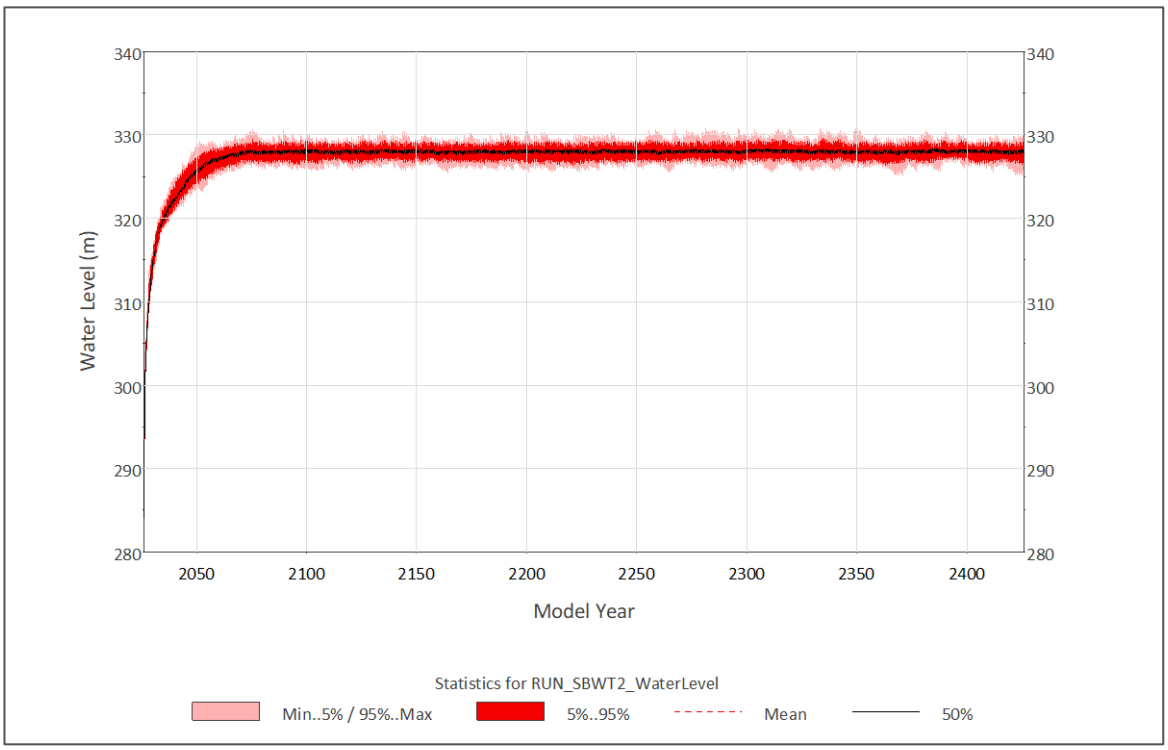

4.2 Sparrow Lake

The post-closure predicted pit lake fluxes for the Sparrow Lake pit are presented in Figure 4.3 and predicted pit lake rebound is presented in Figure 4.4. Results for the pit lake rebound include the minimum, maximum, median, 5th percentile and 95th percentile Monte Carlo statistical results and are summarised in Table 4.2.

Table 4.2: Summary of Sparrow Lake steady state conditions

Parameter	Units	Minimum	5th percentile	Average	Median	95th percentile	Maximum
Sparrow Lake water levels	mAHD	303.0	305.3	306.9	307.0	308.4	310.5

The median result shows that the steady state water level in the Sparrow Lake pit occurs at 307 mRL after around 71 years post closure and with a maximum variation of around 5 m, indicating that the pit will remain a groundwater sink over the long term under the modelled conditions.

The long-term average of post-closure pit water level is expected to remain below the local groundwater level, and therefore it is not expected to spill to the surface or contribute water to local aquifers.

Figure 4.3: Sparrow Lake post-closure pit flux

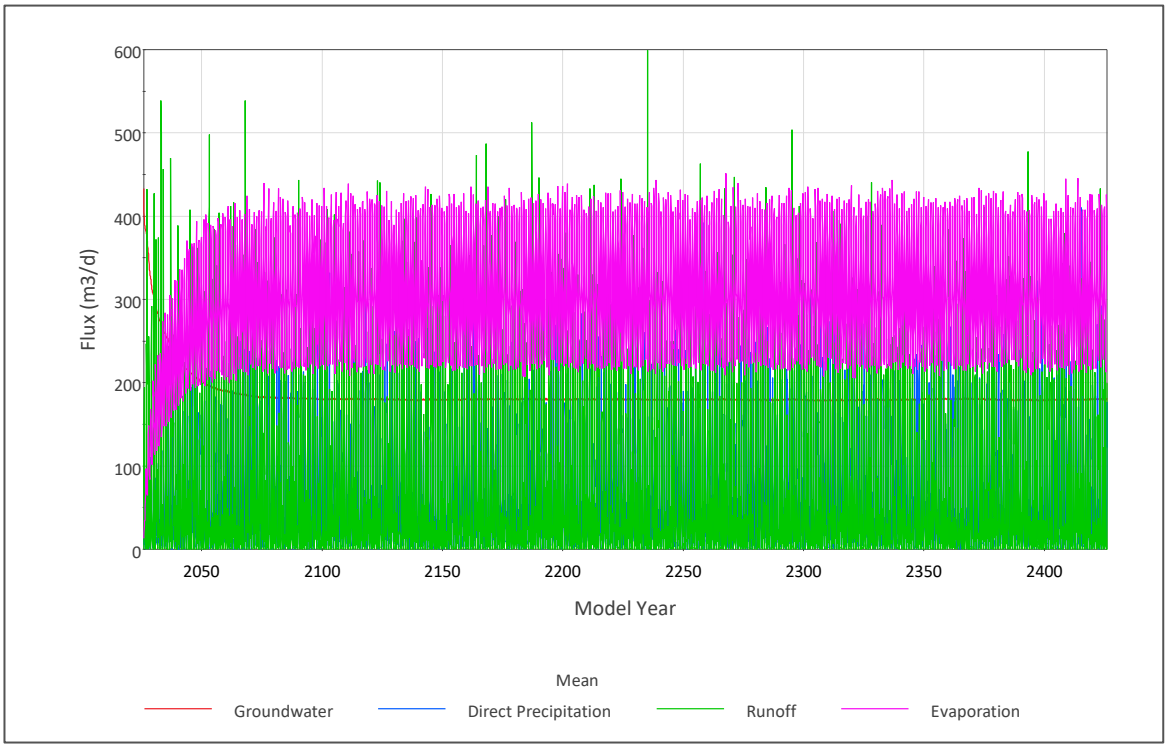

Figure 4.4: Sparrow Lake pit lake rebound

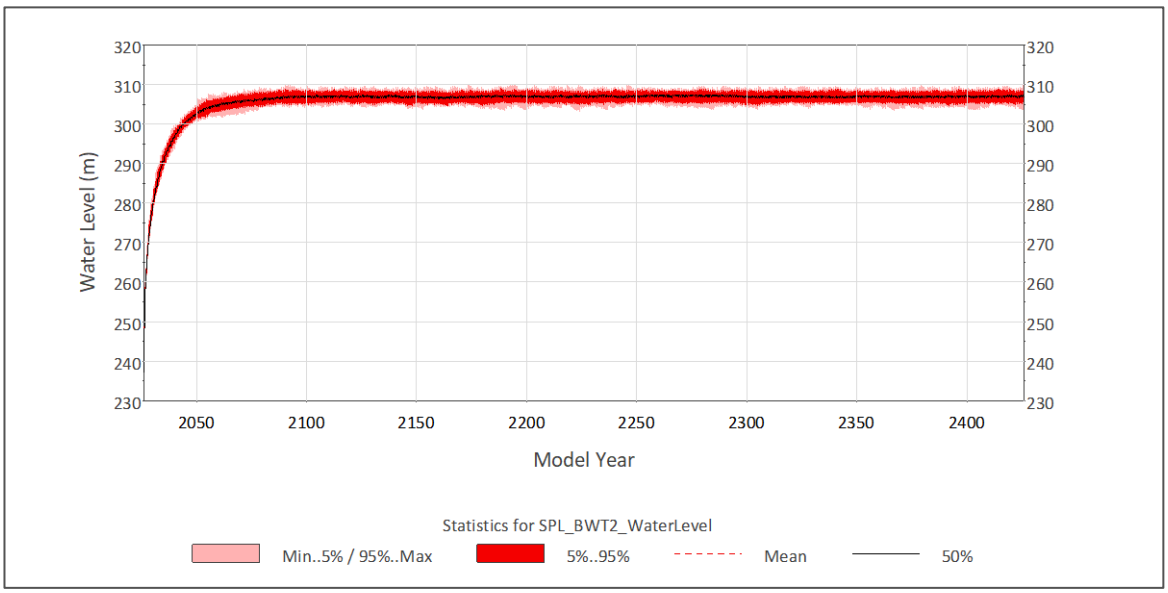

4.3 Shark Gully

The post-closure predicted pit lake fluxes for the Shark Gully pit are presented in Figure 4.5 and predicted pit lake rebound is presented in Figure 4.6. Results for the pit lake rebound include the minimum, maximum, median, 5th percentile and 95th percentile Monte Carlo statistical results and are summarised in Table 4.3.

Table 4.3: Summary of Shark Gully steady state conditions

Parameter	Units	Minimum	5th percentile	Average	Median	95th percentile	Maximum
Shark Gully water levels	mAHD	389.9	391.2	392.8	393.4	394	396.6

The median result shows that the steady state water level in the Shark Gully pit occurs at 393 mRL after around 31 years post closure and with a maximum variation of around 4 m, indicating that the pit will remain a groundwater sink over the long term under the modelled conditions.

The long-term average of post-closure pit water level is expected to remain below the regional groundwater level, and therefore it is not expected to spill to the surface or contribute water to local aquifers.

Figure 4.5: Shark Gully post-closure pit flux

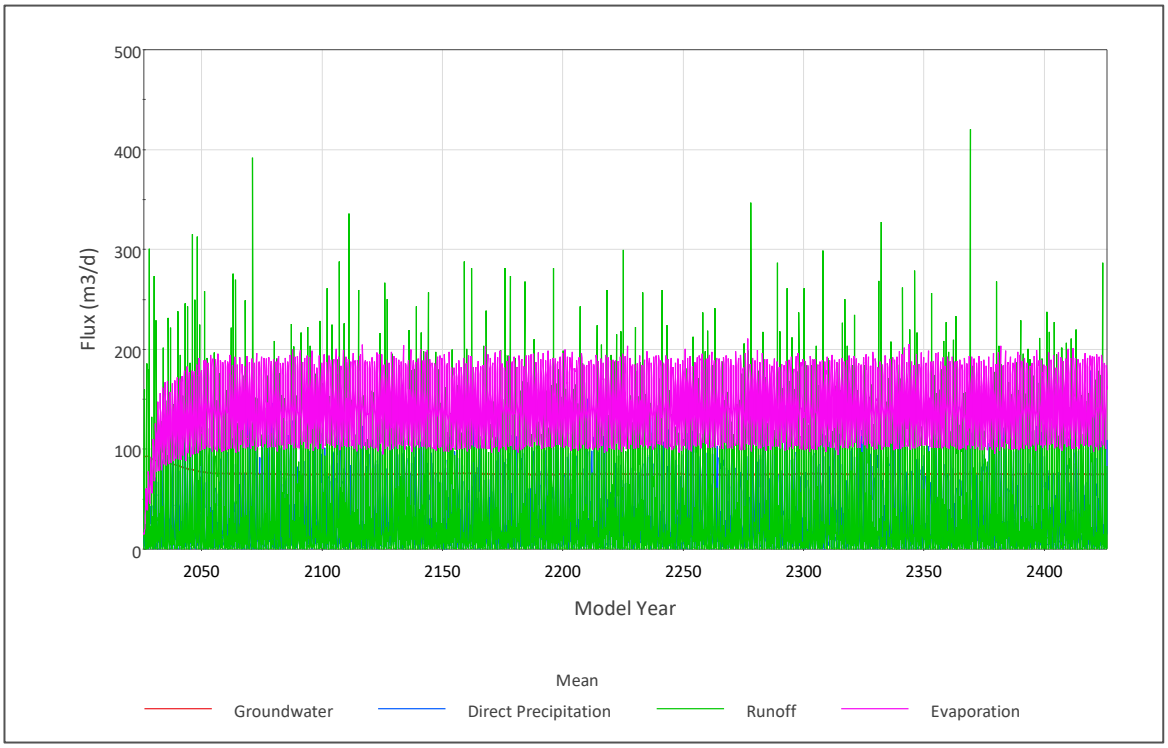

Figure 4.6: Shark Gully pit lake rebound

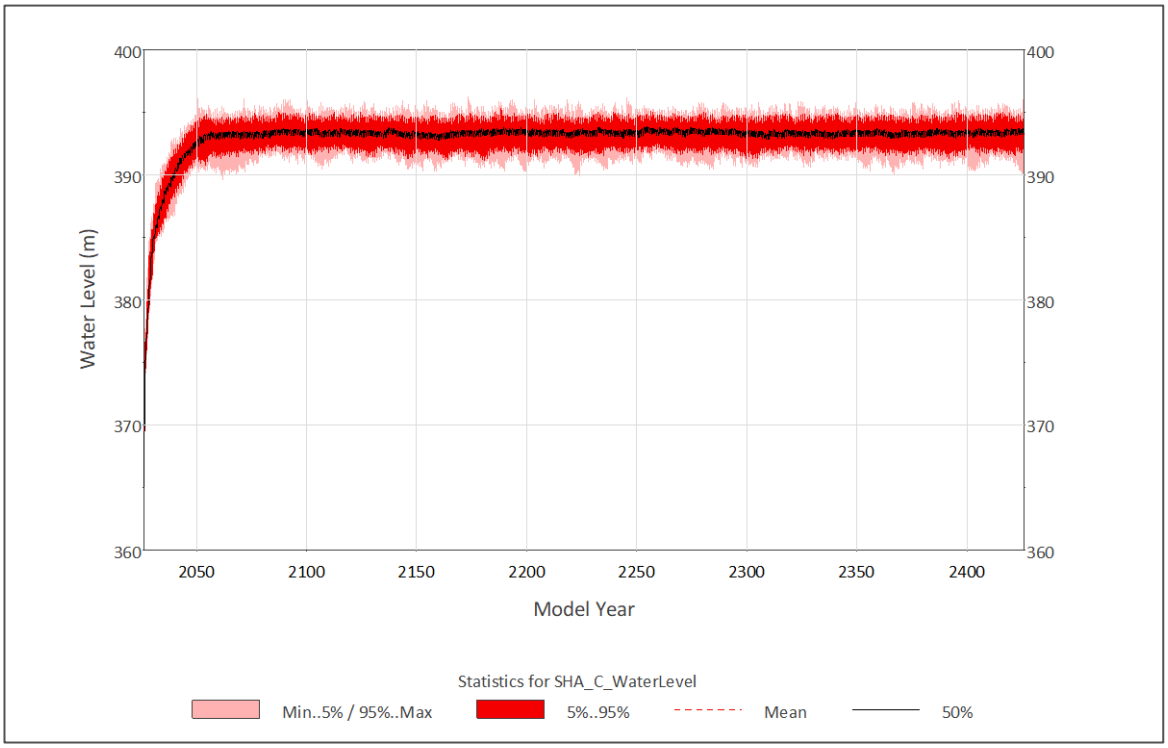

This memorandum, Pit Void Water Balance Modelling: Sanjiv Ridge Stage 5 Below Water Table Mining Hydrogeology Study, WA, Australia was prepared by

Lachlan Gibbins
Principal Consultant (Hydrogeology)

Richard Cheal
Senior Consultant (Hydrogeology)

References

Boughton, W C, 2003. The Australian Water Balance. Model, accepted for publication in Environmental. Modelling and Software, Elsevier, in press October 2003.

SILO (Scientific Information for Land Owners) [https://www.longpaddock.qld.gov.au/silo//. [Accessed station 4106, December 2024].

SRK, 2025. Numerical groundwater model report: Sanjiv Ridge Stage 5 Below Water Table Mining Hydrogeology Study, WA, Australia.

Appendix G Numerical Groundwater Model Report

Final

Sanjiv Ridge Stage 5 Below Water Table Numerical Model Report

Sanjiv Ridge Below Water Table Mining Hydrogeology Study, Western Australia
Atlas Iron Pty Ltd

SRK Consulting (Australasia) Pty Ltd ▪ ATL009 ▪ 4 July 2025

srk consulting

Final

Sanjiv Ridge Stage 5 Below Water Table Numerical Model Report

Sanjiv Ridge Below Water Table Mining Hydrogeology Study, Western Australia

Prepared for:
Atlas Iron Pty Ltd
1314 Hay Street
West Perth, WA, 6005
Australia

+61 8 6228 8000

Prepared by:
SRK Consulting (Australasia) Pty Ltd
Level 3, 18–32 Parliament Place
West Perth, WA, 6005
Australia

+61 8 9288 2000
www.srk.com

ABN. 56 074 271 720

Lead Author: Zip Boniecki **Initials:** ZB
Reviewer: Brian Luinstra **Initials:** BL

File Name:
ATL009_Sanjiv Ridge Stage 5 Below Water Table Numerical Model_Rev5

Suggested Citation:
SRK Consulting (Australasia) Pty Ltd. 2025. Sanjiv Ridge Stage 5 Below Water Table Numerical Model Report. Final. Prepared for Atlas Iron Pty Ltd: West Perth, WA. Project number: ATL009. Issued 4 July 2025.

Cover Image:
Corunna Downs

Disclaimer: The opinions expressed in this Report have been based on the information supplied to SRK Consulting (Australasia) Pty Ltd (SRK) by Atlas Iron Pty Ltd (Atlas). The opinions in this Report are provided in response to a specific request from Atlas to do so. SRK has exercised all due care in reviewing the supplied information. While SRK has compared key supplied data with expected values, the accuracy of the results and conclusions from the review are entirely reliant on the accuracy and completeness of the supplied data. SRK does not accept responsibility for any errors or omissions in the supplied information and does not accept any consequential liability arising from commercial decisions or actions resulting from them. Opinions presented in this Report apply to the site conditions and features as they existed at the time of SRK's investigations, and those reasonably foreseeable. These opinions do not necessarily apply to conditions and features that may arise after the date of this Report, about which SRK had no prior knowledge nor had the opportunity to evaluate.

Contents

Tables

Figures

Appendices

1 Introduction

Atlas Iron Pty Ltd (Atlas) is currently developing the Sanjiv Ridge (formerly Corunna Downs) project (the Project) from Stage 4 (above the water table) to Stage 5 (below the water table). The Project is located in the Pilbara region of Western Australia and involves the mining of iron ore from five open pits using conventional drill and blast methods. Atlas engaged SRK Consulting (Australasia) Pty Ltd (SRK) to complete hydrogeological drilling, testing and modelling during the Stage 4 mining studies that were completed in 2019. Atlas further engaged with SRK during 2023 and 2024 on the following Stage 5 studies:

- hydrogeological drilling and testing
- surface water catchment characterisation and flood modelling
- groundwater numerical modelling
- pit void water balance modelling
- geochemical review, assessment and analysis.

A numerical groundwater model was previously built (Revision 1) for the *Corunna Downs Mine Water Supply H3 Hydrogeological Assessment* (original H3 assessment) (SRK, 2019). The model was validated and updated with new drilling and testing data and 2 years of operational and observation data in 2022 (Revision 2) for the *Sanjiv Ridge Mine Water Supply H3 Hydrogeological Assessment Update* (updated H3 assessment) (SRK, 2023). A minor update to model scenarios (with no additional calibration) was also performed to add recently drilled bores CRD0137, and CRD0143 to replace bores that were being decommissioned by mining (2025 updated abstraction regime (SRK, 2025)).

For the Stage 5 mine plan, the Glen Herring, Runway, Shark Gully and Sparrow Lake (formerly Split Rock) pits will be mined below water table up to 2032. In support of the extension of the pits below water table, further field programs were conducted, including drilling and testing of additional bores and further surface water studies.

Further refinement of Revision 2 of the model was required to extend the depth of the model and incorporate drilling and testing data to predict impacts of the Stage 5 below water table mine plan. This refined and updated model is utilised as the basis of the groundwater impact assessment for the Stage 5 H3 hydrogeological assessment.

This report outlines the numerical groundwater model refinement, calibration and predictive scenarios. The current updated model and predictions will be referred to as the Revision 3 groundwater model for the remainder of this document.

1.1 Model objectives

The main objectives of the model were to perform predictive scenarios for the Stage 5 mine plan at Sanjiv Ridge to:

- simulate operational dewatering flow rates
- assess the effectiveness of existing bores to meet water supply requirements and dewater pits
- assess the drawdown impacts from dewatering during operations
- contribute to the assessment of the long-term pit lake level at equilibrium within the water balance.

2 Conceptual groundwater model

The conceptual groundwater model from previous assessments at Sanjiv Ridge (SRK, 2019) is summarised as follows:

- The fractured bedrock aquifer (FBA) system is highly compartmentalised and anisotropic, with higher permeability, hydraulic connection and groundwater flow in the north–south direction than in the east–west direction.
- The elevated groundwater levels within the banded iron formation (BIF) ridge lines, coupled with the observed steep groundwater gradient between the ridges and low-lying areas, suggest that groundwater discharges very slowly out of the ridge and generally is not in good connection with the surrounding regional hydrogeology. Despite this, some discrete high-flow features within the BIF ridge may have connection to the regional groundwater system.
- It is probable that hydraulic connection between the BIF ridge and the Hardy Formation and Mt Roe Basalt is limited.
- Recharge is expected to occur in areas where the FBA is exposed at surface during seasonal high rainfall events. Alluvial deposits are expected to increase recharge into the FBA during high rainfall events; however, due to high rates of evaporation and evapotranspiration, the alluvial aquifer is expected to act overall as a groundwater sink during the dry period.
- Any potential groundwater discharge from the ridge, if present, is likely to take place into surface water pools where gorges are incised across the ridge through water-bearing fractures.
- The Mt Roe Basalt and Hardy Formation show some degree of compartmentalisation, but in general are likely to have better hydrogeological connection to the regional groundwater system, as demonstrated by gentler hydraulic gradients and higher amplitude response to rainfall events recorded in available hydrographs, particularly near creeks.
- Limited data are available for the formations to the east and west of the Project area, though water levels from Water Information Reporting database bores and bores CRD0016 and CRD0004 indicate a gentler groundwater gradient than in the BIF, likely due to a higher hydraulic conductivity of the regional FBA than the BIF (not including the discrete high flow features).

Water level data collected from 5 years of water supply abstraction reinforce this conceptualisation of a highly anisotropic and heterogeneous hydrogeological system, particularly in monitoring bores at Runway Pit where 25 m drawdown has been recorded along strike with only 1–4 m drawdown recorded across strike at bores located similar distances (300–500 m) from a pumping bore. Additionally, the same operational data show connection in at least some areas between the low hydraulic conductivity FBA and the discrete high flow features. Finally, a large reduction (>200%) in flow rates upon drawdown of high flow bores, and very slow water level recovery rates once the bore stops pumping (e.g. CRD0014) confirm the presence of high flow feature that have limited storage and a low hydraulic conductivity background aquifer within the ridge.

3 Groundwater model build

Revision 2 of the model was used as the basis of the Revision 3 update. Specifics are detailed in the sections below. The model code was updated from MODFLOW2005 to MODFLOW USG to allow for an unstructured grid and better performance during dewatering from pits.

3.1 Grid and extent

The model extent was kept the same as Revision 1 and Revision 2 of the model (Figure 3.1). The grid was redefined with a quadtree refinement to keep the total number of cells low while increasing refinement at the pit areas from 50 m to 30 m and adding three additional layers. An example of cell refinement around pits is shown in Figure 3.2.

Figure 3.1: Model extent

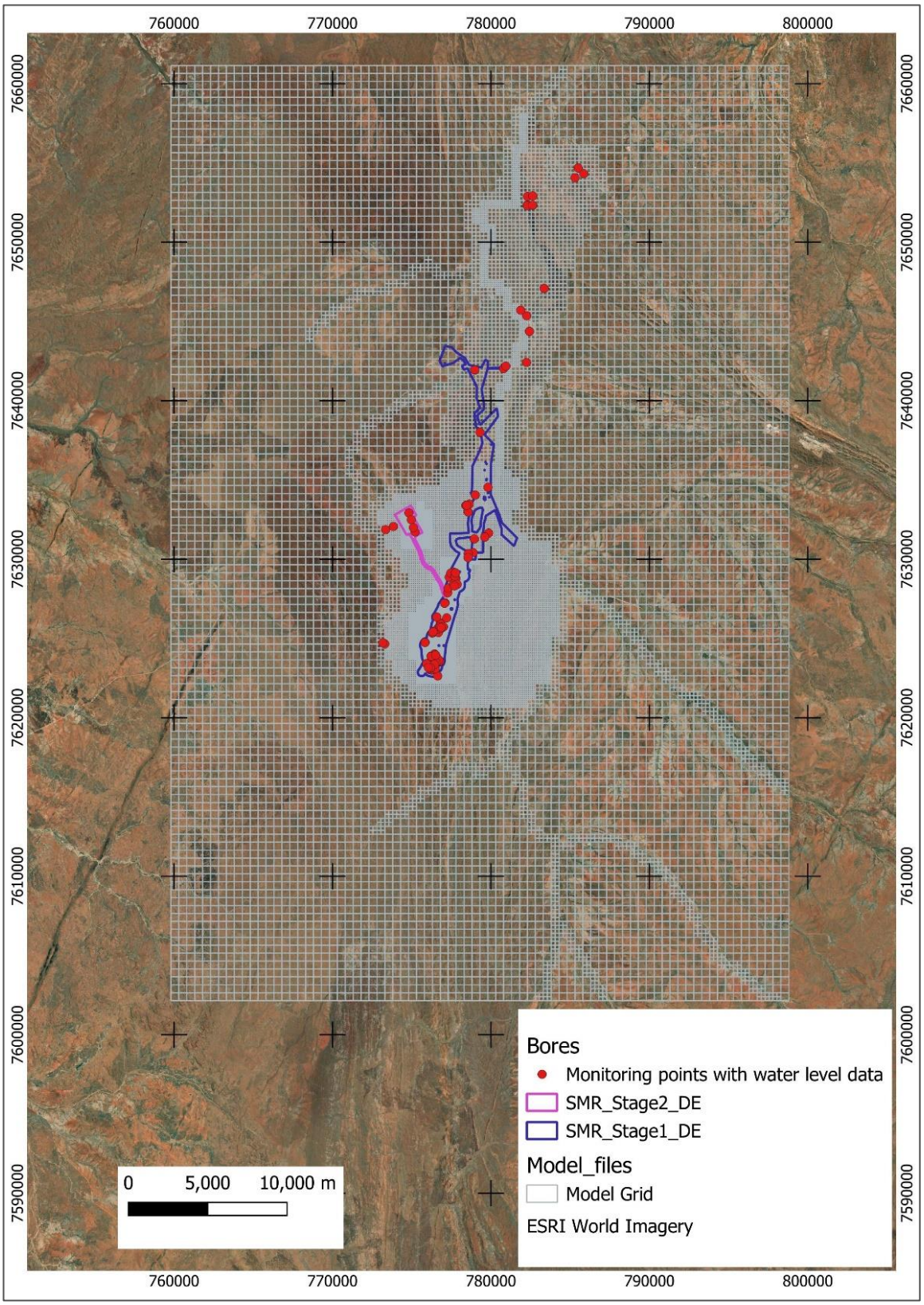

Figure 3.2: Example of Grid refinement in pit areas

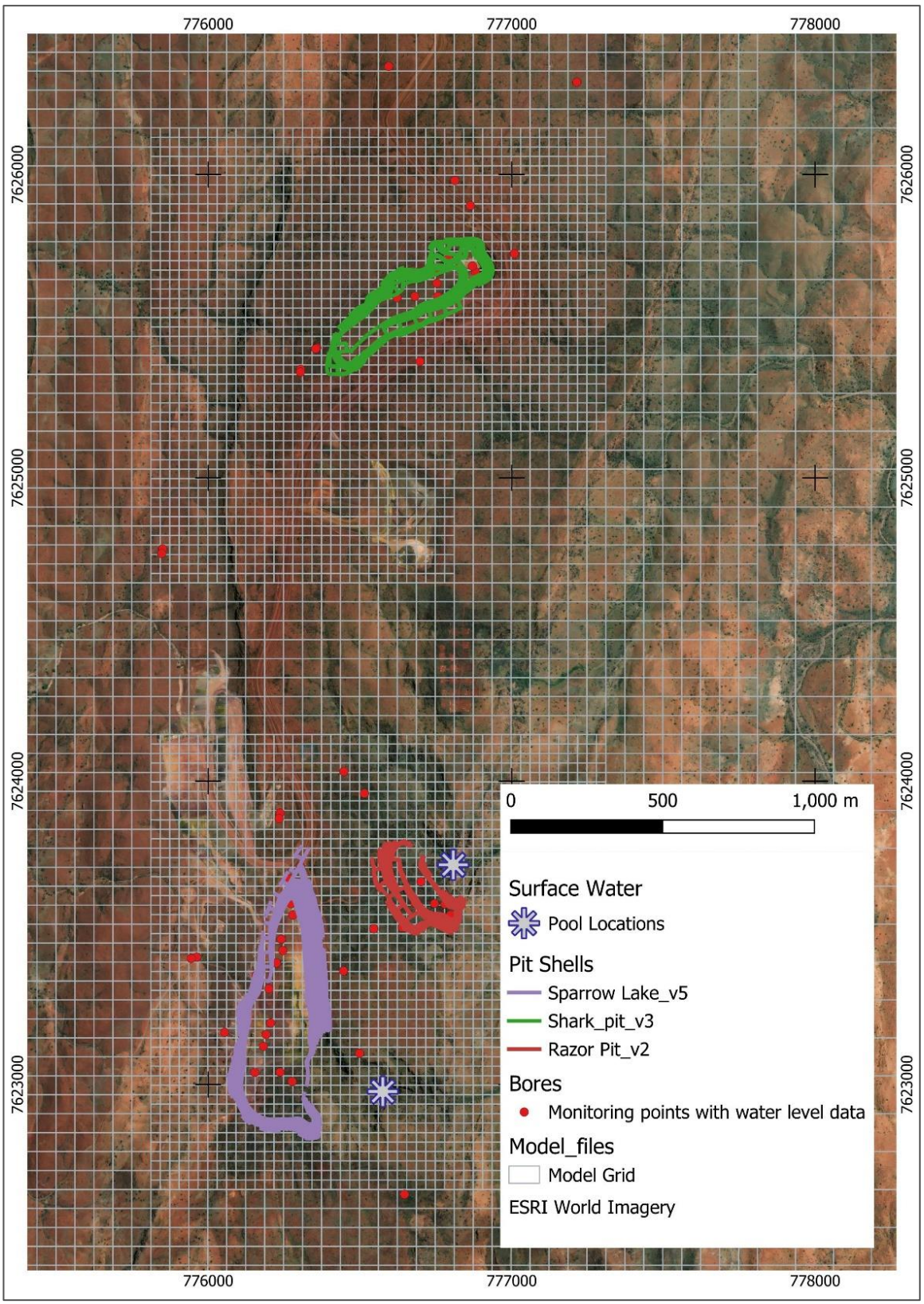

3.2 Layers and elevations

The number of model layers was increased from two to five to allow for better refinement of pit progression and test the impact of varying depth of high flow features. However, the bottom two layers were maintained as a low hydraulic conductivity basement lower than 280 mBGL, with the exception of some high flow features during calibration and sensitivity.

The top elevation was adjusted after quadtree refinement to the topography files (prioritising higher resolution lidar) to have better definition within the BIF ridge and the gorges incised within it.

Layer thicknesses were maintained at a constant thickness of 80 m in the first layer and 100 m for all other layers.

3.3 Boundary conditions

Boundary conditions were largely retained from Revision 2 of the model, with the exception of the addition of river boundary conditions which were applied as drains (act only to remove water) to simulate groundwater flow to gorges and alluvium during times of high groundwater after rainfall. Boundary conditions within the model are summarised in Table 3.1 and presented in Figure 3.3.

Table 3.1: Model boundary conditions

Boundary condition	Values	Unit	Description
Recharge	9.5E-6 to 2E-4	m/d	Values and zones were applied from previous revisions of the model. Higher values were applied to the BIF ridge to represent direct recharge on outcrop and reflect higher water levels and gradients. Recharge multipliers were assigned based on climate data and cross-checked against surface water modelling. Values of zones were occasionally adjusted during calibration.
Evapotranspiration	0.0005 to 0.002	m/d	Evapotranspiration was placed on the entire model domain, with higher extinction depths and rates in alluvium and vegetated areas to simulated groundwater outflow.
General head	140 north 320 south	mAHD	A general head boundary condition was placed on the southern and northern borders of the model to represent regional groundwater inflow and outflow. Values were kept the same as Versions 1 and 2 of the model, as these boundaries were sufficiently far from abstraction zones to have little to no impact on model calibration and predictions.
Well	Historical abstraction	m^3/d	Bores were used to simulate historical abstraction during the calibration phase and simulate future water supply and dewatering impacts during the predictive phase.
Drain	Mine plan pit progression	mAHD	Drains were used in the predictive phase of the model only to represent pit progression and measure required sump pumping rates and resulting drawdown influences.
River	Placed along topography	-	A river boundary condition was placed in major water courses and gorges to remove baseflow during groundwater peaks after rainfall. The condition was set as a drain only to remove water.

Figure 3.3: Assigned boundary conditions

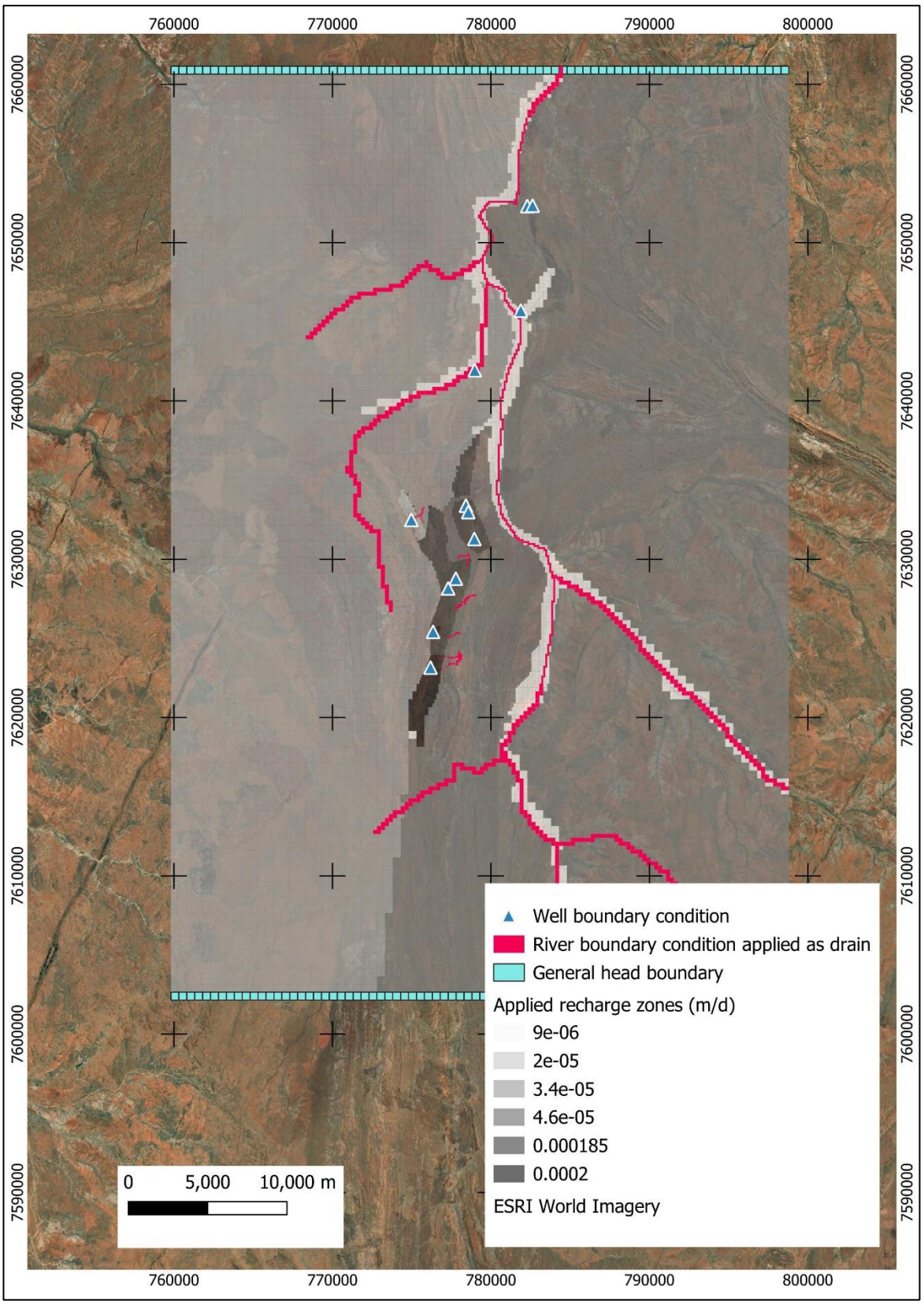

3.4 Stress periods

Monthly time steps were used for model calibration and operational predictive scenarios to allow for reproduction of observed abstraction and rainfall rates during the calibration phase and pit progression below water table during the predictive phase.

3.5 Initial parameters

Initial parameters and zones were copied from the Revision 2 model into the new grid structure. Hydraulic conductivities required changes during calibration to maintain an equal transmissivity due to changes in layer thicknesses and addition of layers.

4 Calibration

The model was calibrated to abstraction, climate and groundwater level observation data collected between early 2020 and early 2025.

The level of observation data, testing, and operational data that were used in the calibration of the Revision 3 of the model included:

- Water supply bores operating at Runway and Shark Gully pits have good observations of drawdown that are of a similar magnitude (30–40 m drawdown) and duration (observations for 2–4 years) of the predictions of dewatering requirements for Stage 5 below water table mining.
- Sparrow Lake does not have same span and scale of operation data as Runway and Shark Gully (limited to 6 months of abstraction at a low average rate ~0.2 L/s). However, there have been three pumping tests performed, the most recent round of which had good drawdown response data in bores up to 750 m away.
- Run of mine (ROM) water supply bores have a good operational and observation record and the simulated operations have rates similar to those that the bores are currently operating.
- Glen Herring has the least amount of data; however, the pit maximum depth does not go below the water table by a large amount (1–2 m).
- Data prior to 2020 was utilised outside of the calibration to inform relative levels in areas that did not have any (or much) data within the calibration period (for example the area of Razor Back pit). The calibration was not extended to include data prior to 2020 as little variation in groundwater levels and no stresses from abstraction were observed during this period and extending the calibration would have extended simulation times without adding much value to the outcome.

The calibration update between Revision 2 and Revision 3 of the model incorporates 2–3 additional years of operational data and five additional pumping tests.

4.1 Discussion

The hydrogeological system at Sanjiv Ridge is conceptualised to be highly anisotropic, heterogenous and compartmentalised (SRK, 2019), and is challenging to represent and calibrate within a numerical groundwater model.

As with previous modelling, hydraulic conductivity within the ridge had to be kept very low (between 1E-5 m/d and 1E-3 m/d) with a high anisotropy (1:10, kx:ky) to maintain high water levels as observed in bores drilled in the ridge. Zones of higher hydraulic conductivity in the ridge represented the discrete high flow features that were intercepted during drilling and testing. The combination of low background hydraulic conductivity and discrete higher flow features was required to maintain high water levels observed in the ridge and match variation in some bores, and to match drawdown data from high abstraction rate pumping tests as well as abstraction from water supply bores.

During calibration, the simulated water levels were matched to observations and graphed by spatial zones/areas (Figure 4.1). The main findings during the model calibration are outlined for each of these areas below.

Figure 4.1: Spatial distribution of zones for calibration to observations

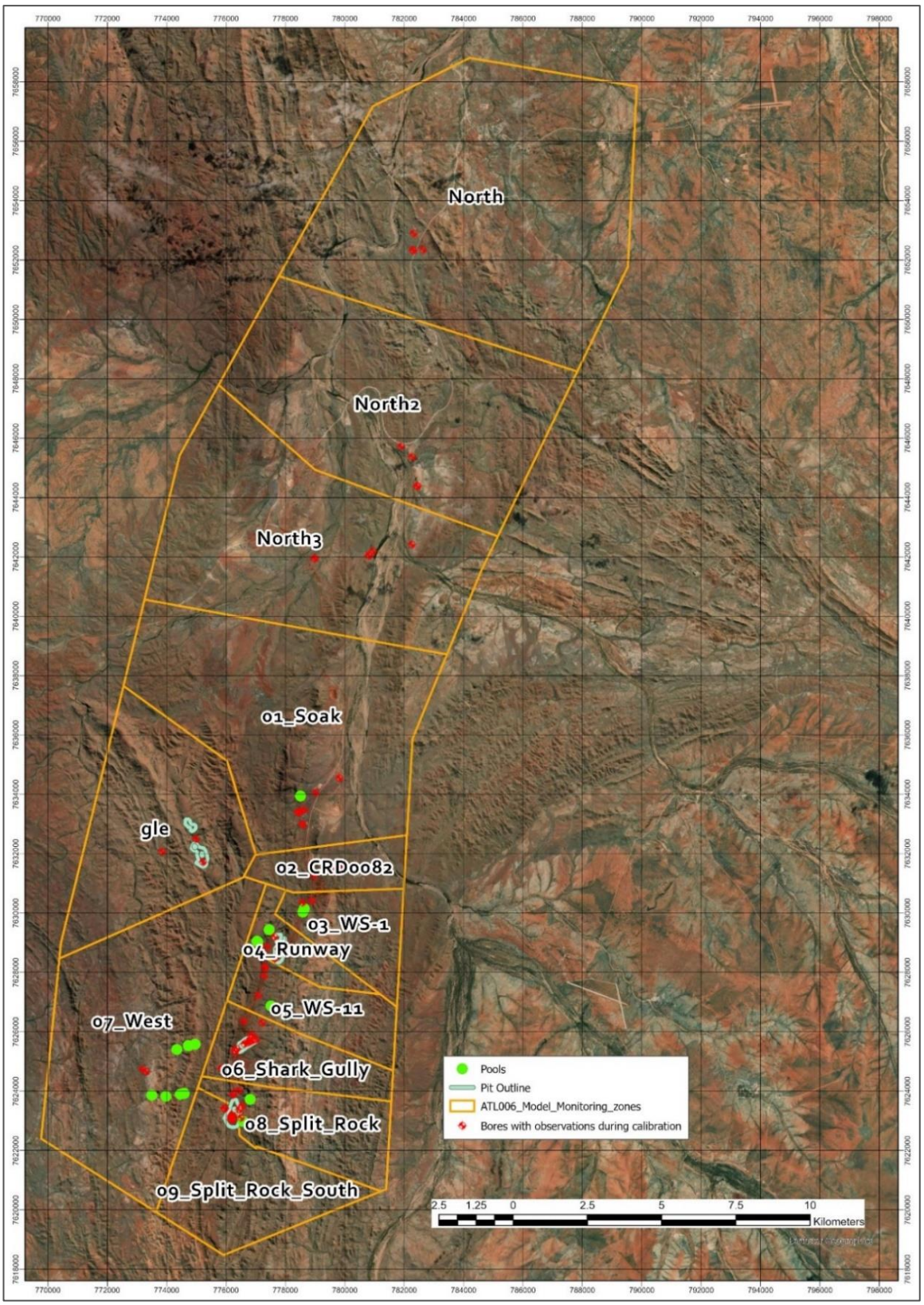

Processing Plant (ROM)

The calibration at the Processing Plant (occasionally referred to as ROM in figures) water supply bores (CRD083 and CRD082) is generally good, with seasonal fluctuations from rainfall and response to abstraction well represented. Simulated levels do not match as well at CRD0027 and CRD0034, with higher simulated than observed water levels evident in Figure 4.2. This should not cause an issue for predictions, as overall the trends away from pumping bores are well represented and only the relative levels are misaligned.

Glen Herring

The Glen Herring Pit area has the least amount of data to calibrate to and calibration is limited, relying on sparse time series data for water levels and three pumping tests with drawdown propagation limited to the nearest observation bore.

Therefore, limited zonation of hydraulic conductivity and storativity zones was applied. A reasonable calibration was achieved to water levels and drawdown responses to the pumping tests. The amount of data is considered to be sufficient, as Glen Herring is not planned to extend below the water table in the Stage 5 mine plan.

Runway

The focus of the calibration at Runway was to match simulated drawdown from abstraction at CRD0101, particularly the large differences between drawdown at bores that were similar distances from the pumping bore (CRD0092, CRD0006 and CRD0096 – Figure 4.3). The high level of drawdown directly south of the pit (CRD0096, 25 m drawdown ~350 m from CRD0101) was matched by assigning high flow zones in the model, while the relatively low drawdown at CRD0006 (4 m drawdown, 430 m north of CRD0101) and CRD0092 (1 m drawdown, 430 m west of CRD0101 – slightly overpredicted in the model) was matched by the addition of some moderate/low hydraulic conductivity zones with low storage and adjustments of anisotropy (higher along strike). The observed drawdowns and adjustments required to match them further reinforce the conceptualisation of a highly anisotropic and heterogenous groundwater system with ground water flow dominated by high conductivity, low storage features.

Shark Gully

Minor adjustments were made to the Shark Gully zones and hydraulic conductivity, as the response to pumping at CRD0122 was reasonable in Revision 2 of the model. The calibration focused on achieving a better response to monitoring in the west (CRD0090 and CRD0007 – Figure 4.4) and in the pumping bore.

Sparrow Lake

High and moderate hydraulic conductivity zones were expanded from the previous model revisions (Figure 4.5) to get a good response to pumping at bores CRD0143 and CRD0141 (Figure 4.9) and relative water levels.

The moderate hydraulic conductivity zone was also placed below Razor Back in the first layer for a more realistic match to water levels below Razor Back based on old (2013) water level readings from reverse circulation holes. This moderate hydraulic conductivity zone could be placed in either Layer 1 or Layer 2 to improve the calibration. Layer 1 was chosen for the base calibration to better align with the conceptualisation of reducing background hydraulic conductivity with depth.

Drawdown predictions were sensitive to this change, and the moderate hydraulic conductivity zone at Razor Back has caused drawdown predictions to extend to pool CO-WS-14 (discussed in Section 5.2.1).

Connection to the east and west of the ridge is unclear, but it is likely that there is some connection due to lower water levels in bores in the east–west orientated gorge that passes on the southeast of Sparrow Lake Pit (pool CO-WS-09). A better calibration to water levels is achieved with some level of connection to the east and west south of Sparrow Lake.

North

The area north of Sanjiv Ridge was previously used for water supply during the construction of the haul road. These bores have not been active at full rates since 2021 (bores are occasionally used for ad hoc water supply). While the area is included in the model and abstraction and observations were used in the calibration, the area was not the focus of the project and calibration, and little time was spent on calibration of the model in this area. The modelled water levels are generally 5 m higher than observed, but show good responses to abstraction impact.

The calibration in this area has no impact on predictions of drawdown or operational flows at Sanjiv Ridge.

Figure 4.2: ROM calibration

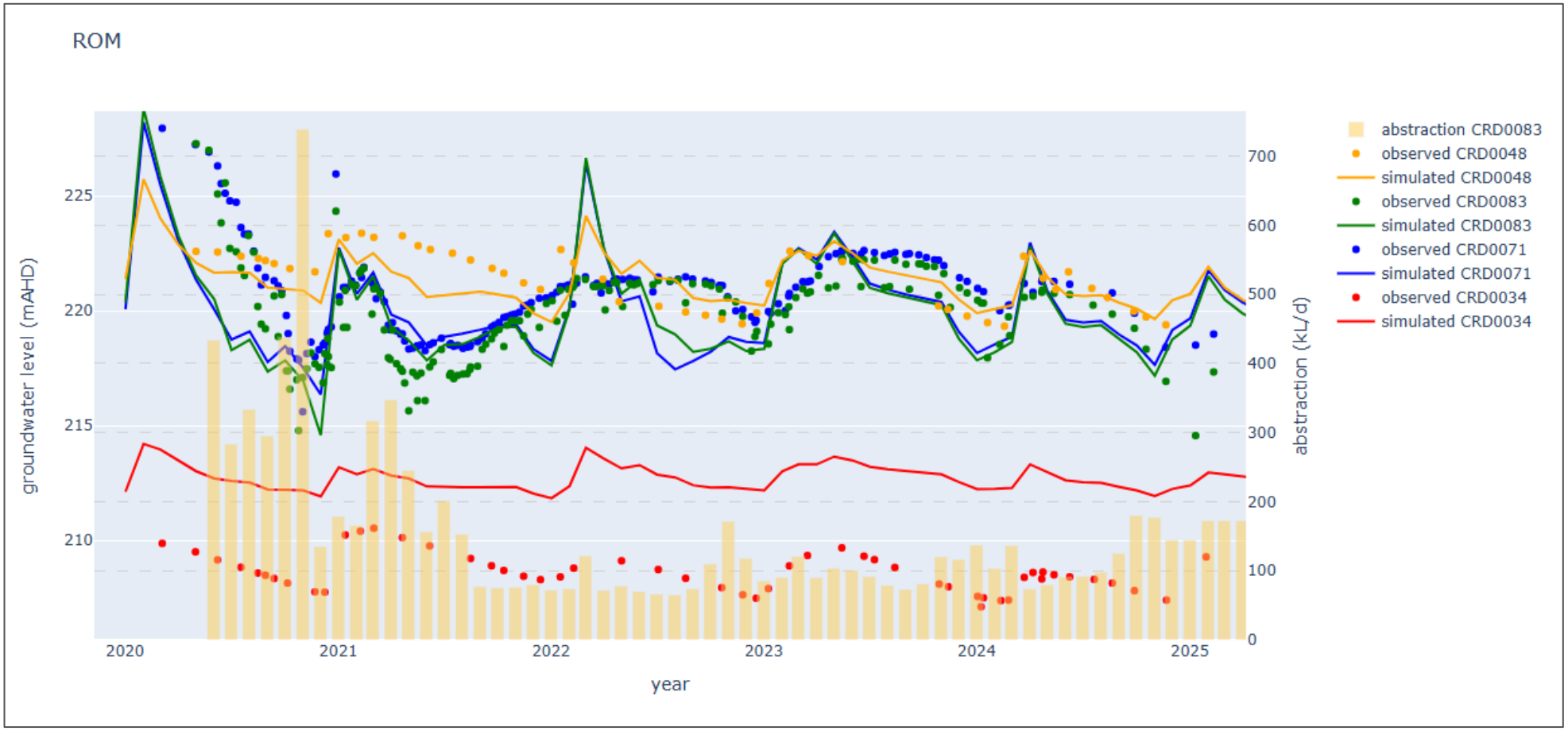

Figure 4.3: Runway Pit calibration

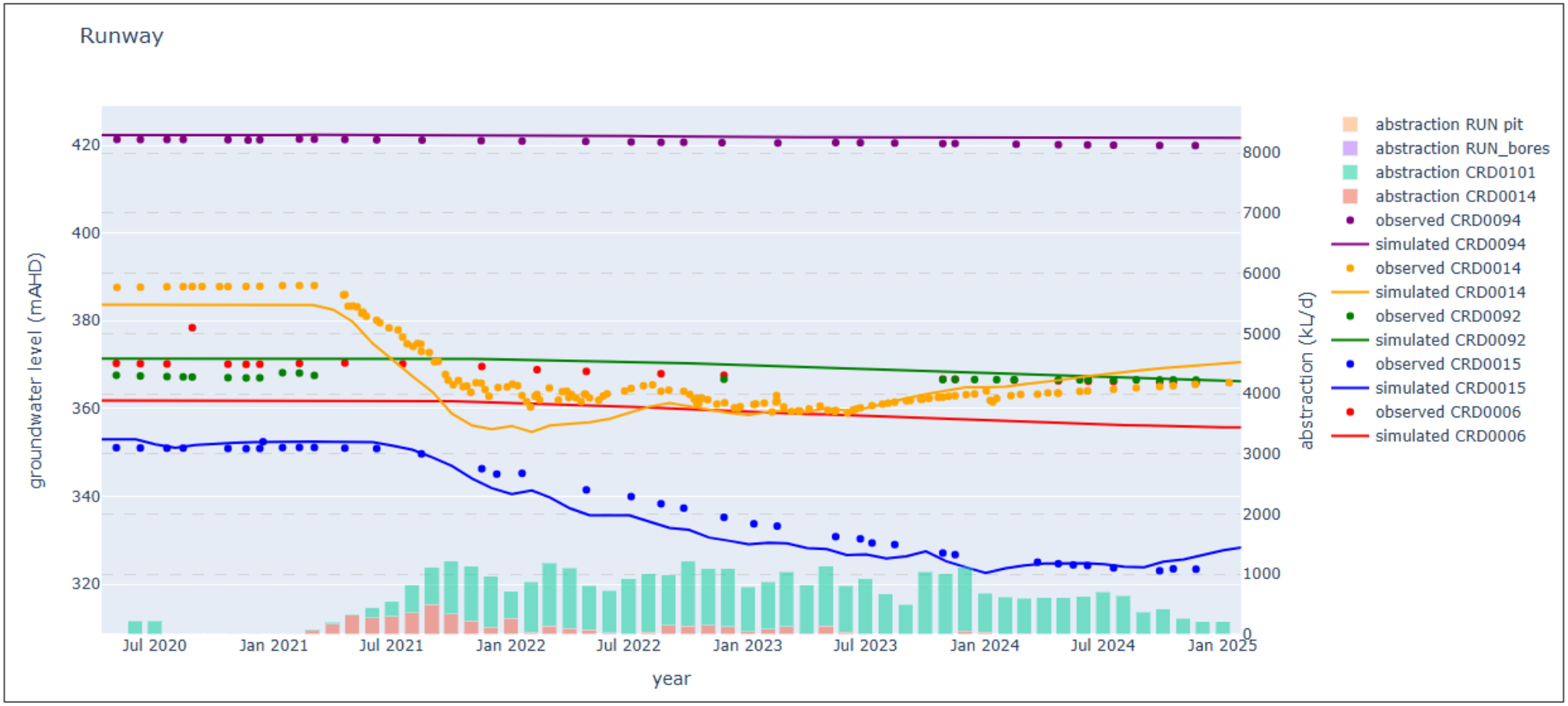

Notes: Calibration to propagation of drawdown was prioritised over relative levels

Figure 4.4: Shark Gully Pit calibration

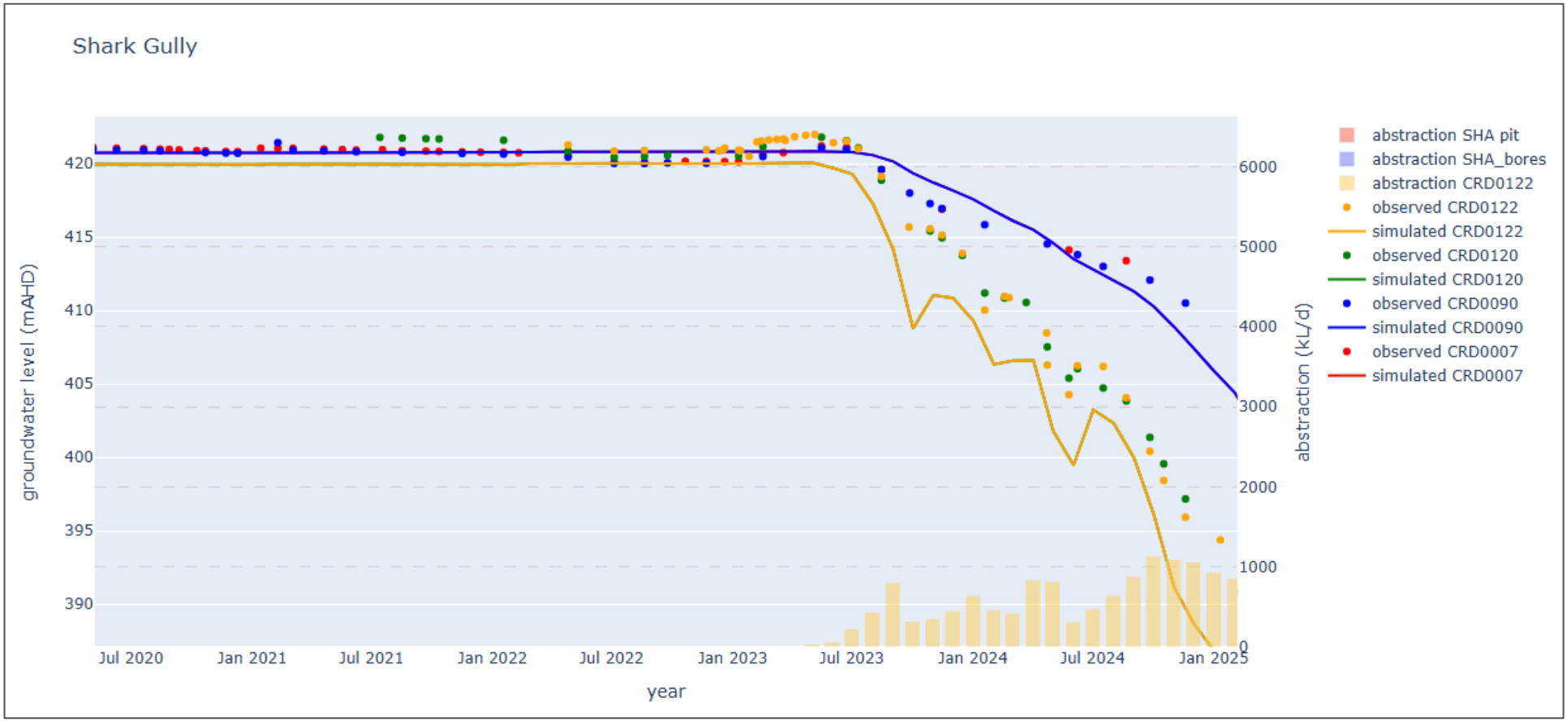

Figure 4.5: Hydraulic conductivity zones at changes between Revision 2 and Revision 3 of the model

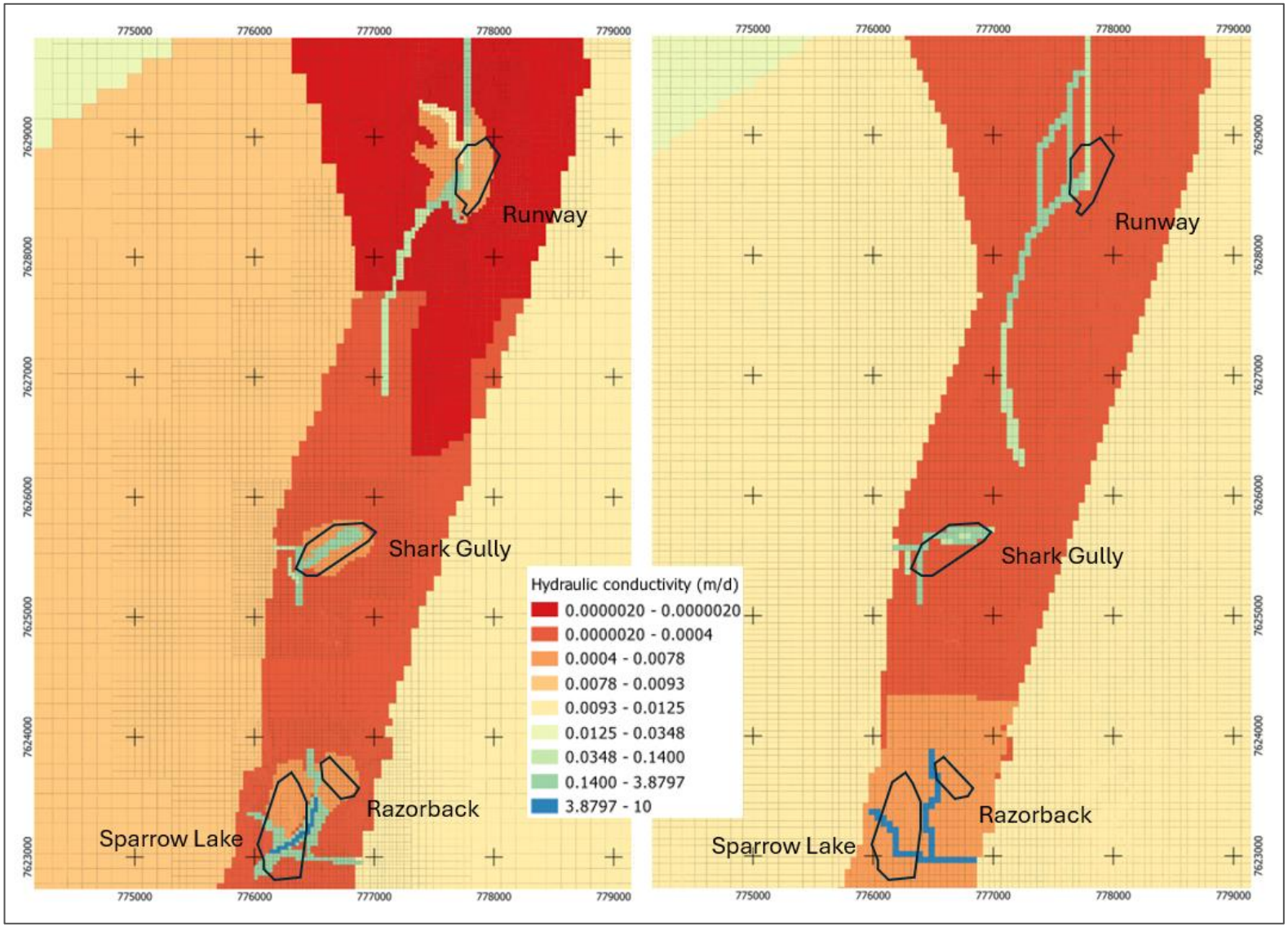

Notes: Left revision 3 of the model; right revision 2 of the model.

4.2 Sensitivity

The main sensitivities and uncertainties in Revision 3 of the model were the same as in Revision 1 and Revision 2 of the model. Notably:

- The high relative levels and high gradients in the BIF ridge were sensitive to a combination of hydraulic conductivity and recharge values. Relatively high recharge values (10–14% of rainfall) were adopted in the base calibration consistent with all previous modelling, and a conceptualisation that groundwater is recharged where the FBA is exposed at surface. Recharge is aligned to the runoff coefficient modelled in the surface water modelling (average 3–50% runoff with higher runoff during the wet season, this leaves an excess of 50% of rainfall for evaporation and recharge). Additionally, evapotranspiration in the model removed excess recharge. However, lower recharge values still allow for a good calibration, but required lower hydraulic conductivities of the BIF ridge. The lower recharge/hydraulic conductivity model makes little difference to the operational inflows due to the presence of high flow features, but reduces drawdown extent during operations (less impact during closure) and reduces pit inflows once high flow features are drawn down. The calibration was not as good with lower recharge values in the Sparrow Lake area.
- Propagation of drawdown towards pool CO-WS-14 from Sparrow Lake is sensitive to the placement of high and moderate hydraulic conductivity zones and their boundaries. During pumping, tests bores between Sparrow Lake and pool CO-WS-14 exhibited drawdown, but there were no monitored bores closer to pool CO-WS-14 to confirm the ultimate extent of drawdown.
- The calibration was sensitive to the combination of the extent of high flow features and the hydraulic conductivity, anisotropy and storativity and specific yield of these features. While matching the drawdown from long-term pumping, these parameters were adjusted iteratively in combination.

4.3 Limitations

The limitations of the previous models (Revisions 1 and 2) are mostly consistent with the current assessment, except where limitations are addressed with extended operational data (the ROM area, Runway Pit and Shark Gully Pit). The main limitations of the model are:

- Aquifer compartmentalisation is poorly represented where no long-term operational pumping and water level data exist. Calibration of these areas relies heavily on aquifer testing data. Aquifer testing data are limited in providing insight where hydrogeological connection may exist due to the short duration of pumping tests and limited stresses. Conversely, where operational data have created an extensive and uneven drawdown distribution, more understanding of connection can be inferred.
- Calibration in the north (old haul road water supply) was not the focus of the model and is not as good as in the mining areas. This has no impact on predictions within the ROM and BIF ridge areas.
- The model assumes full connection between the surficial aquifers and underlying FBA. Small, localised perched aquifers may exist at Sanjiv Ridge, however identifying and characterising these aquifers to a degree allowing model representation is not feasible or warranted for this investigation. If pools or creeks are fed solely by an unidentified perched aquifer system that is

disconnected from high flow features deeper in the BIF ridge, simulated drawdown from water supply and pit dewatering would not eventuate in reality.

4.4 Calibration results

Comparison of simulated and observed water levels in bores during the final calibration had a root mean square (RMS) error of 5.76 % and a scaled root mean square (SRMS) error of 1.6%. Drawdown responses to water supply were reasonably well represented by the model (drawdown at the bore was matched and propagated to distal bores where drawdown was observed in the field) at the ROM, Runway Pit and Shark Gully Pit, and pumping test responses at Sparrow Lake and Glen Herring were also represented in the simulation. Overall, the calibrated model had a reasonable match to observed water levels (Figure 4.6) and observed drawdown during aquifer testing (Figure 4.9), and had a good match to the large vertical range of water level observation data (Figure 4.8). The final calibrated parameters are presented in Table 4.1 (variation between Revision 2 of the model are partially due to layer thickness changes, i.e. hydraulic conductivity changed to match transmissivity).

The current calibration was assessed against a validation of Revision 2 of the model that was updated with the most recent data (Figure 4.7). While Revision 2 performed acceptably (RMS error of 6.6% and SRMS error of 2.1%), the Revision 3 calibration significantly increased the match to observed data, particularly drawdown at the ROM, drawdown distal from Runway Pit, drawdown at Shark Gully Pit and relative levels at Sparrow Lake.

Table 4.1: Calibrated hydraulic parameters

Hydrostratigraphic unit	Hydraulic conductivity (m/d)		Anisotropy (Kx/Ky)		Specific storage (m^{-1})	
	From	To	From	To	From	To
Alluvium	*15*		*0.5*		*1E-7*	
Alluvium (updated)	**9**		**1**		**1E-7**	
Regional Archaean basement (including Mt Roe Basalt)	*0.03*	*1*	*0.1*	*1*	*3E-6*	*2E-5*
Regional Archaean basement (including Mt Roe Basalt) (updated)	**0.03**	**1**	**0.1**	**1**	**3E-6**	**2E-5**
Cleaverville Formation (BIF Ridge)	*0.00003*	*0.01*	*0.01*		*3E-5*	*4E-3*
Cleaverville Formation (BIF Ridge) (updated)	**0.00003**	**0.001**	**0.01**		**3E-5**	**4E-3**
Euro Basalt and Duffer Formation (west of Ridge)	*0.009*		*0.1*		*2E-6*	
Euro Basalt and Duffer Formation (west of Ridge) (updated)	**0.009**		**0.8**		**3E-6**	
Hardy Formation (north of Ridge)	*0.01*	*0.2*	*0.5*		*2E-6*	
Hardy Formation (north of Ridge) (updated	**0.01**	**0.5**	**0.9**		**2E-7**	
Wyman Formation and Dalton Suite (east of Ridge)	*0.1*		*0.25*		*2E-6*	
Wyman Formation and Dalton Suite (east of Ridge) (updated)	**0.1**		**0.15**		**1E-6**	
Local high flow zones	*0.09*	*8*	*0.1*	*0.5*	*3E-5*	*4E-3*
Local high flow zones (updated)	**0.09**	**3**	**0.1**	**1**	**3E-6**	**4E-3**
Local moderate flow zones (updated)[1]	**0.005**	**0.006**	**0.1**	**0.5**	**1E-7**	**4E-3**

Notes: Revision 2 model parameters in italics; current Revision 3 parameters in bold.

[1] Added in Revision 3 of the model.

Figure 4.6: Transient calibration graphs for the current (Revision 3) version of the model

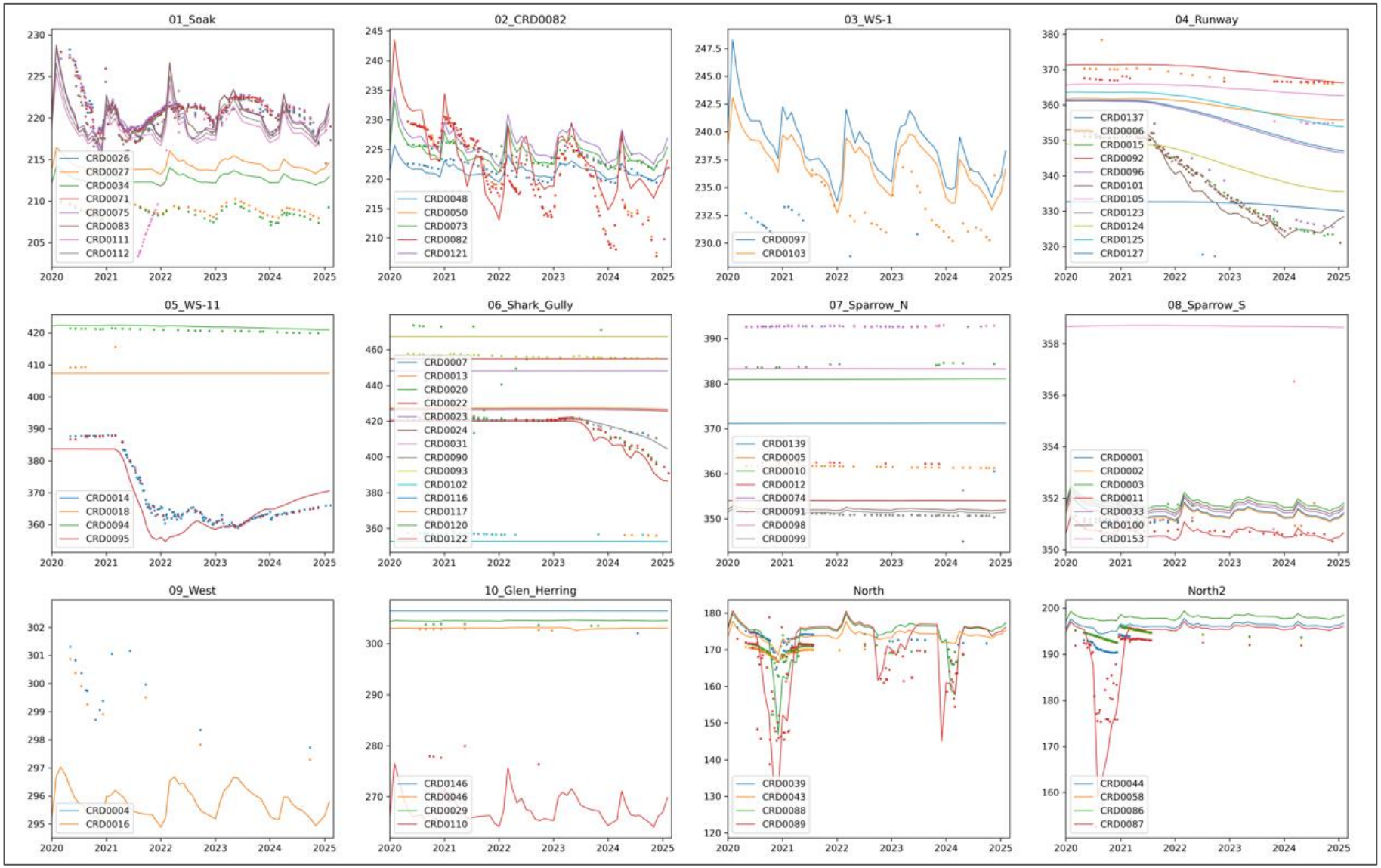

Notes: Points represent observed water levels and lines represent simulated water levels.

Figure 4.7: Validation of previous model (Revision 2) with update data

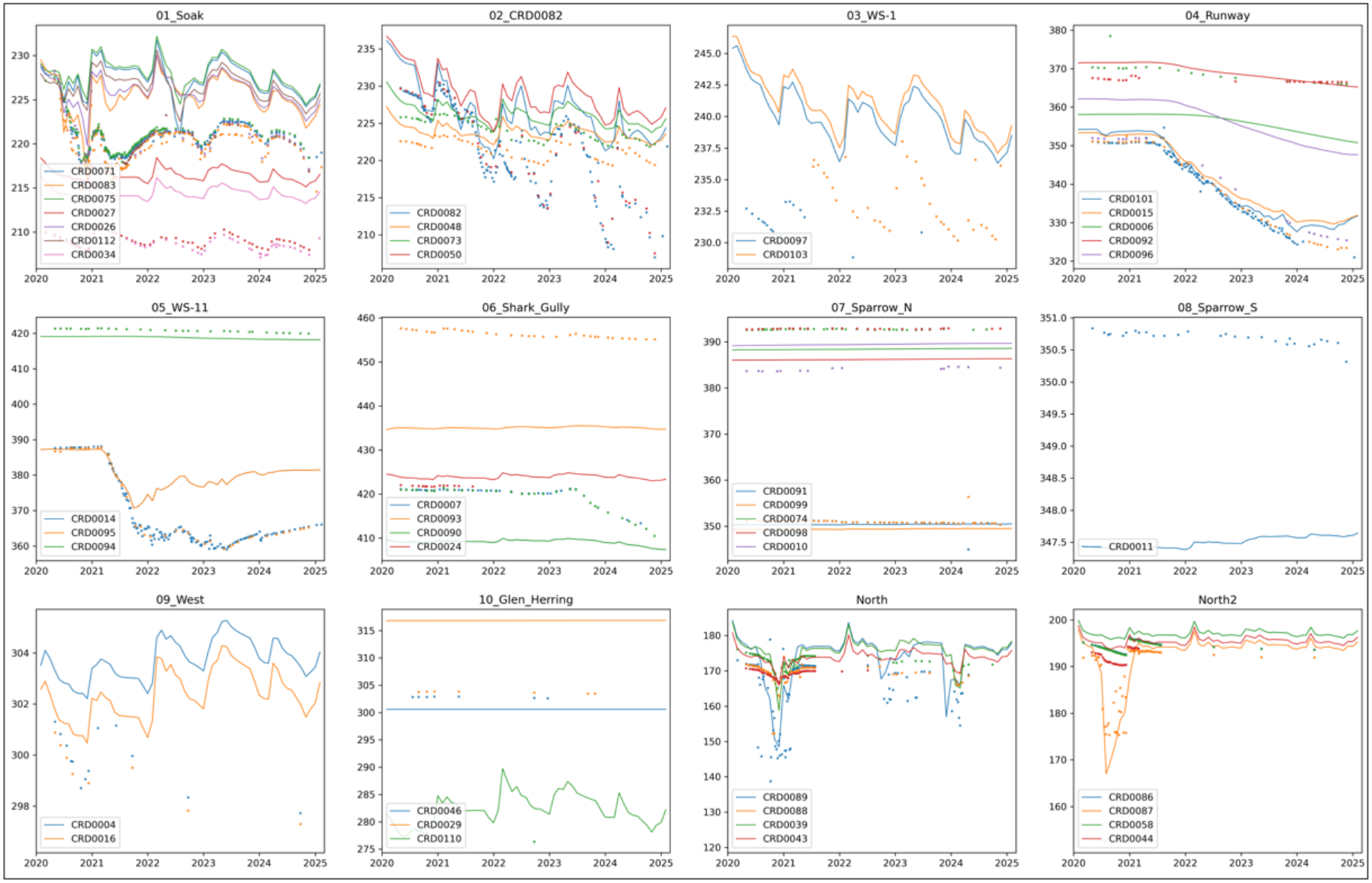

Notes: Points represent observed water levels and lines represent simulated water levels.

Figure 4.8: 1:1 modelled versus observed water levels during transient calibration

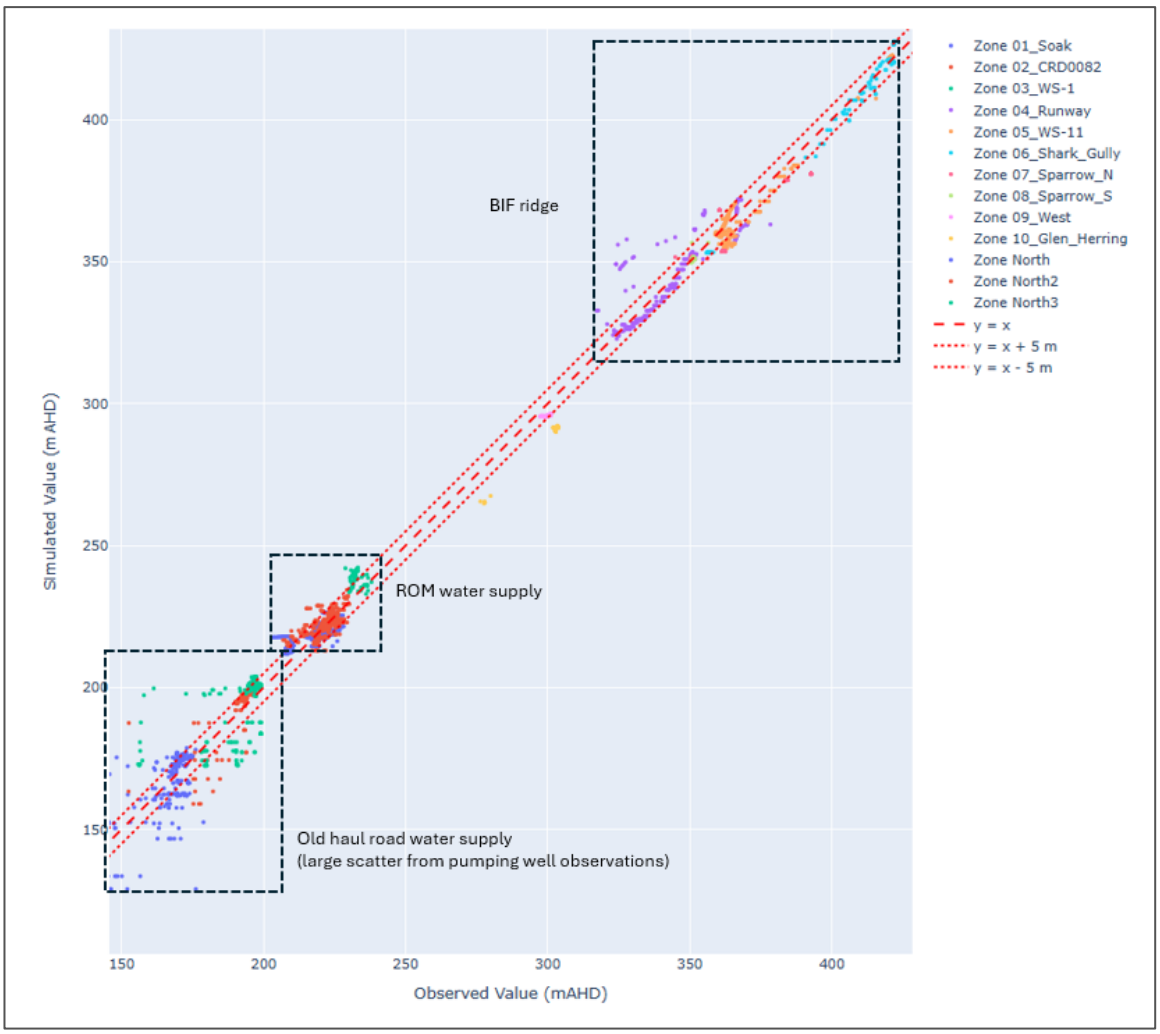

Figure 4.9: Simulated drawdown during pumping tests

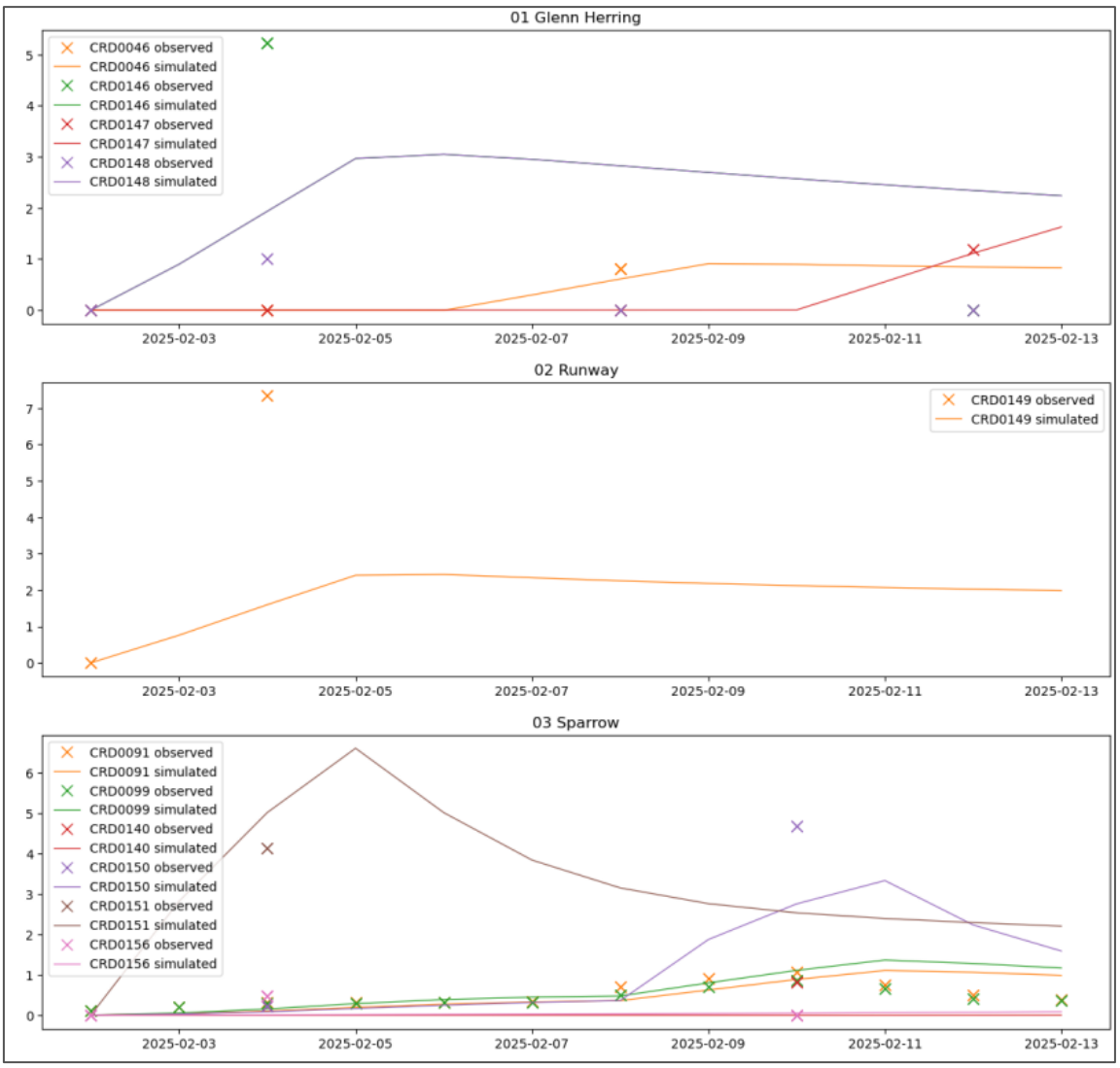

Notes: Points represent observed drawdown and lines represent simulated drawdown. Where the pumping bore has a monitoring bore on the pad, only the monitoring bore is shown if there was a large amount of drawdown in the pumping bore to represent aquifer drawdown and not well losses that are not represented in the model.

5 Predictive scenarios

5.1 Scenario set-up

5.1.1 Operational

The calibrated model was extended to 2032 for the predictive scenarios to assess dewatering rates and drawdown impacts from dewatering and water supply.

Recharge for predictive scenarios was kept constant in the numerical groundwater model so that predictive drawdowns isolated the impacts from pit dewatering and water supply. Changes in rainfall due to climate change are represented in the water balance model which then inform the pit lake water levels during the closure and rebound scenarios (sections 5.1.2 and 5.1.3).

Water supply bores were assigned the water requirement rates from the previous updated H3 assessment (SRK, 2023) and the 2025 updated abstraction regime (SRK, 2025), abstraction rates are provided in Table 5.1. Water supply bores (CRD0127, CRD0137 at Runway, CRD0122 at Shark Gully and CRD0143 at Sparrow Lake) function as both water supply and advanced dewatering. Glen Herring Pit is not planned to progress below the water table in the Stage 5 mine plan.

Additionally, a drain boundary condition was applied at the pit progression (Figure 5.1) to simulate how much extra dewatering may be required from sumps (in addition to ex-pit dewatering) as the pit progresses below the water table. The drain boundary condition also ensured that simulated drawdown extents should reflect the total drawdown generated by both bore and pit dewatering.

Figure 5.1: Pit progression

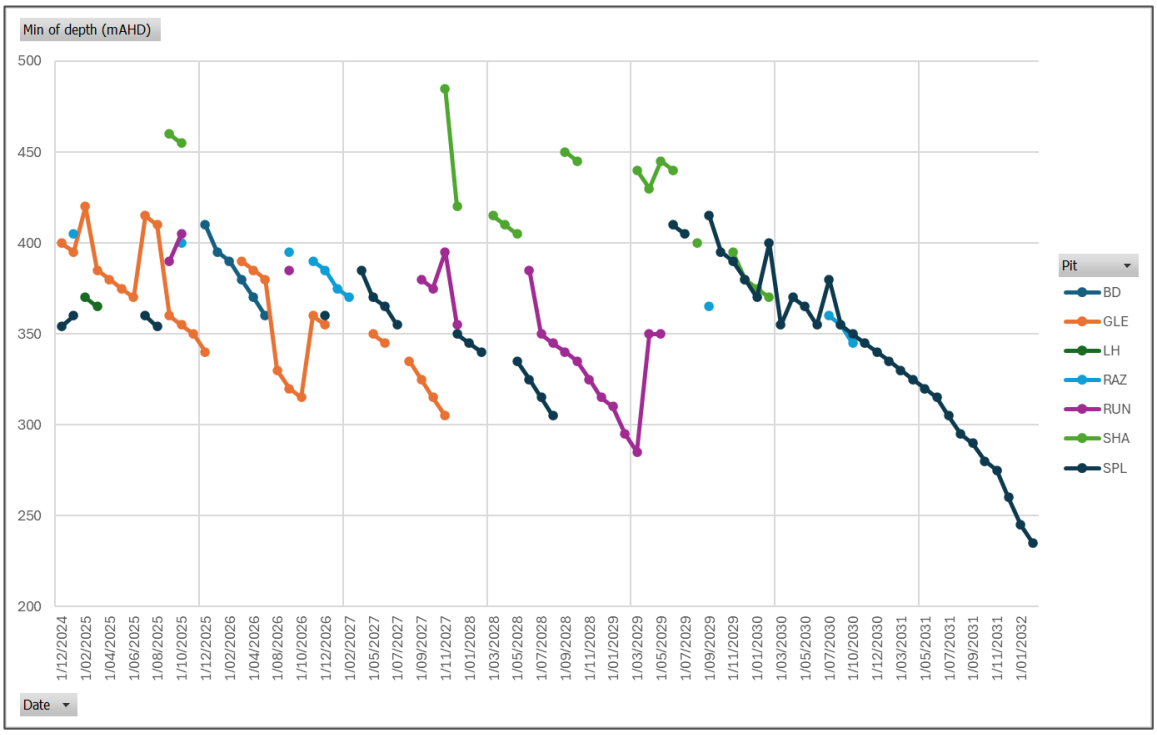

Notes: Planned pit depth in mAHD presented as the deepest values of active strips within a pit.

Table 5.1: Bore abstraction rates for predictive scenarios

Period	Average historical abstraction[1]	H3 assigned rate[2]	Future assigned rate[3]	Comments
Bore ID	**Flow (L/s)**			
CRD0083	1.7	2	2	ROM water supply
CRD0082	4.1	7	7	ROM water supply
CRD0014	1.2	0.5	0.5	Bore recorded reduced flow in 2022
CRD0101	7.1	10	–	To be replaced by CRD0137, original H3 assess impacts of 14 L/s until July 2026
CRD0121	–	2	2	ROM water supply
CRD0122	6.6	9	19	For water supply and advanced dewatering at Shark Gully
CRD0102	–	2	0	Unlikely to be required if water supply can be sourced from Shark Gully dewatering (sumping or CRD0122)
CRD0005	–	1	0	Unlikely to be required if water supply can be sourced from Sparrow Lake dewatering (sumping and/or CRD0143)
CRD0137	–	6	6	For water supply and advanced dewatering at Runway
CRD0143	–	15	15	For water supply and advanced dewatering at Sparrow Lake

Notes:

[1] Average operation rate for the bore.

[2] Combination of the Updated H3 (SRK, 2023)and the 2025 updated abstraction regime (SRK, 2025).

[3] Assigned rate for water supply and advanced dewatering. For dewatering bore this rate decreases as aquifer is dewatered.

5.1.2 Post-closure

An iterative approach between the numerical groundwater model and the water balance was adopted to simulate groundwater and pit lake conditions at closure once conditions had reached equilibrium (the period between operations and equilibrium is discussed in section 5.1.3).

The groundwater model simulated steady-state groundwater inflows at set elevations using the drain boundary condition to simulate the inflow to the pit once a pit lake had equalized with groundwater inflows, surface water inflows and evaporation outflows (assuming the pit is a groundwater sink). These inflows represent the long-term (>400 years) inflows once the low hydraulic conductivity aquifer has been dewatered by filling of the pit and evaporation from the pit.

Groundwater inflows were imported into the water balance model (SRK, 2025) to simulate a final resting pit lake water level for each pit (fluctuating around a mean level that represents the steady state level).

This final resting level was then re-imported back into the groundwater model as a drain (the resting level was below the current groundwater table) and the groundwater model was run as steady state to simulate the drawdown impact of all the pits as permanent evaporative groundwater sinks. The iterative approach between the water balance and groundwater model enables modelling of complex surface water, evaporation, and groundwater interactions with the pit void geometry to determine the pit lake water level in equilibrium with a level of accuracy that would not be possible in just the groundwater model.

The resting water levels during closure and rebound output from the water balance and the time for the system to achieve equilibrium are presented in sections 5.2.3 and 5.2.4.

5.1.3 Rebound period between operation and post-closure equilibrium

The period between cessation of operations and equilibrium between groundwater level and the pit lake water levels was also modelled to assess drawdown rates at pools during this period.

An iterative approach between the groundwater model and the water balance model, similar to the post-closure scenario, was adopted to assess rebound rates and drawdown in groundwater during this phase. Groundwater inflow rates during a rebounding water level after cessation of mining were simulated in the groundwater model at set depths and then applied within the water balance model to simulate the rate of pit lake level rebound. The rate of rebound was then re-input into the groundwater model as a drain to cross-check that groundwater inflow rates were the same as those initially provided to the water balance. If the rates were similar enough to not make a material difference to pit lake rebound, the water balance pit lake rebound levels over time were then used in the groundwater model to assess the evolution of groundwater drawdown at pools during the rebound of pit lakes.

5.2 Scenario outputs

5.2.1 Drawdown from abstraction and dewatering during operations

Drawdown contours are presented as the 1 m drawdown contour at the completion of mining in Figure 5.5. Drawdown contours are presented for January 2032, when mining ends at the deepest below water table pit (Sparrow Lake). Drawdown will continue to extend within the BIF ridge during rebound after completion of mining as pits (and dewatered high flow features) refill with water, effectively dewatering the low permeability surroundings until pit lakes equilibrate between surface water and groundwater inflows and outflow through evaporation.

ROM

Drawdown extending from the ROM bores (CRD0121, CRD0082 and CRD0083) is similar to previous assessments due to application of the same abstraction rates for the extended period (Figure 5.5). Drawdown extent from previous assessments had not eventuated in some bores further from the pumping bores (CRD0027) due to a lower actual rate being used than that used in the model.

Runway

Runway Pit is planned to progress another 35–40 m below the current water level by 2029 and will require sump pumping (or in-pit bore/s) to supplement ex-pit dewatering at CRD0137 (to replace the current water supply bore CRD0101 which is located in the centre of the planned pit).

Simulated drawdown extents from the Stage 5 below water table mining at Runway are simulated to extend up to 700 m to the northwest and up to 1,400 m to the south (Figure 5.5).

Drawdown from abstraction for water supply at CRD0101 is currently reported as being over 28 m and extends strongly along strike with 25 m of drawdown at CRD0096 which is 340 m to the south of the pumping bore. Conversely drawdown weakly propagates across strike with 4 m drawdown at CDR0006 located 416 m northwest of the pumping bore, and 1 m of drawdown at CDR0092 located 436 m west-northwest of the pumping bore. Drawdown at these bores will continue with up to 40 m simulated at CRD0096, and 10 m simulated at bores CDR0006 and CDR0092 (Figure 5.2).

While drawdown is not simulated to reach pools CO-WS-10 and CO-WS-12 during operations due to the low permeability of the BIF and high degree of compartmentalisation within the FBA represented in the model, the level of drawdown will ultimately depend on the extent of high flow pathways and their connection to surficial FBA that cannot be predicted within the model.

Figure 5.2: Current and simulated drawdown at Runway Pit

Notes: Rebound in CRD0015 is due to shift from abstraction at CRD0101 to CRD0137

Shark Gully

Mining is planned up to 50 m below the current water table. Due to dewatering at CRD0122 and additional sump pumping (or in-pit bore/s) in areas of the pit, drawdown is simulated to be limited within the BIF ridge (to 200 m from the pit edge) but will propagate out up to 1,200 m towards the west (Figure 5.5).

CRD0122 is already dewatering the area (23 m in CRD0120 next to CRD0122, and 10 m in CRD0090, 80 m southwest of CRD0122) and planned mining represents a 6 year continuation of abstraction and drawdown from this bore (Figure 5.3)

The extent of drawdown has not increased from previous assessments as the pit level and sump abstraction would not represent a deeper point of water level than the simulated drawdown at CRD0122 from water supply. A reduction of the drawdown contour to the west when compared to the Revision 2 model predictions is due to the Revision 3 model limiting abstraction from CRD0122 as the water level approaches the bottom of the bore to not create an unrealistic drawdown at the bore.

Figure 5.3: Current and simulated drawdown at CRD0122 and Shark Gully Pit

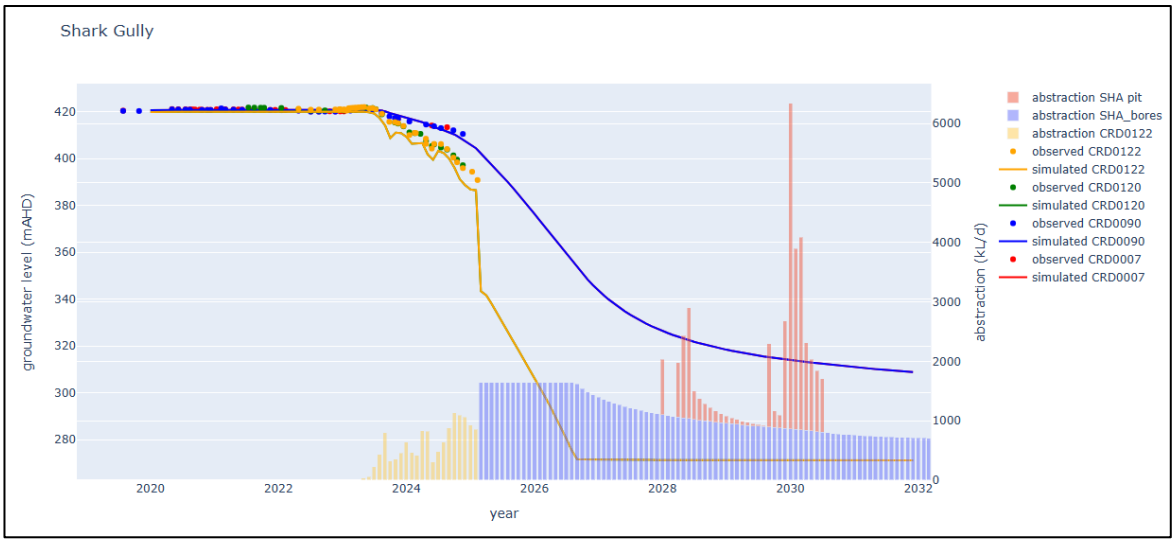

Notes: Sharp decline in water level in CRD0122 is related to increase in applied abstraction

Sparrow Lake

Mining at Sparrow Lake is planned to progress ~115 m below the current water table.

Drawdown extent from Sparrow Lake is simulated to extend up to 600 m from the pit edge within the BIF ridge, and up to 3,000 m east of the ridge to join drawdown from the ROM east of the ridge within the Euro Basalt and Mt Roe Basalt (Figure 5.5). Modelled drawdown extends up to 2,000 m westward from the ridge.

Drawdown is simulated to extend towards pools CO-WS-09 and CO-WS-14 during operations with a simulated >10 m at CO-WS-09 and 1–6 m drawdown at CO-WS-14, respectively, at the end of operations (Figure 5.4).

It is important to note that the drawdown extent is highly sensitive to the extent of higher flow zones that are currently informed by 3-day pumping tests only and not long-term abstraction. Additionally, the connection with depth between high flow features that were test pumped at Sparrow Lake and the surficial formations that feed pool CO-WS-14 is uncertain and has not been tested with test pumping (there is no bore at pool CO-WS-14). It is possible that the low hydraulic conductivity formations at surface will not be impacted by drawdown within the deeper aquifer

Drawdown extent at Sparrow Lake is significantly larger (1,000 m larger extent) than simulations in the previous assessment due to the deep progression of the pit and associated dewatering. The shape of the extent differs slightly from previous predictions (more drawdown towards the west and

less drawdown towards the east) due to changes in hydraulic conductivities and extents of high hydraulic conductivity features during the calibration.

Figure 5.4: Simulated water levels at Pool 14 and Sparrow Lake

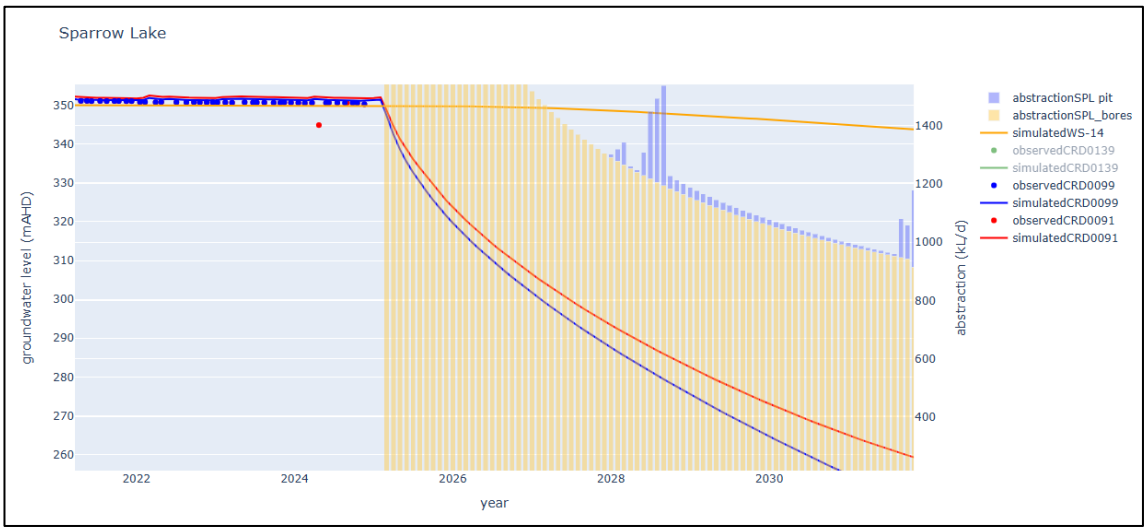

Figure 5.5: Drawdown extents at end of operations

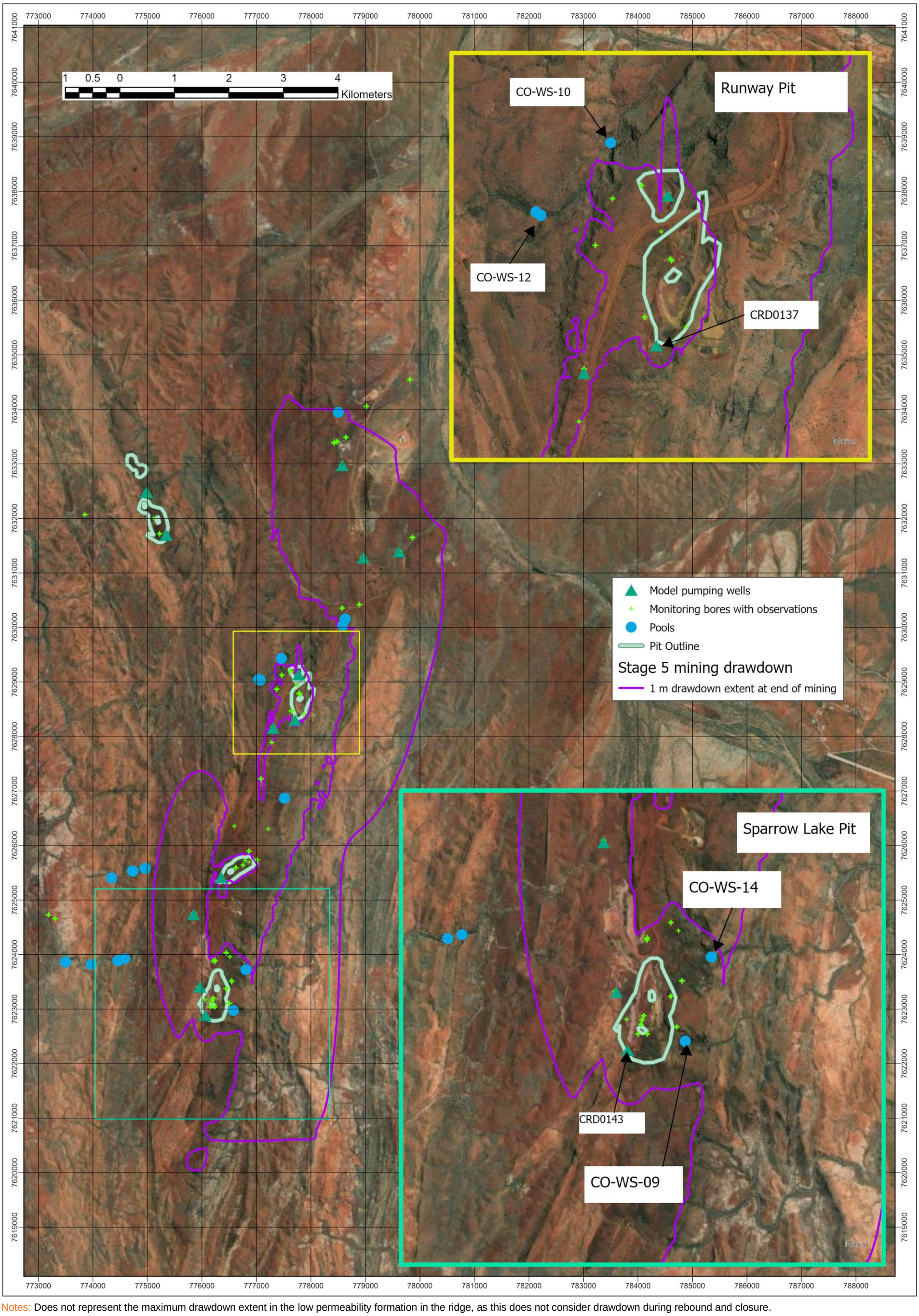

Notes: Does not represent the maximum drawdown extent in the low permeability formation in the ridge, as this does not consider drawdown during rebound and closure.

Table 5.2: Simulated drawdown at pools during operation

Pool	Simulated drawdown during operations (m)	Comment
CO-WS-14	1 to 6	Drawdown is highly sensitive to placement of moderate hydraulic conductivity. Range is indicative of different sensitivity scenarios.
CO-WS-09	>10	Pool has been identified as not groundwater dependent; high level of drawdown is due to high K zone placement and may be unrealistic.
CO-WS-10	<1	Drawdown not simulated to reach pool with the currently assigned hydraulic conductivities.
CO-WS-12	<1	Drawdown not simulated to reach pool with the currently assigned hydraulic conductivities.
CO-WS-01	5.5	From propagation of drawdown from CRD0082, bore does not usually operate at full flow and to date only seasonal fluctuation at monitoring bores near the pool (CRD0103) have been observed.

5.2.2 Operational dewatering requirements

The model simulates the planned pit progression and advanced dewatering rates from ex-pit bores. Preliminary results from the modelling suggest that the use of auxiliary sumps will be required as pits progress to support dewatering ahead of planned mining. In some areas, existing ex-pit dewatering bores will not extend deep enough or intersect areas with sufficient hydraulic connection to the aquifer to facilitate dewatering without the use of sumps. Additional ex-pit bores (or in-pit bores) may decrease the requirement for sump pumping during pit progression below the water table, and delay the time at which sump pumping is required. The effectiveness of additional bores will depend on the depth of fractures and high flow zones; if pit depths extend to the lowest point of high flow zones or the fractured area, some level of sump pumping to dewater at the base of the pit will be required. Examples of simulated water levels from dewatering bores alone compared with planned pit progression are provided in Figure 5.6.

Actual abstraction for water supply is typically lower than rates previously (and currently) used in simulations and if bore abstraction is restricted to water supply requirements (instead of being optimised for dewatering) this would not facilitate dewatering in advance of mining. Modelling suggests that even with bores pumping at maximum rates for dewatering (and additional ex-pit bores being installed) some auxiliary sumps will still be required, as the bores will not be sufficient to reduce groundwater levels at the deepest part of the pits.

Regardless of the dewatering strategy (proportion of advance dewatering with bores and sumps), the model simulates a surplus of water at Sanjiv Ridge starting in 2028 as Shark Gully progresses below the simulated water table. The magnitude of the surplus will fluctuate over time as pit progression rates vary (higher progression will result in higher inflow rates) and as the aquifer is dewatered (high initial inflow rates will reduce as the aquifer is dewatered during a pause or slowdown in pit progression).

The simulated dewatering rates from bores (assigned) and pit sumps (simulated) are presented in Figure 5.7 and summarised by calendar year in Table 5.3 for the current mine plan. Bores yields are likely to reduce over time as water levels decrease (and the model does have a reduction in flows at Shark Gully); however, the assigned rates are shown as the highest estimate. Peaks in

dewatering rates are likely overestimated and should not persist. In general, a 30 L/s surplus from pit dewatering is simulated (assuming bores are run at the maximum rate), with peaks of 70 L/s or more possible during periods of rapid pit progression.

Table 5.3: Annual predicted modelled abstraction volumes (m^3) for Sanjiv Ridge

Year	Total abstraction (kL/year)	Haul road construction (kL/year)	ROM (kL/year)	Runway (kL/year)		Shark Gully (kL/year)		Sparrow Lake (kL/year)		Comments
				Sumps	Bores	Sumps	Bores	Sumps	Bores	
2020	580,492	454,029	112,326	-	14,137	-	-	-	-	
2021	468,905	52,089	202,211	-	210,914	-	-	-	3,691	
2022	566,236	33,902	174,085	-	358,249	-	-	-	-	Historical abstraction
2023	647,109[1]	64,045	172,498	-	327,634	-	82,052	-	-	
2024	730,533	74,773	192,363	-	195,196	-	268,201	-	-	
2025	1,567,875	1,639	276,468	-	204,836	-	555,206	957	528,768	
2026	1,717,757	-	283,824	-	236,520	-	584,364	306	612,743	
2027	1,484,380	-	283,824	-	236,520	-	452,244	-	511,791	
2028	1,596,389	-	284,602	4,958	237,168	207,408	377,277	36,910	448,066	Assumed increase in 2025 for advanced dewatering in simulation, but will likely to be less with full increase in abstraction in 2026
2029	2,241,865	-	283,824	847,757	235,788	127,818	333,156	9,587	403,935	
2030	1,691,273	-	283,824	-	236,093	495,390	296,895	5,600	373,471	
2031	1,157,209	-	283,824	-	236,520	-	267,672	23,315	345,879	
2032	297,856	-	72,317	-	60,264	-	65,955	64,778	34,543	Sparrow Lake active until February 2032
2033	-	-	-	-	-	-	-	-	-	

Notes: Abstraction volumes are used for groundwater modelling. Annual volumes presented are taken from Atlas supplied water take records and are based on calendar year so may vary from reported abstraction volumes.

[1] Includes minor (< 1,000 kL) of abstraction from Glen Herring

Figure 5.6: Drawdown at pits with advanced dewatering

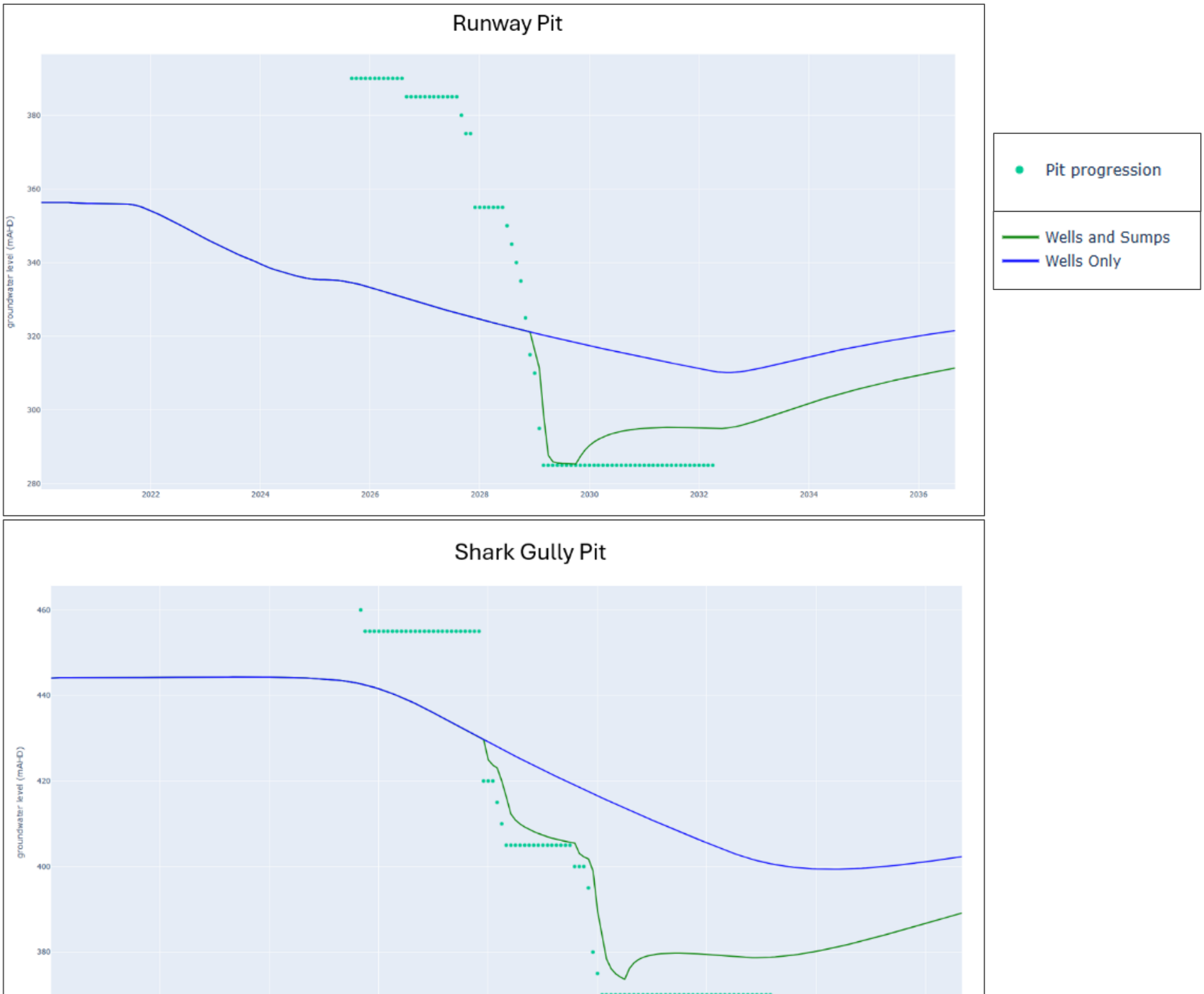

Notes: Sumps (green line) are switched on when pit progression reaches water table and switched off 4 months after the pit reaches its maximum depth.

Figure 5.7: Simulated dewatering rates and bore rates

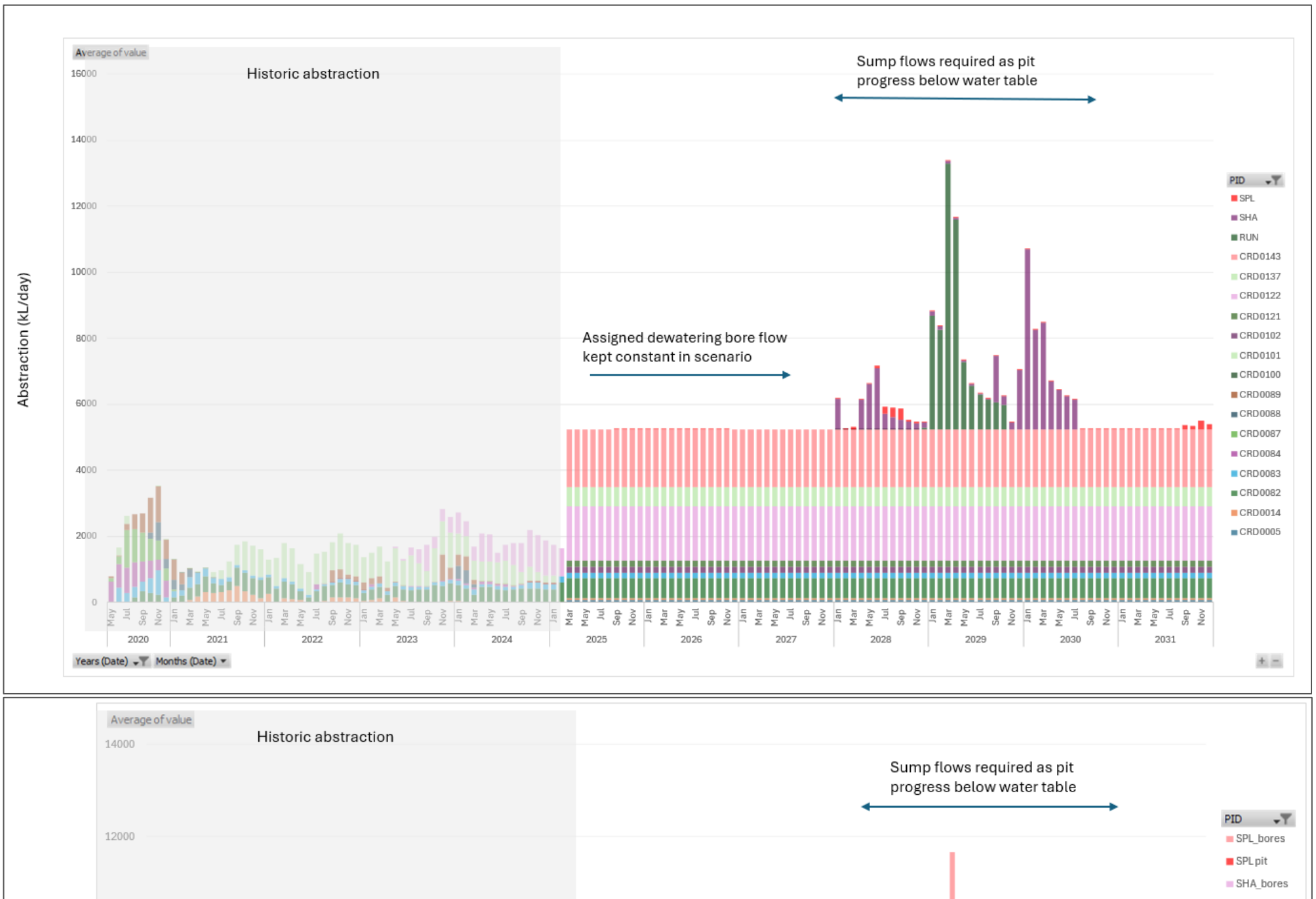

Note: Top graph represents assigned rates; bottom graph represents simulated rates once adjusted for bore reduction due to water level decrease to the base of the bore.

5.2.3 Post closure

Combined outputs from the water balance and groundwater models indicate that pits will act as evaporative groundwater sinks abstracting a net 1.1–2.5 L/s, and equilibrating to a pit lake level that is 24 m to 46 m lower than pre-mining groundwater levels, see Table 5.4 (not including Glen Herring Pit which is only planned to just above the water table).

Table 5.4: Pit lake water levels and evaporations

Pit	Resting pit lake water level (mAHD)	Net outflow[1] (L/s)	Depth below pre-mining groundwater level[2] (m)	Comment
Runway	327	1.6	24	
Shark Gully	380	1.1	41 to 47	Observed level is higher on the eastern side of the pit than on the western side
Sparrow Lake	305	2.5	46	

Notes:

[1] Surface water inflow minus evaporation

[2] Groundwater level before all mining operations including water supply

The resultant simulated drawdown from the permanent pit lakes (evaporation driven groundwater sinks) is presented in Figure 5.8 as drawdown from the simulated pre-mining water level.

Modelling results simulate drawdown extending to some pools (Table 5.5) within the ridge (CO-WS-14, CO-WS-10, and CO-WS-12) as a result of the simulated effective drawdowns of 24 m at Runway and 46 m at Sparrow Lake post-closure. Some post-closure drawdown is simulated at pools CO-WS-13 and CO-WS-08 as a result of interference from the respective drawdowns for the Sparrow Lake and Shark Gully pits, however there is less certainty in these predictions due to a lack of drilling, testing and operational data in this area.

Post-closure drawdown extents continue to propagate in some areas, particularly the ridge itself, after mining is completed and pit lakes form due to the low hydraulic conductivity of the FBA, and the resultant lag in dewatering of the aquifer. This results in drawdown extents that are larger than those simulated during mining.

Glen Herring

A pit lake will not form at Glen Herring as the pit will not extend below the water table.

Runway

Drawdown associated with the development of a lake at Runway Pit is comparable to the operation of CRD0101 in perpetuity. This bore has currently drawn down the aquifer ~28 m at the pumping bore and the pumping rate has reduced from 9.8 L/s to 2.4 L/s with no associated rebound in water levels. In comparison, groundwater inflow post-closure is estimated to continue at an estimated rate of 1.6 L/s from the low permeability FBA.

Drawdown is simulated to propagate out towards pools CO-WS-10 and CO-WS-12 and range from 1 m to 4 m as inflows from the low permeability FBA equilibrate over time. This will result in a continuation of the drawdown observed at CRD0006 (located equidistant ~300 m between the pit edge and CO-WS-10) which is currently at 4 m below pre-mining water levels and is still progressing at ~0.06 m/month. The drawdown at this bore is simulated to be ~10 m below pre-operation water levels when equilibrium is achieved with evaporation and surface water inflows in the lake at Runway Pit. The model is likely overestimating drawdown propagation towards the west, as during calibration, drawdown at CRD0092 was over-simulated at 3 m compared to the ~1 m observed at the bore. As such, the simulated post-closure drawdown at CO-WS-12 may be too conservative (overestimated).

Shark Gully

The low inferred hydraulic conductivity at Shark Gully Pit limits drawdown impacts to the ridge immediately adjacent to the pit (simulated up to 400 m from the pit edge).

Drawdown is simulated to extend towards the west in combination with drawdown induced from Sparrow Lake. The estimated post-closure pit lake water level is topographically higher than the pools and, in isolation, unlikely to result in any drawdown impacts on the pools. Any drawdown associated with the pools is predominantly caused by the Sparrow Lake evaporative sink, which may be influenced by a reduction in recharge, and inflow from the ridge to the west due to the Shark Gully Pit lake.

Sparrow Lake

The low post-closure water level simulated for the lake at Sparrow Lake Pit (305 mAHD, 46 m below the water table) relative to the pre-mining water table results in simulated drawdown extending beneath CO-WS-14 within the ridge (located ~500 m north east of the pit edge) and propagating out towards CO-WS-13 and CO-WS-08.

Local hydrogeological conditions may prevent drawdown from extending to the pools. However, water levels at Sparrow Lake and Razor Back are generally lower than in the rest of the ridge and have a gentler groundwater gradient suggesting higher background hydraulic conductivities within the FBA than other areas of the ridge. Additionally, drawdown from pumping tests (and low relative levels) in bores that had a very low or no airlift yield (CRD0099 and CRD0091) suggest that even in the low hydraulic conductivity basement there is some connection to the higher hydraulic conductivity features. Predicted drawdowns between Sparrow Lake Pit and Razor Back Pit are therefore considered to be sensible when compared with observed pumping test drawdowns at Sparrow Lake. The connection between Sparrow Lake and Razor Back is further supported by water strikes and airlift yields that were recorded for the length of drilling at bores CRD0140 and CRD0150, which are located between the two pits. Airlift data recorded during drilling from the water table to depth at these locations suggest connections between these pits.

It is possible to simulate zero drawdown from the pit lake at CO-WS-14 post-closure but only when a continuous aquitard with a low hydraulic conductivity (less than 5E-6 m/d) is placed between CO-WS-14 and Razor Back Pit. Bores north of the pit do suggest the presence of a lower hydraulic conductivity aquitard formation based on high relative water levels, early termination of pumping tests, and the lack of water encountered during drilling in some bores (CRD0139). However, no drilling or testing data is available to confirm the hydrogeological conditions directly between Razor Back Pit and CO-WS-14.

Table 5.5: Drawdown at pools post-closure

Pool	Drawdown (m)	Comment
CO-WS-14	2–14	Dependent on assigned hydraulic conductivity at Razor Back Pit. Zero drawdown is possible if a continuous aquitard of <5E-6 m/d is present between the pit and CO-WS-14 but this is not tested with pumping data. Additionally, the pool may be supported by a perched water system (similarly not tested).
CO-WS-12	0–3	
CO-WS-10	2–5	
CO-WS-08	2–4	
CO-WS-13	2–3	
CO-WS-09	>20	This pool is identified as not groundwater dependent. Drawdown is sensitive to placement of high hydraulic conductivity features.

Note: ranges are taken from different sensitivity scenarios that include different placement of hydraulic conductivity zones and lower hydraulic conductivity and recharge scenarios.

Figure 5.8: Drawdown extent post-closure

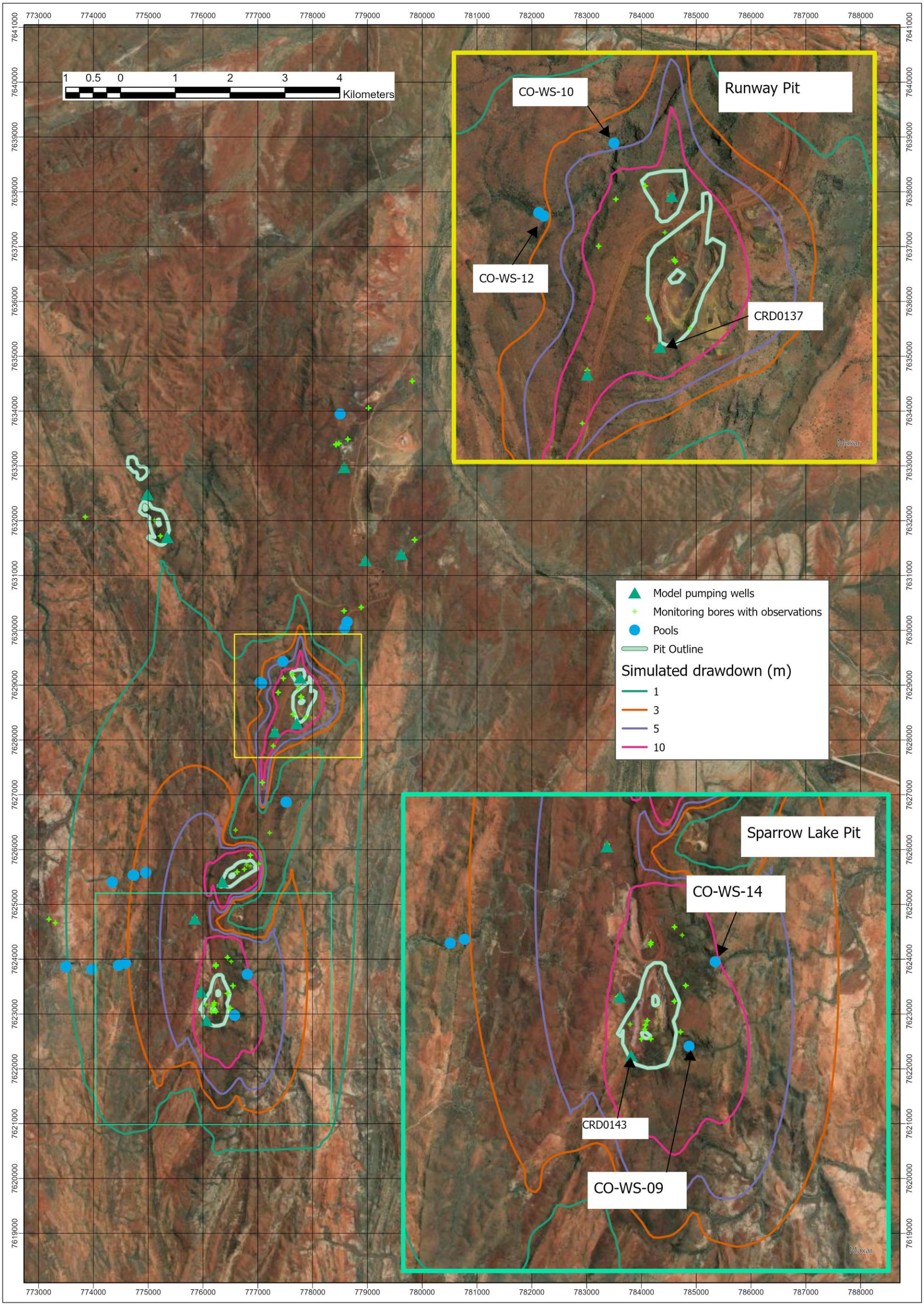

5.2.4 Rebound period between operation and post-closure equilibrium

The pit lake rebound rates that were output from the water balance model are presented in Figure 5.9. Rebound rates in all pits are highest during the first 5–10 years due to a high hydraulic gradient and larger groundwater inflows. All three pits are simulated to have equalised groundwater inflow with net evaporation by 2060 and water levels will fluctuate around a mean level from this time. Some change in groundwater levels will continue after this time due to the low hydraulic conductivity of the FBA; while this will have an impact on pit inflow rates, the changes are considered negligible and would not have much of an impact on pit lake water levels As such, there is a slight discrepancy between inflows used in the water balance and the groundwater water model but further iteration is considered not required at this phase due to the negligible difference that it would cause to predictions.

Drawdown rates were assessed from the rebound scenario outputs as the year-on-year change at pools that were identified as having impacts at closure. Table 5.6 presents the year-on-year changes during operations and post cessation of mining. Drawdown rates during the rebound period are below 0.5 m per year (m/yr) with the highest rates observed at CO-WS-14 between 0.146 m/yr and 0.192 m/yr between 2039 and 2070 after which time the rate of drawdown starts to decrease, reaching negligible rates of less than 0.01 m/yr by 2201 and further reducing to 0.001 m/yr by 2401.

Drawdown rates at CO-WS-10 and CO-WS-12 are far lower than Pool 14 (Figure 5.11) with a rate as high as 0.017 m/yr at CO-WS-10 and 0.009 m/yr at CO-WS-12. Additionally, the peak in rate of drawdown lags about 100 years after cessation of mining due to the low hydraulic conductivity assigned to the FBA in the area.

The cumulative drawdown in the rebound period approached but did not quite reach the total drawdown simulated by the closure scenario in steady state, by the end of the rebound period simulation (year 2500). While the drawdown rate is almost negligible, there are some changes in water level suggesting that the system will not have achieve complete equilibrium until after 2500. However, the impact on the system after this date would be very small relative to the overall impacts (i.e. the system would be more than 80% recovered to final equilibrium by 2500).

Figure 5.9: Water level rebound in pit lakes at end of operations

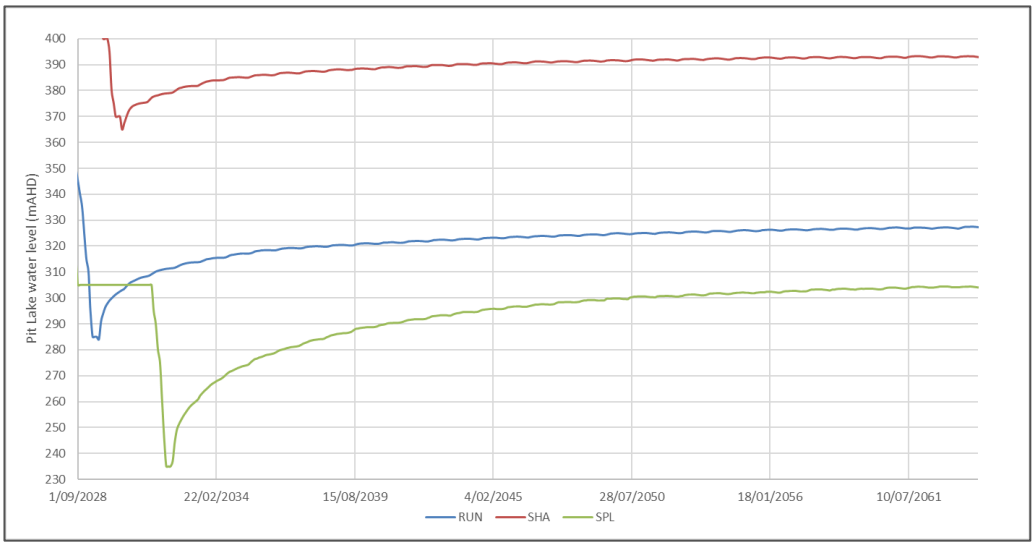

Figure 5.10: Drawdown during rebound at Pool 14

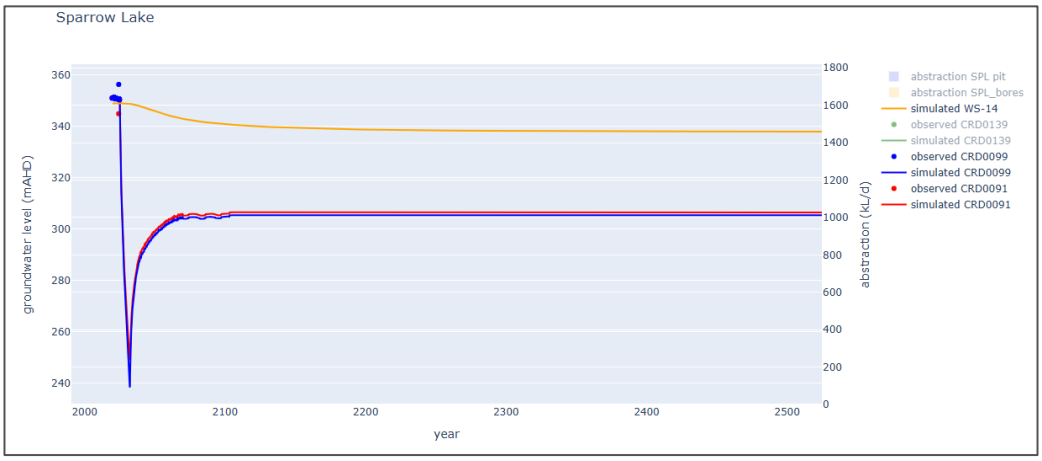

Figure 5.11: Drawdown during rebound at Pools 10 and 12

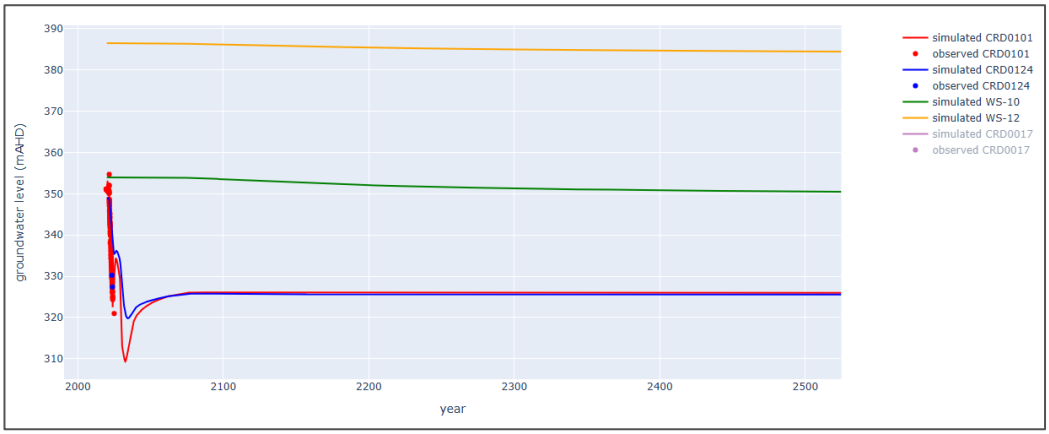

Table 5.6: Drawdown rates in m/yr at pools between operation and post-closure equilibrium

Year from	Year to	CO-WS-10	CO-WS-12	CO-WS-13	CO-WS-14	CO-WS-8	CO-WS-9
				Maximum drawdown rate in m/yr during period			
2033	2040	-	0.000	0.001	0.168	-	-
2041	2050	0.001	0.003	0.002	0.192	0.002	-
2051	2060	0.005	0.006	0.003	0.186	0.004	-
2061	2070	0.009	0.007	0.003	0.146	0.004	0.031
2071	2080	0.012	0.008	0.003	0.113	0.005	0.130
2081	2090	0.015	0.008	0.004	0.075	0.005	0.117
2091	2100	0.016	0.008	0.004	0.057	0.005	0.116
2101	2150	0.017	0.008	0.004	0.046	0.005	0.002
2151	2200	0.015	0.007	0.004	0.017	0.005	0.002
2201	2250	0.012	0.007	0.004	0.010	0.006	0.001
2251	2300	0.008	0.004	0.004	0.005	0.005	0.001
2301	2350	0.006	0.003	0.003	0.003	0.004	0.000
2351	2400	0.004	0.003	0.003	0.002	0.004	0.000
2401	2450	0.004	0.002	0.003	0.001	0.003	0.000
2451	2500	0.003	0.002	0.003	0.001	0.003	0.000
Cumulative drawdown by 2500		**3.47**	**2.06**	**1.68**	**11**	**2.22**	**34.5**
Drawdown at equilibrium		**4**	**2.5**	**2.5**	**14**	**3**	**35**

Notes: Drawdown is presented as the maximum rate in m/yr between the indicated period.

6 Conclusions

The existing numerical model was updated to develop predictions of the impact of Stage 5 below water table mining at Sanjiv Ridge. The calibration update between Revision 2 (SRK, 2023) and the updated (Revision 3) model incorporated 2–3 additional years of operational data and five additional pumping tests.

The level of observation data, testing and operational data that was used in the calibration of the updated model is considered appropriate for predictions simulated by the model, specifically:

- Water supply bores operating at Runway and Shark Gully pits have good observations of drawdown that are of a similar magnitude (30–40 m drawdown) and duration (observations for 2–4 years) to the predictions of dewatering requirements for Stage 5 below water table mining.
- Sparrow Lake does not have the same span and scale of operation data as Runway and Shark Gully (limited to 6 months of abstraction at a low average rate ~0.2 L/s). However, there have been three pumping tests performed, the most recent round of which had good drawdown response data in bores up to 750 m away.
- ROM water supply bores have a good operational and observation record and the simulated operations have rates similar to those that the bores are currently operating.
- Glen Herring has the least amount of data available for calibration; however, the pit does not progress below the water table.

A predictive operational scenario was set up with a continuation of water supply bores at rates outlined in the previous H3 assessment (with some substitutions for bores inside the pit area) and drains to represent the planned pit progression. Water supply bores near to pit (CRD0137, CRD0122 and CRD0143) will also act as advanced dewatering. However, sumps will be required to facilitate dewatering in advance of mining as the rate of pit progression is predicted to overtake the rate of drawdown from the bores. Sumps will likely be required, potentially at lower pumping rates, even if additional ex-pit dewatering bores are drilled and operated.

Regardless of the dewatering strategy (proportion of advance dewatering with bores and sumps), the model predicts a surplus of water at Sanjiv Ridge starting from 2028 as Shark Gully progresses below the simulated water table. The magnitude of the surplus will fluctuate over time as pit progression rates vary and the aquifer is dewatered but is estimated to range between 30 L/s and 70 L/s.

Regionally, drawdown during operation of Stage 5 mining will be similar to that simulated in the previous assessment, with the following notable similarities and differences:

- Drawdown at Runway will extend further towards pools CO-WS-10 and CO-WS-12, as the pit will progress 35 m lower than the current water level. However, the predictive simulation does not predict drawdown at these pools during the operational phase of the mine.
- Drawdown at Sparrow Lake is simulated to extend towards the east and northeast of the BIF ridge significantly more (>1,000 m) than previous modelling due to the depth of the pit (~115 m below current water level) and associated dewatering. Drawdown is also simulated to extend past pools CO-WS-09 (identified as not groundwater dependent) and CO-WS-14 (Pool 14 did not have any impacts predicted from water supply by previous assessments). The predicted

drawdown during operations at CO-WS-14 is simulated to reach 1 m (6 m in the more conservative scenario).

Combined outputs from the water balance and groundwater models indicate that pits will act as evaporative groundwater sinks abstracting a net 1.1 L/s to 2.5 L/ at closure resulting in pit lake levels that are lower than pre-mining groundwater levels – 24 m lower at Runway and 46 m lower at Sparrow Lake. Based on these simulated levels, drawdown may extend to some pools post-closure within the ridge (pools CO-WS-14, CO-WS-10, and CO-WS-12). Some (1–3 m) post-closure drawdown is simulated at CO-WS-13 and CO-WS-08 from a combination of Sparrow Lake and Shark Gully.

Simulated drawdowns for operational, rebound and post-closure equilibrium represent a maximum possible drawdown within the FBA at the assigned hydraulic conductivities. Drawdown extents may be lower, as the hydrogeological system is highly heterogenous. Additionally, the aquifer systems feeding the pools within the ridge (e.g. Pools 14, 10 and 12) may be perched and disconnected from the broader FBA aquifer. If a perched, disconnected aquifer system is present at pools, simulated drawdown from pits would not impact groundwater flow to pools so long as the surface water catchment of the pools was not disturbed, or aquitard formations were not fractured through blasting.

The groundwater system is simulated to take over 400 years to achieve complete equilibrium; however, drawdown rates away from pit lakes will reduce to less than 0.01 m/yr after 100 to 200 years. During the rebound period between the cessation of mining and achieving of equilibrium within the groundwater system, the maximum rate of drawdown simulated at pools is 0.192 m/yr.

Recommendations

The following actions are recommended to further refine the model in the future, confirm model predictions, or optimise predictions:

- Continue data collection of abstraction volumes and water levels to allow further refinement of model predictions.
- Perform further field investigations (tracer testing, isotope sampling, and possibly drilling and testing) for pools with predicted drawdown to assess the degree of connection with the FBA or if a perched aquifer system feeds the pools.
- If possible, install a monitoring bore with a deep and shallow screen (with a good seal between the two) between Razor Back pit and Pool 14 to monitor (or lake thereof) impacts from water supply and dewatering at Sparrow Lake. A bore in this location, together with isotope analysis and tracer testing, would assist with conceptualisation of the aquifer system at Pool 14 and identify if a perched aquifer system that is disconnected from the FBA feeds the pool.
- Dewatering rate peaks maybe reduced by performing optimisation within the model by testing different abstraction regimes, in including in pit bores. The effectiveness of installing and operating additional ex-pit bores can also be tested during optimisation.
- Impact of excess water from dewatering can be assessed in the model and optimised together with the dewatering regime.

Closure

This report, Sanjiv Ridge Stage 5 Below Water Table Numerical Model Report, was prepared by

Zip Boniecki
Principal Consultant

and reviewed by

Brian Luinstra
Principal Consultant

All data used as source material plus the text, tables, figures and attachments of this document have been reviewed and prepared in accordance with generally accepted professional engineering and environmental practices.

References

SRK, 2019. *Corunna Downs Mine Water Supply H3 Hydrogeological Assessment,* Perth: Atlas.

SRK, 2023. *Sanjiv Ridge Mine Water Supply H3 Hydrogeological Assessment Update ,* s.l.: s.n.

SRK, 2025. *Numerical groundwater modelling for updated abstraction regime at Sanjiv Ridge,* s.l.: s.n.

SRK, 2025. *Sanjiv Ridge Stage 5 Water Balance Model Report,* s.l.: s.n.

Appendix A Model run log

Model Version Log

Model Version	Report Name	POW date	Mine Schedule	Pit shells	Scenarios completed	Scenario Name
1	Corunna Downs Mine Water Supply H3 Hydrogeological Assessment 2019	2018	NA, above water table	NA above water table	Drawdown assessment from water supply	K9tt2_gv23
					Drawdown assessment from increased water supply	K9tt2_gv24
2	Sanjiv Ridge Mine Water Supply H3 Hydrogeological Assessment Update 2023	2022	NA, above water table	NA above water table	Drawdown assessment from water supply – abstraction regime updated from previous H3	ATT015_SCP1
	2025 updated abstraction regime				Drawdown assessment from increased water supply - abstraction regime updated from previous H3	ATT015_SCP2
3	Sanjiv Ridge Stage 5 Below Water Table Mining Hydrogeology Study - H3 Hydrogeological Assessment	2024	T2_FY25_MTP_Recut_LOM_S1_V1 SMR TMM	SMR_Stage5_Pits	Drawdown assessment from BWT mining	SJR082P
	ATL009_Sanjiv Ridge Stage 5 Below Water Table Numerical Model_Rev2				Drawdown assessment from BWT mining - sensitivity for hydraulic conductivity	SJR083P
					Drawdown assessment from BWT mining - sensitivity for recharge and hydraulic conductivity	SJR058par6
					Drawdown assessment at closure	SJR082SS
					Drawdown assessment at closure - sensitivity for hydraulic conductivity	SJR083SS
					Drawdown assessment at closure - sensitivity for recharge and hydraulic conductivity	SJR058par6SS
					Assessment of rebound period between cessation of mining and equilibrium	SJR0082Re
					Assessment of rebound period between cessation of mining and equilibrium - sensitivity for hydraulic conductivity	SJR0083Re

Run Register

Type	Model file name	Description
Previous Model	ATT015	Version 2 of the Sanjiv Ridge/Corunna Downs model
Calibration	SRJ082	Calibrated to extra two years of operational data and 5 extra pumping tests. Updated to MODFLOW USG, layers added, and quadtree refinement implemented
Predictions and sensitivities	SJR082P	Drawdown assessment from BWT mining
Scenarios run during the historic phase and the predictive phase to assess impacts of parameter changes to both calibration and predictions	SJR083P	Drawdown assessment from BWT mining - sensitivity for hydraulic conductivity
(Informal sensitivity runs performed during calibration not listed)	SJR058par6	Drawdown assessment from BWT mining - sensitivity for recharge and hydraulic conductivity
	SJR082SS	Drawdown assessment at closure once groundwater level and pit lake water levels reach equilibrium
	SJR083SS	Drawdown assessment at closure - sensitivity for hydraulic conductivity
	SJR058par6SS	Drawdown assessment at closure - sensitivity for recharge and hydraulic conductivity
	SJR0082Re	Assessment of rebound times and rates between operation and equilibrium
	SJR0083Re	Assessment of rebound times and rates between operation and equilibrium - sensitivity for hydraulic conductivity

Appendix H Preliminary Pit Lake Water Quality Assessment

SRK Consulting (Australasia) Pty Ltd
Level 3, 18–32 Parliament Place
West Perth WA 6005
Australia

ABN: 56 074 271 720

+61 8 9288 2000

info@srk.com.au
www.srk.com

Final

Technical Memorandum

To	David Nyquest	**Client**	Atlas Iron Pty Ltd
From	Pierre Rousseau	**Project**	ATL009
Cc	Sam Nixon, Larissa Byrne, Paul Livesey	**Date**	20 June 2025

Subject Preliminary pit lake water quality assessment

1 Introduction

Atlas Iron Limited (Atlas) requested SRK Consulting (Australasia) Pty Ltd (SRK) to carry out a pit lake study to assess expected pit lake water balances and water quality for the Sanjiv Ridge iron ore project. The objective of the water balance is to predict whether the pits will be terminal sinks or release water to the environment (e.g. via overtopping). This entails tracking of water inflows to and outflows from the pits, as well as water stored in the pit under investigation. The water balance forms a key component of the water quality assessment, where the composition of the pit lake requires evaluation of the chemical composition of all components of the water balance.

This work was included as part of a larger site wide hydrological assessment being completed by SRK for the Stage 5 (below water table) mine plan. This memorandum documents the preliminary results from the modelling based on the data available to date (with literature values used to supplement gaps in the current dataset). This study supplements other hydrological studies to assess the risk of the pit lakes to the local environment. Specific considerations include the potential for contaminant migration to surface water and groundwater and for development of hazardous water quality in the pit lake post closure. Further phases of the pit lake study will include refinements to the model as more data become available, to be documented in a more comprehensive report.

The Sanjiv Ridge mine includes five pits – Glen Herring, Runway, Shark Gully, Razorback, and Sparrow Lake (Figure 1).

Outcomes from work completed by Mine Earth indicate that pit wall exposures at four of the five pits comprise low sulfur, non-acid forming (NAF) materials (Mine Earth, 2024; 2025a; 2025b). However, wall rock with higher sulfur content and greater acid generation potential will be exposed on completion of mining of the Sparrow Lake pit. Water quality modelling has therefore focused on the Sparrow Lake pit, as the water in this pit is likely to represent a worst case.

To assist in quantifying the risk posed by exposed wall rock, Mine Earth selected eight samples for kinetic testing. The samples are listed below, together with the rock type (and stage of mining in parenthesis):

- S1 – Shale (Stage 5)
- S2 – Chert (Stage 5)
- S3 – Goethite/hematite (Stage 5)

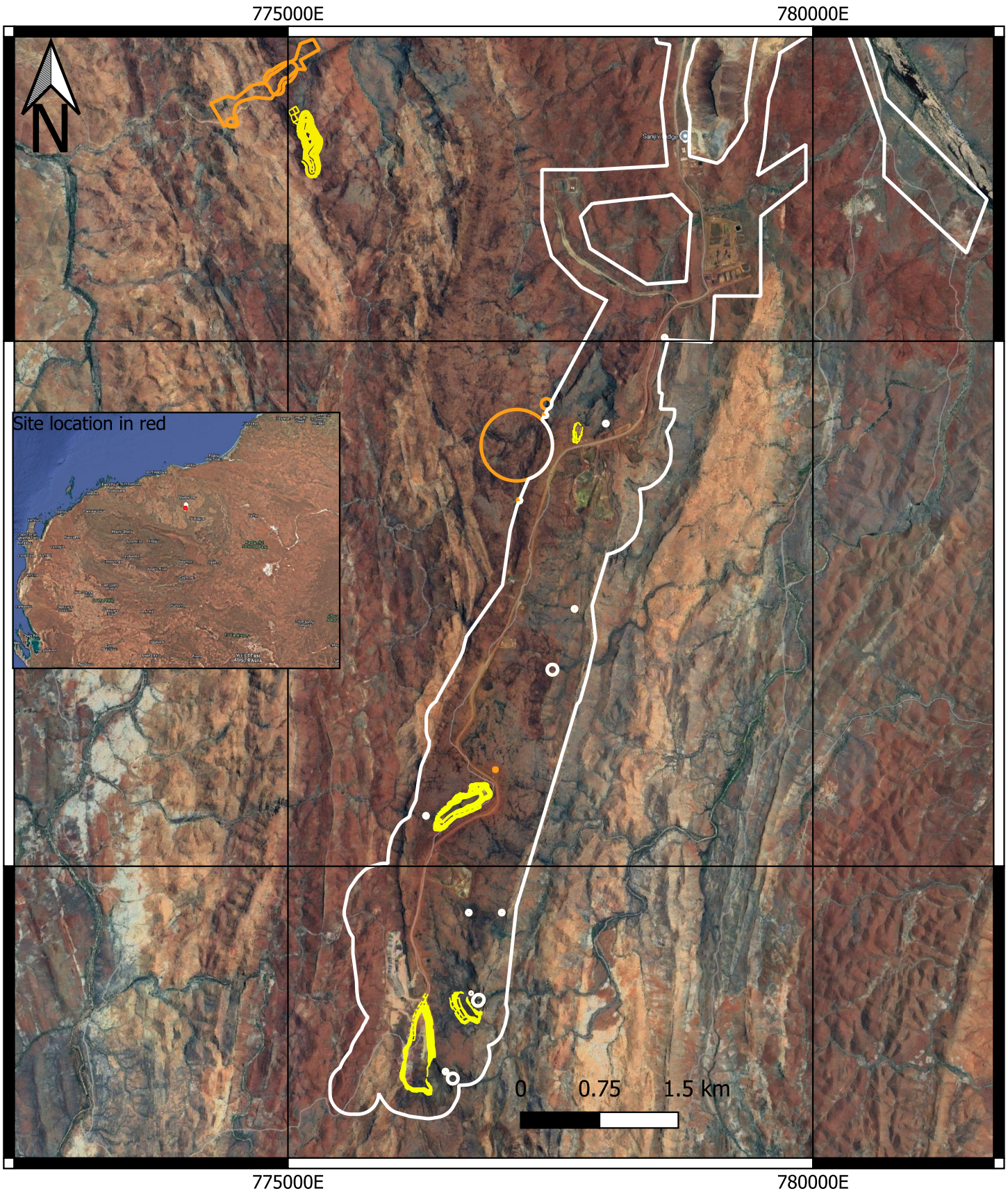

Legend

- Pit Designs
- SMR_Stage1_DE
- SMR Environmental Exclusion Areas

Client:	Altas Iron Ore
Project:	Sanjiv Ridge Below Water Table Assessment
Project Number:	ATL009
Figure Number:	Figure 1
Figure Title:	Sanjiv Ridge Iron Ore Project locality map.

Date: 28/05/2025
Coordinate System: GDA2020 / MGA zone 50
EPSG: 7850
Scale: 1:50,000

srk

- S4 – Banded Iron Formation (BIF) (Stage 5)
- S5 – Shale (Stage 5)
- S6 – Goethite/hematite (Stage 4)
- S7 – Chert (Stage 4)
- S8 – BIF (Stage 4)

These samples were exclusively derived from drill holes intersecting the Sparrow Lake pit volume and wall rock. The following static tests were completed prior to commencing kinetic testwork:

- acid base accounting (ABA)
- particle size distribution (PSD)
- oxygen consumption rate (OCR) and carbon dioxide release rate (CDRR)
- MEND deionised (DI) water leaching tests at 1:2 solid to liquid ratio.
- net acid generation (NAG) liquor elemental analysis.

Kinetic column leach testing is currently underway, with data for use in pit lake water quality modelling pending (likely available in 3 to 4 months). Due to the lack of data, an alternative approach has been implemented, which is outlined in Section 2.

2 Assumptions and limitations

The preliminary pit lake modelling provides indicative results that may be used to inform potential risks to the environment. Modelling provides an early indication of risks and identifies gaps to guide later phases of work. This preliminary pit lake model is based on the following assumptions:

- Leaching behaviour of wall rock and talus has been modelled based on analogue materials with comparable sulfide concentrations and lithological characteristics. There are expected to be differences between the analogue material and the Sparrow Lake pit material that will influence the results of modelling – for example, uncertainty due to likely differences in mineralogical compositions, elemental compositions and ratios, physical characteristics and site-specific water–rock interactions. The extent to which these factors may influence pit lake water quality can only be confirmed through kinetic test data on samples collected from site (as indicated, this testwork is underway).
- The model is based on mean water balance time series and hence does not account for extreme conditions associated with high or low pit lake water levels. This is not considered to be a major limitation, as the pit lake water level is only forecast to vary by ±4 m from the mean value. This translates to a volume difference of approximately 20% between the minimum and maximum pit lake storage volume.
- Solute concentrations in rainwater falling directly onto the pit lake are assumed to be zero. Due to the low concentrations of solutes in rainwater and the dominance of groundwater in the pit lake water balance, this assumption is not considered to be a model limitation.

3 Approach and methodology

The Sparrow Lake pit-lake water quality model was developed in an Excel workbook and incorporates:

- water balance outputs from a GoldSim water balance model (developed by SRK, 2025)
- geochemical source terms derived from average groundwater quality for Sparrow Lake near-pit bores (as shown in Section 4.2.1)
- literature-derived leaching rates for pit wall rock, classified by sulfur content.

The water quality is calculated for each of the following inflows to the pit:

- pit wall surface water run-off:
  - talus
  - pit wall rock
- groundwater.

The pit wall run-off component is subdivided into exposed contact areas based on block model sulfur concentrations on exposed wall rocks, according to the following classifications i) <0.01% S, ii) 0.1% to 0.2% S, iii) 0.2% to 1% S and iv) >1% S. Other solute concentrations for each material type were scaled relative to sulfate for that material. Such scaling is an industry standard approach for modelling water quality based on kinetic leach testing of sulfidic samples. Elements may be released directly from the breakdown of sulfide minerals, or from other minerals that come into contact with sulfuric acid released through sulfide oxidation. Direct rainfall over the pit lake is assumed to contribute a negligible proportion of the overall chemical load as indicated in Section 2.

As mentioned in Section 1, kinetic testing is currently underway and test data for modelling are pending. To facilitate preliminary water quality modelling of pit wall rock run-off, analogue data for sulfidic shales at different sites has been used, interpolated from kinetic data for Mt McRae Shales, as published by Linklater et al. (2015). Further model development and refinement will be carried out once sufficient site-specific kinetic column data are available, since there are likely to be differences in material properties that will influence the modelling results. The current pit water quality model excludes the contribution from the proposed in-pit dump (shown in Figure 1) due to lack of available data. The contribution from the in-pit dump is dependent on the composition of the waste rock (i.e. sulfide content and neutralising capacity) and the amount of material present above the long-term pit lake water level. The intention at the time of writing is for in-pit potentially acid forming (PAF) waste to be deposited in the Sparrow Lake pit waste dump, although this is subject to change depending on the environmental risks posed. The potential impact of waste rock disposal on pit lake water quality will be investigated as more information becomes available and will be included in later revisions of the model as appropriate.

Figure 1: Current planned pit layout and long-term steady-state water level (in-pit dump shown circled in the inset image)

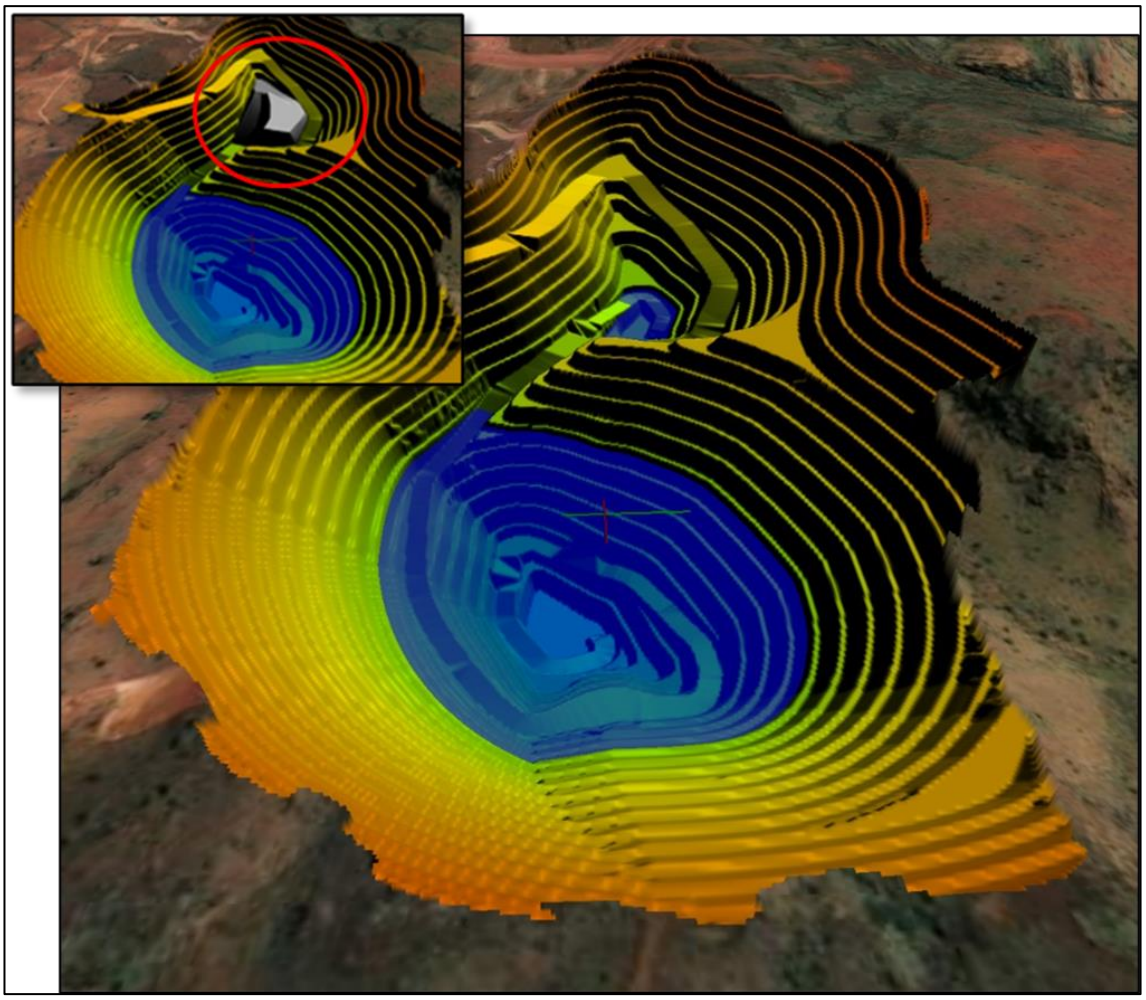

Source: SRK

Notes: The small image insert shows the pit layout with the proposed in-pit waste rock dump, for illustrative purposes. The large image shows the modelled steady-state water level over the entire pit.

4 Input data

4.1 Water balance

Input water balance data were obtained from the GoldSim water balance model (SRK, 2025). Data were converted to monthly frequency from the daily timestep implemented in the GoldSim model, to align with the timestep of the spreadsheet-based pit lake water quality model. The water balance indicated that all modelled pit water levels would be below the pre-mining water level (i.e. all pit lakes are likely to be terminal sinks). The GoldSim model output shows that the mean pit water level for Sparrow Lake pit would be in the range 307 ±4 mAHD.

A graph indicating relative inflows from surface water and groundwater sources to the Sparrow Lake pit is included in Figure 2. Based on cumulative inflows in the groundwater model, the

average contributions to pit inflows over the modelled period of 400 years is 59% groundwater, 21% pit wall run-off and 20% direct rainfall recharge over the pit lake. The predicted long-term steady-state water level is approximately 44 m below the pre-mining water level.

Figure 2: Modelled monthly inflows to the Sparrow Lake pit and pit lake volume, derived from the daily GoldSim water balance model (SRK 2025)

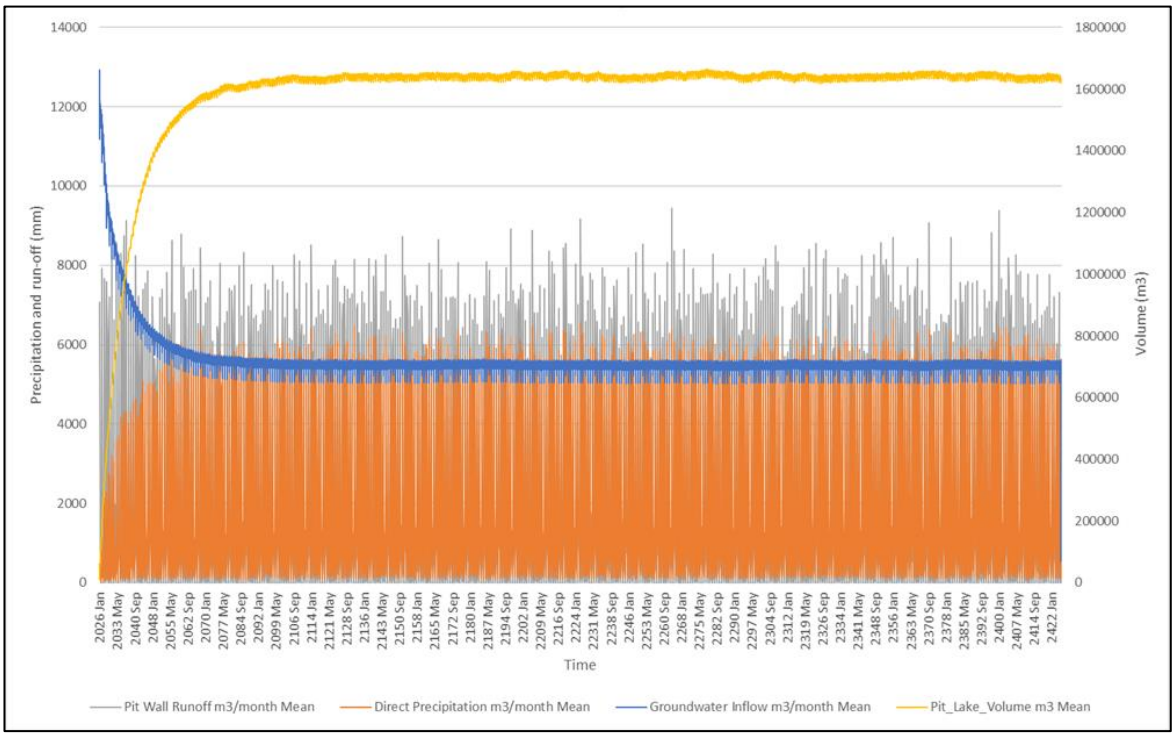

Source: SRK

4.2 Geochemistry

4.2.1 Groundwater

Groundwater quality data were collated for all groundwater bores allocated to the Sparrow Lake pit in the groundwater quality database and the mean values for selected parameters were used to calculate the groundwater contribution to pit lake chemistry in the pit lake water quality model. The data span a period between April 2014 and November 2024 and include between 1 and 10 samples per monitoring bore (see Figure 3). Groundwater chemistry statistics for Sparrow Lake pit bores are included in Table 1, with mean values used for water quality modelling highlighted in yellow.

Figure 3: Data included in groundwater quality statistics.

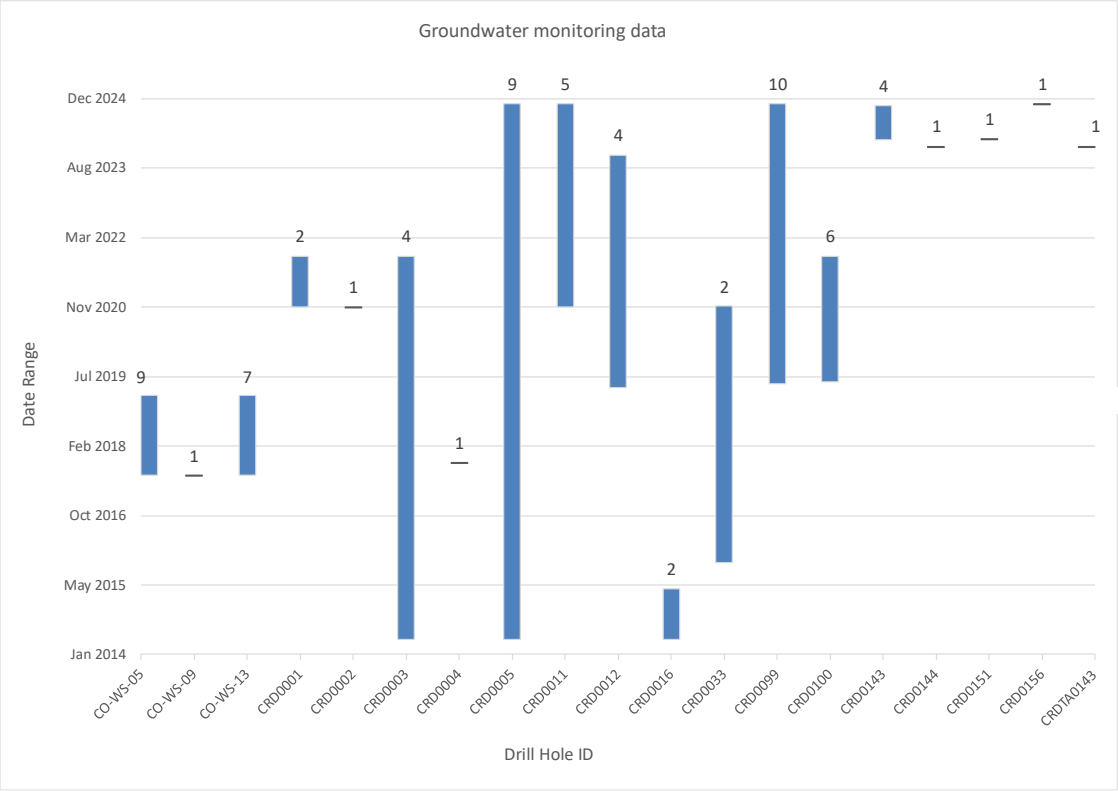

Sources: \\srk.ad\dfs\au\per\ATL009 - Sanjiv Ridge Below Water Table Mining Hydrogeology study\04_Working_Files\Geochemistry\Pit Lake WQ Modelling\Raw water quality data.xlsx"

Notes: Bars start at the first sampling date and end at the last sampling data in the dataset. Sample counts for each sampling location are shown above the bar.

The pH of the groundwater is in the near-neutral range (between pH 6.3 and 8) and contains alkalinity (average of 183 mg$CaCO_3$/L). The water is of low salinity (average electrical conductivity – EC of 610 µS/cm), with modest concentrations of major cations (e.g. Ca) and anions (e.g. Cl and SO_4). Trace element concentrations are generally low.

Table 1: Water quality statistics for the Sparrow Lake pit groundwater samples

Parameter	Statistic						
	Unit	Count	Mean	Minimum	50%	Maximum	Std Dev.
pH	pH units	54	7.2	6.3	7.2	8	0.49
EC	µS/cm	42	610	150	560	1,300	180
SO_4	mg/L	55	55	1	70	89	29
Cl	mg/L	55	66	4	67	150	25
Si	mg/L	28	7.9	1.7	7.4	18	3.6
Total alkalinity as $CaCO_3$	mg/L	53	180	63	130	460	120
Total suspended solids	mg/L	51	2,600	5	12	92,000	14,000
Total dissolved solids	mg/L	54	370	87	330	710	120
Ca	mg/L	55	31	1.2	22	80	20
Mg	mg/L	55	37	0.6	37	66	12
Na	mg/L	55	41	1.4	39	69	12
K	mg/L	55	2.9	0.4	2.4	12	1.7
Al	mg/L	45	0.0069	0.005	0.005	0.01	0.0024
Sb	mg/L	45	0.00058	0.0002	0.0003	0.0022	0.00045
As	mg/L	47	0.0026	0.0002	0.001	0.02	0.0049
B	mg/L	47	0.13	0.008	0.11	0.3	0.048
Ba	mg/L	45	0.041	0.003	0.03	0.14	0.032
Cd	mg/L	47	0.00013	0.00005	0.00007	0.001	0.00023
Co	mg/L	45	0.0019	0.0001	0.001	0.0057	0.0017
Cr (total)	mg/L	42	0.00088	0.0002	0.0004	0.005	0.0013
Cr (VI)	mg/L	44	0.0013	0.001	0.001	0.002	0.00045
Cu	mg/L	47	0.0014	0.0005	0.001	0.01	0.0018
F	mg/L	51	0.27	0.1	0.3	0.5	0.1
Fe	mg/L	47	0.74	0.002	0.04	5	1.3
Pb	mg/L	47	0.0017	0.0001	0.0001	0.02	0.0049
Mn	mg/L	47	0.53	0.0029	0.45	1.6	0.43
Hg	mg/L	45	0.000056	0.00004	0.00004	0.0001	0.000026
Mo	mg/L	45	0.00069	0.0001	0.0003	0.008	0.0012
Ni	mg/L	47	0.009	0.0005	0.0028	0.046	0.013
NO_2 + NO_3 as N	mg/L	43	0.67	0.005	0.01	10	1.7
Se	mg/L	47	0.0038	0.0002	0.0008	0.05	0.012
Ag	mg/L	42	0.0004	0.0001	0.0001	0.001	0.00043
Sr	mg/L	45	0.11	0.02	0.089	0.63	0.089
Sn	mg/L	45	0.0028	0.0002	0.0002	0.01	0.0042
Zn	mg/L	47	0.17	0.002	0.022	5.1	0.74

4.2.2 Pit wall and talus run-off and seepage

Wall rock and talus solute release rates for selected parameters, based on analogue kinetic leaching rates reported in Linklater et al. (2015), are shown in Table 2. Scaling factors used in modelling are summarised in . The solute release rates are based on the abovementioned assumptions of analogous behaviour of similar lithologies and the scaling factors are based on typical observed physical properties of similar materials, along with published results of field studies. Scaling factors are applied because there will be differences between conditions in the laboratory and the field (e.g. particle size, fraction contacted by water) – they are approximations to allow scaling up of laboratory data to field conditions.

Wall areas used for each material type are shown for each elevation interval in Figure 4. Two important observations from Figure 4 are:

- There is variability in area versus elevation due to different slope angles of benches and batters affecting exposed surface area over a given elevation interval.
- There is a decrease in exposed area versus elevation above the 353–357 m interval (contrary to expectation), due to the spill level of the pit occurring within that interval and air gaps in the pit wall at higher levels, as can be observed in Figure 1.

Table 2: Selected kinetic leaching rates applied to wall rock and talus materials

Parameter	Leaching rate (mg/kg/week) by sulfur category			
	>1%	0.2–1%	0.1–0.2%	<0.1%
SO_4	36.1	3.6	1.81	0.01
Ca	5.42	0.542	0.271	0.001
K	1.45	0.145	0.072	0.000
Mg	5.42	0.542	0.271	0.001
Co	0.036	0.004	0.002	0.000
Cu	0.001	0.0001	0.000	0.000
Fe	0.005	0.001	0.000	0.000
H	0.108	0.011	0.005	0.000
Ni	0.145	0.014	0.007	0.000
Si	9.03	0.903	0.452	0.002
Se	0.004	0.0004	0.000	0.000
Zn	0.014	0.001	0.001	0.000

Table 3: Laboratory to field scaling factors

Item	Units	Scaling factor	
		Talus	Exposed wall rock
Surface area correction	-	0.2	0.01
Fraction flushed by rainfall	-	0.5	0.1
Temperature correction	-	1	1
Assumed thickness oxidising material	m	1	0.1
Bulk density	kgm^{-3}	1,600	2,540
Mass, per m^2	kg	1,600	254

Figure 4: Exposed wall areas as a function of elevation and sulfur content

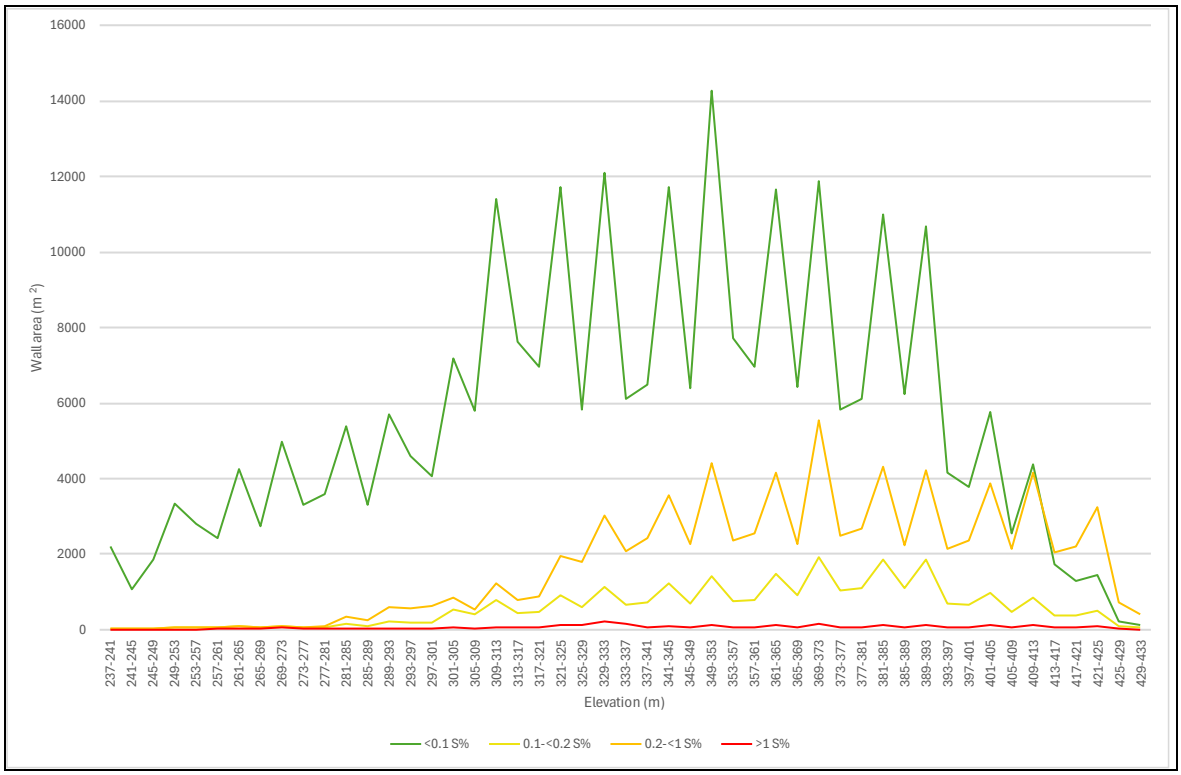

Source: SRK

Figure 5: Sulfur distribution in Sparrow Lake pit, indicating sulfur concentration classes identified in the resource block model.

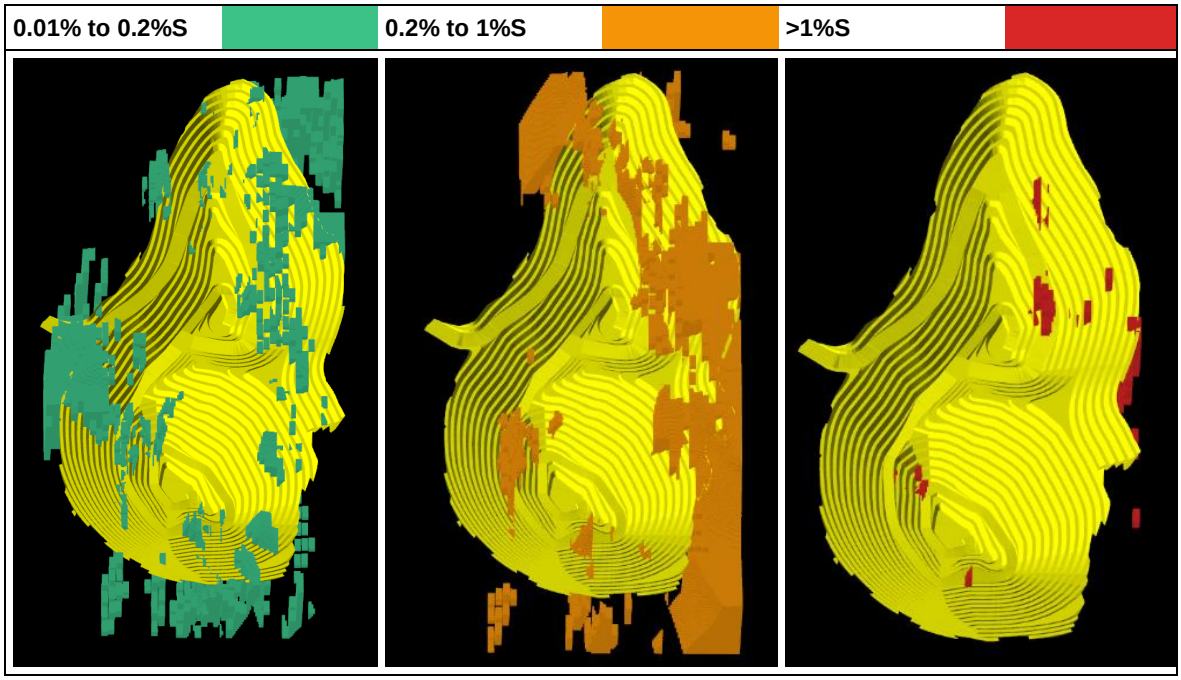

Source: SRK

Notes: Areas not covered by any of the categories are attributed to <0.01% S concentration.

5 Results and discussion

Water quality model results were generated from the spreadsheet model and speciated using PHREEQC geochemical modelling software.

Sensitivity analyses were carried out by calculating speciation at redox values of pe = -2 (reducing conditions), pe = 4 (mildly reducing conditions) and pe = 12 (oxidising conditions). For the Pilbara region, the most likely conditions would be oxidising to mildly reducing, due to limited presence of organic matter. Additionally, sensitivity to CO_2 alkalinity buffering was set using log pCO_2 fugacities of -3.5 (atmospheric CO_2 concentration) and -2.0 (CO_2 saturated groundwater/soil water concentration). The effect of varying pe and pCO_2 on solution pH can be seen in Figure 6.

Due to the use of analogue Mt McRae Shale data for modelling water quality, metal concentrations are not reported, as they may be substantially different to those that would be generated from the Sparrow Lake pit lithologies and are dependent on the source rock trace element geochemistry, which tends to be location-specific. Dissolved metal concentrations would also strongly depend on pH, which is considered to be key in evaluating the risk of poor water quality developing in the pit lake, partly associated with the likelihood of mobilising potentially toxic elements.

Modelled pH values over time for the different pe–pCO_2 combinations evaluated in PHREEQC are shown in Figure 6. The modelled results indicate that water in the Sparrow Lake pit is likely to remain neutral to alkaline. This is consistent with the alkalinity–acidity cumulative load balance

calculated for the pit lake water quality model, shown in Figure 7, as well as being consistent with expectations given the water balance and associated water qualities.

Modelled major ion concentrations are shown in Figure 8 for illustrative purposes and are considered to be indicative of future pit water quality, assuming that the average modelled groundwater inflow rate and average measured chemistry, used for modelling pit lake water quality, are representative. This premise is based on the understanding that groundwater accounts for approximately 60% of the water inflow volume to the pit and that it is dominant relative to the pit wall run-off component (given the limited exposure of material with >0.2% S). Materials with >1% S make up <1% of the pit wall according to the block model, thereby limiting the influence of potentially acid generating lithologies on pit lake water quality.

The decreasing concentration of calcium modelled shown in Figure 8 is attributable to calcite precipitation, as shown in Figure 9.

Figure 6: Modelled pH for selected pe–pCO_2 combinations

pe	Log pCO_2 = -3.5	Log pCO_2 = -2.0
12	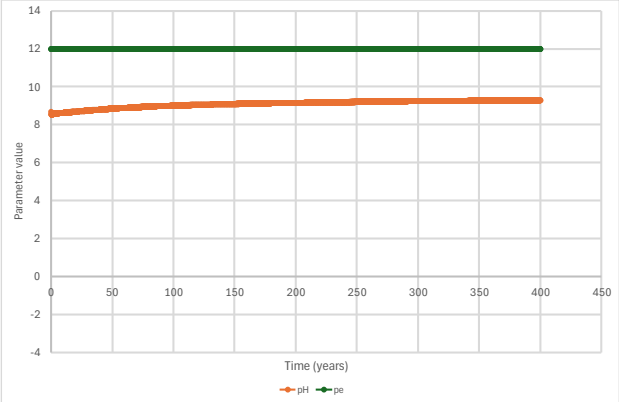	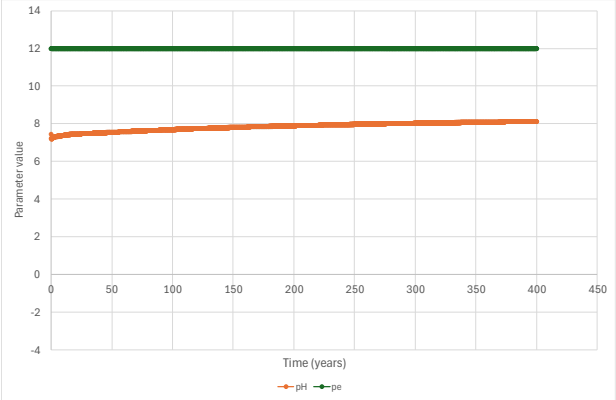
4	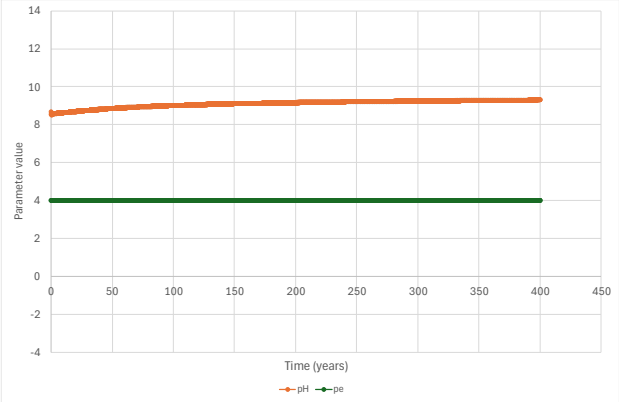	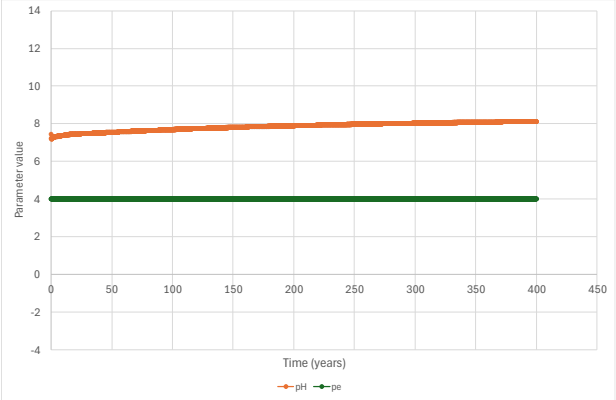
-2	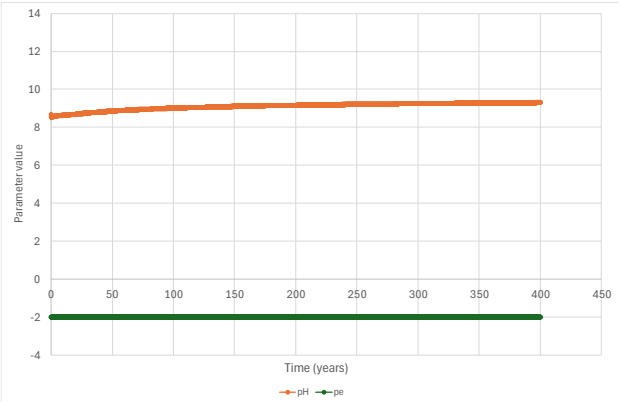	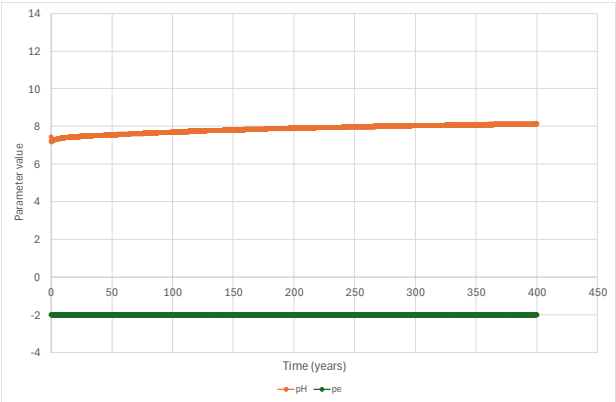

Sources: SRK

Figure 7: Comparison of cumulative acidity and alkalinity modelled to flow into the Sparrow Lake pit from groundwater and surface run-off

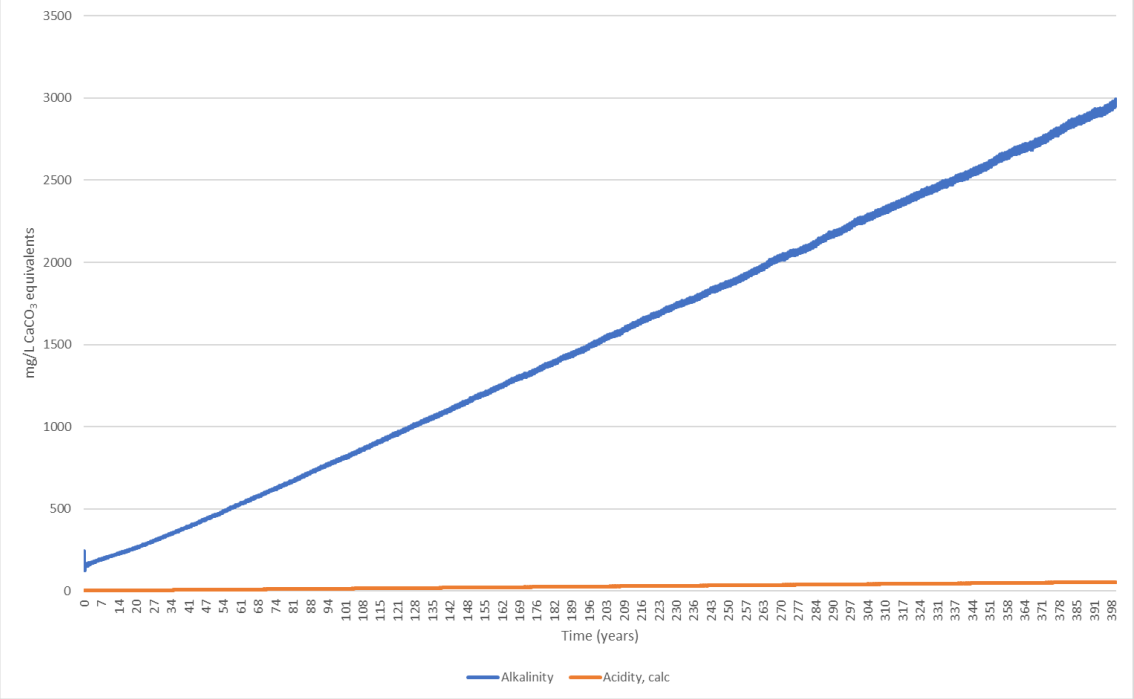

Source: SRK

Notes: Alkalinity and acidity calculated cumulatively from input source term chemistries.

Figure 8: Modelled major ion concentrations for the pe 12, Log pCO_2 -3.5 solution

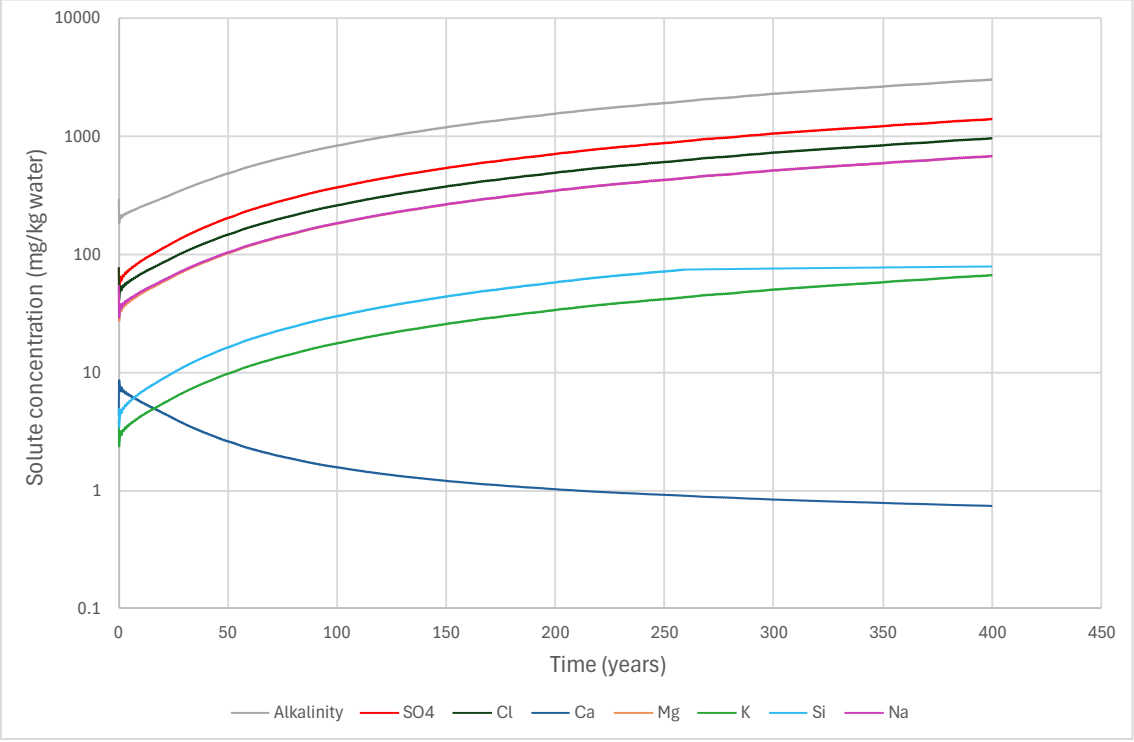

Source: SRK

Minerals that were modelled to precipitate according to PHREEQC calculations are shown in Figure 9 for illustrative purposes. The accuracy of this mineral precipitation modelling may be influenced significantly by factors such as:

- the actual metal leaching concentrations from the Sparrow Lake pit wall materials differing substantially from model input chemistry
- trace metal sorption onto solid phases such as ferrihydrite ($Fe(OH)_3$)
- water temperature and variability between pure phase compositions modelled in PHREEQC
- actual mineral compositions in mineral groups that form solid solutions
- errors associated with thermodynamic data in PHREEQC that do not contain temperature correction parameters for temperatures that deviate significantly from 25ºC
- inclusion or exclusion of minerals for modelling water chemistry in PHREEQC.

Mineral reaction kinetics would also play an important role, as some of the phases that are modelled to precipitate would likely take a substantial period to form, during which time elevated dissolved metal concentrations may persist. Significant differences in major ion solute concentrations derived from wall rock or talus may change the mineral composition of any precipitation reactions and must be confirmed during the model update.

The possibility of biological reduction of $Fe(OH)_3$ and other oxidised iron minerals must also be considered in the long term, although this depends on the availability of organic carbon in the pit lake environment. This could occur through biological activity within the lake due to the availability of water to both aquatic and terrestrial plants and animals. If biological reduction of iron minerals occurs, besides the release of Fe^{2+}, other metals may also be released through desorption.

Figure 9: Mineral precipitation predicted by PHREEQC speciation, assuming equilbrium conditions at 25°C

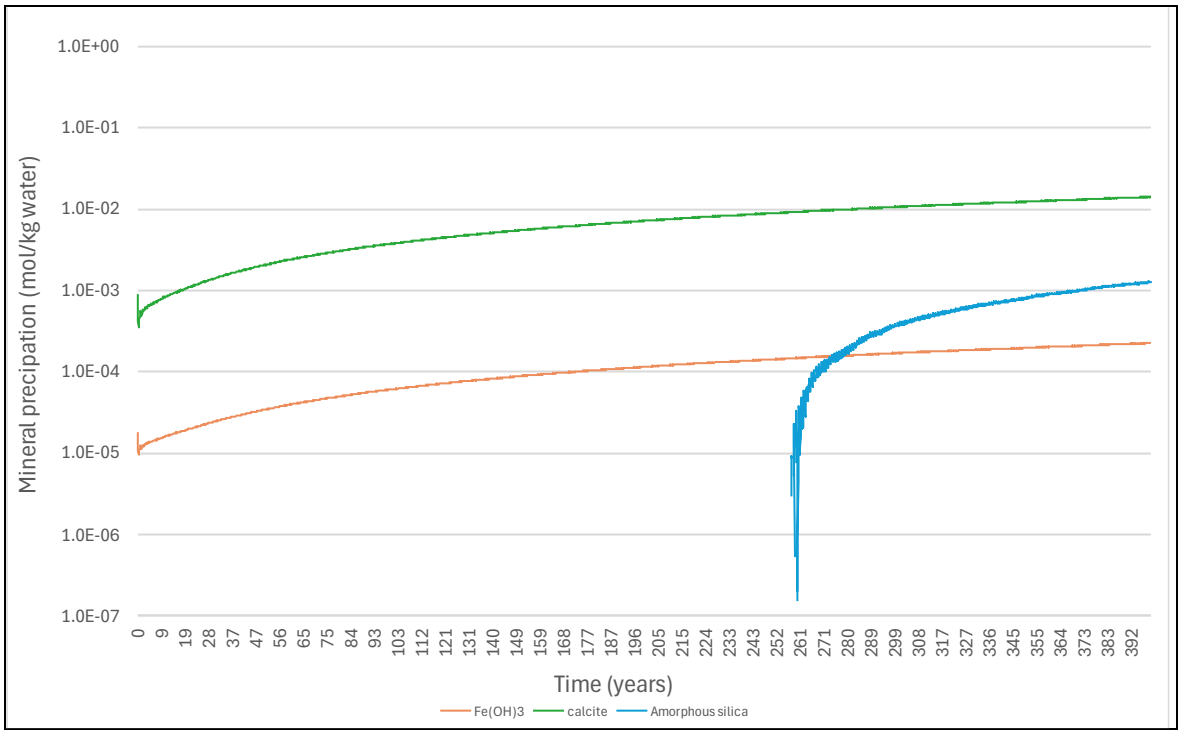

6 Summary and conclusions

Preliminary pit lake water quality modelling was carried out using a simplified spreadsheet approach and the resulting pit lake concentrations were speciated using PHREEQC geochemical modelling software. Inflows to the pit were obtained from the pit water balance, constructed in GoldSim (SRK, 2025). Average bore water chemistry for the Sparrow Lake pit was used to represent inflowing groundwater chemistry. Pit wall run-off chemistry was simulated using published data for Mt McRae Shale kinetic tests (Linklater, et al., 2015), which were scaled according to pit wall sulfur content, estimated from the block model provided by Atlas.

The model results indicate that the Sparrow Lake pit is likely to remain circum-neutral and that the risk of acidification is low. This is due to the large excess of predicted groundwater inflows relative to pit wall run-off volumes and the relatively low sulfur concentration in most of the pit wall exposure, according to block model intersections.

It is noted, however, that these conclusions do not consider potential changes in groundwater flow rates and/or groundwater quality over time. It is not known to what extent the average groundwater quality that was used for modelling is representative of the pore volume that will be dewatered. The groundwater model was being completed at the time of drafting this memorandum and hence was not yet available for this work. Allocation of relevant borehole monitoring data to zone budgets obtained from the Modflow model will enable calculation of a weighted groundwater quality for known groundwater sources, which will improve confidence in the representativeness of the groundwater solute load that will enter the pit lake.

The representativeness of the Mt McRae Shale kinetic data that were applied for this work is uncertain and should only be interpreted as indicative of the risk of acidification of a future pit lake in the Sparrow Lake pit. Since acidification is the most significant environmental risk associated with a pit lake, the results nevertheless indicate that the risk associated with the Stage 5 Sparrow Lake pit design is limited. The model indicates that the presence of PAF rock in the pit walls is not expected to result in pit lake acidification The potential for saline or metalliferous drainage could not be assessed based on the available data.

The contribution of the in-pit waste rock dump was not assessed at this stage of the project, as representative geochemical data for the proposed waste rock is not yet available.

7 Recommendations

A refined pit lake water quality model should be developed once sufficient laboratory data are available to populate it. It is recommended that the refined model be constructed in GoldSim (as originally intended), incorporating the water balance model as a sub-component. Suggested model refinements include:

- more rigorous evaluation of likely groundwater inflow volume and chemistry over time, to provide more accurate weighting of contributions from different groundwater zones
- addition of the proposed in-pit waste dump as a source term in the pit lake model
- accounting for source term mass depletion in wall rock, talus and any in-pit waste rock disposal
- inclusion of representative kinetic data to define source terms for wall rock, talus and waste rock. These representative samples are currently undergoing testing.

Regards

SRK Consulting (Australasia) Pty Ltd

Pierre Rousseau
Principal Consultant

Alex Watson
Principal Consultant

References

Linklater, C. et al., 2015. *Weathering and Oxidation in Black Shales - A Comparison of Laboratory Methods.* Santiago, Chile, International Mine Water Association.

Mine Earth, 2024. *Sanjiv Ridge Stage 4 - Waste Rock Assessment. Detailed Geochemical Characterisation,* s.l.: s.n.

Mine Earth, 2025a. *Sanjiv Ridge Stage 5 - Waste Rock Assessment. Interim Report - Preliminary Geochemical Characterisation,* s.l.: s.n.

Mine Earth, 2025b. *Sanjiv Ridge Stage 5 - Waste Rock Geochemical Characterisation - Sparrow Pit Update,* s.l.: s.n.

Sellman, L., 19 April 2024. *Memorandum - SMR Stage 4 PAF disposal strategy,* s.l.: Atlas Iron.

SRK, 2025. *Pit Void Water Balance modelling: Sanjiv Ridge Stage 5 Below Water Table Mining Hydrogeology Study, WA, Australia,* Perth: SRK.